MANUFACTURING AND CHARACTERIZATION OF UNIFORMLY POROUS
AND GRADED POROUS POLYMERIC STRUCTURES VIA SELECTIVE
LASER SINTERING

A THESIS SUBMITTED TO
THE GRADUATE SCHOOL OF NATURAL AND APPLIED SCIENCES
OF
MIDDLE EAST TECHNICAL UNIVERSITY

YUSUFU ABEID CHANDE JANDE

IN PARTIAL FULFILLMENT OF THE REQUIREMENTS
FOR
THE DEGREE OF MASTER OF SCIENCE
IN
MECHANICAL ENGINEERING

DECEMBER 2009

Approval of the thesis:

MANUFACTURING AND CHARACTERIZATION OF UNIFORMLY POROUS AND

GRADED POROUS POLYMERIC STRUCTURES VIA SELECTIVE LASER

SINTERING

Submitted by **YUSUFU ABEID CHANDE JANDE** in partial fulfillment of the requirements for the degree of
Master of Science in Mechanical Engineering Department, Middle East Technical University by,

Prof. Dr. Canan Özgen   _____
Dean, Graduate School of **Natural and Applied Sciences**

Prof. Dr. Süha Oral   _____
Head of Department, **Mechanical Engineering**

Assist. Prof. Dr. Merve Erdal Erdoğmuş   _____
Supervisor, **Mechanical Engineering Department, METU**

Assoc. Prof. Dr. Serkan Dağ   _____
Co-supervisor, **Mechanical Engineering Department, METU**

Examining Committee Members:

Prof. Dr. Mustafa İlhan Gökler
Mechanical Engineering, METU   _____

Assist. Prof. Dr. Merve Erdal Erdoğmuş
Mechanical Engineering, METU   _____

Assoc. Prof. Dr. Serkan Dağ
Mechanical Engineering, METU   _____

Prof. Dr. Suat Kadıoğlu
Mechanical Engineering, METU   _____

Prof. Dr. Serhat Akın
Petroleum and Natural Gas Engineering, METU   _____

Date: _____

I hereby declare that all information in this document has been obtained and presented in accordance with academic rules and ethical conduct. I also declare that, as required by these rules and conduct, I have fully cited and referenced all material and results that are not original to this work.

Yusufu Abeid Chande JANDE

ABSTRACT

MANUFACTURING AND CHARACTERIZATION OF UNIFORMLY POROUS AND GRADED POROUS POLYMERIC STRUCTURES VIA SELECTIVE LASER SINTERING

JANDE, YUSUFU ABEID CHANDE

M.Sc., Department of Mechanical Engineering

Supervisor: Asst. Prof. Dr. Merve ERDAL

Co-Supervisor:Assoc. Prof. Dr. Serkan DAĞ

December 2009, 254 pages

Selective laser sintering is a rapid prototyping method (RP), which was originally developed, along with other RP methods, to speed up the prototyping stage of product design. The sole needed input for production being the solid model of the part, the mold/tool-free production characteristics and the geometric part complexity that can be achieved due to layer-by-layer production have extended the applicability/research areas of these methods beyond prototyping towards new applications and material development.

Local pore formation in a part that occurs as a result of the discrete manufacturing nature of selective laser sintering is normally considered a defect. In the current research, this is viewed as an opportunity for material development: Exploitation of rapid prototyping methods to produce composites/functionally graded materials with controlled porous structures. That the material interior structure (porous structure) and exterior shape are formed during the same course renders selective laser sintering process as an attractive manufacturing alternative for producing complex-geometry composite/porous materials, which may be difficult or impossible to manufacture with other techniques. In this thesis, the use of selective laser sintering (a rapid prototyping method) in producing uniformly porous and graded polymeric graded porous structures is studied. The material used was polyamide powder (PA 2200) and the selective laser sintering machine used was the EOSINT P 380 system. In this research, three process parameters of the SLS system, the hatching distance, the laser power and the laser scanning speed were varied to produce parts that have different porosities. Porous parts with a homogenous porous microstructure (uniformly porous parts) could be produced, as well as graded porous parts. The results of uniformly porous structure production were utilized to build graded porous structures by imparting different porosities along a certain direction within a single part. Both, uniformly porous and graded structures were characterized physically and mechanically. The porous parts (both uniformly porous and

graded porous) were infiltrated with epoxy resin to produce epoxy-PA composites and graded materials. The physical and mechanical properties of these parts were compared with those of the uninfiltrated (porous PA) structures.

Keywords: Selective laser sintering, porous structures, microstructure, factorial analysis

ÖZ

LAZER SİNTERLEME HIZLI PROTOTİPLEME YÖNTEMİ KULLANILARAK DERECELENDİRİLMİŞ HOMOJEN VE GÖZENEKLİ PÖLİMERİK MALZEME ÜRETİMİ VE KARAKTERİZASYONU

JANDE, YUSUFU ABEID CHANDE

Yüksek Lisans,Makina Mühendisliği Bölümü

Tez Yöneticisi: Y.Döç.Dr.Merve ERDAL

Ortak Tez Yöneticisi:Döç.Serkan DAĞ

Aralık 2009, 254 sayfa

Lazer Sinterleme, diğer hızlı prototipleme yöntemleri gibi ürün tasarım sürecini hızlandırmak amacıyla geliştirilmiş bir üretim yöntemidir. Üretim için yalnızca parçanın katı modelinin gerekli olması, kalıp/takımdan bağımsız üretim özelliği ve katman-katman üretim sayesinde karmaşık parçaların üretilebilmesi, konunun çalışma alanlarını genişletmiş; araştırmacıları yeni uygulama alanlarına ve malzeme geliştirmeye yönlendirmiştir. Lazer sinterlemede üretimin ayrık doğası sonucu parçada yerel gözenekler oluşur. Bu gözenekler çoğunlukla hata gibi görülse de, bu çalışmada kontrollü gözenek yapılarına sahip derecelendirilmiş/kompozit malzeme geliştirilmesi

açısından bir fırsat olarak değerlendirilmiştir. Lazer sinterleme yönteminde parçanın iç (gözenekli yapı) ve dış (şekil) yapısı aynı anda üretildiğinden, diğer üretim yöntemleriyle üretilmesi zor yada imkansız olan karmaşık şekilli parçalar bu yöntemle üretilebilir. Bu özellik lazer sinterleme yönteminin cazip bir alternatif üretim metodu olarak değerlendirilmesini kılmaktadır. Bu tezde lazer sinterleme (hızlı prototipleme yöntemi) kullanılarak, düzenli ve derecelendirilmiş gözenekli polimerik malzeme üretimi araştırılmıştır. Üretimde EOSINT P380 lazer sinterleme makinesi ile poliamid PA2200 plastik toz kullanılmıştır. Farklı gözenekliliğe sahip parçalar üretmek için lazer tarama aralığı, lazer gücü ve lazer tarama hızı üretim parametreleri değiştirilmiştir. Bu sayede homojen (düzenli) gözenekli ve derecelendirilmiş gözenekli yapıya sahip parçalar üretilebilmiştir. Düzenli gözenekli parça üretiminden elde edilen sonuçlar kullanılarak, tek bir parça içinde belli bir yönde farklı gözenekliliğe sahip derecelendirilme verilebilmiş ve bu tip derecelendirilmiş gözenekli parçalar üretilmiştir. Düzenli ve derecelendirilmiş gözenekli parçalar hem fiziksel hem de mekanik olarak karakterize edilmiştir. Gözenekli (düzenli ve derecelendirilmiş) parçalara epoksi reçine emdirilerek epoksi-PA kompozit ve derecelendirilmiş malzemeler üretilmiştir. Bu parçaların fiziksel ve mekanik özellikleri, reçine emdirilmeyen (gözenekli) plastik parçaların özellikleri ile karşılaştırılmıştır.

Anahtar Sözcukler: lazer sinterleme, gözenekli yapılar, mikroyapı, parametre analız.

To My Family,

ACKNOWLEDGEMENT

TABLE OF CONTENTS

LIST OF TABLES

LIST OF FIGURES

NOMECLATURE

CT   : Computed Tomography

SLS   : Selective laser sintering

SEM   : Scanning Electron Microscope

HD   : Hatching Distance

LP   : Laser Power

LS   : Laser scanning speed

IUPAC   : International Union of Pure and Applied Chemistry

UTS   : Ultimate tensile strength

PA   : Polyamide

ED   : Energy Density

p   : Applied pressure

D   : Pore diameter

γ : Surface tension of mercury

φ : Contact angle between mercury and the pore wall

CHAPTER 1

INTRODUCTION

1.1 Rapid Prototyping

Rapid Prototyping (RP) is the family of solid free form fabrication methods where the production of parts is based on additive technology. In these processes product is constructed in a layer by layer fashion (Figure 1.1). The virtual design of a part model is created via Computer Aided Design (CAD) packages, and then transferred into a physical object without human intervention. The RP technology was invented to speed up prototyping stage of product development. The required product models can be quickly and easily built via RP approach compared to the traditional production methods like chip removal technique [1]. In this manner the term rapid prototyping was born.
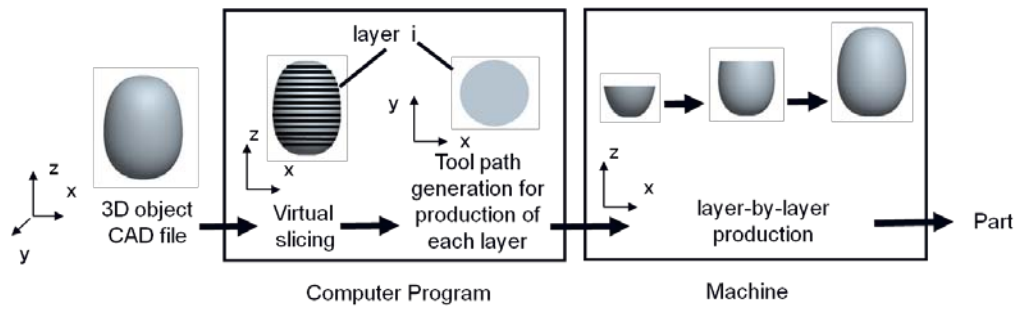
Figure 1.1: Layer by layer Production

In all RP systems, the solid model of the part to be produced is virtually sliced into planar layers and the actual production is carried out by constructing the part, layer by layer. No tooling is required and for production of a new part, or a modification on the old, an RP system needs only the relevant 3-D part geometry data as input. Layered nature of manufacturing also enables the production of complex shapes, which are difficult or perhaps impossible to manufacture by other means, by forming and stacking relatively simple 2-D layers, (Figure 1.2). As such, RP methods have found applications beyond building models, as in rapid/additive manufacturing and rapid tooling, which use RP to directly manufacture the end-product or the tooling for producing the end-product [2-5].

There are a variety of RP processes. Among these, the most commonly used processes are fused deposition modeling (FDM), stereolithography (SLA), 3D printing (3DP), and selective laser sintering (SLS) [6]. In FDM process, the thermoplastic filament is extruded in molten state from the heated nozzle (extruder) which is kept just above the melting temperature of the extruded material. The extruder moves on deposition plane depositing material at the select locations to construct the layer. After the first layer is finished the second layer is built. This procedure is repeated until the desired part is produced. In case of SLA process, the raw material is liquid resin which is deposited onto the platform to form a thin layer.

Figure 1.2: Examples of complex geometry parts produced via RP methods produced at the Biltir Center; METU

Laser scans the resin layer at the select locations in order to cure. After the curing process in the first layer is over the second layer is deposited and the same building process follows as in the previous layer. Layering process continues in this manner until the whole part is built. For the 3DP the thin layer of powder particles is selectively bonded using the droplets of binder. After the binding process is over for the current layer the new layer is deposited and the binding process is performed. These procedures are repeated until the desired part is built. In this thesis the SLS process is used, and the process is explained in details in the next section.

1.2 Selective Laser Sintering

In selective laser sintering (SLS) process product layers are formed by sintering a layer of powder material with a laser at select locations. The process has relatively higher flexibility in terms of type of material used [7, 8]. The powder can be thermoplastic or metal or ceramic powder with appropriate binder in it. Thermoplastic powder locally melts and solidifies to form a solid layer. For the metal or ceramic powder laser melts the binder in the powder (not the metal or ceramic powder). Therefore, binder melts and solidifies to hold the metal or ceramic particles together forming the solid

layer. But then after SLS these parts need to be sintered at high temperature to bond actual particles together.

The SLS process is composed of the controlling terminal (computer) and the production unit as in all other RP processes. The control terminal is a computer for human interface such as for loading product geometry files, production preparation, and manual control of the machine whenever necessary. The production unit is composed mainly of processing chamber and laser source. In the processing chamber there are heaters for initially heating the deposited powder; the powder is sintered layer by layer using the laser beam to produce the desired model.

The solid model of the part to be produced is virtually sliced into layers on which the tool (laser beam) paths will be generated. The slice thickness is chosen during the virtual slicing process. The new generated file which contains the laser beam paths is loaded into the computer of the SLS system. The desired production parameters are selected before the production begins. Before production starts the processing chamber is heated to just below the melting temperature of the powder that will be sintered.

Figure 1.3 indicates the production steps for an SLS machine. The machine is composed of the powder bins, recoater, exchangeable frame, platform, and laser source. The powder bins hold the powder to be used in the production. Sufficient powder is put into the bins so as to meet the demand of the whole production at a given time. The recoater is loaded with powder from the powder bins and can move back and forward on the platform so as to deposit powder onto the platform. The exchangeable frame supports the platform, where the powder is deposited, so that it can move up and down when necessary. The laser source, on the other hand, produces the laser beam for locally melting the deposited powder so that the inter-particle and inter-layer fusion happens.

The first step of the SLS process is to fill the recoater with powder from the powder bin which is just above the recoater position. In this case the recoater is on the left and it accepts powder from the left powder bin. Then, the recoater moves to the right depositing powder onto the platform from its opening at the bottom (step 2). The amount of powder deposited is calculated based on the desired layer thickness chosen. In the third step, the laser beam is directed to select locations on the layer in order to fuse powder particles and to fuse the current layer to the previous one. After the current layer is sintered the platform moves one layer-thickness down. The step

movement is equal to the desired layer thickness. The production of the next layer proceeds through recoater filling and depositing (step 5 and 6). The steps continue until all layers have been produced, forming the part geometry.

1-Bins, 2-Recoater, 3-Frame
4-Platform, 5-Laser source

Step-1: Powder fill the recoater from the left-bin

Step-2: Recoater moves to the right (deposits powder)

Step-3: Laser beam fuses powder

Step-4: Platform moves one-step down

Step-5: Powder fill the recoater from the right-bin

Step-6: Recoater moves to the left (deposits powder)
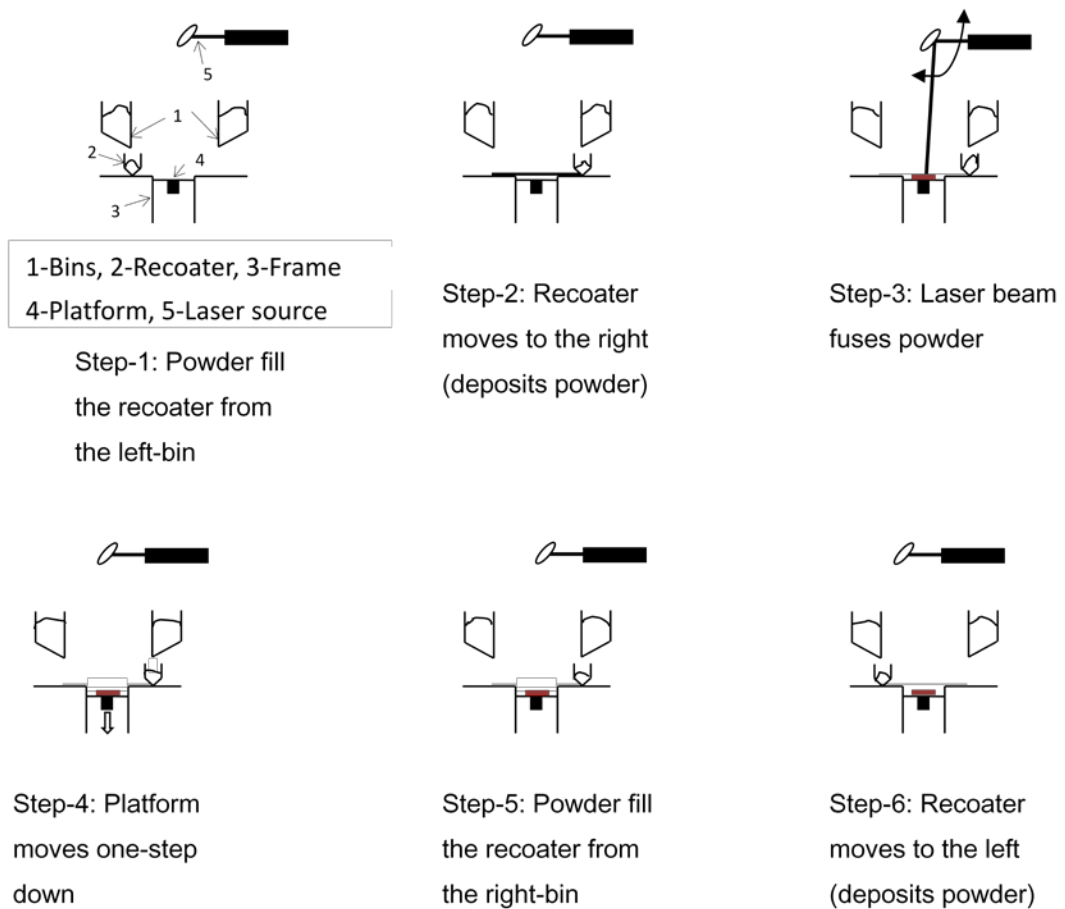
Figure 1.3: Production steps of the SLS process

1.3 Porous Structures Production Using Rapid Prototyping Methods

Due to the discrete nature of manufacturing, all parts produced via RP exhibit some porosity, the degree and the locality of which vary with respect to the particular method used. This is usually an undesired trait as the porosity undermines the structural integrity of the part, important especially in applications such as rapid tooling/manufacturing. However, this same trait, often regarded as a defect, can be viewed as an opportunity to use RP methods for producing porous parts with controlled porosity/controlled interior pore structure. As such, a considerable number of studies are being conducted on using layered manufacturing techniques to produce porous structures for various applications.

In tissue engineering, research is conducted to develop complex shaped scaffolds using RP methods, as implants for the purpose of growing tissues [9-17]. Controlled porosity is also a desired feature in studies conducted towards developing drug-delivery devices via layered manufacturing [18-20]. A number of different RP methods are employed in these studies, varying from fused deposition modeling to 3D printing to selective laser sintering. A variety of materials are used in these studies, including ceramics and metals, but mostly polymers.

1.3.1 Porous Structures Production Using SLS

The internal structure and the porosity of the parts produced via SLS are affected by the processing parameters. A number of studies involving the effect of processing parameters on properties of parts produced via SLS have been reported in the literature [21-24]. In [21], samples were built using polyamide powder (PA2200-EOSINT) to assess the effect of laser power and laser scan speed on the material properties (volumetric density, stress at 10 % strain, flexural modulus). The individual effect on material properties were investigated using the factorial design. Laser power was found to have the largest effect on volumetric density and stress at 10% strain. But, the flexural modulus was affected by both scan speed and laser power. In [22], the effects of laser scanning speed and laser power on parts built from steel powders of different carbon content on the porosity, yield stress, and microhardness were investigated. The pores volume fraction in carbon steels produced using SLS decreased as the scan speed and scan spacing decreased. Compared to wrought steels density, the required energy density for full densification decreases with an increase in the amount of carbon content.

In another study the porosity of the parts, built from CastForm TM Polystyrene (CF), were produced using SLS process by only changing the laser power [23]. The apparent densities of samples produced at various energy densities were found, and also the sintered parts were infiltrated with red-wax. Also, it was found that the density of the sintered parts increased with an increase in laser energy density up to a certain value and started to decline due to the material degradation. There has been one another study involving porous polyamide parts (other than the current one), in which the effect of laser power on part density and mechanical properties were reported, by producing samples on a DTM Sinterstationplus SLS machine using DuraFormTM Polyamide powder of 3D Systems [24]. The laser power was varied and the parts were produced at different orientations. It was found that porous parts built at different orientations but same processing parameters exhibited varying physical and mechanical properties.

1.3.2 Production of Graded Porous Structures using SLS

There have been some studies in the literature towards developing graded structures via SLS. The grades could be given by changing the relative compositions of several materials in a part [26-29] or by varying porosity [30-31]. In [26], the production settings were kept constant while the amount of

one component (Zirconium) was changed from 0% to 10% within another component (Waspaloy® - nickel-based superalloy) along production layers [32]. In [27], one of the process parameters, the scan speed, was varied along with change in relative composition of two material components (silica nanoparticles in nylon-11). In [28], polycarbonate-nickel material duo was used in different relative concentrations to produces grades. In [29], glass beads - nylon-11 material duo was used in different relative concentrations

In [30], the particle size of the same powder material (high density polyethylene) was changed along the layering direction so as to achieve porous graded structures. In [31], one of the processing parameters, he laser power, was varied to induce varying porosity within parts, towards developing drug delivery devices from biodegradable materials.

1.4 The scope of the thesis

The ability to produce complex 3-D shaped parts in layered manufacturing offers a range of research opportunities in designing and developing porous materials that can find other applications, such as those in thermal insulation and filtration. Furthermore, the porous structures can be infiltrated with a second material to produce composites [33] that have complex outer shapes,

or graded materials, if the porosity can be varied within the part during production. The successful realization of all such depends on the degree of control over creating the desired interior structure (porosity/pore architecture), as well as the availability of the appropriate material for the intended application. In order to attain the necessary control over the interior structure generation during production, the relations between the processing parameters and the resulting part interior structure must be established. This is the focus of the current study.

In this study, the ability to produce porous structures using selective laser sintering (SLS) process is investigated. The aim of the study is to obtain uniformly porous structures and graded porous structures in a controlled and repeatable manner from polyamide powder, which can exhibit variations in porosity by changing specific process parameters. The starting point for this research lies in a previous study conducted by İlkgün [25] in which uniformly porous structures were produced by varying three process parameters: hatching distance, laser power, and laser scanning speed. In that study, the apparent densities of the produced porous structures were related to the three production parameters. In this study, thorough characterization (both physical and mechanical) is performed to obtain the physical and mechanical properties of the porous parts that can be produced by varying the three

process parameters used in [25]. Once the uniform production and characterization are completed; next the production and the characterization of graded porous structures are carried out. The infiltration capabilities of porous structures (uniform and graded) are also studied. The conducted research is presented in the rest of this thesis in the following manner:

In Chapter 2, the production and the physical and mechanical characterization methodology of uniformly porous polyamide structures are presented. In order to impart different part porosities, design of experiment is used to plan production in this part. In Chapter 3, the production and the physical and mechanical characterization methodology of graded porous polyamide structures are presented. In this part of the study, grades are given to a part by varying the porosity within the part in a controlled manner. In Chapter 4, the uniformly porous structures and graded porous structures are infiltrated using an appropriate liquid resin in order to find out impregnability or infiltration characteristics. The produced infiltrated parts are characterized using physical characterization methods and mechanical tests. The results of the studies outlined in Chapters 2 to 4 are presented and discussed in Chapter 5. Conclusions of the current work and recommendations for future work are given in Chapter 6.

CHAPTER 2

PRODUCTION AND CHARACTERIZATION OF UNIFORMLY POROUS
POLYAMIDE STRUCTURES

The first part of the thesis work involves producing and characterizing uniformly porous structures. Uniformly porous means the interior microstructure of the produced part is more or less, uniform. The local density from one location to the other does not vary. In production, the type of SLS machine used is EOSINT P 380 available at Biltir Center at the Department of Mechanical Engineering in Middle East Technical University (Figure 2.1). This machine is used to produce all samples in this study. The machine technical specifications are given in Table 2.1. The material used in EOSINT P 380 is a fine polyamide powder (PA 2200) provided by the machine vendor. This is a type of Nylon 12 [34, 35]. The average diameter of the powder particles is approximately 60 µm. The powder is thermoplastic, which soften/melts with heat and freezes (solidifies) when cooled. The material datasheet for PA 2200 is in Appendix A.

Figure 2.1: EOSINT P 380 Laser Sintering Machine in Biltir Center-METU

Table 2.1: EOSINT P 380 SLS System Technical specifications

Effective Building Volume	340 mm x 340 mm x 620 mm
Building Speed	10-25 mm height / hour
Layer Thickness	0.15-0.20 mm
Laser Type (max. power)	CO_2 (50W)
Laser Scan Speed (max.)	5000 mm/s
Power Supply	32 A
Power Consumption (max.)	4kW/h

In this study, in order to impart porosity and change the amounts of porosity in part produced through SLS, three processing parameters are varied (Appendix C). These processing variables are hatching distance (HD), the laser power (LP), and the laser scanning speed (LS). By setting these parameter values to different values, the amount of porosity in a sample can be controlled. The porosity formation is related to degree of fusion between powder particles and these processing parameters are used to vary the fusion amount.

Figure 2.2 gives the description of the three parameters. For a given layer, the laser beam moves along x and y coordinates on the layer plane (xy-plane). Hatching distance is the distance between two adjacent scan paths of the laser beam on a layer. The smaller the hatching distance is, the smaller the amount of overall fusion between particles will be. During the scanning process, the amount of laser power applied into the region of interest also affects the amount of intra-particle and inter-layer fusion. The speed with which the laser beam moves along its path on a layer is the laser scanning speed. If the speed is high, the time a unit area of powder exposed to laser beam is small which affects the degree of fusion (weak fusion between particles and between successive layers). The combined effect of the three processing parameters is expressed in terms of energy density (ED) as

$$ED = \frac{LP}{HD \times LS}$$
(2.1)

This is the amount of energy to which a unit layer area of powder is exposed during production. As energy density increases better fusion happens and it is likely to have less porosity. But, when the energy density decreases poor fusion occurs and is the part is likely to have higher porosity. If the energy density is too low sintering becomes impossible due to lack of fusion between powder particles and between successive layers. On the other hand, if the amount of energy density is too high, the material degrades [23, 25]. The processing window (parameter setting range) must be such that the production of parts lies between these two limits. An earlier work conducted by İlkgün [25] involved determining the upper and lower limits of these three process parameters to avoid these pitfalls. In this study, the limitations values of the three parameters have been chosen based on the results of [25]. These limits are presented in Table 2.2.
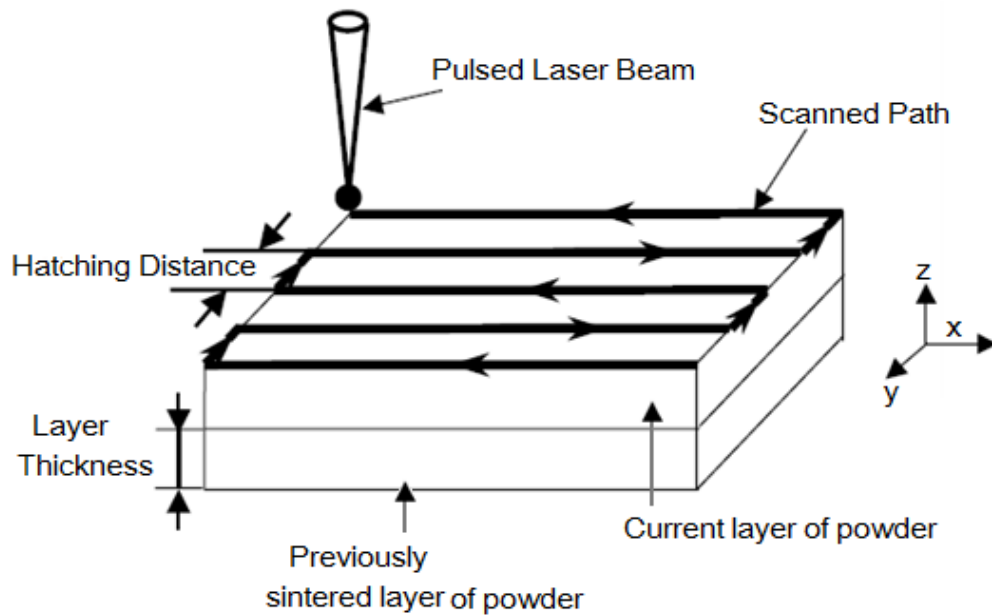
Figure 2.2: Production parameters used to assess the properties of sintered parts

Table 2.2: Maximum and minimum values of the processing parameters

Factor	HD(mm)	LP (%)	LS (mm/s)
Min. value	0.30	66.3	4000
Max. value	0.45	90.0	5000

2.1 Production Planning and Production of Uniformly Porous Parts

The design of experiment is used to plan the production in which parts with different porosities can be produced. In this production there are three processing parameters (factors) and each parameter has two "levels" (the maximum and minimum values of Table 2.2). The two levels of each factor are denoted as "high" and "low". The combination of the three factors at two

levels yields 2^3 (eight) production settings. This is a "factorial design" of the

production in which all factors (parameters) are varied together to assess the

response of the system of process [45]. The factorial design is different from

the traditional way of doing experiment where the one-factor-at-a-time is

varied in the experiment.   In this research, in addition to the eight settings

generated by factorial design the default parameter setting of the SLS

machine is also included for study. The default parameter setting has been

identified by the machine manufacturer as the recommended production

setting for producing models (the original purpose of the SLS system). The

nine different processing parameter setting are presented in Table 2.3.

Table 2.3: Processing parameter settings used for producing uniformly
porous parts

Processing Setting	Hatching Distance(mm)	Laser Power (%)	Scanning Speed(mm/s)	Energy ** Density(J/mm^2)
1	0.45	66.3	5000	0.016
2	0.45	66.3	4000	0.019
3	0.45	90.0	5000	0.020
4	0.30	66.3	5000	0.024
5	0.45	90.0	4000	0.025
6	0.30	66.3	4000	0.029
7	0.30	90.0	5000	0.030
8[*]	0.30	90.0	4500	0.033
9	0.30	90.0	4000	0.037

* Default machine setting (recommended production setting for producing models)

** Energy Density is obtained using equation (2.1) and laser power (LP) is in Watt which is converted to (%) using laser power characteristics curve in Appendix B

Production from each setting is expected to produce different porosity sample. Apart from the three factors there is a layer thickness which can be varied, but in this research the layer thickness is kept at 0.15mm. The SLS machine also has two standard laser exposure types (the way laser beam scans powder layers) which are sorted and unsorted. These two types differ only on the exposure path (Figure 2.3). The "Sorted" strategy searches the shortest exposure way across the part, whereas the "Unsorted" strategy moves across the part in the easiest way [36]. In this study sorted exposure type has been used for all parts, therefore the scanning strategy is not a parameter.

(a) Sorted Hatching

(b) Unsorted Hatching
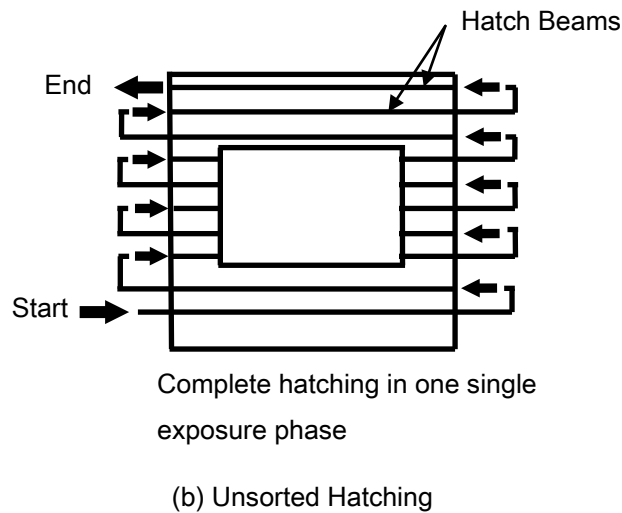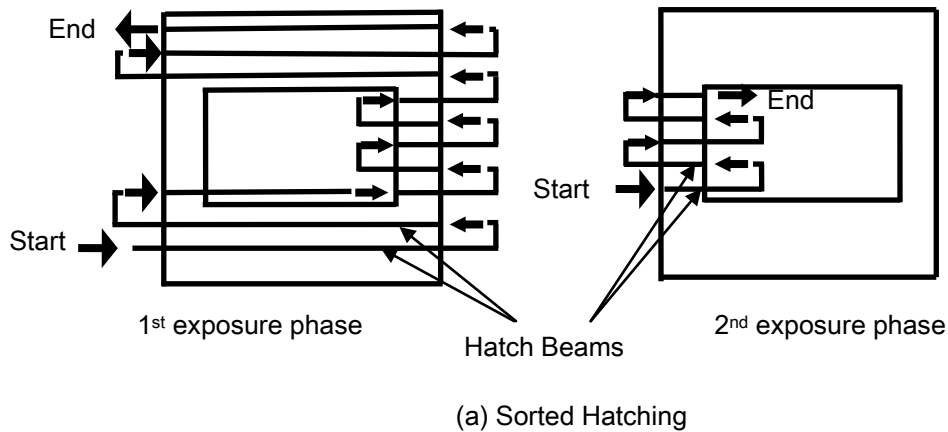
Figure 2.3: Standard laser exposure types: sorted hatching and unsorted hatching

In Figure 2.4 different hatching categories are indicated: hatching in x-direction, hatching in y-direction, hatching in both x and y direction, and alternating hatching. Hatching in x-direction implies that in each layer laser paths are only in x-direction (Figure 2.4 (a)), hatching in y-direction means in each layer laser paths are in y-direction only (Figure 2.4(b)), hatching in x and y-direction implies that hatching in each layer is performed in both

directions: x-and y-direction (Figure 2.4(c)). Alternating hatching means the laser paths from one layer to the other alternates between x and y-directions (Figure 2.4 (d)). For the standard application alternating hatching is being used. In this research this hatching category has been used for all production.
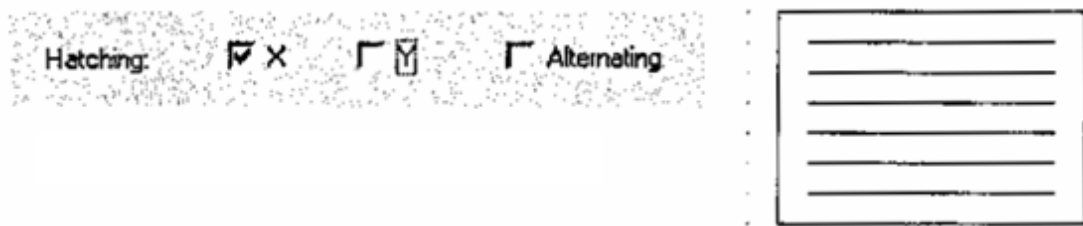
(a) Hatching in x-direction only
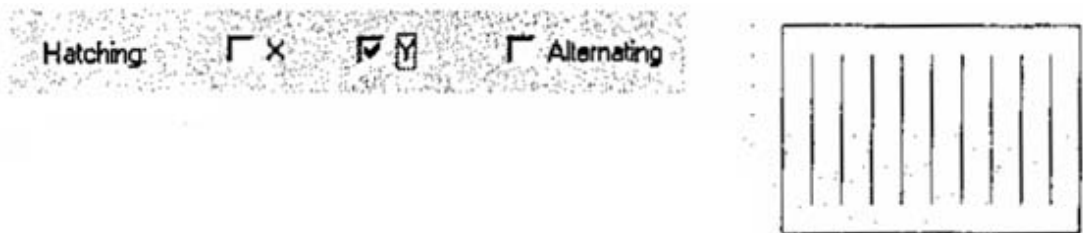
(b)Hatching in y-direction only
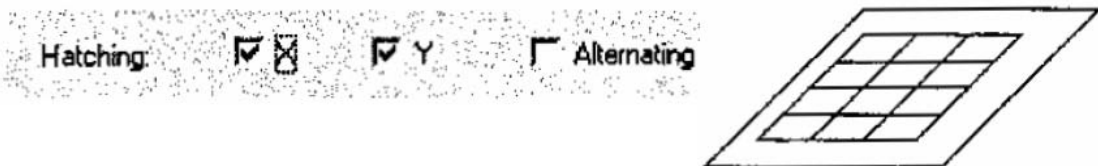
(c) Hatching in x and y direction

(d) Alternating hatching

Figure 2.4: Hatching categories

There are other factors which may affect the porosity of the sintered parts like location of the parts on the platform (due to an uneven temperature distribution), layer thickness and part orientation. In EOSINT P 380 layer thickness can be changed: either 0.15mm or 0.20mm. Different physical and mechanical properties of the sintered parts can be achieved if different layer thickness is used. In this research, 0.15 mm-layer thickness has been used throughout. The uneven temperature distribution (location of the part on the platform) and part orientation are not parameters, but they can influence the properties of the sintered parts. The parts to be sintered can positioned on the same location to minimize the effects of temperature. The orientation of the parts mostly influences parts which are not symmetric. Trying to produce parts from the same process parameter from the same orientation can minimize the effect. In this research, location of the parts and orientation of the parts on the platform have not been taken into consideration.

Once samples are produced, they will be characterized to assess their porous structures and related properties. For the physical characterization of the parts Helium Pycnometer, Mercury Porosimeter, Computed Tomography (CT) and Scanning Electron Microscope (SEM) were used. For each characterization method, different sample geometries needed to be produced at the processing settings of Table 2.3. All samples for physical characterization are shown in Table 2.4. The sample geometries and sizes are determined based on the requirements of each characterization method.

The mechanical properties of the produced samples are also to be obtained. Since the parts are expected to have different porosities at different processing settings, their mechanical properties are also expected to change. The sample geometry for the mechanical characterization is given in Figure 2.5. The geometry for the mechanical test (tensile test) is in accordance with ASTM Standard D 638-03 (2003) [37].

Table 2.4: Parts for physical characterization, dimensions in mm

Sample for characterization and density measurement	
Porosimeter Sample	
CT Sample	
SEM Sample	
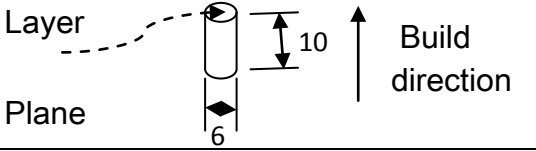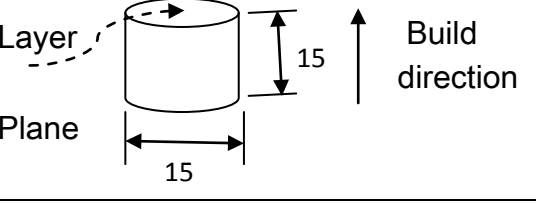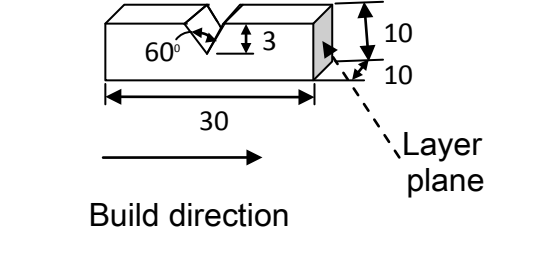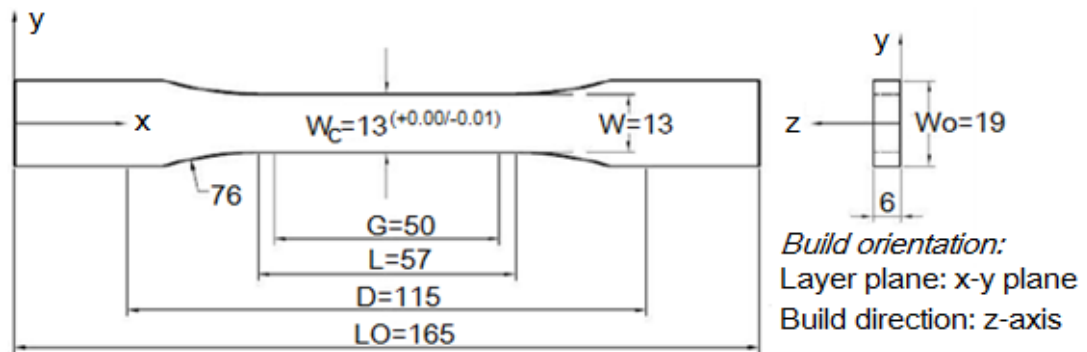
W: Width of narrow section	WO: Overall width
W_c: Width at the center	LO: Overall length
L: Length of narrow section	D: Distance between the grips
	G: Gage length

Figure 2.5: Sample geometry for mechanical characterization and the layering direction (dimensions in mm) [37]

2.2 Characterization of Uniformly Porous Structures

2.2.1 Physical Characterization

Helium pycnometer, mercury porosimeter, computed tomography (CT), and scanning electron microscope (SEM) are used to physically characterize the uniformly porous samples. Helium pycnometer is used for determining the true density of polyamide; mercury porosimeter reveals the pore size and size distribution. CT is a non-destructive method used for indirectly visualizing the microstructure in the sintered parts. SEM directly visualizes

26

the interior microstructure of the sintered parts. The characterization methods are explained in this chapter. The results are presented in Chapter 5.

2.2.1.1 True Polyamide Density via Helium Pycnometer Measurements

The helium pycnometer tests are conducted at the Central Laboratory at the Middle East Technical University (Quantachrome Corporation, Ultrapycnometer 1000, shown in Figure 2.6). The device employs Archimedes' principle of fluid displacement and Boyle's Law to determine pore volume and true density of a specimen. The Ultrapycnometer 1000 has three different sample cells with different volumes (135, 50 and 10 cm^3), (Table 2.5). The samples must be bulk solids, powders or foams, the amount of which should be able to fit in one of the three cells. The sample geometry of pycnometer test is about 1.178cm^3 (Table 2.4), thus the 10 cm^3 cell is used. At each processing parameter setting of Table 2.3 two samples were produced and tested, for repeatability assessments.

Figure 2.6: Quantachrome Corporation, Ultrapycnometer 1000

Table 2.5: Quantachrome Corporation, Ultrapycnometer 1000 Specification
[38]

Cell Size (cm^3)	Accuracy	Reproducibility
135	$< \pm0.02\%$	$< \pm0.01\%$
50	$< \pm0.02\%$	$< \pm0.01\%$
10	$< \pm0.03\%$	$< \pm0.015\%$

In Table 2.6 the average values of the mass, the true volume (measured in pycnometer) and the true density (calculated based on the mass and measured true volume) of samples produced at each processing setting are presented. Though the true density represents the density of solid part (without pores) and it is expected to be the same for all sintered parts, there

is some variation among different process settings. The mean PA true

density is calculated to be 1.0039 g/cc with a standard deviation of

0.0235g/cc, respectively. Figure 2.7 presents the true density of the samples

produced at different energy densities (different process settings). The true

density variation from one processing parameter to the other is very small.

The true PA density will be used to determine the macroscopic porosity of

parts produced at different production settings (each of Table 2.3).

Table 2.6: Results for true polyamide volume and density

Energy Density(J/mm^2)	Mass(g)	True Volume(cc)	True Density(g/cc)
0.016	0.9425	0.8975	1.0501
0.019	1.0260	1.0043	1.0216
0.020	1.0255	1.0058	1.0196
0.024	1.0702	1.0808	0.9902
0.025	1.0798	1.0911	0.9896
0.029	1.0690	1.0693	0.9997
0.030	1.1139	1.1277	0.9878
0.033	1.1195	1.1145	1.0045
0.037	1.1202	1.1529	0.9716
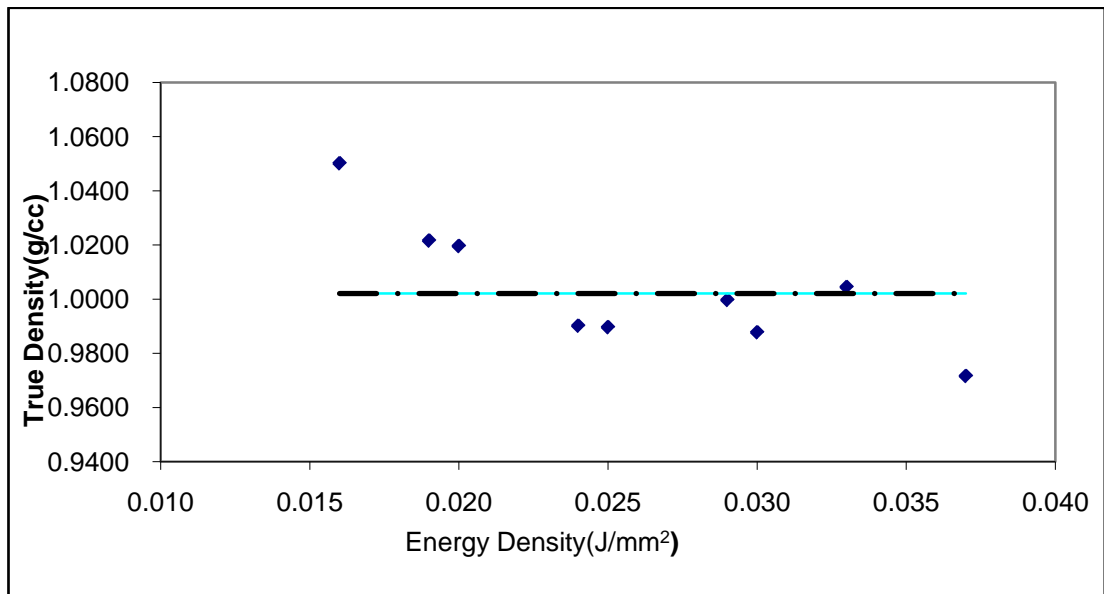
Figure 2.7: The true density of the uniformly porous polyamide parts at different process settings

2.2.1.2 Apparent Density

Apparent density is the density calculated by using the apparent volume of a porous part, rather than the true solid volume. Thus, it includes the contribution of pores. The same samples that are in pycnometer tests are used in evaluating apparent density. The density of the parts is acquired through volumetric analysis. The mass of the samples are measured by weighing them on a digital triple beam balance. The apparent volume of each sample is calculated from the measured outer dimensions. The samples are cylindrical in shape. The diameter and height of each sample is measured at different locations and using the average height and diameter for each

sample the overall (apparent) volume is calculated. The apparent density is

then calculated based on equation 2.2.

$$Apparent\ density = \frac{Sample\ Mass}{Sample\ Apparent\ Volume} \qquad (2.2)$$

Four different samples produced at each processing setting of Table 2.3 are

used to calculate an average apparent density at each setting along with

part-to-part variation (standard deviation) at each setting.

2.2.1.3 Macroscopic Porosity

The percent macroscopic (overall) porosity of each sample is found as

$$\%\ porosity = (1 - \frac{Apparent\ Density}{True\ Density}) \times 100 \qquad (2.3)$$

The apparent density of each sample (produced at each processing of Table

2.3) is found from previous section. The true density is obtained from the

pycnometer tests as explained in section 2.2.11. Hence, the macroscopic

porosities of all porous samples produced at each of a processing setting of

Table 2.3 are obtained.

2.2.1.4 CT Test for the Assessment of Production Uniformity

Computed Tomography (CT) tests are conducted to study the uniformity of porosity in the sintered parts. For this purpose Philips Tomoscan TX 60 CT machine is used. The degree of uniformity is assessed by comparing a parameter called CT number from one location to the other within the sample. CT number is the Hounsfield unit which measures the amount of x-ray attenuation used in CT scans [39]. Each voxel is assigned a value (CT number) on a scale in which air has a value of −1000; water, 0; and so on [39]. A voxel is a 3-D pixel [46] and it is in the shape of a cube. In CT, the two-dimensional image is displayed on the screen, but the 3D image has been constructed during CT scanning in which every scan has a thickness. Taking CT scans and reading CT numbers are not performed simultaneously. Firstly, images are taken and then CT numbers are read.

Attenuation refers to the reduction of the radiation intensity, upon passage through matter, resulting from all types of interaction. The CT number is defined as

$$CT_{number} = \left(\frac{\mu}{\mu_w} - 1 \right) 1000 \qquad (2.4)$$

where μ: effective linear attenuation coefficient for the x-ray beam passing through the scanned material and $μ_w$: effective linear attenuation coefficient for the x-ray beam passing through water [39].

Table 2.7 indicates the CT machine parameters for the CT tests. Each parameter shown in Table 2.7 is defined as follows: slice thickness is the nominal thickness of the CT image that is scanned. Every CT image normally has a thickness and the attenuation across this thickness is measured. Scan time is the time interval between the beginning and the end of the acquisition of attenuation data. Field of view is the maximum diameter of the scanned area or reconstructed image (the image produced after CT scanning). The area to be scanned is assigned a diameter (the field of view) and this is normally larger than the specimen or casing to be scanned. The diameter value is set (entered) before the CT machine starts to operate. The elemental area refers to the actual area over which the CT number is read. This area is expressed in terms of voxels and can be adjusted to the desired value. On the CT image when the elemental area is adjusted, the CT value is displayed instantly and it corresponds to the area of the voxel.

Table 2.7: Parameters used for in CT imaging of uniformly porous structures

Parameter	Value
Slice thickness (mm)	3
Scanning time (s)	3
Field of view (cm)	16
Elemental area (number of voxels used for reading the CT number)	4

To obtain the corresponding area of 4 voxels the following procedures can be followed:

$$A_{1v} = \frac{\pi F^2}{4(512)^2} \tag{2.4}$$

where A_{1v}: area of one voxel and F: field of view and area of 4 voxels: $4 \times A_{1v}$.

The volume of 4 voxels is found by multiplying the area of 4 voxels with the slice thickness. The field of view has a resolution of 512 pixels x 512 pixels. A single voxel area is equivalent to 1x1 pixel area. The samples produced for CT testing are cylindrical (as shown in Table 2.4). The CT scanning is performed on the three xz-planes (slices) shown in Figure 2.8. Each plane is a layer plane. The scans are performed at three different slices along the parts, with the first layer at 1/4th of the height, second layer at 1/2 of the height, and the last one at 3/4th of the height. On each layer, CT numbers

are read at five different locations, shown in Figure 2.9, and averaged for that slice (layer). The elemental area used to read each CT value is that of 4 voxels (minimum value setting of the machine) as presented in Table 2.6.
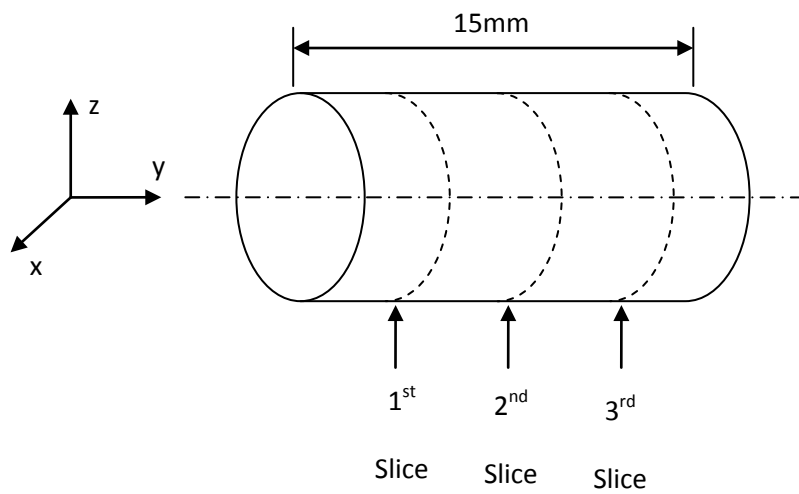
Figure 2.8: Scanned layers during CT imagery
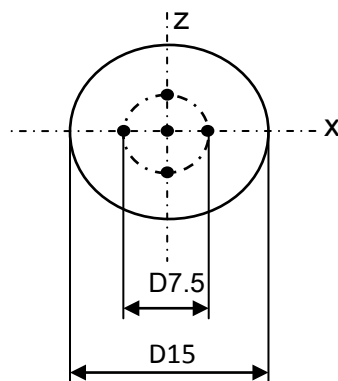
Figure 2.9: Positions of reading CT numbers on a slice (layer) (dimensions are in mm, each scan "point" is 4 voxels big)

The produced CT samples are placed in a casing which has cavities for all samples to be scanned during the same CT session. Figure 2.10 shows a CT image of a slice of the specimens in the casing. The average CT number on a slice (a layer) in a part built at a specific processing setting is calculated by taking the average of the five CT numbers read on the slice, as was mentioned before. The standard deviations are also calculated to assess the uniformity within a layer.   The overall CT number corresponding to a specific part (i.e., a specific production setting) is determined by averaging all CT values read on all layers.
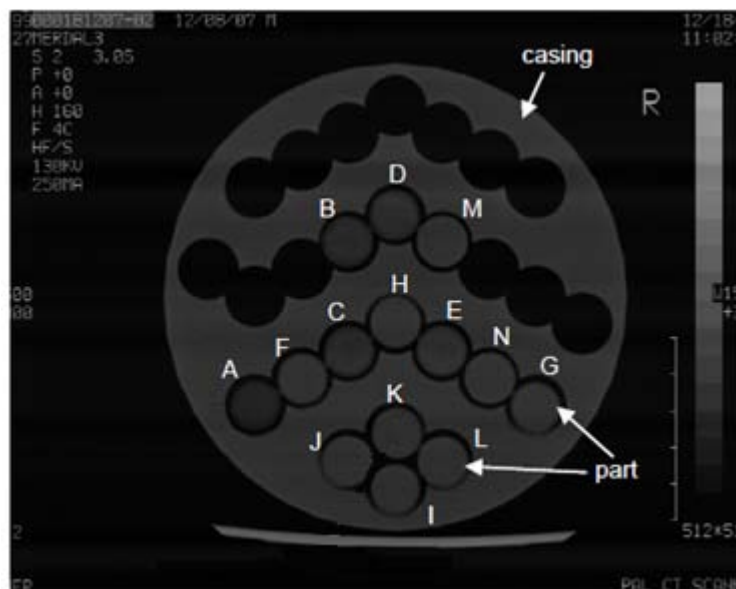
Figure 2.10: CT image of the produced specimens on layer (x-z) plane at 1/4th the specimen height

Figure 2.11 presents the variation of CT number with the laser energy density (process parameter setting, i.e. different porosities) for the porous samples produced. At a given energy density the CT number variation within a layer and from one layer (slice) to the other is very small. Thus, the variations in microstructure from one layer to another are small and uniformly porous structures could indeed be produced by SLS. There is variation in CT number from one energy density (process parameter setting) to the other. This is expected as the CT number is an indicator of density (porosity). By changing the process settings (the energy density), the imparted porosity (and density) are changed.
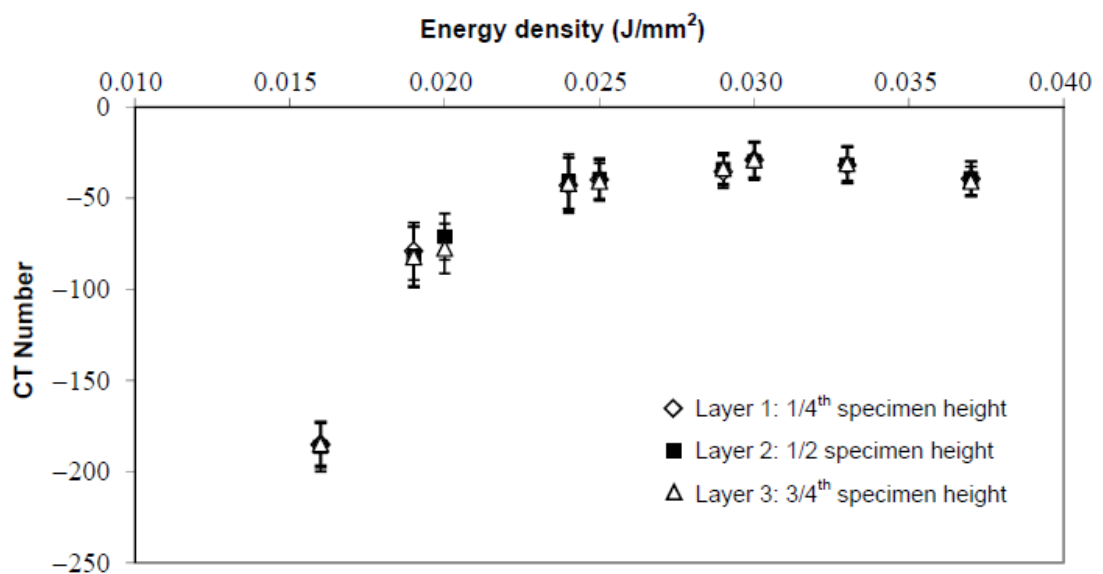
Figure 2.11: Variation of the CT number with Energy Density

2.2.1.5 Visualization of Microstructure through SEM

In order to visualize and analyze qualitatively the microstructure of the porous parts scanning electron microscopy (SEM) is used. The JEOL JSM electron microscope in the Department of Metallurgical and Materials Engineering of METU is used for SEM imaging (Figure 2.12). The sample geometry for SEM test was presented in Table 2.4. With SEM, the as-processed surfaces are to be visualized. Therefore, preparation of the surface is important and this as-processed surface is obtained by fracturing the specimens along a notch at very low temperature for a brittle fracture, so that the fractured surface is undeformed (as-processed).

Figure 2.12: SEM located at Metallurgy Department in METU

The sample preparations before SEM experiment are as follows:

1. Immersing specimens in a liquid Nitrogen bath using tongs and waiting for one to two minutes before taking them out. The Nitrogen bath is a beaker filled with liquid Nitrogen. Liquid Nitrogen (at $-196^{o}C$) can be stored in a steel thermos for long periods of time.

2. Fracturing specimens along the notch immediately after they are taken out of the Nitrogen bath, using a simple 3-point bend configuration.

3. Positioning the fractured specimens with the fracture surface up, by fixing the other end in a box with sticky tape. The surfaces to be visualized are the fracture surfaces. Because the specimens are cooled before fracture, the failure is brittle with little or no deformation, resulting in a planar surface, appropriate for SEM visualization. The surfaces are coated with gold prior to SEM scanning. Figure 2.13 shows the fractured surface and gold-coated surface. For visualization of uniformly porous structures, samples were produced at three different process settings (three different macroscopic porosities); not all settings. These settings correspond to the energy densities 0.016, 0.025, and $0.037 J/mm^2$ in Table 2.3 (settings 1, 5 and 9).
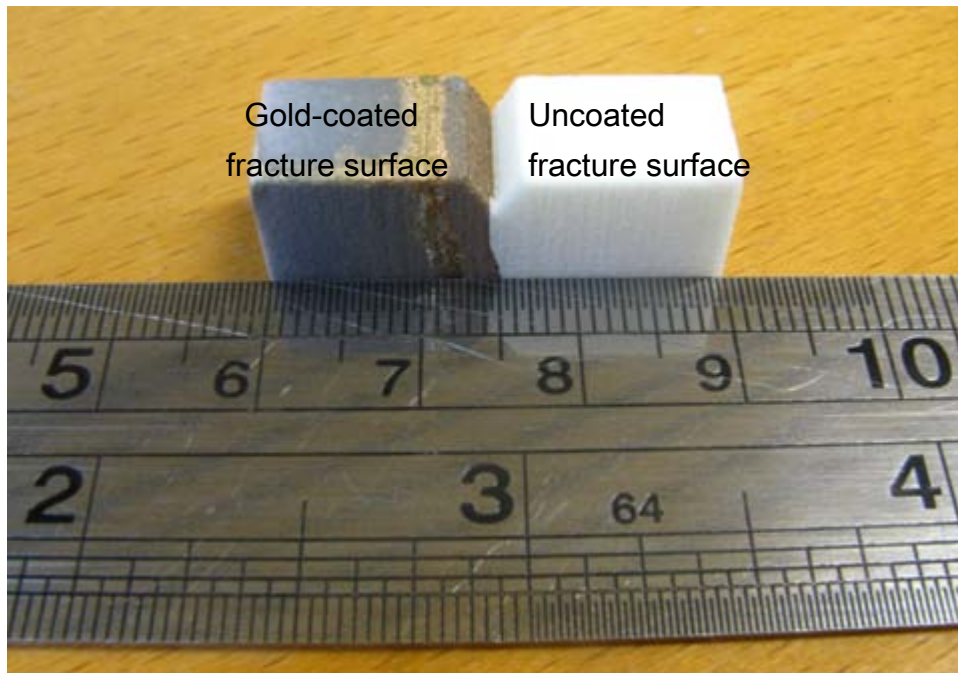
Figure 2.13: Fractured SEM sample showing gold-coated and uncoated surfaces

2. 2.1.6 Pore Size and Size Distribution from Porosimeter Measurements

The information about size of the pores formed, as well as the size distribution of pores in the uniformly porous samples is obtained using mercury porosimetry. Poremaster 60 (Quantachrome) (Figure 2.14) porosimeter at the Central Laboratory in METU is used for this characterization. The operation of mercury porosimeter depends on the physical principle that a non-reactive, non-wetting liquid will not penetrate fine

pores until sufficient pressure is applied to force its entry. The relationship between the applied pressure and the pore diameter is given by the Washburn equation [40]:

$$D = \frac{-4\gamma\cos{(\varphi)}}{p}$$ (2.5)

where p is applied pressure, D is pore diameter, γ is the surface tension of mercury (480 dyne/cm), and φ is the contact angle between mercury and the pore wall (usually 140°). The specimen geometry used in the porosimeter test was shown previously in Table 2.4. These specimens were produced at different process settings of Table 2.3, to compare the changing porous properties due to different production settings. The specimens were infiltrated with mercury by gradually increasing infiltration pressure. The volume of infiltrated mercury is recorded. By comparing pressure and mercury volume, the pore volume of different pore sizes can be determined. The mercury infiltration pressure is raised up to 45 MPa. The polyamide powder supplier reports this value as the material strength for well sintered polyamide parts.

2.3 Mechanical Characterization of the Uniformly Porous Structures

As the porosity changes between samples produced at different settings, the strengths of the samples are expected to change. To relate part porosity to

the structural integrity, the ultimate tensile strength of the sintered parts is measured. Tensile tests are performed in accordance with ASTM D 638-03 standard using a Zwick/Roell Z020 test machine. At each processing setting of Table 2.3, five tensile test specimens of Figure 2.5 are produced to assess repeatability. The testing is carried out by Murat C. Tekin, who has conducted a related study in which mechanical properties of polyamide parts were thoroughly determined [42].

Figure 2.14: Quantachrome Corporation, Poremaster 60 [41]

CHAPTER 3

PRODUCTION AND CHARACTERIZATION OF GRADED POROUS

POLYAMIDE STRUCTURES

A major goal of current research is to investigate the ability of SLS process to produce graded porous structures by varying the porosity. In this chapter, the production of these parts is presented. All produced graded PA structures are characterized physically and mechanically. The characterization results are compared with those of uniformly porous parts in Chapter 5

3.1 Production of Graded Porous Structures

The grades in the mono-material (PA) porous part are formed by changing the porosity from one location to the other within the part. In order to do this, the processing parameters must be varied during the production of a part. In producing uniformly porous structures with different porosities, the three processing parameters, (hatching distance, laser power, and laser scanning speed), were set to different value-combination to induce changing porosity.

In order to impart grades in a single porous part, it was planned to vary the values of the three processing parameters within the part. From uniformly porous part tests (after physical and mechanical characterization) the relation of process energy density (to denote the process setting) to porosity will be known. When energy density is changed (by changing the values of the three parameters), porosity will change (the expected porosity will be known from the results of uniformly porous parts). Therefore, the graded part production is planned by changing energy density (by changing the three parameter values) during production of a single part.

In the SLS system used, the software that plans and controls production does not allow the processing parameters to be changed during the production of a "solid model". A single part produced through SLS is represented by its solid model. Therefore, normally it is not possible to impart varying porosity in a single part by changing process settings. For that purpose, a single part is modeled as comprising of several solid models (as if each model is a different part). The solid models are "stacked" on top of one another. The stacked geometry is the part and each model (stack) is a different "grade". That is, to each solid model in the stack, a different process

setting (a different of combination of the three process parameters-a different

energy density) can be assigned. In this way, the program is "fooled into

believing" that different parts are being produced on top of one another

(Figure 3.1). The only limitation in this methodology is that grades can only

change from layer to layer (cannot be changed on a layer). The geometry of

the graded porous samples that are produced for characterization is tensile

specimens, shown in Figure 2.5.

Part to be Produced   where n: desired number of grades
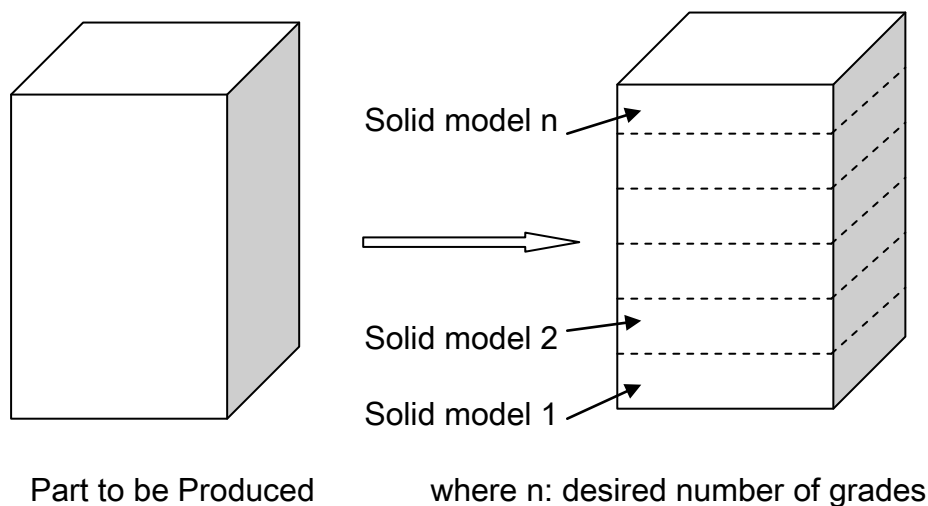
Figure 3.1: Representation of a grades as different solid models

in a graded porous structure

The mechanical properties of graded porous specimens will be compared with those of uniformly porous specimens. The building of the graded porous parts is along the thickness direction. The grades will be along the thickness direction, (z-direction), indicated by Figure 3.2. Depending on the desired number of grades (n grades), n solid models are constructed and stacked along the thickness direction to form n-number of grades. The produced graded porous structures are of two types: 'Type I' and 'Type II'. The difference between these two types is the maximum and minimum energy densities used. In imparting grades in a specimen, the porosity is to be varied from minimum to maximum from one end of the thickness to the other end. The porosity depends on the energy density (ED), thus the grades are designed between minimum and maximum energy value. In Type I specimens, the minimum and maximum energy densities are 0.016 and 0.030 J/mm^2 respectively. Type II has 0.019 and 0.033 J/mm^2 as the minimum and maximum energy density values, respectively.
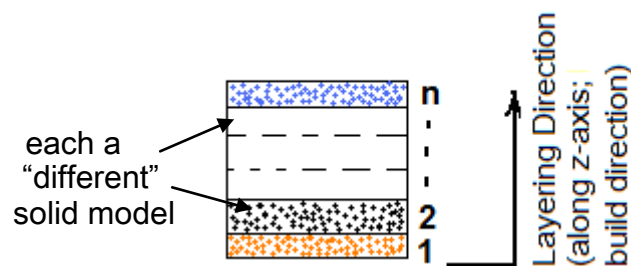
Figure 3.2: Distinct layers throughout the thickness of graded porous specimen

The energy density for each grade as well as the minimum and maximum energy density values are chosen among the process settings that were used to produce uniformly porous specimens (Table 2.3 in Chapter 2). For each type, there are three categories of graded porous structures in which the number of grades differ. There can be three grades, five grades or seven grades. All graded samples have the same geometry and dimensions (dog-bone shape), thus sample thicknesses are the same. Each grade in a sample has the same thickness. Thus, the grades with the smallest thickness are in 7-grade samples and the grades with the largest thickness are in 3-grade samples. The process settings for each grade, for different specimen types and grade categories, as well as design grade thickness are presented in Table 3.1. The process settings, which are represented by energy densities, compared to specific combinations of the three process parameters, also shown in Table 3.1.

Table 3.1: The process settings corresponding to each grade, expressed in terms of energy density (ED)

Energy Density in J/mm^2, used for producing each grade

	3-grades	5-grades	7-grades
Type I	0.016	0.016	0.016
		0.020	0.019
			0.020
	0.024	0.025	0.024
			0.025
		0.029	0.029
	0.030	0.030	0.030
Type II	0.019	0.019	0.019
		0.024	0.020
			0.024
	0.025 ;	0.025	0.025
		0.030	0.029
			0.030
	0.033	0.033	0.033

	Design Grade Thickness*
3-grade	2 mm
5-grade	1.2 mm
7-grade	6/7 mm

*

All specimens dog-bone-shaped with the specimen design thickness = 6mm

Process Setting	Hatching Distance(mm)	Laser Power (%)	Scanning Speed(mm/s)	Energy Density(J/mm^2)
1	0.45	66.3	5000	0.016
2	0.45	66.3	4000	0.019
3	0.45	90.0	5000	0.020
4	0.30	66.3	5000	0.024
5	0.45	90.0	4000	0.025
6	0.30	66.3	4000	0.029
7	0.30	90.0	5000	0.030
8	0.30	90.0	4500	0.033

3.2 Characterization of Graded Porous Structures

For graded porous structures macroscopic properties like the macroscopic

porosity do not mean much as they do in uniformly porous structures. The

property variations within the graded porous structures need to be examined. Two methods are employed to visualize microstructure in order to analyze porosity variation. The non-destructive computed tomography (CT) is used in a similar manner to that outlined in Chapter 2, to detect variations in density through the CT number and relate them to variations in porosity. The produced dog-bone shaped specimens are also mechanically tested to compare strength values with those of uniformly porous samples. The fracture surfaces of the broken samples are studied in scanning electron microscope (SEM) to assess directly the presence of grades. In this section, the characterization methods are explained and the results will be presented in Chapter 5.

3.2.1 CT Imaging of Porous Grades

The grades are to be observed indirectly by reading the CT numbers across the thickness of graded sample, which is also the direction along which the grades change. CT numbers are directly related to density, and hence, the porosity of the grades. For quantifying the apparent density/porosity in a grade, a reference apparent density versus CT number (or porosity versus CT number) scale is constructed using uniformly porous samples (as outlined in Chapter 2, Section 2.2.1.4). Since the grade process settings are chosen

among the process settings used to produce uniformly porous samples, the grades are expected to have densities/porosities corresponding to the particular uniformly porous sample that was produced with the same process setting as the grade. Thus, the reference scale explained above can be used to determine the porosity/density in a grade indirectly. The uniformly porous samples (for the construction of CT-density/porosity reference scale) and graded porous samples are characterized at the same time in the CT machine so that the uniform and the graded porous sample microstructure could be compared visually. For CT imaging of uniformly porous samples, Table 3.2 presents the imaging settings. In Figure 3.3, the CT casing used to hold the eight uniformly porous samples is shown. Specimens are for the eight different process settings for which the grades are produced, i.e. eight different energy densities: 0.016, 0.019, 0.020, 0.024, 0.025, 0.029, 0.030, and 0.033 J/mm^2.

Table 3.2: Parameters used for reading CT numbers on uniformly porous structures

Parameter	Value
Slice thickness(mm)	3.0
Scanning time(s)	3.0
Field of view(cm)	16
Number of voxels used to read CT number	4
Step movement along a graded part	1 pixel (~0.277mm)
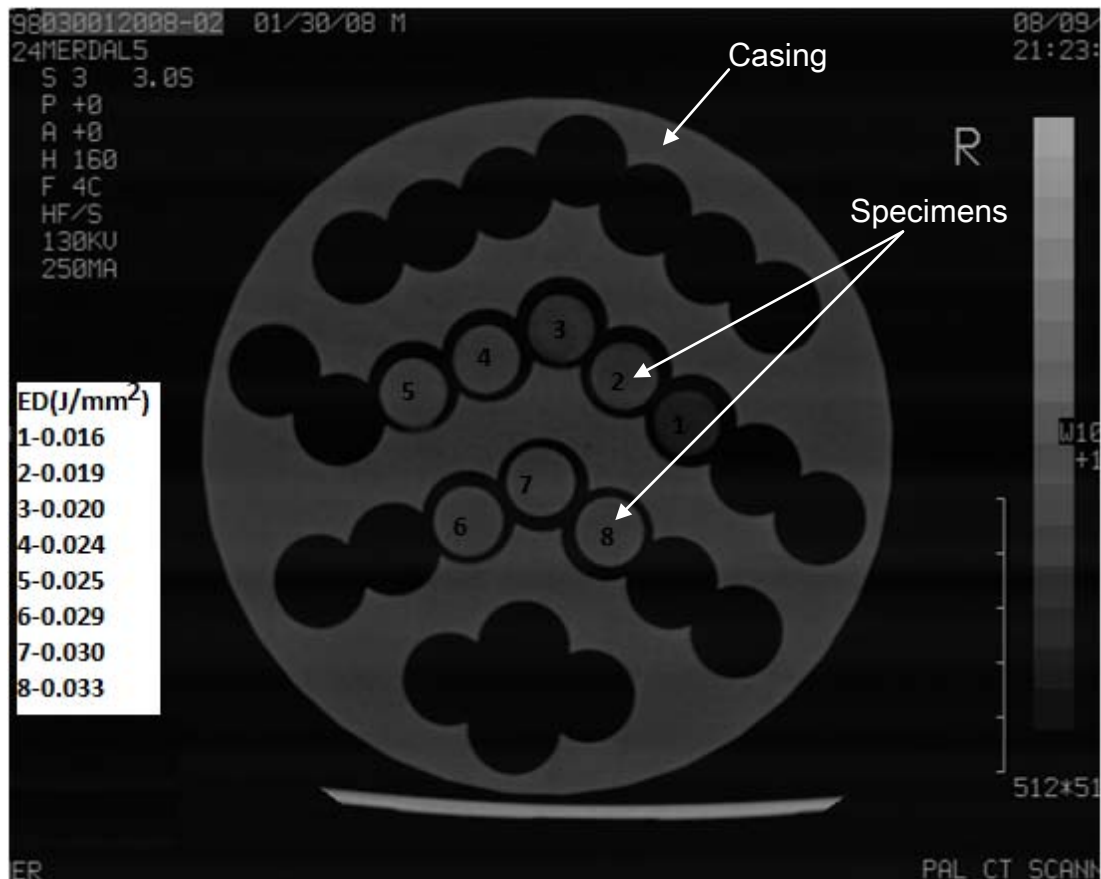
Figure 3.3: Scan image during the computed tomography of uniformly porous samples for obtaining reference CT scale to be used in characterizing graded porous structures

Figure 3.4 shows how CT numbers are read on a graded sample view. The diagram represents a zoomed view on a single specimen among those shown in Figure 3.5. The thickness of each graded porous parts is approximately 6 mm. The grade layers are along the thickness direction (build direction). Scanning along the thickness of each sample yields the microstructure variation due to the grades.

All produced graded porous samples are housed in the casing shown in Figure 3.5. The specimens are stacked as shown. The shown view for the samples is a section within the "test gauge (gauge) length", cut perpendicular to the length of the dog-bone specimens. The grades are along the thickness direction, i.e. the 6 mm side. Graded samples that have the same number of grades (same grade category) are placed on the same column, while those of the same type (Type I or Type II) are on the same row as seen in Figure 3.5. At each type/number of grades (category) setting, three specimens were produced in order to assess repeatability.
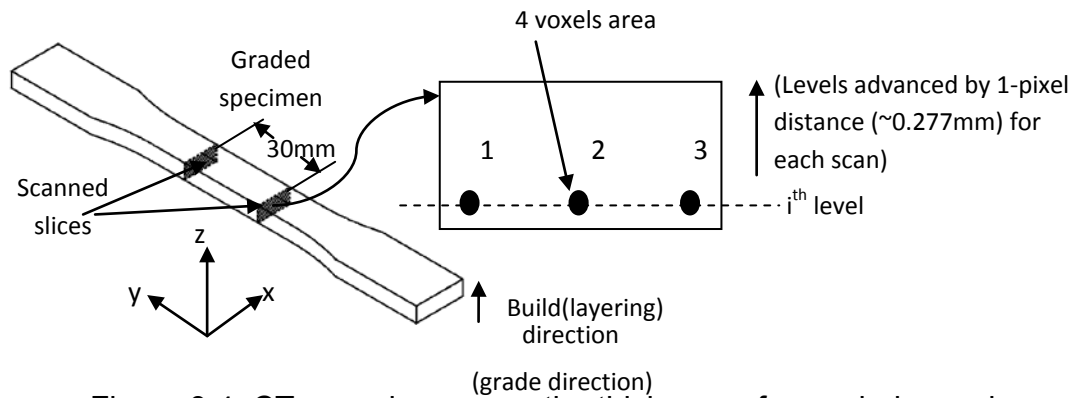
Figure 3.4: CT scanning across the thickness of a graded sample
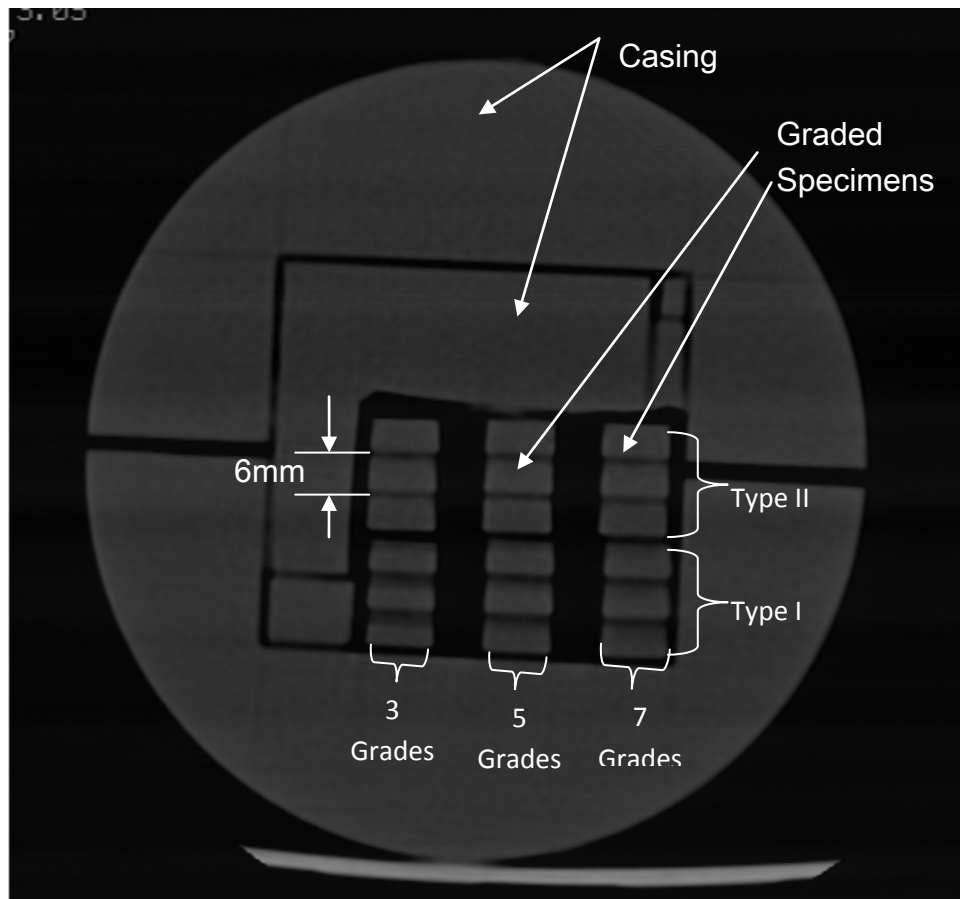
Figure 3.5: Scan image during computed tomography of graded porous
samples

The scanning is performed "level-by-level" at changing z-coordinates, shown in Figure 3.5. At a given level (i^{th} level, in Figure 3.5), CT numbers are read in three different locations (labeled 1, 2, and 3 in Figure 3.5) spread evenly along the constant z-level. CT numbers are from an element area created by 4 voxels of each dot given in Figure 3.5. For the CT machine used (Philips Tomoscan TX 60), 4 voxels is the minimum value for which the corresponding CT number can be read. From the six locations (two slices available, three locations from each slice) shown in Figure 3.5, the average CT number for that level (z coordinate in the part) is computed. The scanning position is then advanced by 1 pixel (step movement along the part) and the readings are repeated.

3.2.2 Mechanical Testing of Graded Porous Structures

The tensile testing of all produced graded porous specimens was conducted to assess their macroscopic mechanical strength and the compare with uniformly porous part strengths. The overall strength of the graded sample is expected to be different from that of the individual grade which is made from a specific process parameter setting (the energy density). The procedures used in section 2.3.2 are utilized in this section using the same machine and testing standard (ASTM D 638-03 standard, Zwick/Roell Z020 test machine).

The mechanical test results of all graded porous samples are presented in Chapter 5.

3.2.3 SEM Imaging of Graded Porous Structures

The SEM imagery was conducted for the fracture surface resulting from tensile testing (Figure 3.6). The SEM samples were cut off a small specimen below the fractured surface using a saw (Figure 3.6). The fracture surfaces were scanned in SEM. The rest of the SEM test procedures used to visualize the microstructure successfully are similar to that explained in section 2.2.1.5. The SEM images are presented in Chapter 5.
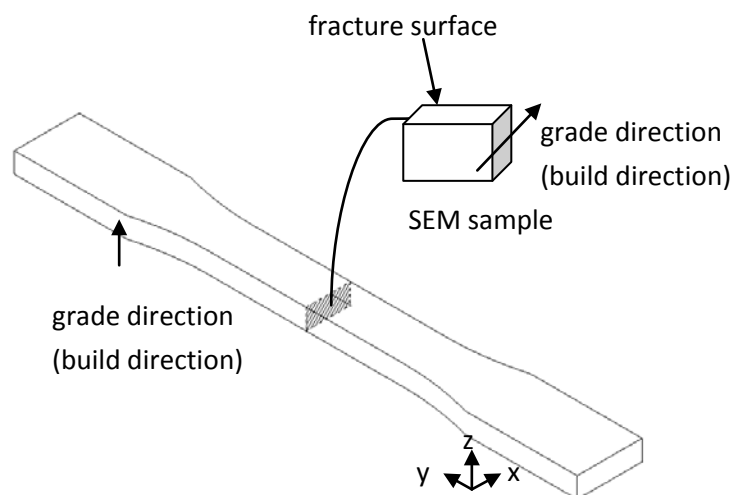
Figure 3.6: Fracture surface for SEM from tensile test fracture surface

CHAPTER 4

PRODUCTION AND CHARACTERIZATION OF EPOXY-POLYAMIDE

COMPOSITES AND GRADED MATERIALS

As a natural extension of the current research, it was further inquired whether solid composite materials could be produced using SLS. In this context, the produced porous parts were considered as "preform" that could be infiltrated with a liquid resin. The liquid resin must have a low viscosity in order to infiltrate a structure, which is likely to have very small pores. Furthermore, the resin must be a thermosetting resin, so that it cures "hardens" after infiltration. The curing stage must be performed at a temperature that will not be too high so as to deform/degrade the polyamide preform. A survey of available resins was conducted and a two-part epoxy resin (epoxy: Araldite® LY 564, hardener: XB 3486) was chosen as infiltrating resin mainly due to its low viscosity. The processing characteristics and the material properties are given in Appendix F.

4.1 Infiltration of Uniformly Porous Structures with Liquid Resin

The composites were produced from porous PA samples manufactured in the shape of a dog-bone for mechanical testing. The production is outlined as follows: An identical set of porous samples for mechanical testing of Figure 2.5 is produced with the production settings of Table 2.3. For repeatability assessment, three samples are produced at each process setting. The porous samples are placed in a container, which is an open rectangular specimen-holder, shown in Figure 4.1. It has two chambers: one chamber has the capacity of accommodating three specimens and the other one accommodates up to six samples. The dimensions of the smaller chamber are 5x7x22cm and that of the larger one are 5x11x22cm. The specimen holder is placed in a vacuum dessicator, which is used for the resin infiltration process.
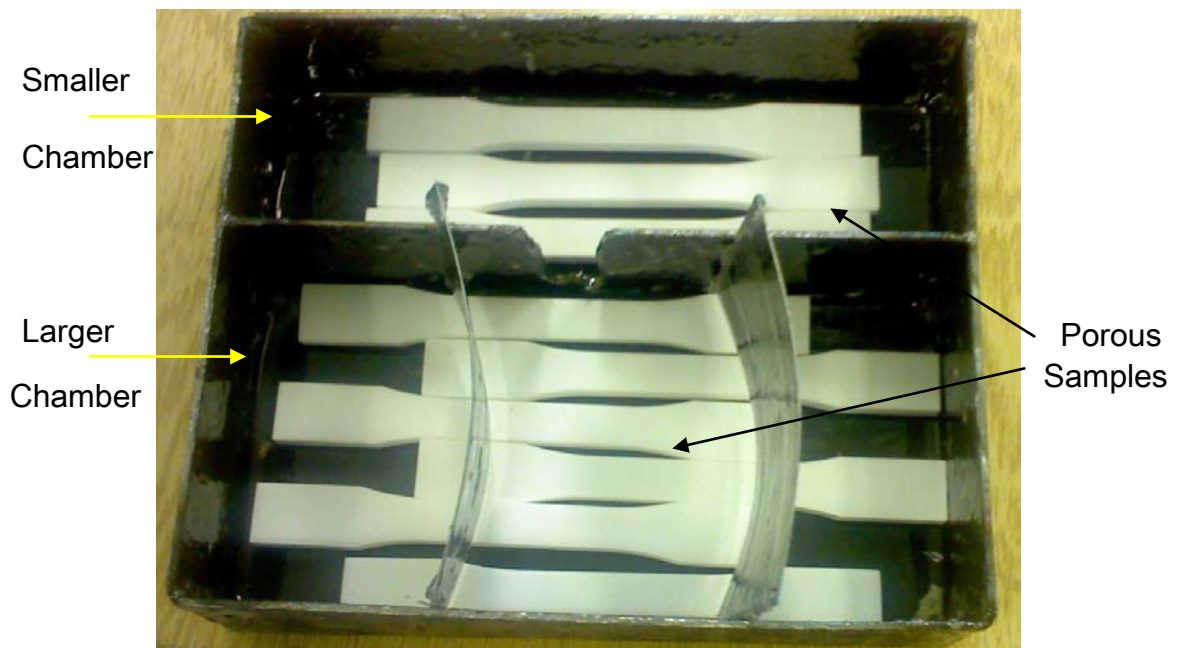
Figure 4.1: Specimen-holder during infiltration

Figure 4.2 shows the dessicator system. Dessicator is a transparent glass container with a lid. A resin line and vacuum line are connected to the top of the dessicator lid, each with a valve. The vacuum line is plastic tubing that connects to a vacuum pump. The resin line is a plastic tube whose other end is immersed in an open resin reservoir in which is epoxy resin that has been catalyzed with the hardener. At first, the resin line valve is closed. The vacuum line valve is opened and the vacuum pump is started. Air is evacuated from the desiccator using the vacuum pump until the vacuum gauge indicates at least 600 mmHg of vacuum pressure. The valve of the resin is then opened to allow the flow of resin from the resin reservoir to the

specimens-holder. The resin is allowed to fill until all parts are soaked under the resin (takes about 10 to 15 minutes). The resin flows due to the pressure difference between desiccator inside and outside. Afterwards, the resin line valve is closed. The pump continues to pump at an on-off interval of 15 minutes for a total of four hours so that vacuum state is maintained throughout this time. The desiccator can be shaken very gently from time to time to help capillary infiltration and to release air bubbles. Resin impregnation into porous sample is by capillary action. After four hours, the vacuum line valve is closed and the pump is stopped.
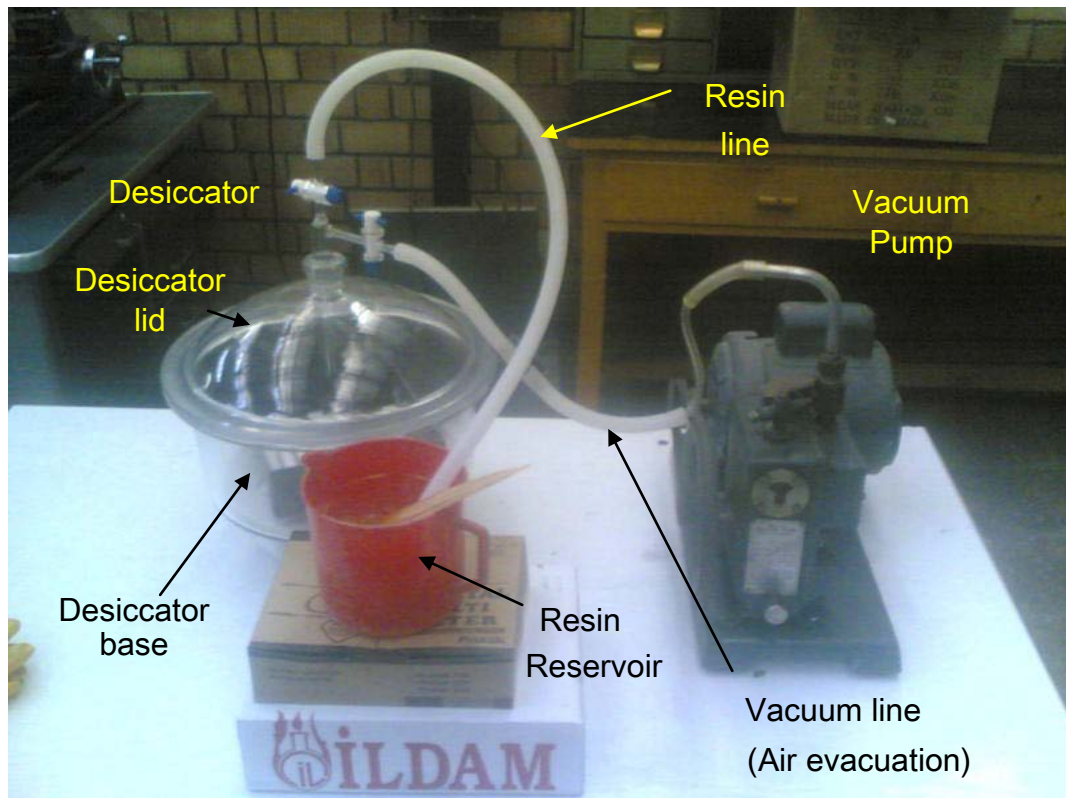
Note: when dessicator is in vacuum state, the lid presses onto the base (seals) due to outside atmospheric pressure

Figure 4.2: Vacuum and resin line

The resin valve is opened to allow air from the resin line whose end is no longer immersed in resin, but exposed to atmosphere. As the pressure in dessicator rises, resin in the specimens-holder further pushes into the porous structures. After infiltration is complete, the samples must be placed in an oven to cure the epoxy resin so that it hardens, completing the production of composites. The desiccator lid is removed and the parts are taken out. Since

the resin is still in liquid form (has not hardened), the outside surfaces are wiped with a clean cloth and the samples, placed on a metal plate, are put immediately in a pre-heated oven. In order to prevent sticking of the samples to the plate during resin curing, the plate is coated earlier with a mold-release agent (Renlease® QZ 5111). The coating is applied twice with an interval of at least 15 minutes (for drying). The plate must be completely dry before samples are placed on it. Based on the available cure cycles for the resin the cure temperature is chosen to be 50°C (Appendix F). This temperature is low enough for the thermoplastic polyamide portion to retain its solid form. The samples are cured at this temperature for 15 hours in the oven (Lab-Line Instruments, 1071) (Figure 4.3). To avoid distortion/curling of the cured parts, a plate (coated with mold-release agent, Renlease® QZ 5111) is placed on top of the specimens. But, the plate does not touch specimens (small clearance is left between specimens and this plate by using steel bars (Figure 4.3)).
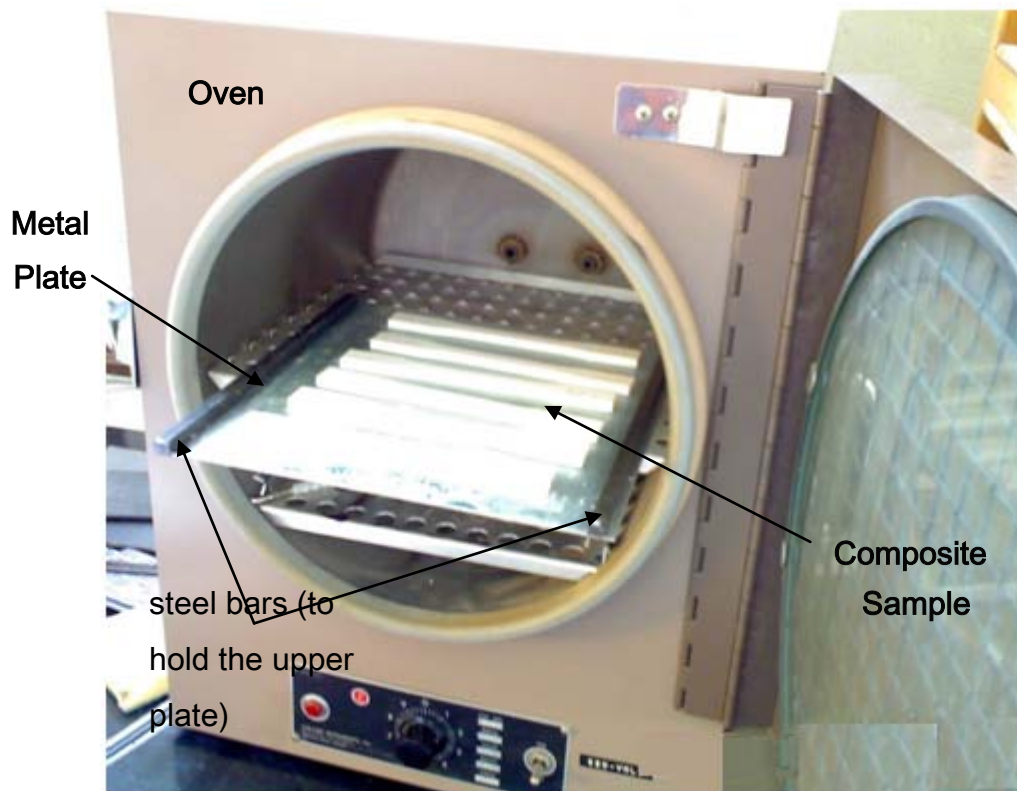
Figure 4.3: Oven for curing infiltrated parts

4.2 Characterization of Epoxy-Polyamide Uniform Porous Structures

The uniformly porous parts after epoxy infiltration were characterized mechanically and physically. Tensile testing for the epoxy-polyamide structures were carried out with ASTM D 638-03 standard using a Zwick/Roell Z020 test machine. At each processing setting of Table 2.3, three epoxy infiltrated tensile test specimens of Figure 2.5 were produced to assess repeatability. The testing is carried out by Murat C. Tekin, who has conducted a related study in which mechanical properties of polyamide parts

were thoroughly determined [42]. The results are presented in Chapter 5. The SEM samples were extracted from the tensile test fracture surface in the same way as that for graded porous specimens explained in section 2.2.1.5. Samples from the process energy density 0.016, 0.025, and 0.037 J/mm^2 were extracted for visualization. The SEM procedure for these parts is exactly the same as that explained in section 3.2.3. The results are presented in Chapter 5.

4.3 Epoxy- Polyamide Graded Porous Structures

The Type I graded structures produced through SLS and infiltrated with epoxy resin using the procedure outlined in Section 4.1. These parts are in the shape of the dog-bone of Figure 2.5 since they will be tested mechanically. All three types of Type I: Type I-3 grades, Type I-5 grades, and Type I-7 grades were infiltrated with epoxy. Three samples were produced from each graded category for repeatability. The epoxy-polyamide graded porous structures were tested mechanically and physically (visualizing microstructure). The mechanical test procedure explained in section 4.2 is applied to these parts. For the SEM images, the fracture surfaces from the tensile testing are utilized in the same manner as that explained in section 4.2. The microstructure and mechanical properties are compared with those

of graded PA porous polyamide structures. The results are presented in

Chapter 5.

CHAPTER 5

RESULTS AND DISCUSSION

In this study uniformly porous parts and graded porous parts were built using selective laser sintering process from polyamide powder (PA 2200 of type nylon 12). The selective laser sintering machine used was EOSINT P 380, available in the Biltir Center at the Department of Mechanical Engineering at the Middle East Technical University. In building the polymeric structures, three machine processing parameters were varied to attain distinct microstructures (porosities) and mechanical properties. These parameters were the hatching distance, the laser power, and the laser scanning speed. All sintered parts were characterized physically and mechanically through various techniques. In this Chapter, the results of the physical and mechanical tests are presented and analyzed, and the obtained properties are discussed.

5.1 Uniformly Porous Part Properties

The properties of the uniformly porous structures produced at different process settings (Table 2.3) are presented in this section. The methods used to obtain properties of the uniformly porous parts have been explained in Chapter 2. In this section the apparent density, the macroscopic porosity, microstructures, and the mechanical strengths are presented

5.1.1 Apparent Density

At the process settings of Table 2.3, uniformly porous samples for apparent density measurements were produced. Four samples were produced at each setting for repeatability. The results are presented at Figure 5.1. In this figure, the variation of the apparent density of samples with process setting (energy density) is presented. As seen, the value of the apparent density increases with an increase in the amount of energy density. This is expected, since higher energy process setting means better particle fusion and higher apparent density. The apparent density of the sintered parts ranges between 0.7100 and 0.9505 g/cc, depending on the processing parameters used during production. The density increase slows down and remains about the same after an energy density of about 0.029 J/mm^2.
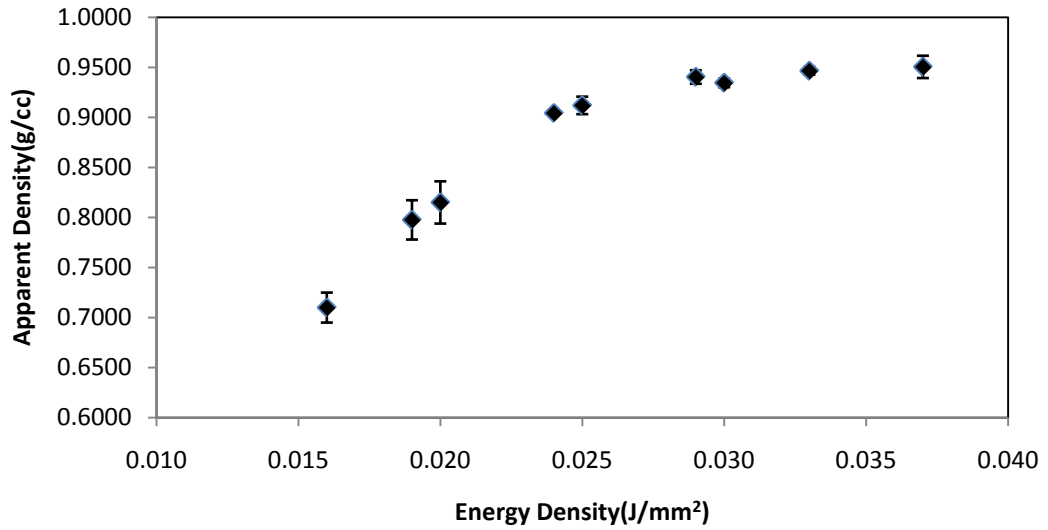
Figure 5.1: Variation of apparent density of the sintered parts with energy density

The apparent density of the parts produced at a certain energy density process setting exhibit deviation from the mean. This might be contributed by producing them at different location on the SLS platform (uneven temperature distribution on the platform). In this research, the location of the parts on the platform is not taken into consideration during production.

5.1.2 Porosity

The macroscopic porosity of the uniformly porous samples is calculated from equation 2.3 using the true density values obtained from pcynometer measurements in Table 2.6. Figure 5.2 presents the porosity variation as process setting (energy density) is changed. The porosity decreases with an increase in the energy density.
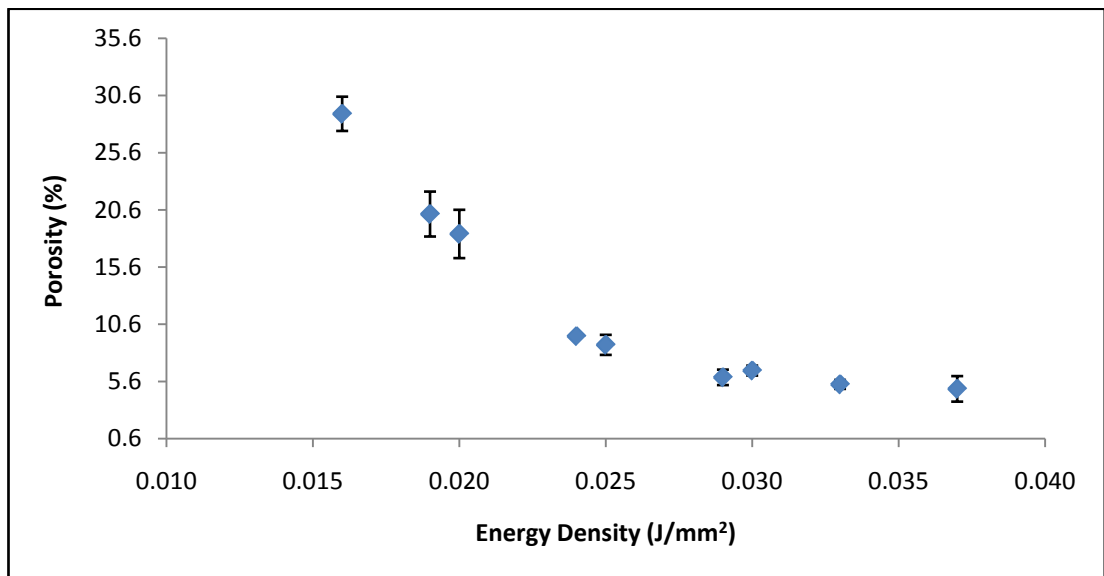
Figure 5.2: Porosity variation with energy density

Like the apparent density the porosity reaches an asymptotic value beyond energy density of approximately 0.029 J/mm². Further increase in energy density may lead to thermal degradation of polyamide. While apparent density increases with energy density, porosity decreases with an increase in energy density. To have highly porous parts, process settings should be chosen to yield low energy densities. The limitation in achieving higher porosities is the poor bonding of powder particles and inter-layers when very low energy densities are used. For the process settings used in the production, the achieved porosity is between 4.9 % and 29 %. At a given energy density process setting of Figure 5.2, the macroscopic porosity deviation is observed. Like the apparent density, the repeat parts had been produced at different locations on the platform (uneven distribution of temperature) which might affect the physical properties.

5.1.3. Uniformity of Porosity within the Parts

Possible variations in the microstructure of each specimen were indirectly observed through computed tomography (CT) and quantified by the CT number (explained in Chapter 2). The aim was to assess the accuracy of using a single "macroscopic porosity" to express the porosity of a specimen. The results shown in Chapter 2 (Figure 2.11) indicated that the porosity

within the parts was indeed uniform and a macroscopic porosity value could be used to describe the porous structure.

5.1.4 Microstructure

The microstructure of the uniformly porous specimens was examined qualitatively using SEM imagery (JEOL JSM electron microscope). The detail of the methodology is explained in section 2.2.1.5. Samples with energy density (ED) values of 0.016 J/mm^2 (high porosity), 0.025 J/mm^2 (medium porosity) and 0.037 J/mm^2 (low porosity) were produced as specified in Table 2.4 and the fracture surfaces were scanned. Figures 5.3 and 5.4 show the SEM images of these samples. The microstructure of the low porosity sample (produced at an energy density of 0.037 J/mm^2) is drastically different from the medium and high porosity samples. The particles are well fused forming an even layer with pores placed sparsely (Figure 5.3). The individual PA powder particles are indistinguishable.
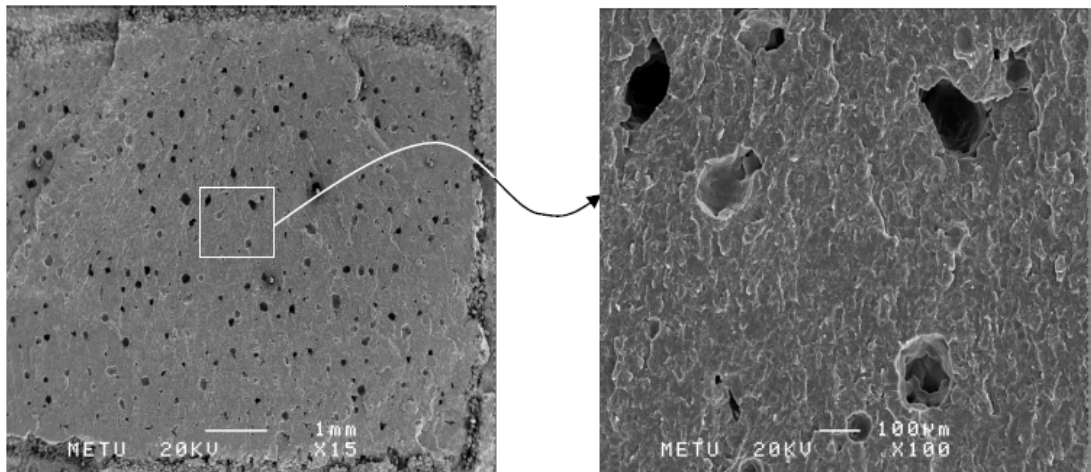
Figure 5.3 Microstructure of a low porosity sample (ED = 0.037J/mm^2)
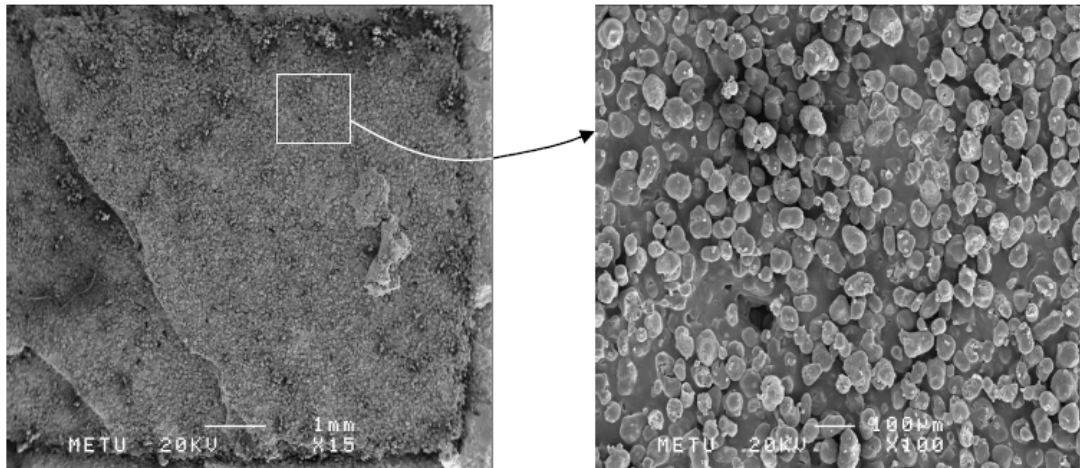
Figure 5.4 (a) Microstructure of medium porosity (ED = 0.025J/mm^2)
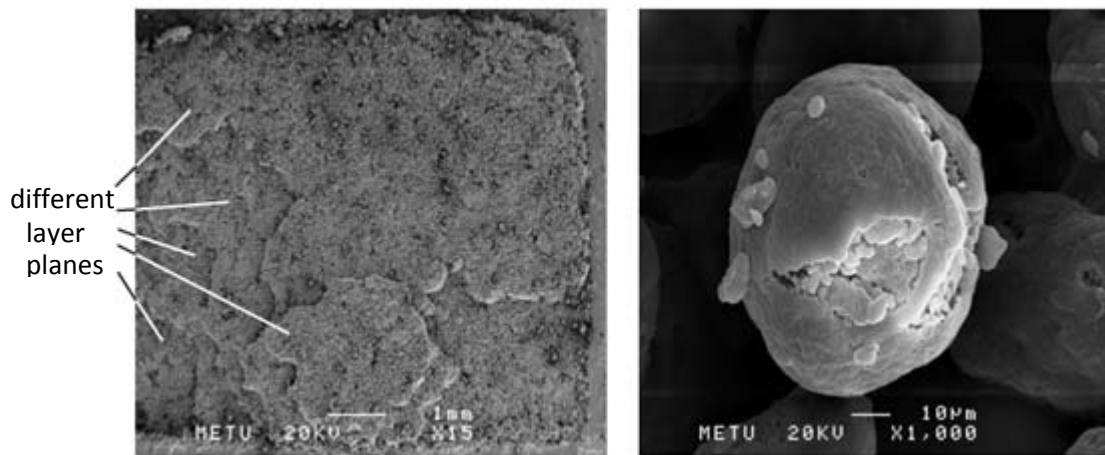
Figure 5.4 (b) Microstructure of high porosity (ED = 0.016J/mm^2)

On the medium and the low porosity sample layer surfaces, particles are clearly distinguishable with the pores formed in between them (Figure 5.4). The powder particle size as reported by the manufacturer is, on the average, 60 μm. The images confirm this however, there are also smaller particles present and the individual powder particles also have some pores in them (Figure 5.4.b). The fracture surface for the low porosity sample is a single layer, whereas for the medium and low porosity samples, the fracture surface consists of several layers. As the process energy density gets smaller, the fusion between the layers gets weaker, the specimen fracturing along multiple numbers of layers.

5.1.5 Pore Size and Size Distribution

The pore size distributions in uniformly porous samples were determined using mercury porosimetry (Quantachrome Corporation, Poremaster 60). The details of the methodology are explained in section 2.2.1.6. The samples shown in Table 2.4, were impregnated with mercury at progressively increasing pressure. The pore size through which mercury can infiltrate at a given pressure is known (equation 2.5). Tracking the amount of mercury infiltrated at each pressure and using the pressure-pore size correlation, the pore size distributions were obtained. For the three production settings

(energy density, ED = 0.016 J/mm^2 (high porosity), 0.025 J/mm^2 (medium porosity), and 0.037 J/mm^2 (low porosity)), the results are presented in Figure 5.5 and the results from the rest of the process settings are in Appendix E. As expected, the largest volume of pores is in the high porosity part (lowest ED), with the overall pore volume decreasing as the energy density, ED, increases and the porosity decreases. The size distribution in all cases is in the shape of a bell curve, with the majority of the pores in the size range of 5-100 μm. According to the International Union of Pure and Applied Chemistry (IUPAC) standards, pores with size greater than 50 nm are classified as macropores [44].Thus, the formed pores are macropores. The largest volume of pores occurs at the pore size of around 20 μm in all process settings. It could be argued that different production settings which yield significantly different microstructures observed in Figure 5.3 and 5.4 would yield the largest concentration of pore volume at different pore sizes. However, Figure 5.5 clearly shows this is not the case, implying that the powder particle size, which is the fixed effective parameter in all settings, is the major influence on the size of the largest volume of pores, regardless of the process setting.
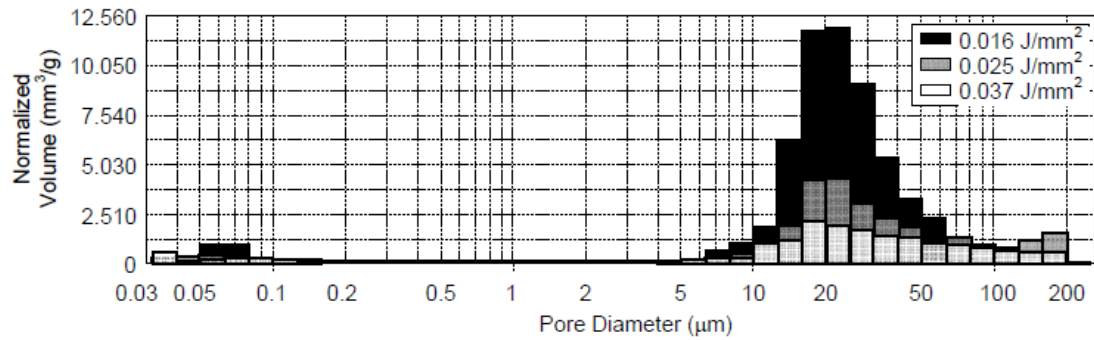
Figure 5.5: Pore size distribution in uniformly porous specimens produced at ED = 0.016 J/mm^2 (high porosity), 0.025 J/mm^2 (medium porosity) and 0.037 J/mm^2 (low porosity)

5.1.6 Mechanical Properties

The ultimate tensile and rupture strengths of the specimens produced using the energy density (process parameter settings) of Table 2.3 are determined by conducting tensile tests as described in section 2.3. To assess repeatability five samples were produced from each process setting of Table 2.3. Figure 5.6 shows the graph of ultimate tensile strength (UTS) and the rupture strength versus the energy density (process parameter settings). It is seen that the energy density (process settings) level used during selective laser sintering significantly influences the ultimate tensile strength and the rupture strength of the specimen.
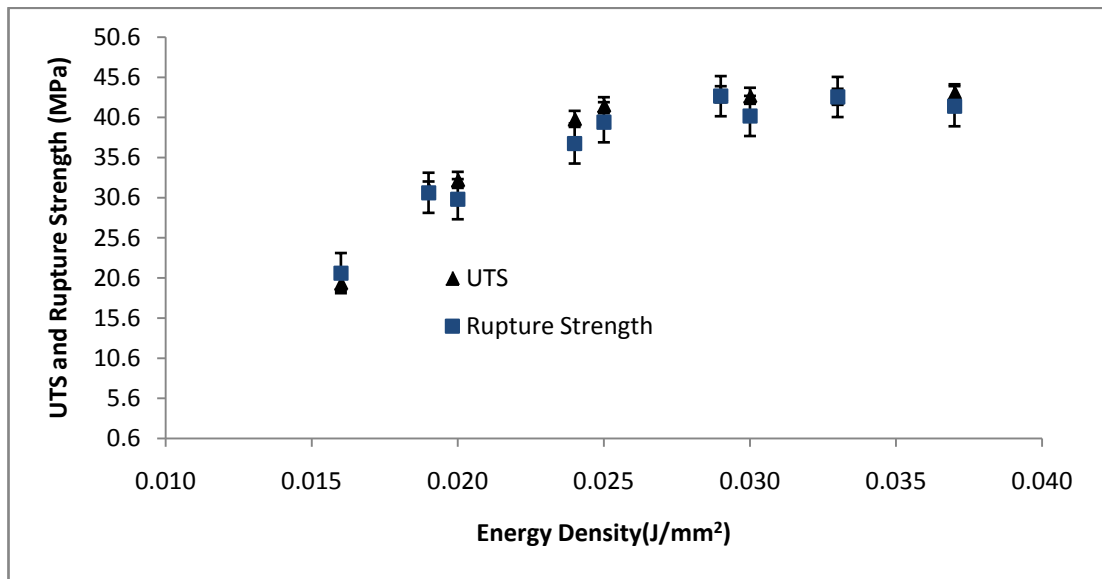
Figure 5.6: UTS and rupture strength of the uniformly porous parts

The initial value of the ultimate tensile strength is about 20 MPa whereas the maximum value is close to 45 MPa. This indicates a 125% increase in the ultimate tensile strength with the corresponding increase in the energy density level. The increase in the ultimate tensile strength is expected due to superior particle fusion and reduced porosity with increased energy density. The trends observed in Figure 9 are parallel to those demonstrated in Figures 5.1 and 5.2. The mean rupture strength has a trend similar to the trend observed for the ultimate tensile strength. The mean rupture strengths are found to be close to the mean ultimate tensile strengths. This implies that

parts fracture soon after reaching their maximum strength, before undergoing necking.

5.2 Factorial Design Analysis for the Uniformly Polyamide Porous Structures

In planning production in order to impart a range of porosities, three processing parameters were used, each at two levels. Their combined effect was characterized by the energy density (ED), which also denoted the particular processing setting. The parameter settings directly influence the resulting part properties. In this section, the methodology for determining the effect of each of the three processing parameters on porous part properties as well as the interaction of the parameters is presented. This is based on the results of the 2^3 factorial design based on which the production was planned. The details of 2^3 factorial design can be found in [45]. In this study, the analysis is carried out using the MINITAB statistical software.

5.2.1 Main Effects

Main effects refer to the effects contributed by the design factors to the response value, due to the change in level of those factors [45]. To explain how main effects are calculated, the following example is presented: It is supposed that there are two design factors (parameters) that affect the response of a system. In designing the experiment (or testing the system),

each factor takes a low and a high value. The low and high values of the two

factors can be denoted as A⁻, A⁺ (for factor "A"), and B⁺, B⁻ (for factor "B"),

respectively. The change in the response of the system or process due to the

change in the level of factor A when factor B is at lower level is given by A_{B^-}

as

$$A_{B^-} = A^+B^- - A^-B^-$$
(5.1)

and the change in response of the system or process due to the change in

the level of factor A when factor B is at higher level is given as

$$A_{B^+} = A^+B^+ - A^-B^+$$
(5.2)

In equations 5.1 and 5.2, A⁺B⁻, A⁻B⁻, A⁺B⁺ and A⁻B⁺ denote the response

values corresponding to the specific high/low level combination of the two

factors.

The average effect of factor A on the system or process is

$$A = \frac{A^+B^+ + A^+B^-}{2} - \frac{A^-B^+ + A^-B^-}{2}$$
(5.3)

and the average effect of factor B on the system or process is

$$B = \frac{B^+A^+ + B^+A^-}{2} - \frac{B^-A^+ + B^-A^-}{2}$$
(5.4)

In the above equations, A is the value of the change in response when the

factor "A" changes from low to high level. The sign and magnitude of A

denote whether the response increases or decreases, and by how much,

respectively. Similarly, B is the value of the change in response when the factor "B" changes from low to high level. In Appendix G, how main effects are computed in this study has been shown.

5.2.1.1 The Effect of Individual Process Parameters on Apparent Density

In Figure 5.7, the main effects of each processing parameter (design factors) on the apparent density (the response) are given. In each graph in Figure 5.7, the vertical axis is the apparent density scale and the horizontal axis is the parameter (design factor) scale.   The average densities in Figure 5.7 are obtained by considering the average apparent density of the sintered parts when a parameter is at its low level or when it is at its high level (Table 5.1). For example, at the low level of hatching distance (HD=0.30mm) there are four process setting configuration, disregarding the default in Table 2.3. The apparent density values at these four settings presented in Table 5.1, which are 0.9044, 0.9404, 0.9345, and 0.9505 g/cc and their mean is 0.9325 g/cc presented at the last row in Table 5.1. The mean values at the low and high hatching distance levels are plotted in Figure 5.7. The slope in the graph of Figure 5.7 presents the effect of a factor while other factors are kept constant.

The apparent density of the sintered parts decreases as the hatching distance increases. When the level of the laser power is increased from lower to higher level the apparent density also increases. In case of the laser scanning speed, its effect to the density of the sintered parts is similar to that of hatching distance; as speed increases from low to high level, apparent density decreases. The energy density increases when laser power increases and this in turn, increases the apparent density of the produced samples. When either laser scanning speed or hatching distance is decreased the energy density increases and this in turn increases the apparent density.
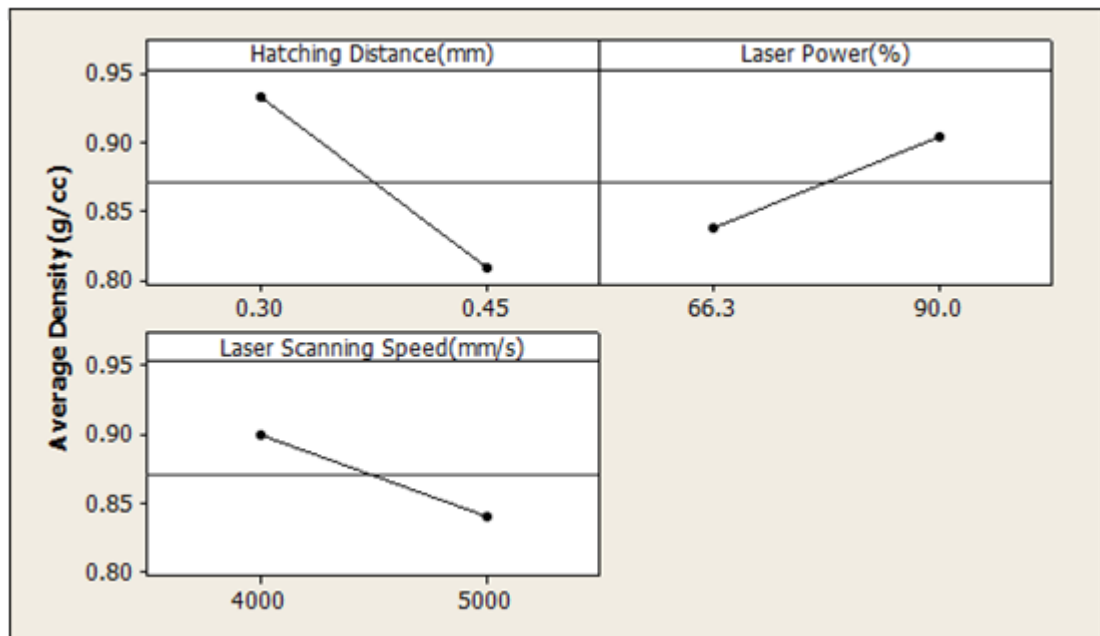
Figure 5.7: Main effects plots for apparent density

Table 5.1: Main effects (in g/cc) of the three parameters on apparent density when the parameters are at their respective levels

HD (mm)		LS (mm/s)		LP (%)	
0.30(low)	0.45(high)	4000(low)	5000(high)	66.3(low)	90(high)
0.9044	0.7100	0.7976	0.7100	0.7100	0.8151
0.9404	0.7976	0.9120	0.8151	0.7976	0.9120
0.9345	0.8151	0.9404	0.9044	0.9044	0.9345
0.9505	0.9120	0.9505	0.9345	0.9404	0.9505
M= 0.9325	M=0.8087	M=0.9002	M=0.8410	M=0.8381	M=0.9030

HD: hatching distance, LS: laser scanning speed, LP: laser power

M: mean of four apparent density values above it at a given level of parameter

5.2.1.2 The Effect of Individual Process Parameters on Ultimate Tensile Strength

In Figure 5.8 the main effect of each processing parameter (design factors) on the ultimate tensile strength (UTS - the response) are given. In each graph in Figure 5.9, the vertical axis is the UTS scale and the horizontal axis is the parameter (design factor) scale. The average UTS in Figure 5.8 are obtained by considering the UTS of the sintered parts when a parameter is at its low level or when it is at its high level (Table 5.2). For example, at the low level of hatching distance (HD=0.30mm) there are four processing setting configurations, disregarding the default, in Table 2.3. The UTS values at these four settings are presented in Table 5.2, which are 40.422, 43.494, 43.302, and 43.736 MPa and their mean is 42.739 MPa presented at the last

row in Table 5.2. The mean values at the low and high hatching distance levels are plotted in Figure 5.8. The slope in the graph of Figure 5.8 presents the effect of a factor while other factors are kept constant. The UTS of the sintered parts decreases as the hatching distance increases. When the level of the laser power is increased from lower to higher level, UTS also increases. In case of the laser scanning speed, its effect to the UTS of the sintered parts is similar to that of hatching distance. When speed from low to high, apparent density decreases.

Table 5.2: Main effects of the three parameters on apparent density when the parameters are at their respective levels

HD (mm)		LS (mm/s)		LP (%)	
0.30(low)	0.45(high)	4000(low)	5000(high)	66.3(low)	90(high)
40.422	19.980	31.620	19.980	19.980	32.822
43.494	31.620	42.126	32.822	31.620	42.126
43.302	32.822	43.494	40.422	40.422	43.302
43.736	42.126	43.736	43.302	43.494	43.736
M=42.7385	**=31.6370**	**=40.2440**	**=34.1315**	**=33.8790**	**=40.4965**

HD: hatching distance, LS: laser scanning speed, LP: laser power

M: mean of four apparent density values above it at a given level of parameter
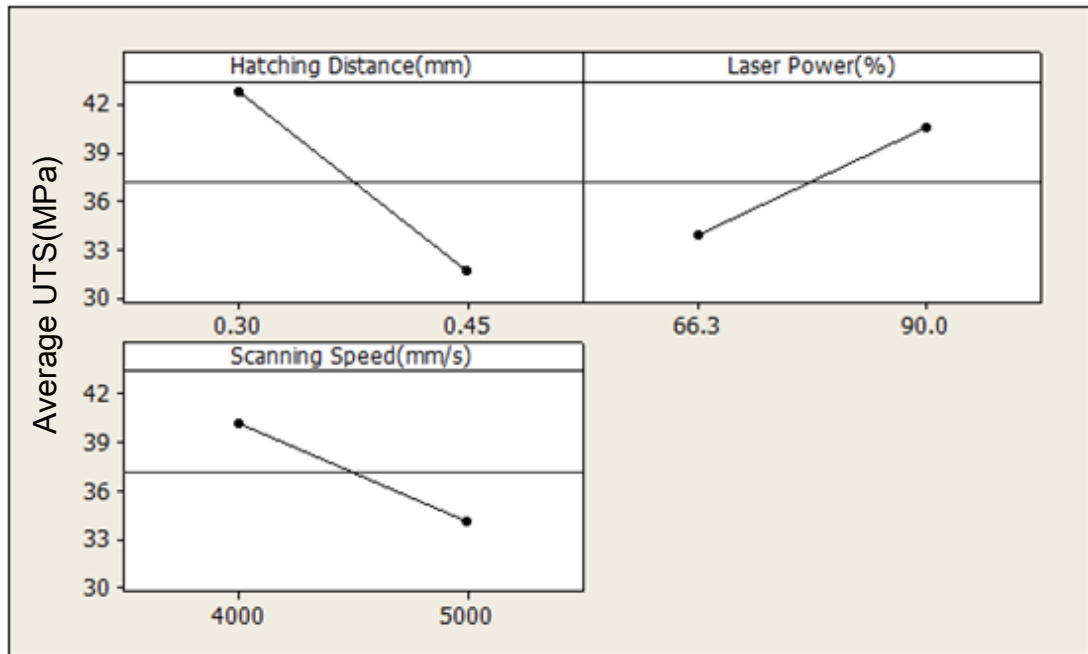
Figure 5.8: Main Effects Plots for UTS

5.2.2 Interaction Effects

In the previous section, the determination of the effect and individual factor (i.e. the process parameters) on the system response (porous part properties) was shown; they are the main effects. In practice, the way a single factor influences the response of a system, may depend on the level (value) of the other factors [45]. Referring to the two-factor scenario of section 5.2, increasing the value of factor "A" may increase the response value. If the amount of increase in the response for the same change in

factor "A" varies at different levels of factor "B", then, factors "A" and "B" are interacting. This interaction effect may be significant and must be known, to understand how the factors and their combinations at different levels influence the response. The AB interaction is defined as the average difference of A_{B-} and A_{B+}. A_{B-} is the change in the response of the system or process due to the change in the level of factor A when factor B is at lower level and A_{B+} is the change in the response of the system or process due to the change in the level of factor A when factor B is at higher level. The AB interaction is:

$$AB = \frac{A_{B+} - A_{B-}}{2} \tag{5.5}$$

From equations 5.1 and 5.2,

$$AB = \frac{A^+B^+ - A^-B^+}{2} - \frac{A^+B^- - A^-B^-}{2} \tag{5.6}$$

In Figure 5.9 the two-parameter interaction plots for the apparent density are shown. Minitab statistical software was used to draw those graphs [45]. The graph number 1 represents hatching distance and laser power interaction effect, graph number 2 represents the interaction between hatching distance and laser scanning speed, and graph number 3 represents the interaction effects between laser power and laser scanning speed. In each graph, the apparent density (vertical axis) is plotted against one of the parameters (the horizontal axis) at the low and high levels of the second parameter, while the

third parameter is kept constant. For instance, the two lines in graph 2 denote how the apparent density varies with laser scanning speed at the high (red dashed line) and the low (black solid line) levels of the hatching distance. In each graph, if the lines are parallel, it means the parameters are not interacting. The response of the apparent density to changing laser power at low and high levels of hatching distance are not the same (Graph 1) and the lines are not parallel to each other. This indicates that the hatching distance and the laser power interact and for each one, its effect on apparent density would depend on the level of the other. In graph number 2, at low and high level of hatching distance the apparent density responses are not the same when the laser scanning speed is varied, and the lines are also not parallel to each other. This also implies that there is an interaction effect between hatching distance and laser scanning speed. On the other hand, when laser power is kept either at low value or high value while changing laser scanning speed the response of the apparent density shows the same slope (almost parallel to each other). This implies that there is no interaction effect observed between laser scanning speed and laser power. That is, how the laser scanning speed influences the apparent density does not depend on the level of laser power, and vice versa.

In Figure 5.10 the two-parameter interaction plots for the UTS are shown. The graph number 1 represents hatching distance and laser power interaction effect, graph number 2 represents the interaction between hatching distance and laser scanning speed, and graph number 3 represents the interaction effects between laser power and laser scanning speed.
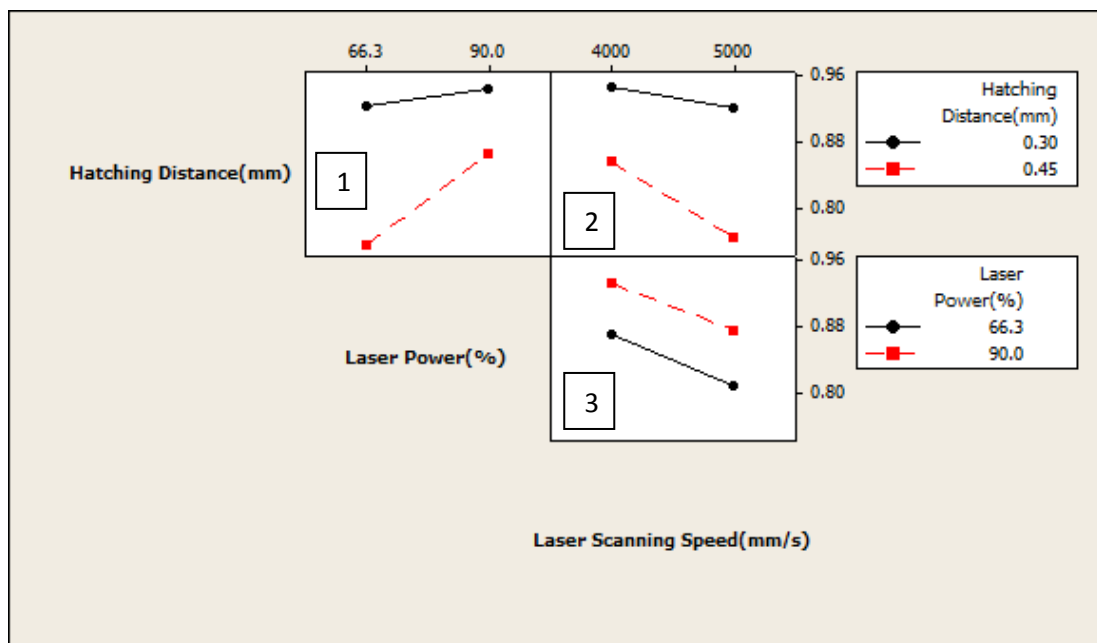
Figure 5.9: Interaction Effects Plots for the Apparent Density (g/cc)

The UTS values (vertical axis) are plotted against one of the parameters (the horizontal axis) at the low and high levels of the second parameter, while the third parameter is kept constant. The slopes of the two plots found in each of graph 1 and graph 2 are not parallel to each other. In graph 1, this indicates interaction between the hatching distance and the laser power, which means the amount that each parameter influences UTS depends on the value of the other parameter. In graph 2, the nonparallel trend indicates interaction between the hatching distance and the laser scanning speed. In graph 3, the two plots are almost parallel to each other, implying no interaction between the laser power and the laser scanning speed.
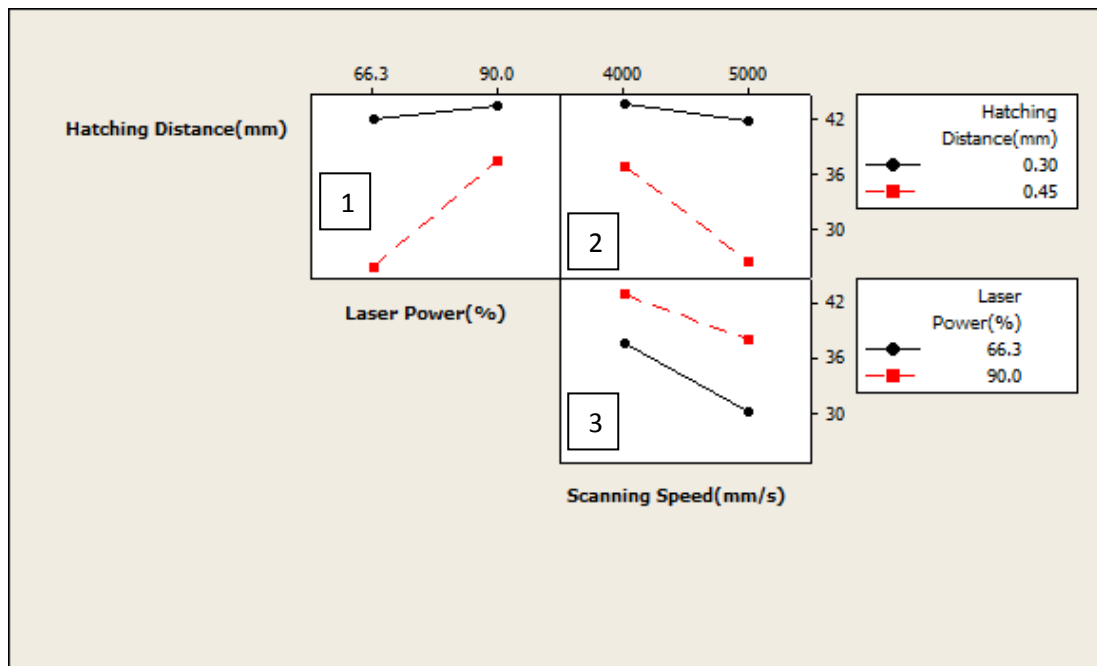
Figure 5.10: Interaction Effects Plots for UTS (MPa)

5.2.3 Pareto Charts

The Pareto Chart indicates the absolute standardized effects of the factors on the response of the system or process. How the standardized effects are calculated are presented in Appendix G. The Pareto chart of the absolute standardized effects shown in Figure 5.11 gives information about the degree of effects onto the apparent density by the process parameters. The horizontal axis is the change in response (the effects) that is presented in a scaled (standardized) manner. The vertical line drawn at the standardized effect 2.06 presents the threshold for defining the significance level of the factors. A statistically significant effect means the factor (parameter) influences the response. A statistically insignificant effect means the factor does not influence the response; the change in response is due to noise. Above the threshold the effects are significant. The threshold value is due to the significance level denoted as α in the Minitab software and by default it is 0.05; and refer to [45] for details on the statistical terms in order to understand more. The hatching distance has the largest effect on apparent density of the sintered parts while the laser power-laser scanning speed (BC) interaction is the least. Figure 5.12 shows the Pareto chart for the UTS. The horizontal axis presents the absolute standardized effects for UTS.
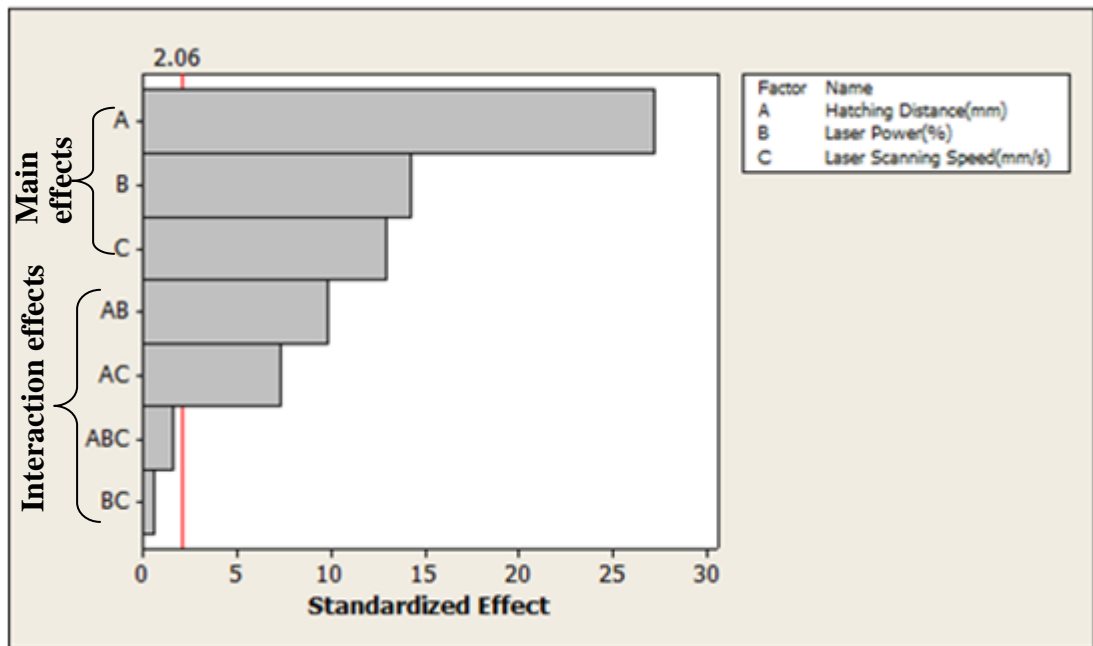
Figure 5.11: Pareto chart of the absolute Standardized Effects for Apparent Density
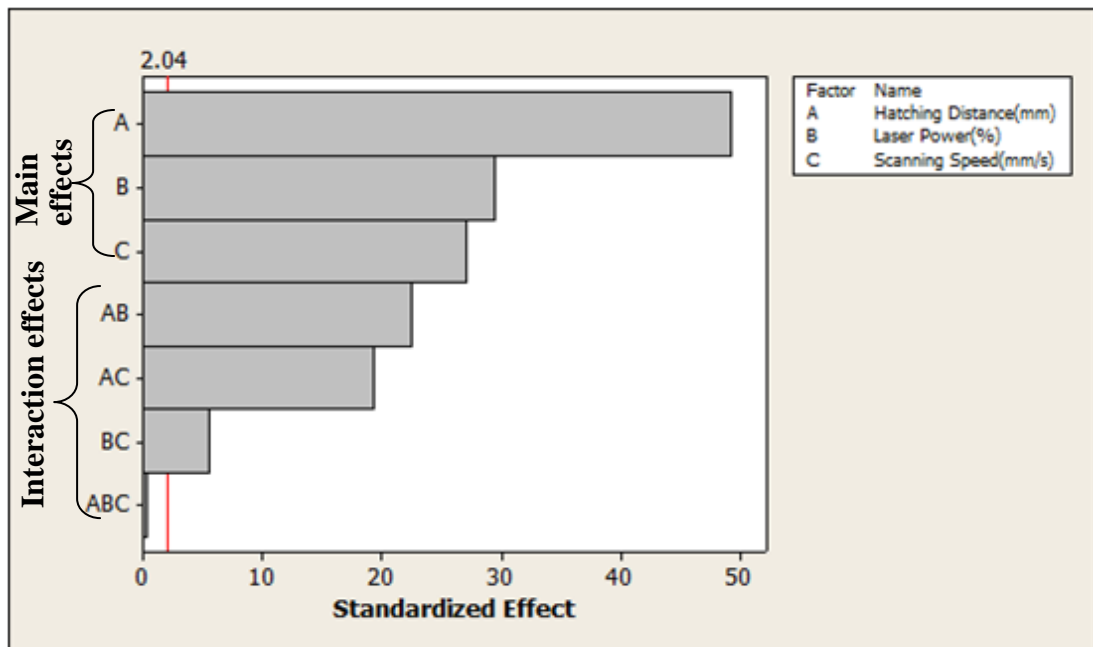
Figure 5.12: Pareto chart of the absolute Standardized Effects for UTS

The ultimate tensile strength of the porous structures is affected by the hatching distance. The interaction of the three parameters (hatching distance, laser power and laser scan speed) has the least effect onto the UTS of the porous polyamide parts. The standardized effects have been calculated and presented in Appendix G.

5.3 Characterization Results for Epoxy-Polyamide Composites: Uniformly Porous Structures Infiltrated with Epoxy Resin

In this section the microstructure and mechanical properties of the resin infiltrated uniformly porous structures is presented.

5.3.1 Microstructure

Figure 5.13 shows the fracture surface of the infiltrated uniformly polyamide porous structures produced at three different process settings; energy densities: 0.016, 0.025 and 0.037 J/mm^2. The build directions are shown in each image. The fracture plane and the build direction (layering direction) are perpendicular to each other due to brittle failure. The individual layers are visible in Figure 5.13 (a) and (b). Qualitatively there is a change in microstructure after parts have been infiltrated with resin. This change is mostly observed for the parts with low energy density compared to that with

high energy density. Parts from low energy density exhibit larger porosity and open pores, and this allows easier impregnation of resin (Figure 5.4). On the other hand, parts which have been sintered using higher energy density posses low porosity and possibly closed pores (Figure 5.3). The flow of resin becomes almost impossible within the material matrix due to the absence of paths. Therefore, the morphology of unfiltrated and infiltrated parts looks similar for the parts built at higher energy densities (Figure 5.3).
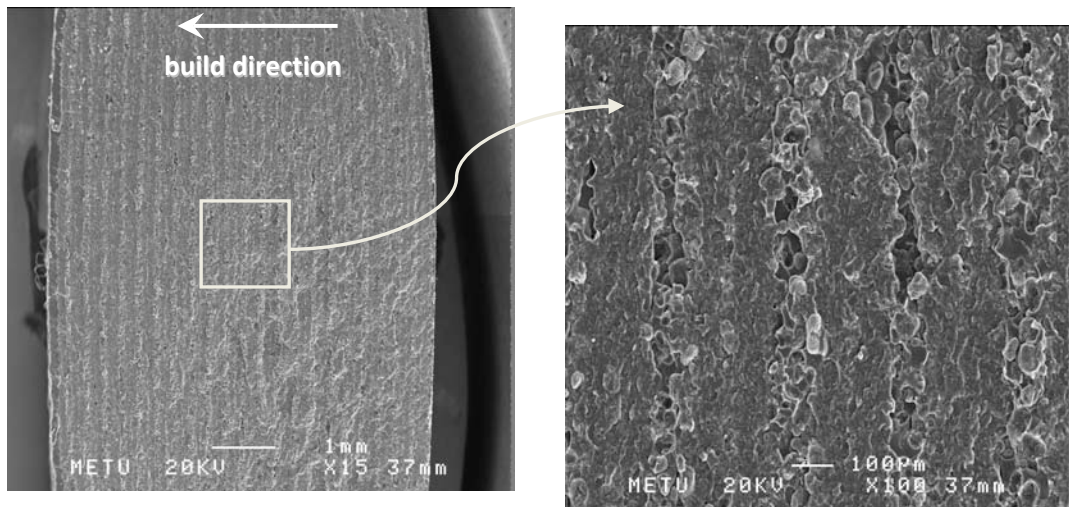
Figure 5.13: Microstructure epoxy-PA (a) ED=0.016J/mm^2 (high porosity)
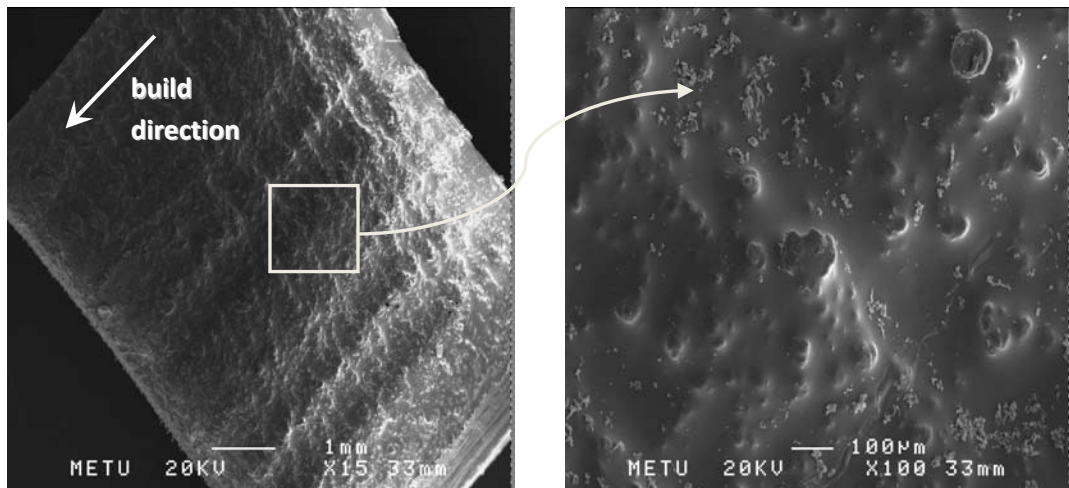
Figure 5.13: Microstructure epoxy-PA (b) ED=0.025J/mm^2 (medium porosity)
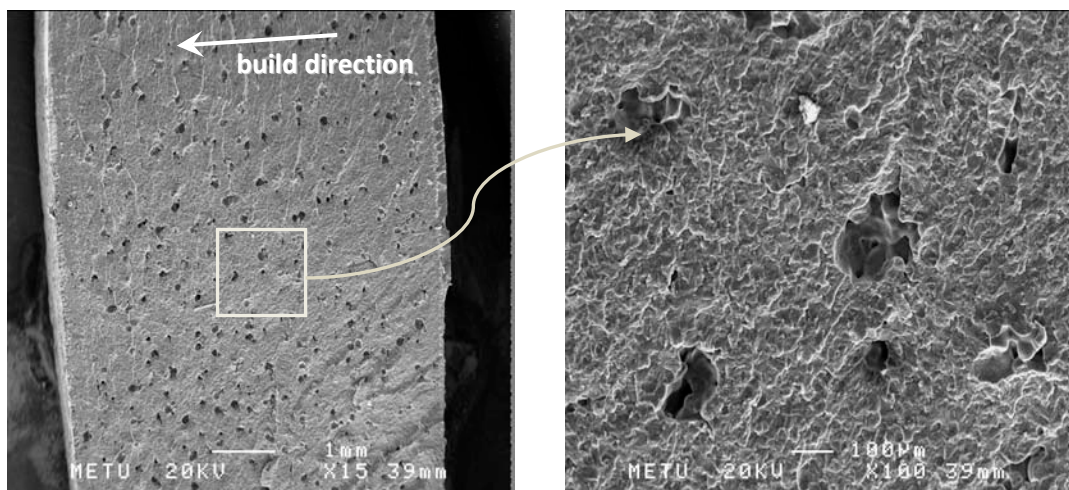
Figure 5.13: Microstructure epoxy-PA (c) ED=0.037J/mm^2 (low porosity)

5.3.2 Mechanical Properties

The strength of the infiltrated structures is assessed through tensile test and the results are compared with uninfiltrated porous specimens. This way, the effect of epoxy could be observed. Figure 5.14 presents the results along with the ultimate tensile strength (UTS) values of the uninfiltrated porous parts for comparison. The ultimate tensile strength of the epoxy-polyamide composite structures varies between 36 MPa and 43 MPa. At the lower energy density, the part infiltrated with epoxy has UTS of 36.79 MPa, while that of uninfiltrated uniformly porous part has 19.98 MPa, (Figure 5.14). There is a gain of about 84.1%. At the energy density of 0.20 J/mm^2, the gain is 17.6%. The gain in UTS is clearly due to epoxy. At energy densities greater than $0.025J/mm^2$, there doesn't seem any difference between uninfiltrated polyamide porous parts and epoxy infiltrated parts. At high energy density setting parts become denser and exhibit low porosity and possibly closed pores (SEM image of Figure 5.3). At low energy density settings, built parts have higher porosity and open pores to allow easier epoxy infiltration (SEM image of Figure 5.4).
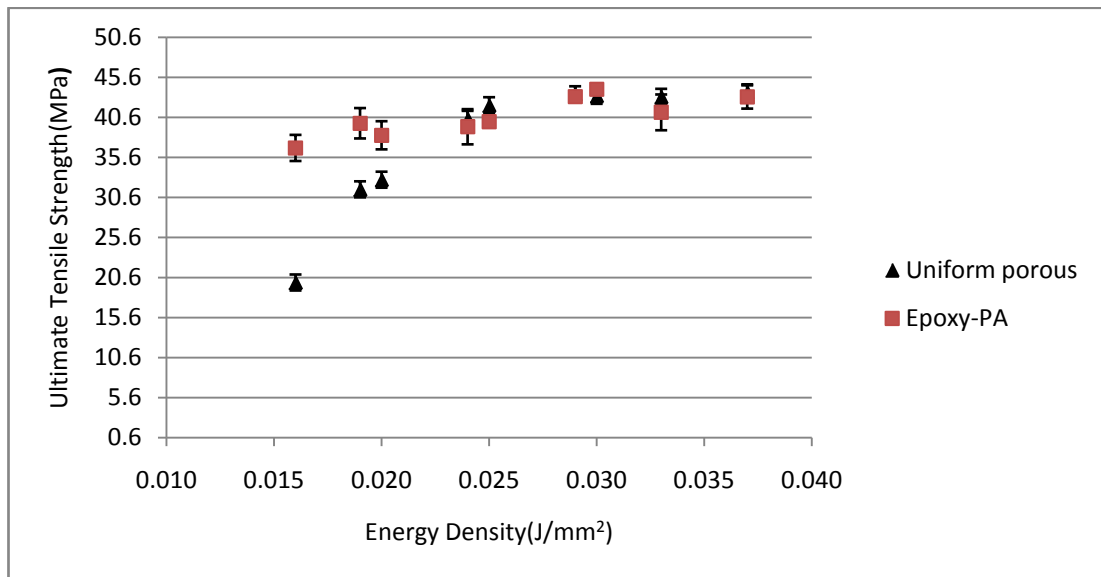
Figure 5.14: Ultimate Tensile Strength of Infiltrated and Uninfiltrated
Uniformly Porous Structures

The tensile strength of epoxy (Araldite® LY 564 and Hardener XB 3486) cured at 50 °C, 15 hrs is 74-78 MPa (Appendix F), the strength of epoxy-polyamide composite for the polyamide parts processed at the lowest energy density (0.016 J/mm^2) process setting is 36.79 MPa and that of uninfiltrated porous polyamide part built at this energy density is 19.98 MPa. The achieved strength of epoxy-polyamide composite lies between the strength of the cured epoxy and the strength of the sintered uninfiltrated porous polyamide structure.

5.3.3 Weight Gain and the amount of porosity left of the Infiltrated Uniformly Porous Structures

The uniformly porous parts infiltrated with epoxy resin were also analyzed to find the amount of resin infiltration in parts of different porosity. The rectangular prism samples were cut off from tensile test specimens for infiltration characterization (Figure 5.15). Three samples were prepared for each process parameter setting (each energy density) for repeatability. Each sample was weighed. The dimensions were measured and the volume was calculated. The mass of uninfiltrated uniform samples were found by multiplying the available apparent density from each process parameter setting (Figure 5.1 and Appendix E) and the volume of these samples.

rectangular prism sample, cut off from from tensile test specimens, for infiltration characterization

side to be cut
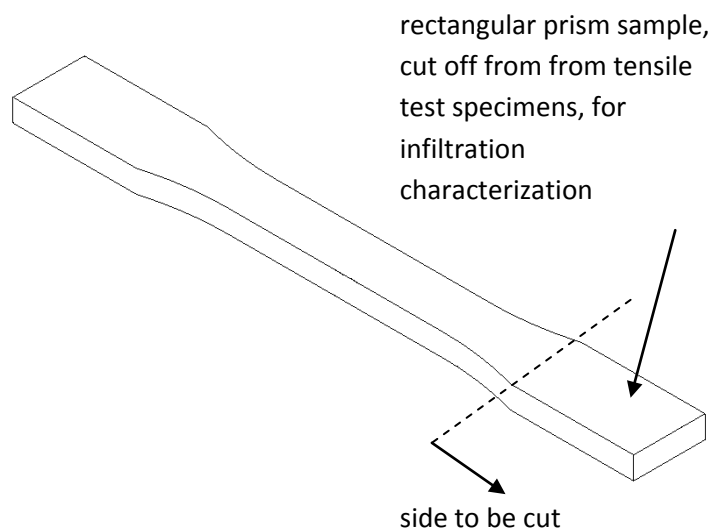
Figure 5.15: Specimen preparation for weight gain analysis for the infiltration of uniformly polyamide porous parts

The difference between the two weights (mass of uninfiltrated graded porous parts and epoxy-PA) gives the weight gain, and if this difference is divided by the volume of the sample gives the normalized weight gain (g/cc). Figure 5.16 presents the variation of the normalized weight gain with the energy density (process parameter settings) (data in Appendix E). As for the porosity of the sintered parts, the increase in energy density decreases the amount of normalized weight gain. The amount of weight gain remains almost zero just above the energy density of 0.025J/mm^2, as for the UTS of the infiltrated uniformly porous structures.

The amount of porosity left after infiltration (effective porosity) for the uniformly porous structures were also found by considering the volume of resin infiltrated and the total volume of the pores (equation 5.7).

$$\varepsilon_{left}(\%)=\frac{V\varepsilon-\dfrac{W_{resin}}{\rho_{resin}}}{V}\times100 \qquad\qquad 5.7$$

where $\varepsilon_{left}(\%)$: percentage porosity left after infiltration, V: volume of the produce sample, W_{resin}:weight of resin and ρ_{resin}:density of resin (Appendix F). The samples used in finding weight gain are used in finding the approximate amount of porosity left after infiltration. Figure 5.16 shows the amount of porosity left after the infiltration from all process settings (energy

densities) of Table 2.3. At low energy density, 0.016 J/mm^2, before infiltration macroscopic porosity were found to be 29% and after infiltration the porosity left is around 5%. For the higher energy density, 0.037 J/mm^2, the macroscopic porosity before infiltration is 5% and after infiltration the porosity did not change. This shows that at higher energy density poor infiltration due to the lack of pores connectivity. In Appendix E the data for finding the porosity left are available.
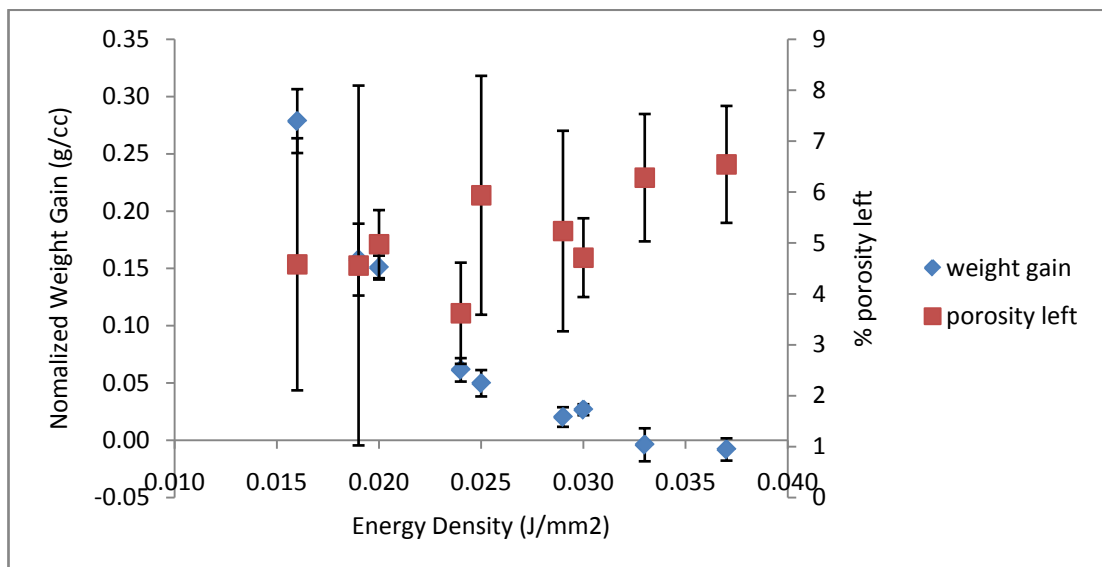
Figure 5.16: Normalized weight gain for the infiltrated uniformly porous parts

5.4 Characterization Results for Graded Porous Polyamide Structures

In this section the polyamide graded porous parts are physically and mechanically characterized. The microstructure and tensile strength of the graded parts will be analyzed.

5.4.1 Analysis of Grades through Computed Tomography (CT)

 Figure 5.17 shows the reference scale for assessing the graded porous parts via computed tomography. In this scale, the average CT numbers for uniformly porous samples produced at different settings (energy densities) are obtained. Using the relation between the energy densities and the macroscopic porosity (Figure 5.16), the CT numbers are related to porosity.
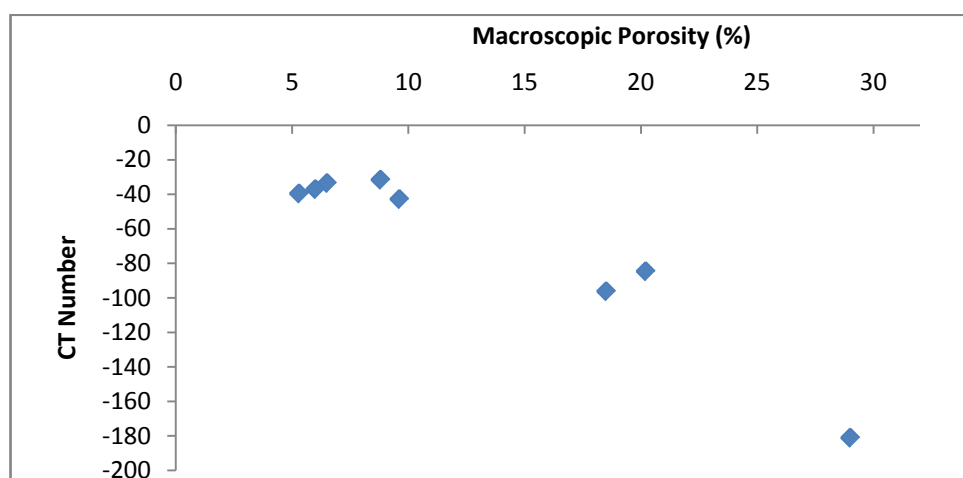
Figure 5.17: Reference scale relating porosity to the CT number

In Figures 5.18 and 5.9, the variation of CT numbers along the thickness direction obtained from CT measurements for Type I and Type II graded parts, respectively, are shown. The expected CT number at each grade is shown in these figures, based on Table 3.1 Using the scale of Figure 5.16; the expected porosity for each grade could also be specified. In all graded specimens, the grade changes occur in a continuous, smooth manner, rather than in step changes as which the process settings were entered into the SLS system. The Type II specimens show significant deviation from expected trends, yielding almost a homogenous CT distribution with little grading, except at the two edges of the parts. The standard deviations of these CT values are also significantly high.
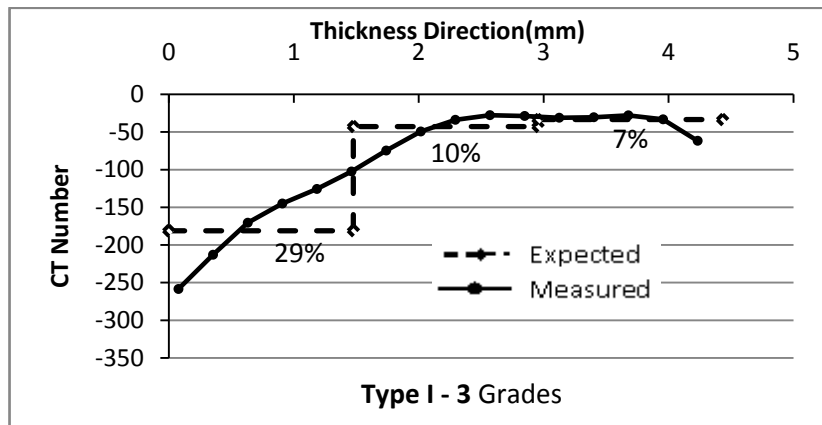
5.18 (a)
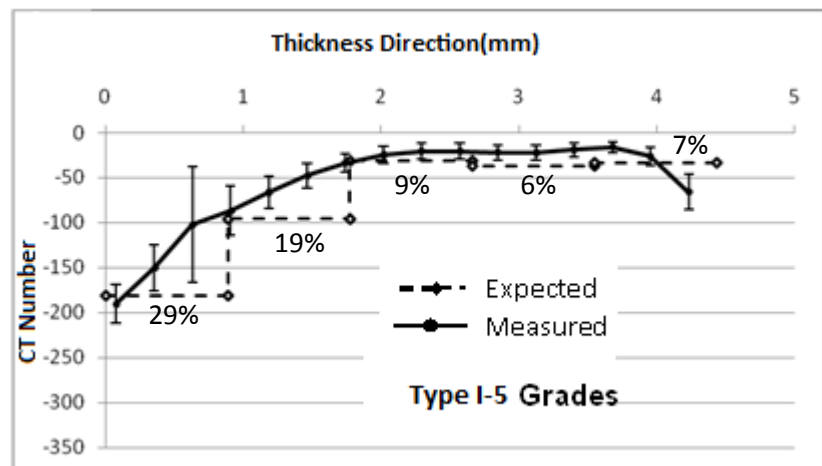
5.18 (b)
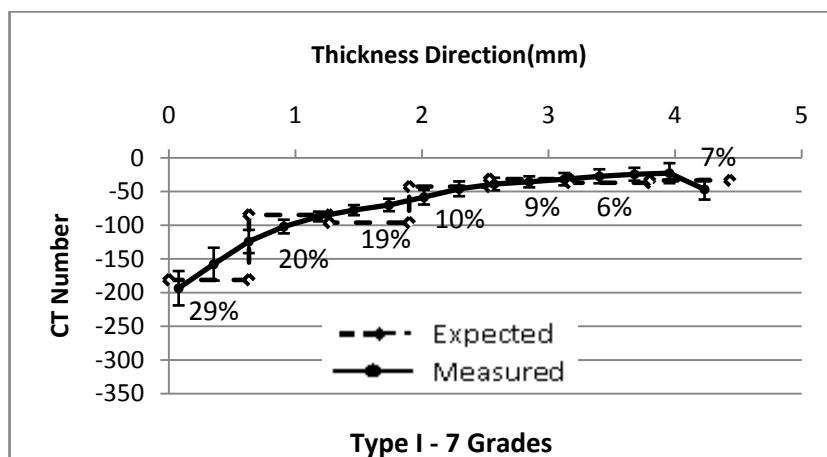
5.18 (c)

Figure 5.18: CT numbers along thickness direction for Type I
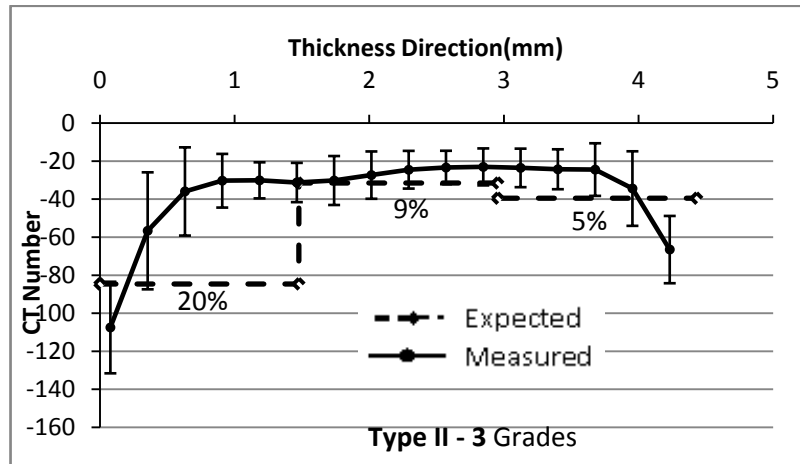
5.19 (a)
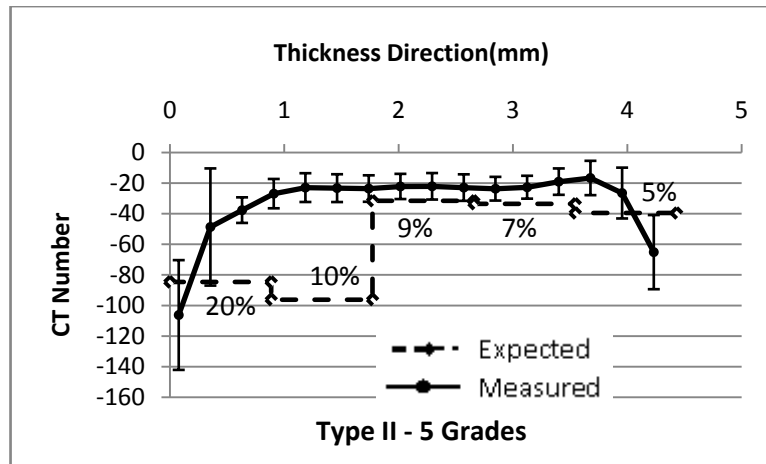
5.19 (b)
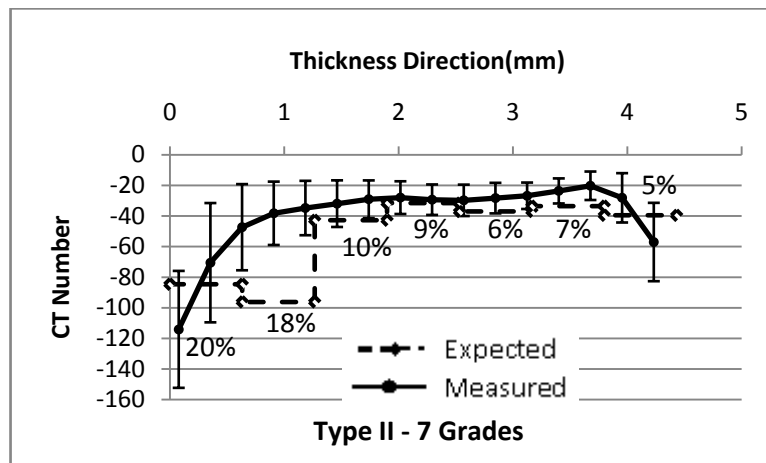
5.19 (c)

Figure 5.19: CT numbers along thickness direction for Type II

On the other hand, the Type I specimens exhibit clear, continuous grades with close match with the expected trends. As the number of grades increase, the measured trends conform more to the expected trends in Type I parts.

5.4.2 Visualization of Grades with Scanning Electronic Microscope (SEM)

Figure 5.20 shows the fracture surface and the build direction for the SEM sample. The graded porous parts were scanned on the fracture surface resulting from the tensile tests. The SEM samples were for Type I parts only, since these parts were shown to exhibit clear grades (section 5.4.1). Due to lower energy density (processing setting) used to built some grades in Type I graded structure, However, SEM samples could be extracted only from 3-Grade and 5-Grade Type I specimens. Some of the 7-Grade specimens' grades were damaged after the tensile tests due to the lower energy density process setting used to build some of the grades which resulted in weak bonding between layers. Figure 5.20 shows the SEM images of the fracture surface of Type I graded porous structures. There are two categories: Type I-3 Grades and Type I-5 Grades. In each category the energy density increases from left to right. The images on the left depict the dense region (low porosity). The images on the right show the weaker (high porosity)

region. In the weak region, the interlayer bonding is weak due to low process energy density used in the production. The production layers are clearly visible in the weaker regions where as the dense side resembles the low porosity morphology of uniformly porous parts (Figure 5.3). The difference in morphology on the denser and weaker regions confirms the results of Figure 5.18, indicating grade change.
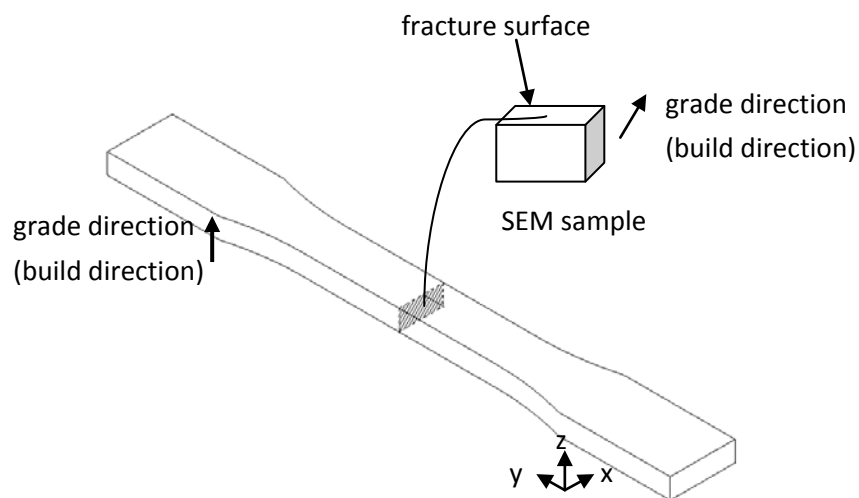
Figure 5.20: Fracture surface for SEM from tensile test
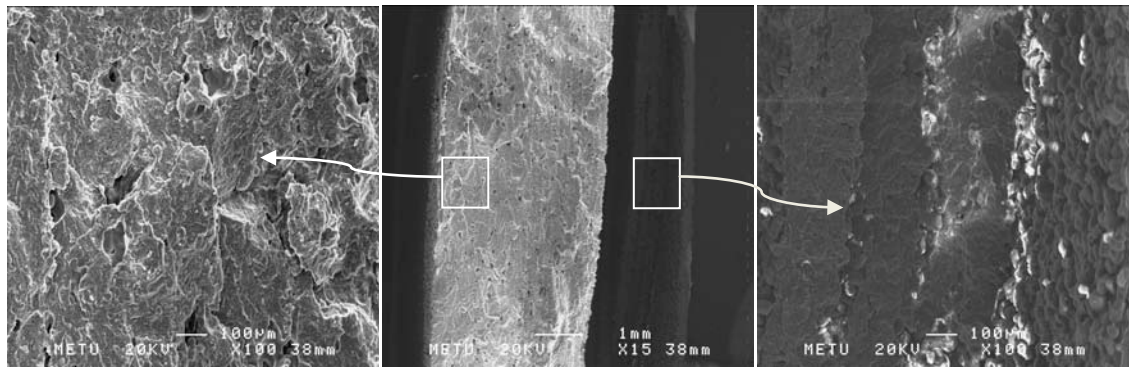
(a): Type I-3 Grades
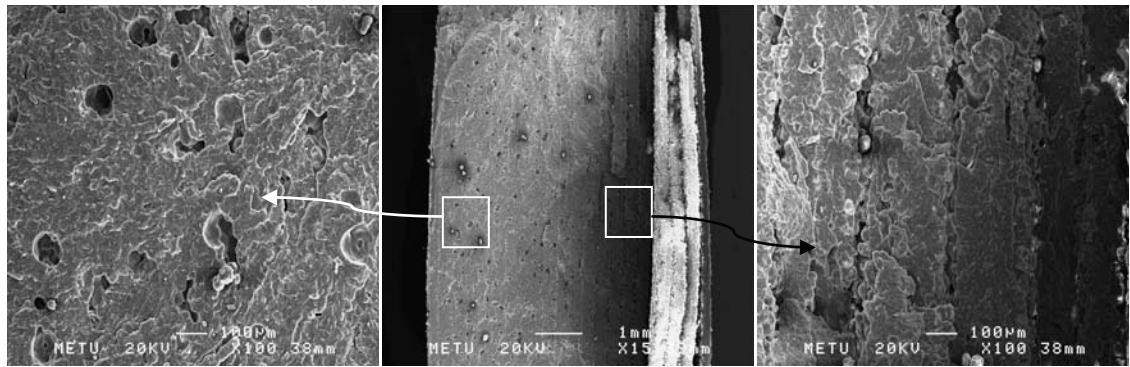
(b): Type I-5 Grades

Figure 5.21: Fracture Surface of Type I Graded Porous Parts

5.4.2 Mechanical Properties

The values of the ultimate tensile strength (UTS) for the graded porous structures are shown in Table 5.3. Three samples were built from each type of graded porous structure to assess repeatability. The Type I samples all have a UTS value around 35 MPa and the Type II samples all have a UTS value around 40 MPa. Within each Type, there is no change in UTS due to

the number of grades, so the number of grades does not change the strength. In Type II specimens, the CT measurements had shown very small grading, with the majority of the specimens resembling homogenous parts built at the energy density of 0.25 – 0.33 J/mm^2. In this ED range, the uniformly porous structures had exhibited strength values around 40 – 44 MPa (from Figure 5.6). The Type II specimen strength values conform to those results. In Type I specimens, the grades could clearly be distinguished in the CT and SEM results. The strength values, though not as high as that corresponding to the largest ED setting (0.30 J/mm^2) – which is about 43 MPa from Figure 5.6, still exhibit a significantly high value around 35 MPa. For the production ED range used in Type I specimens, the individual grade strengths would vary between 20 – 43 MPa per results of Figure 5.6. As such, the Type I graded specimens were not as strong as their weakest grade, but actually stronger, approaching a mid-strength value in the produced grade spectrum.

Table 5.3 (a): The UTS of Type I graded porous structures

Type I			
Sample	3-grades	5-grades	7-grades
	UTS	UTS	UTS
Replicate 1	35.38	36.27	35.11
Replicate 2	34.75	34.31	36.09
Replicate 3	34.49	35.32	35.95
Mean	34.87	35.30	35.72
Standard deviation	0.46	0.98	0.53

Table 5.3(b): The UTS of Type II graded porous structures

Type II			
Sample	3-grades	5-grades	**7-grades**
	UTS	UTS	UTS
Replicate 1	40.08	40.94	40.23
Replicate 2	40.19	40.48	39.75
Replicate 3	39.59	40.66	39.70
Mean	39.95	40.69	39.89
Standard deviation	0.32	0.23	0.29

5.5 Characterization Results for Epoxy-Polyamide Graded Structures

In this section the micrographs (SEM images) and mechanical properties of the graded porous parts infiltrated with epoxy resin are presented. Type II graded porous parts were not infiltrated since they did not exhibit clear grades and would not have made graded composites. Only Type I specimens were used in producing epoxy infiltrated graded parts.

5.5.1 Visualization of Microstructure

The surface for the SEM visualization is similar to that shown in Figure 5.20, i.e. the fracture surface following the tensile tests. Figure 5.22 shows the SEM images of the Type I graded porous structures (Type I-3 Grades, Type I-5 grades and Type I-7 grades) infiltrated with epoxy. In each category, the energy density increases from left to right. The images on the left depict the dense region (low porosity). The images on the right show the weaker (high porosity) region. The layers on the middle image are more clearly visible compared to the graded porous structures of Figure 5.21. The middle images of Figure 5.22 generally have similar microstructure. This feature is absent in Figure 5.21. For all parts, the left side (stronger fusion, lower porosity) shows similar microstructure as those of Figure 5.3 and Figure 5.21. The high energy density used to build these grades result in denser structure and

possibly closed pores. This would hinder the infiltration of epoxy. The weaker regions in epoxy-PA graded specimens are different from those of Figure 5.20. Epoxy resin could be infiltrated from the right side (low energy density side where weak grades are built) due to higher porosity and the presence of open pores (Figure 5.4).
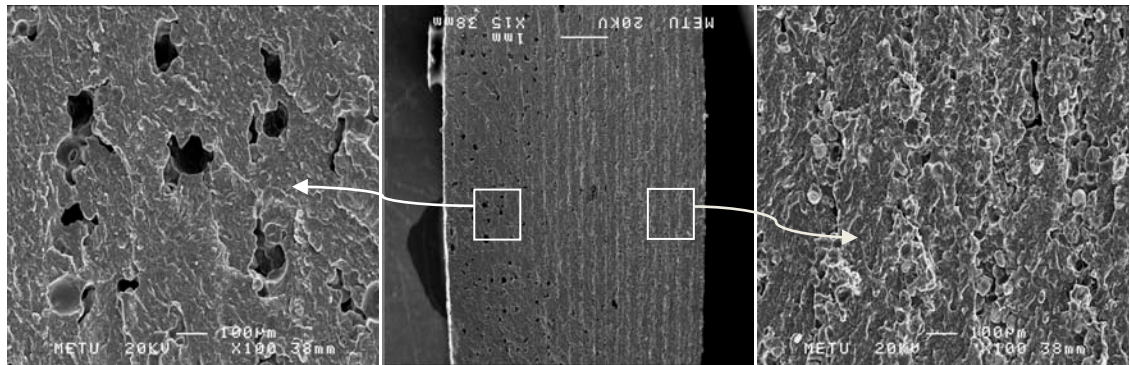
(a): Infiltrated Type I-3 Grades
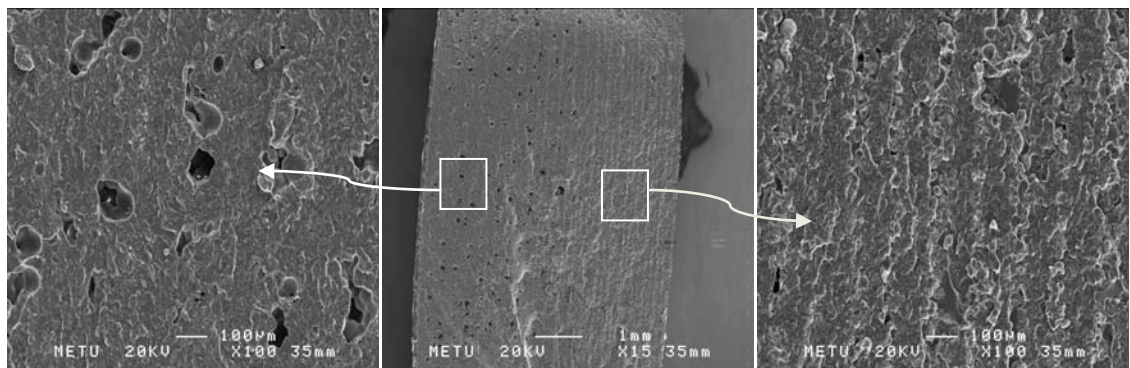
(b): Infiltrated Type I-5 Grades
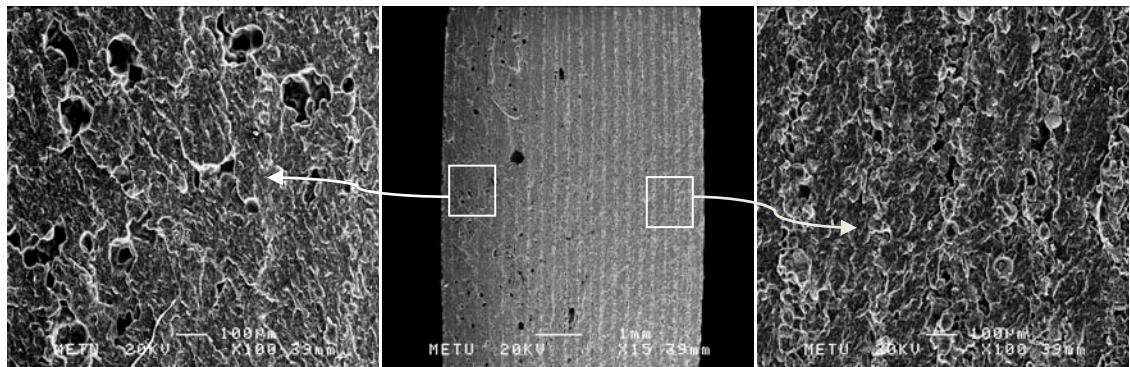
(c): Infiltrated Type I-7 Grades

Figure 5.22: Fracture Surface of Type I Epoxy-PA Graded Parts

5.5.2 Mechanical Properties

The mechanical tests for the epoxy-polyamide graded porous structures have

been conducted to compare the results with those of graded porous PA

specimens in Table 5.1. . Figure 5.23 compares the ultimate tensile strength of the Type I graded porous structures and Type I graded porous structures infiltrated with epoxy. For the Type I-3 Grades the UTS has risen from 34.87 MPa to 37.37 MPa after infiltration. In Type I-5 Grades, the UTS has risen from 35.30 MPa to 38.78 MPa after resin impregnation, and for the Type I-7 Grades the UTS has risen from 35.72 MPa to 37.91 MPa after infiltration. As in graded porous sample results, there is no significant UTS variation with the number of grades in the infiltrated specimens. Generally, the strength gain is about 3 MPa.
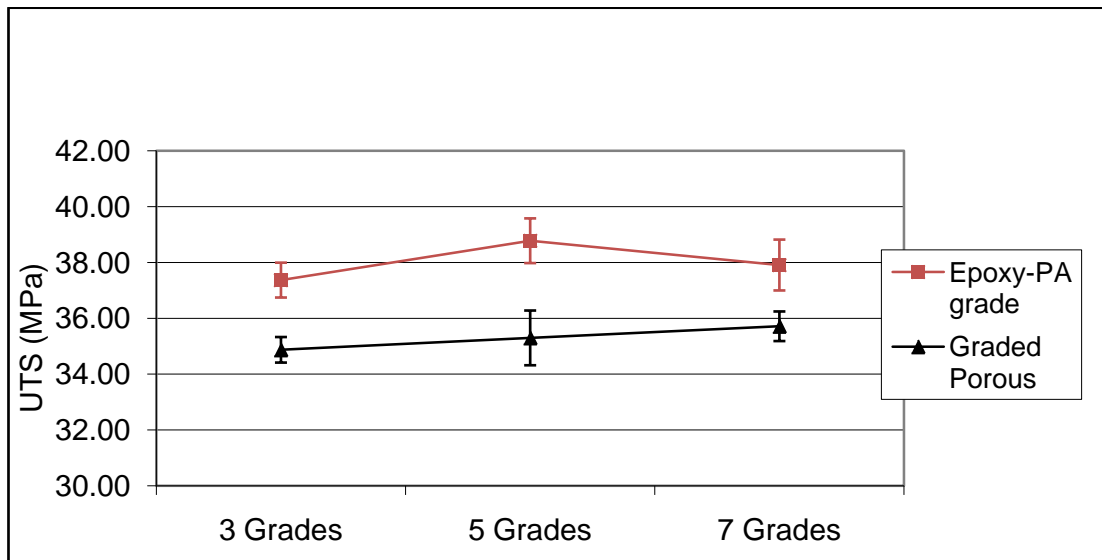
Figure 5.23: Ultimate tensile strength of an uninfiltrated Type I graded Porous structures and infiltrated Type I graded porous structures

5.5.3 Weight Gains of the Epoxy-PA Graded Porous Structures

The weight gain for the infiltrated graded structures were calculated to assess the amount of epoxy resin infiltrated into Type I graded porous structures. Three samples were prepared from the uninfiltrated graded PA samples and three samples from infiltrated graded PA parts. The procedure for preparing samples is similar to that of section 5.3.3. However, the infiltrated samples and uninfiltrated samples were not from the same dog-bone specimens. The normalized weight gains are found by considering the difference between the masses of the uninfiltrated and epoxy-PA graded porous parts. Figure 5.23 shows the weight gains for Type I categories graded porous parts infiltrated with resin. The weight gains have increased with the number of grades. It indicates different behavior from the UTS trend of the graded parts. The UTS of the infiltrated graded porous (Type I) shows almost no difference from one category to the other (Type I-3 grades, Type I-5 grades, Type I-7 grades) (Figure 5.23). The weight gain, on the other hand, increases with an increase in the number of grades (Figure 5.23). In Appendix E, weight analysis data for the epoxy-PA graded porous structures are presented.
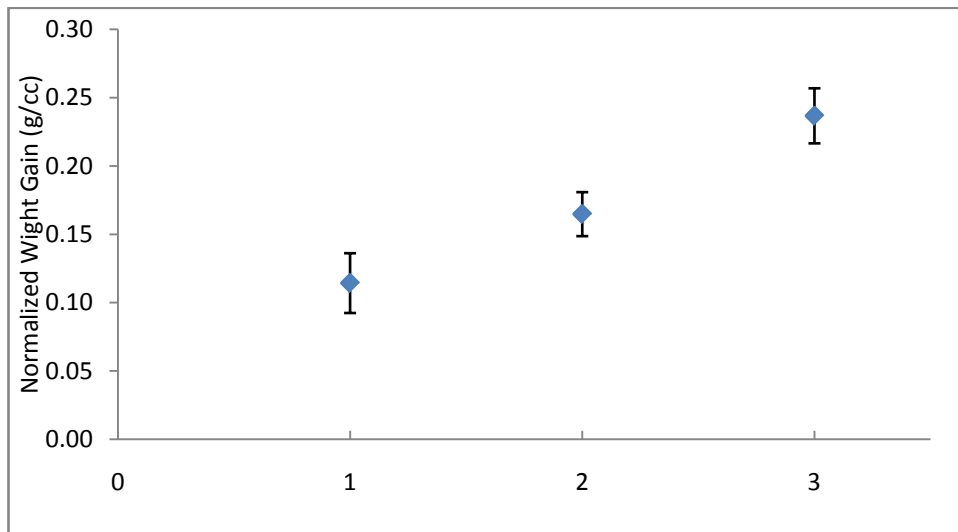
where 1=3-Grades Type I, 2=5-Grades Type I 3=7, -Grades Type I

Figure 5.23: Weight gains for the epoxy-PA graded porous parts

CHAPTER 6

CONCLUSION AND RECOMMENDATIONS

In this thesis, uniformly porous structures from polyamide powder were built using selective laser sintering process and characterized. The microstructure and mechanical properties of parts could be changed by varying the three SLS machine parameters: hatching distance, laser power, and laser scanning speed. A combination of the three parameters; energy density was used to describe the specific process settings. Graded porous polyamide structures were also built by varying these parameters within a simple specimen from layer to layer and were characterized. Uniformly polyamide porous structures and graded polyamide porous structures were infiltrated with epoxy resin and were characterized. The conclusions related in this study and recommendations for future study are presented in this chapter.

6.1 Conclusions

1. The apparent density of the parts sintered using selective laser sintering process varied between 0.7100 g/cc and 0.9505 g/cc for the range of process parameters used in this study. Increasing the energy density enables the apparent density to increase. However, this increase is limited by material degradation.

2. For the process parameter range used, porous parts with macroscopic porosity varying from 4.9 % to 29.0 % could be obtained. If the energy density decreases, the amount of porosity will increase. However, insufficient energy supply could result in insufficient fusion between powder particles and in between successive layers, so this is the obstacle in obtaining higher porosity. At all process settings (energy density) used in the production, the pore sizes were greater than 50 nm, rendering the pore structure as macropores.

3. At all process settings, most of the pores have sizes between 5 and 100 μm. The pore size distribution in all specimens is in the shape of a bell-curve. The highest pore volume in all specimens was found to belong to pores of 20 μm size, regardless of the production setting or the overall porosity. Therefore, if production of parts is from the same

powder (having the same powder particle size), the size of the largest volume of pores will be the similar even if the process parameter settings used in the production are different. Varying process parameter settings influence the macroscopic porosity.

4. The ultimate tensile strength (UTS) of produced parts varied between 19.80 MPa and 43.74 MPa for the process settings used. Like apparent density, UTS increased with increase in energy density.

5. The production was planned according to 2^3-factorial design and an effects analysis was performed. Among the three processing parameters that were used to change porosity and other properties, hatching distance is the most effective on the physical and mechanical properties of the sintered parts. Laser scanning speed was found to be the least effective parameter on property response.

6. The ultimate tensile strength of uniformly porous polyamide samples were improved significantly by infiltration with epoxy resin for highly porous samples. For example, the UTS of the sample built at the energy density 0.016 J/mm^2 (the lowest setting) changed from 19.98 MPa to 36.79 MPa exhibiting a gain of about 84.1% after infiltration. The improvement of strength by infiltration decreased with as the energy density was increased. The improvement in mechanical and physical properties was prominent only when the energy density (as

an indicator of the process setting) was less than 0.025 J/mm^2. Beyond this energy density, pores are closed rather than in a network (Figure 5.3). Also, the porosity at high energy density stay unchanged after resin infiltration (Figure 5.15). This concludes that at higher energy density there is no pores connectivity.

7. It has been found that the ultimate tensile strength of the graded parts (both porous and epoxy-infiltrated) likely depend on the minimum and maximum grade limits and not on the number of grades. The number of grades did not affect the overall strength, however, the maximum/minimum porosity limits (associated with the limiting grades) did.

8. Of the two types of specimens with different grade limits (Types I and II), Type I was shown to have clear, continuously changing grades. These graded porous specimens were found to be stronger than their weakest grade. It is concluded (using CT test) that a desired porosity grade within the limits of the machine capabilities could be induced in polyamide samples produced via SLS. The porosity imparted in Type I where grades were clearly seen ranges between 6 % and 29 %.

9. There is an increase in ultimate tensile strength of the graded porous structures after infiltration with epoxy resin. The infiltration occurs mostly through the highly porous grades where there is not much infiltration into dense grades. Thus, a solid part could not be produced

for the porosity ranges used in the grades. The gain in mechanical strength is contributed to the epoxy infiltrated through highly porous grades.

6.2 Recommendations for Future Study

Further studies could be directed towards producing parts with higher porosities (more than the ones obtained in this research) by trying powder with greater particle sizes (greater than 60 μm), using different laser scanning strategies, and/or changing the layer thickness. In epoxy-PA composite production higher porosity could lead to more infiltration usually when the pores are connected. Also, for easier qualitative visualization of the amount of infiltrated resin, colored resin could be used. The color traces within the material matrix would help to trace the infiltration situation and qualitatively trying to see whether there are closed or open pores. In addition to using colored resin, the infiltration pressure could be varied to a higher value so that the amount of infiltration could be increased.

REFERENCES

[1] Erdal, M., Dağ, S., Jande, Y., and Tekin, C.M., 2010. Manufacturing of Functionally Graded Porous Products by Selective Laser Sintering, Materials Science Forum Vols. 631-632, pp 253-258.

[2] Dunne, P., Soe, S.P., Byrne, G., Venus, A. and Wheatley, A.R., 2004. Some demands on rapid prototypes used as master patterns in rapid tooling for injection molding. J. Mater. Process Tech. 150 (3), pp.201-207.

[3] Chung, S, Im, Y., Jeong, H., Jeong, D., Cho, K, Lee, S., Choi, B. and Choi, H., 2003. Rapid fabrication of aluminum shoe mold using vacuum sealed casting process. J. Mater. Process Tech. 142 (2), pp.326-333.

[4] Tucker, B., Bradley, W., Eubank, P., Norasetthekul, S. and Bozkurt, B., 1997. Zirconium diboride/copper EDM electrodes from selective laser sintering. In: Marcus, H.L., Beaman, J.J., Bourell, D.L., Barlow, J.W., Crawford, R.H. (Eds.), Solid Freeform Fabrication Proceedings, The University of Texas at Austin, pp. 257-266.

[5] Zaw, H.M., Fuh, J.Y.H., Nee, A.Y.C. and Lu, L., 1999. Formation of a new EDM electrode material using sintering techniques. J. Mater. Process Tech. 89-90, pp.182-186.

[6] Bellini, A., 2002. Fused Deposition of Ceramics: A Comprehensive Experimental, Analytical and Computational Study of Material Behavior, Fabrication Process and Equipment Design, PhD Thesis, Drexel University, Philadelphia-USA.

[7] Hongjun, L., Zitian, F., Naiyu, H., Xuanpu, D., 2003. A note on rapid manufacturing process of metallic parts based on SLS plastic prototype. Journal of Materials Processing Technology 142 pp710–713.

[8] Kruth, J.P., Wang, X., Laoui, T., Froyen,L.,2003. Lasers and materials in selective laser sintering. Automation Assembly 23 pp357-371.

[9] Tan, H., Chua, C.K., Leong, K.F., Cheah, C.M., Cheang, P., Abu Bakar, M.S. and Cha, S.W., 2003. Scaffold development using selective laser sintering of polyetheretherketone–hydroxyapatite biocomposite blends. Biomaterials 24 (18), pp.3115-3123.

[10] Kalita, S.J., Bose, S., Hosick, H. L. and Bandyopadhyay, A., 2003. Development of controlled porosity polymer-ceramic composite scaffolds via fused deposition modeling. Mat. Sci. Eng. C 23 (5), 611-620.

[11] Masood, S.H., Singh, J.P. and Morsi, Y., 2005. The design and manufacturing of porous scaffolds for tissue engineering using rapid prototyping. Int. J. Adv. Manuf. Tech. 27 (3-4), 415-420.

[12] Ciardelli, P., Chiono, V., Cristallini, C., Barbani, N., Ahluwalia, A., Vozzi, G. And Previti, A., Tantussi, G., Giusti, P., 2004. Innovative tissue engineering structures through advanced manufacturing technologies. J. Mater. Sci.-Mater. M. 15 (4), 305-310.

[13] Hoque, M.E., Hutmacher, D.W., Feng, W., Li, S., Huang, M.H., Vert, M. and Wong, Y.S., 2005. Fabrication using a rapid prototyping system and in vitro characterization of PEG-PCL-PLA scaffolds for tissue engineering. J. Biomat. Sci.-Polym. E. 16 (12), 1595-1610.

[14] Vozzi, G., Flaim, C., Ahluwalia, A. and Bhatia, S., 2003. Fabrication of PLGA scaffolds using soft lithography and microsyringe deposition. Biomaterials 24 (14) 2533-2540.

[15] Li, J.P., de Wijn, J.R., Van Blitterswijk, C.A. and de Groot, K., 2006. Porous Ti_6Al_4V scaffold directly fabricating by rapid prototyping: Preparation and in vitro experiment. Biomaterials 27 (8), 1223-1235.

[16] Lopez-Heredia, M.A., Goyenvalle, E., Aguado, E., Leroux, C., Dorget, M. and Layrolle, P., 2006. Bone growth in porous titanium implants made by rapid prototyping. Key Eng. Mat. 309-311, 1099-1104.

[17] Hayashi, T., Maekawa, K., Tamura, M. and Hanyu, K., 2005. Selective laser sintering method using titanium powder sheet toward fabrication of porous bone substitutes. JSME Int. J. A-Solid M. 48 (14), 369-375.

[18] Cheah, C.M., Leong, K.F., Chua, C.K., Low, K.H. and Quek, H.S., 2002. Characterization of microfeatures in selective laser sintered drug delivery devices. P. I. Mech. Eng. H. 216 (6), 369-383.

[19] Leong, K.F., Phua, K.K.S., Chua, C.K., Du, Z.H. and Teo, K.O.M., 2001. Fabrication of porous polymeric matrix drug delivery devices using the selective laser sintering technique. P. I. Mech. Eng. H. 215 (2), 191-201.

[20] Low, K.H., Leong, K.F., Chua, C.K., Du, Z.H. and Cheah, C.M., 2001. Characterization of SLS parts for drug delivery devices. Rapid Prototyping J. 7 (5), 262-267.

[21] Beal, V. E., Paggi, R. A.., Salmoria, G. V., and Lago. A., 2009. Statistical Evaluation of Laser Energy Density Effect on Mechanical Properties of Polyamide Parts Manufactured by Selective Laser Sintering, Journal of Applied Polymer Science,Vol. 113, pp.2910–2919.

[22] Takayuki, N., Shirakawa, N., Miyata, Y., Inui, H., 2009. Selective laser sintering of high carbon steel powders studied as a function of carbon content. Journal of Materials Processing Technology 209, pp. 5653–5660.

[23] Ku, C.W., Gibson, I. and Cheung, W.L., 2002. Selective laser sintered castform TM polystyrene with controlled porosity and its infiltration

characteristics by red wax. In: Marcus, H.L., Beaman, J.J., Bourell, D.L., Barlow, J.W. and Crawford, R.H. (Eds.), Solid Freeform Fabrication Proceedings, The University of Texas at Austin, pp 107-114.

[24] Caulfield, B., McHugh, P.E. and Lohfeld, S., 2007. Dependence of mechanical properties of polyamide components on build parameters in the SLS process. J. Mater. Process Tech. 182 (1-3), 477-488.

[25] İlkgün, Ö., 2005. Effects of production parameters on porosity and hole properties in laser sintering rapid prototyping process. Ms Thesis, Mechanical Engineering Department, Middle East Technical University, Ankara-Turkey.

[26] Mumtaz, K.A., Hopkinson, N., 2007. Laser melting functionally graded composition of Waspaloy®. J Mater Sci 42 pp7647–7656.

[27] Chung, H., Das, S., 2007. Functionally graded Nylon-11/silica nanocomposites produced by selective laser sintering. Materials Science and Engineering A 487 pp 251–257.

[28] Petrov A.L., Snarev A.I., Shishkovsky I. V., Scherbakov V.I. Laser synthesis of the functional graded filter elements from metal - polymer powder compositions. P. N. Lebedev Physical institute of Russian Academy of Science, Samara branch.

[29] Chung, H., Das, S., 2006. Processing and properties of glass bead particulate-filled functionally graded Nylon-11 composites produced by selective laser sintering. Materials Science and Engineering A 437 pp226–234.

[30] Salmoria, G.V., Ahrens, C.H., Klauss, P., Paggi, R.A., Oliveira, R.G., Lago, A., 2007. Rapid manufacturing of polyethylene parts with controlled pore size gradients using selective laser sintering. Material Research 10 São Carlos pp1-9.

[31] Leong, K.F., Chua, C.K., Gui, W.S., 2006. Building porous biopolymeric microstructures for controlled drug delivery devices using selective laser sintering. Int J Adv Manuf Technol 31: 483–489.

[32] HAYNES® Waspaloy alloy datasheet.

[33] Erdal, M., Ertoz, L. and Güçeri, S., 1999. Characterization of permeability for solid freeform fabricated porous structures. In: Proceedings of the ASME Materials Division: The Science, Automation and Control of Material Processes Involving Coupled Transport and Rheology Changes, MD-Vol.89, pp. 57-63.

[34] Greses, J., Bullemer, M., Paluzie, V., 2008. Dental restorations, medical/dental implants and medical aids manufactured by laser sintering: fast, flexible and cost-effective. EOS GmbH and RMS S.L.

[35] Wimpenny, D.I., Boivie, K., 2008. Rapid Manufacturing Methods and Materials. Custom-Fit.

[36] EOSINT P380 User Manual.

[37] Bose, S., Darsell, J., Hosick, H. L., Yang, L., Sarkar, D., Bandyopadhyay, A., 2002. ASTM Standard D 638-03, 2003. Standard Test Method for Tensile Properties of Plastics. American Society for Testing and Materials, West Conshohocken, PA, USA..Processing and characterization of porous alumina scaffolds. J. Mater. Sci.-Mater. M.13 pp 23-28.

[38] Automatic Pycnometers Brochure

[39] Akin,S., Kovscek,A.R.,2003. Computed tomography in petroleum engineering research. Geological Society, London, Special Publications; v. 215; pp 23-38.

[40] Gregg, S.J. and Sing K.S.W., 1982. Adsorption Surface Area and Porosity (2nd edition). Academic Press, New York, p. 173-176.

[41] METU Central Lab., http://www.centrallab.metu.edu.tr/?q=en/node/130, last accessed date December 2009.

[42] Tekin, C.M., 2009. Mechanical Characterization of Porous Polymeric Materials Manufactured by Selective Laser Sintering. Ms Thesis, Mechanical Engineering Department, Middle East Technical University, Ankara-Turkey.

[43] Gibson, I., Shi, G., 1997. Material properties and fabrication parameters in selective laser sintering process. Rapid Prototyping Journal, no. 3, v. 4, pp 129-136.

[44] Zdravkov, B.D., Čermák, J.J., Šefara, M., Janků, J., 2007. Pore classification in the characterization of porous materials: A perspective Central European Journal of Chemistry 5 pp385-395.

[45] Montgomery, D.C., 2001. Design and Analysis of Experiments (5th edition). John Wiley & Sons, Inc.

[46] Wikipedia, http://en.wikipedia.org/wiki/Voxel, last accessed date December 2009

APPENDIX A

MATERIAL DATASHEET OF FINE POLYAMIDE PA 2200 FOR EOSINT P 380

Application:

PA 2200 is suitable for use in all EOSINT P systems with fine polyamide option. The recommended layer thickness is 0.15 mm. Unexposed powder can be reused. Depending on building time it has to be mixed with fresh powder by a ratio of 2:1 to 1:1 (old: new) in order to guarantee constant process parameters and persisting part quality.

Typical applications of the material are fully functional prototypes with high end finish right from the process. They easily withstand high mechanical and thermal load.

Table A.1: Material Properties of Fine Polyamide (PA 2200)

Average grain size	Laser diffraction	60	µm
Bulk density	DIN 53466	0,435 - 0,445	g/cm³
Density of laser-sintered part	EOS-Method	0,9 - 0,95	g/cm³

Table A.2: Mechanical Properties of Fine Polyamide (PA 2200)

Tensile Modulus	DIN EN ISO 527	1700 ± 150 N/mm²
Tensile strength	DIN EN ISO 527	45 ± 3 N/mm²
Elongation at break	DIN EN ISO 527	20 ± 5 %
Flexural Modulus	DIN EN ISO 178	1240 ± 130 N/mm²
Charpy - Impact strength	DIN EN ISO 179	53 ± 3,8 kJ/m²
Charpy - Notched impact strength	DIN EN ISO 179	4.8 ± 0.3 kJ/m²
Izod – Impact Strength	DIN EN ISO 180	32.8 ± 3.4 kJ/m²
Izod – Notched Impact Strength	DIN EN ISO 180	4.4 ± 0.4 kJ/m²
Ball indentation hardness	DIN EN ISO 2039	77,6 ± 2
Shore D - hardness	DIN 53505	75 ± 2

Table A.3: Thermal Properties of Fine Polyamide (PA 2200)

Melting point	DIN 53736	172 - 180 °C
Vicat softening temperature	B/50 DIN EN ISO 306	163 °C
Vicat softening temperature	A/50 DIN EN ISO 306	181 °C

* The mechanical properties depend on the x-, y-, z-position and on the exposure parameters used.

APPENDIX B

CALIBRATION CHARTS FOR LASER POWER IN EOSINT P 380
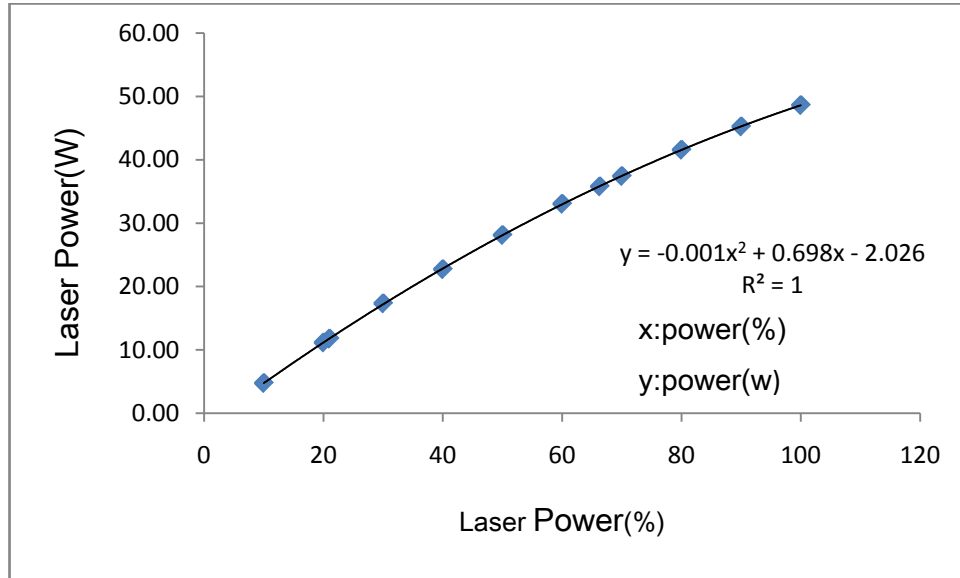
Figure B1: Laser power characteristic curve of EOSINT P 380 SLS machine [25]

Figure B2 presents the laser power characteristics curve obtained during installation. This graph was plotted using the data shown in Table B1.

Table B1: Laser power characteristic data for plotting Figure B2

Laser Power (%)	10	20	30	40	50	60	70	80	90	95	99
Laser Power (W)	4.7	11.4	17.9	24.1	29.9	35.2	39.9	44.4	48.8	50.5	51.8
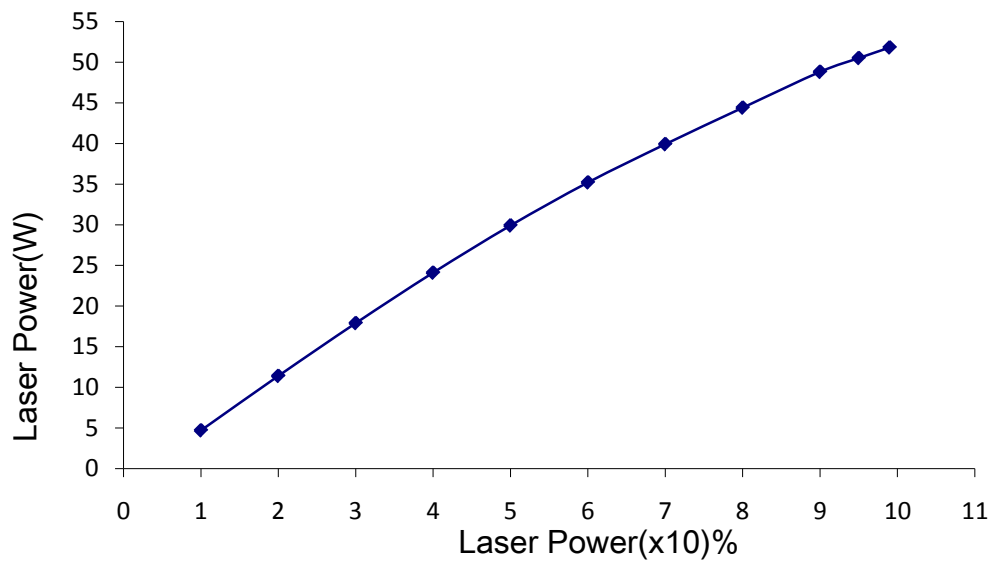
Figure B2: Laser power characteristic curve of EOSINT P 380 SLS machine
obtained during installation

APPENDIX C

SETTING PROCESS PARAMETERS IN SLS MACHINE

Producing prototypes using SLS involves various steps. These can be categorized into two main groups namely post processing and preprocessing. Every category has its own merits for the proper achievements of the product's function. Post processing involves cleaning and packaging of the processed parts. The preprocessing category plays a great role for obtaining the desired mechanical and physical properties of the part like strength, amount of porosity, and pores distribution and this category is explained in details as follows:

Preprocessing:

Outline:

1. Creating Standard Tessellation Language(STL) file

2. Locating the designed part onto the building platform using Magics

3. Slicing by using EOS-RP-Tools

4. Loading parts into PSW P3x0 Software

5. Loading the *filename.job* into the computer which is connected to the RP-Machine.

1. Creating Standard Tessellation Language(STL) file

Within this category there are various activities to be accomplished prior to the production stage. Firstly, the part should be designed using Computer Aided Design (CAD) Software which is capable to store a file in the form of Standard Tessellation Language (STL) format, example *filename.stl.*

In this project Pro/ENGINEER 2001/Wildfire is used for designing and creating STL files. For example, the specimen for Scanning Electron Microscope (SEM) followed these steps:

    a. Draw the specimen

    b. Create STL file via these procedure:

        i. FILE > SAVE A COPY

        ii. CHOOSE FILE TYPE > STL

        iii. OK

        iv. Set chord height to 0. The field will be replaced by a minimum acceptable value.

        v. Set angle control to 1.

        vi. OK

Also see Figures C1, C2, & C3 for more information.
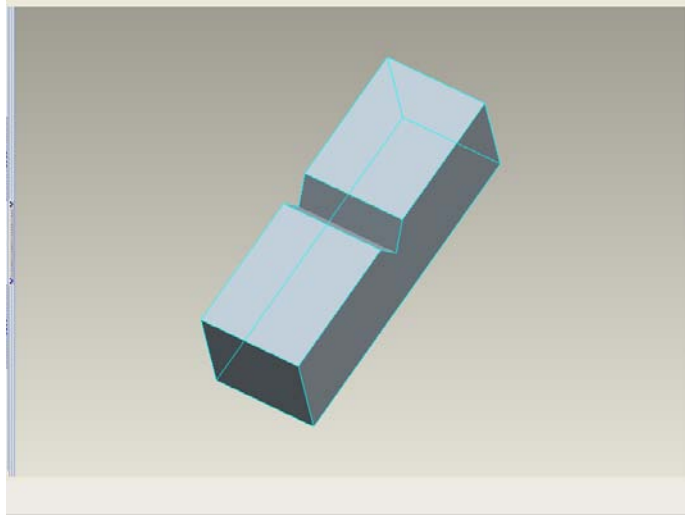
Figure C1: SEM specimen created using ProEngineer
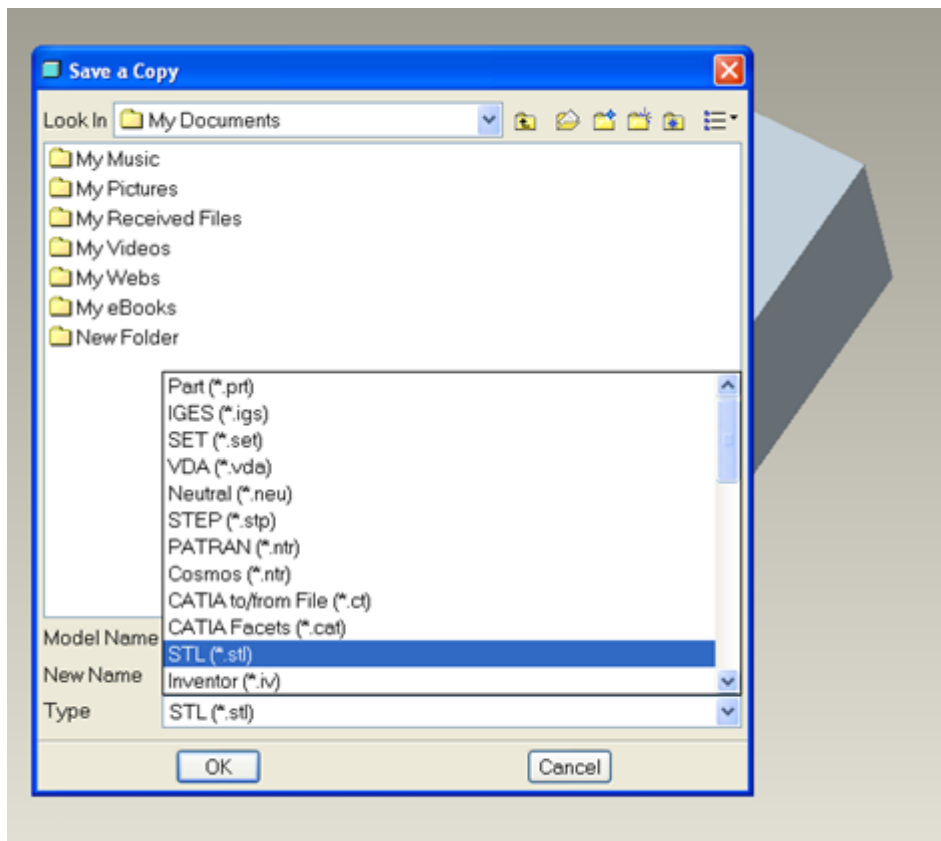
Figure C2: STL file creation on SEM specimen
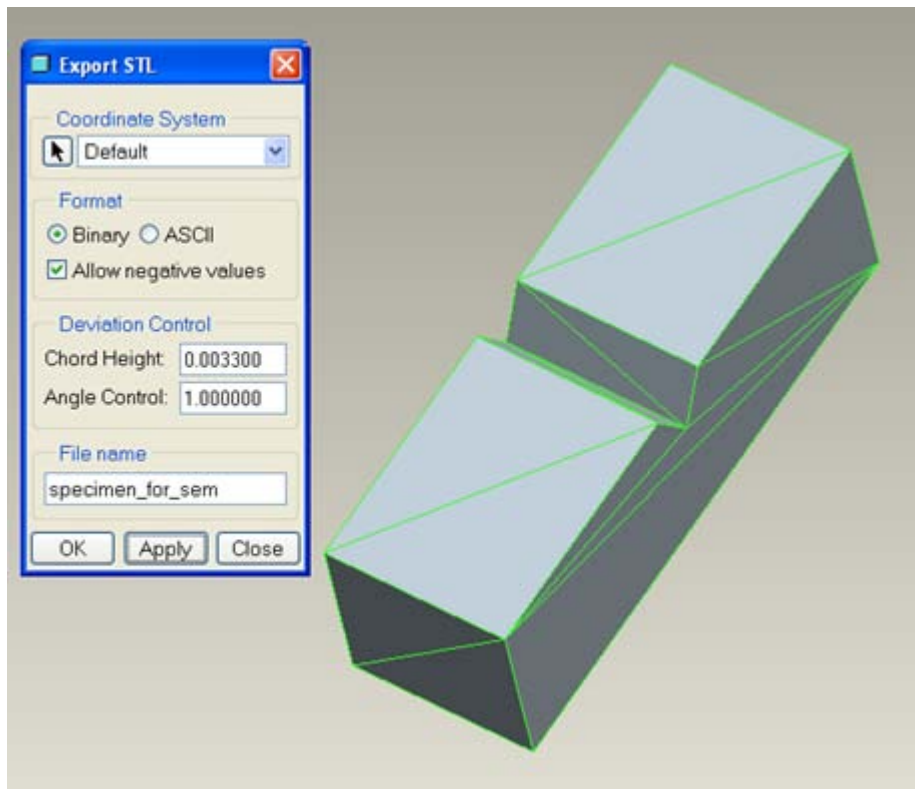
Figure C3: SEM specimen with its triangles

For other software follow the respective steps as explained below.

Pro/ENGINEER (other versions)

1. FILE > EXPORT > MODEL

2. .STL

3. Set chord height to 0. The field will be replaced by a minimum

   acceptable value.

4. Set angle control to 1.

5. OK

SolidWorks 2001

1. FILE > SAVE AS > Set SAVE AS type to .STL

2. STL OPTIONS > Set quality to FINE.

3. OK

4. SAVE > YES

SolidWorks (other versions)

1. TOOLS > OPTIONS > EXPORT

2. .STL OPTIONS

3. Set quality to FINE.

4. File > SAVE AS

5. Set SAVE AS type to .STL

6. SAVE

AutoCAD

1. Set facetres to 10.

2. Use the "STLOUT" command to export your .STL file.

I-DEAS

1. FILE > EXPORT > RAPID PROTOTYPE FILE > OK

2. Select the part to be prototyped.

3. Select PROTOTYPE DEVICE > SLA500.DAT > OK

4. Set ABSOLUTE FACET DEVIATION to 0.000395.

5. SELECT BINARY > OK

IronCAD

1. PART PROPERTIES > RENDERING

2. Set FACET SURFACE SMOOTHING to 150.

3. FILE > EXPORT

4. CHOOSE .STL

Mechanical Desktop

1. Use the AMSTLOUT COMMAND to export your .STL file.

2. The following command line options affect the quality of the .STL and should be adjusted to produce an acceptable file:

    *   Angular tolerance: This command limits the angle between the normals of adjacent triangles. The default setting is 15 degrees. Reducing the angle will increase the resolution of the .STL file.

    *   Aspect ratio: This setting controls the height/width ratio of the facets. A setting of 1 means the height of the facet is no greater than its width. The default setting is 0, ignored.

    *   Surface tolerance: This setting controls the greatest distance between the edge of a facet and the actual geometry. A setting of 0.0000 causes this option to be ignored.

    *   Vertex spacing: This option controls the length of the edge of a facet. The default setting is 0.0000, ignored.

Solid Designer

3. FILE > EXTERNAL > SAVE .STL

4. Select BINARY MODE

5. Select part.

6. Enter filename.

7. Enter maximum deviation distance of .01 MM.

8. OK

Solid Edge

1. FILE > SAVE AS

2. Set SAVE AS TYPE to .STL

3. OPTIONS

4. Set CONVERSION TOLERANCE to 0.001 inch or .0254 MM.

5. Set SURFACE PLANE ANGLE to 45.00.

6. SAVE

Unigraphics

1. FILE > EXPORT > RAPID PROTOTYPING

2. Set OUTPUT TYPE to BINARY.

3. Set TRIANGLE TOLERANCE to 0.0025.

4. Set ADJACENCY TOLERANCE to 0.12.

5. Set AUTO NORMAL GEN to ON.

6. Set NORMAL DISPLAY to OFF.

7. Set TRIANGLE DISPLAY to ON.

Also, CATIA can be used to create STL files. In this project Pro/ENGINEER 2001/Wildfire is used.

2. Locating the designed part onto the building platform using Magics

After the design stage the *filename.stl* is opened by using Magics Software. In Biltir METU-CAD/CAM Center Magics 8.0 is being utilized. This software is intended for rescaling, locating a part on the platform (translation and rotation), checking design errors, and cutting a designed part into different small parts. For the rescaling a designed part it includes also shrinkage compensation as given in Table C1.

Table C1: Scaling Factors for Polyamide (PA 2200) in EOSINT P 380

Specimen height(mm)	x&y (scaling factor	Z(scaling factor)
z<20mm	1.032	1.013
20<z<50mm	1.032	1.014
50<z<100	1.032	1.016
100<z<200	1.032	1.017
z>200mm	1.032	1.018

Scaling factor for any length value in either x or y direction is constant as in Table C1. However, in z-direction scaling factors vary in respect to the height of the part to be manufactured. Furthermore, the platform which is mentioned above corresponds to the building platform of SLS. Therefore, the way the part is z-oriented in the Magics determines the appearance of the layers on the part to be produced. This is the critical stage in preparing a part for production specifically on the aesthetics of the part. However, there is one crucial factor which is the cost of production which depends on part height. This implies that there should be a trade-off between aesthetics and the production cost (C4 & C5).
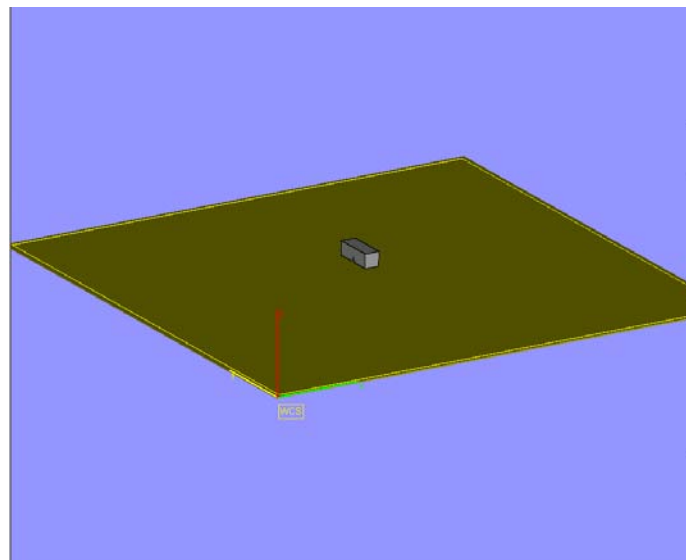
Figure C4: Specimen is in horizontal position on the building platform revealing low cost and poor aesthetics.
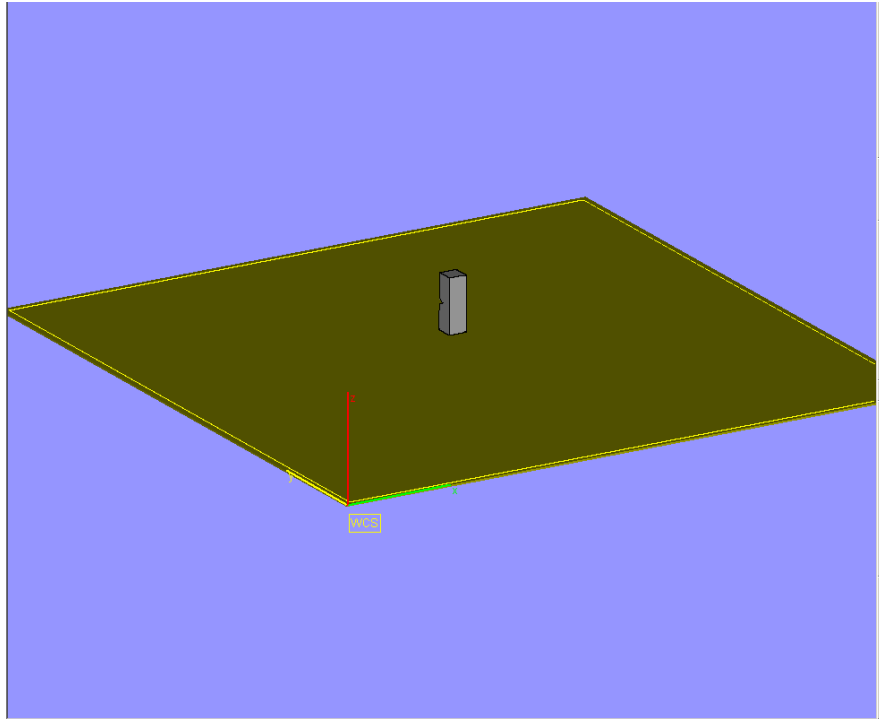
Figure C5: Specimen is in vertical position on the building platform revealing high cost and better aesthetics.

Apart from locating the part on the platform, Magics helps to discover design errors which are not generated due to file conversion to STL, but rather inherited from the in-correct solid models (Figure C6). These errors may cause inconvenience to the RP process.
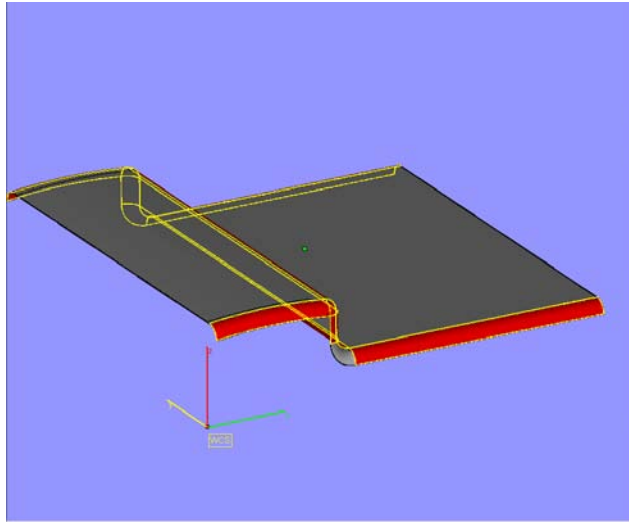
Figure C6: The picture of a STL model generated from an incorrect solid model.

3. Slicing by using EOS-RP-Tools

From Magics follows slicing work which is performed for producing files with *.sli* format. EOSINT P380 uses EOS-RP-Tools for slicing a CAD. It involves only few steps like opening the program followed by opening the file you want to slice and so on. These steps are illustrated by the use of images below (C7, C8 & C9). After slicing business is over the new file will be created with the extension *.sli.* The example file is Fig. C10 which is for the Scanning Electron Microscope (SEM) specimen used in this project.
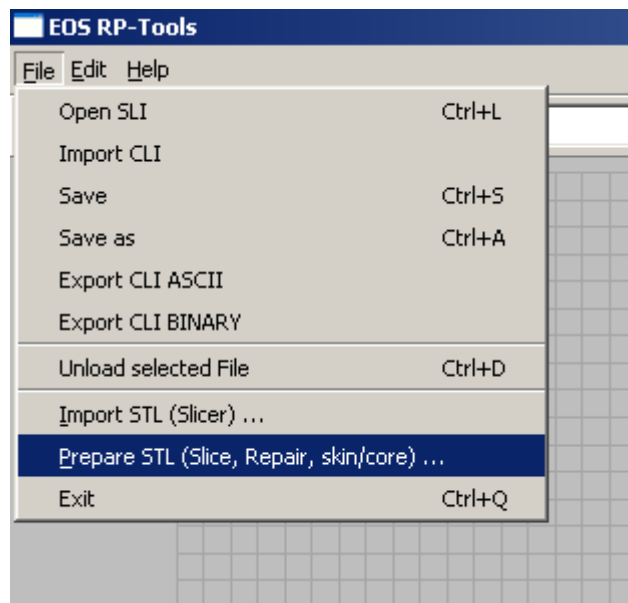
Figure C7: Loading Part for Slicing
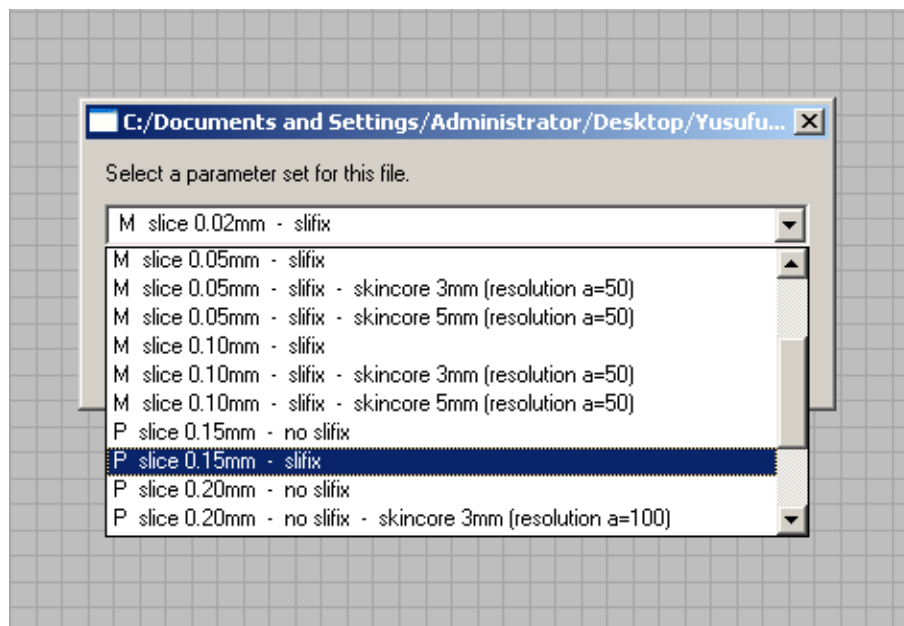
Figure C8: Choosing the material type and slice thickness
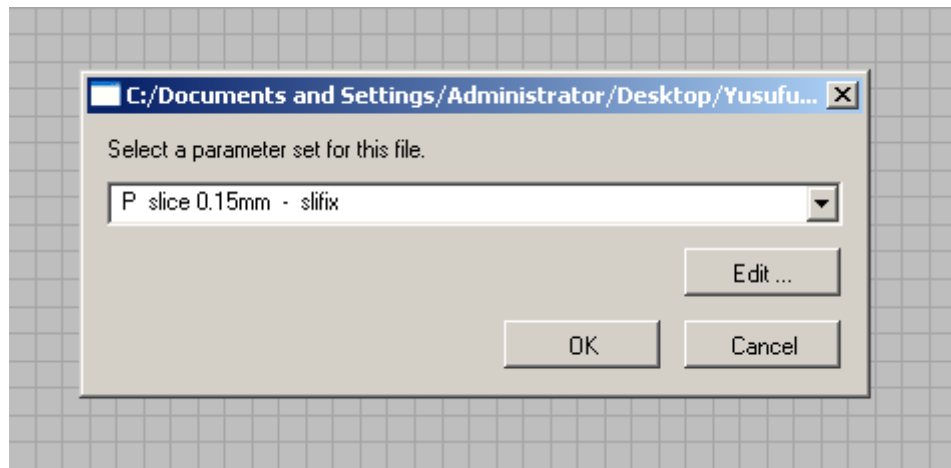
Figure 9: Click Ok and Slicing begins

Figure.10: .sli File for the SEM Specimen

4. Loading parts into PSW P3x0 Software

SLI files before they are used for production one more step is vital which is usually known as job creation which results in *filename.job* file format. There are various activities which have to be accomplished as explained step by step below:

- Create a new folder like Manuf_13_03_2007-05-22

- Copy all EOS Layer Files into this folder

- Open PSW P3x0

- File>Load Parts(See Fig.C11)
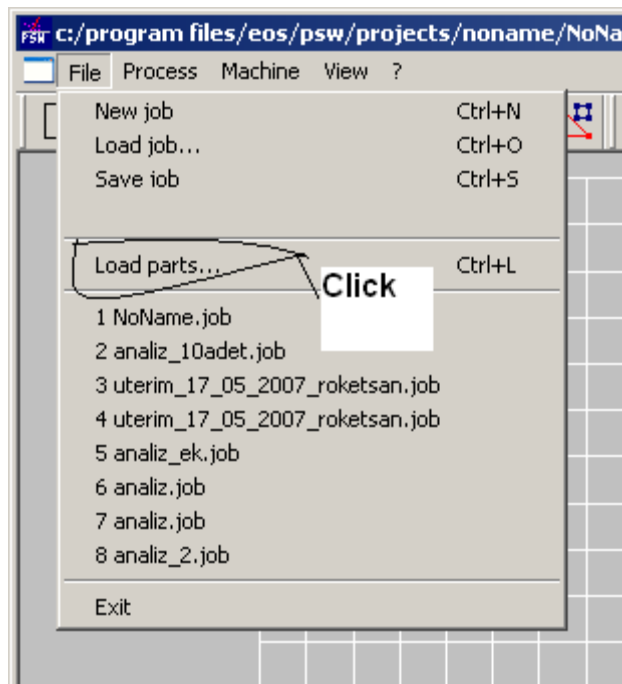
Figure.11: Loading Parts

- Choose all parts to be manufactured (Fig.C12) and click open

- Locate every part to the required position

- Assign the required exposure parameter to every part if necessary. To do so follow these steps:

  1. Click the exposure parameter icon (Fig.C13).

  2. Under new exposure type write down the exposure name, example s1.

  3. Click New.

  4. To modify the parameter values , click the exposure parameter name example s1 example (Fig. C14).

Make all necessary modification of exposure parameters.

5. Click either OK or Apply.

6. Choose the specimen by clicking it as shown in Fig.C15.

7. Click Job Parameters' icon (Fig.C16)

8. Go to exposure type and then scroll down to the appropriate exposure name, example s1. (Fig.C17) and then click ok.
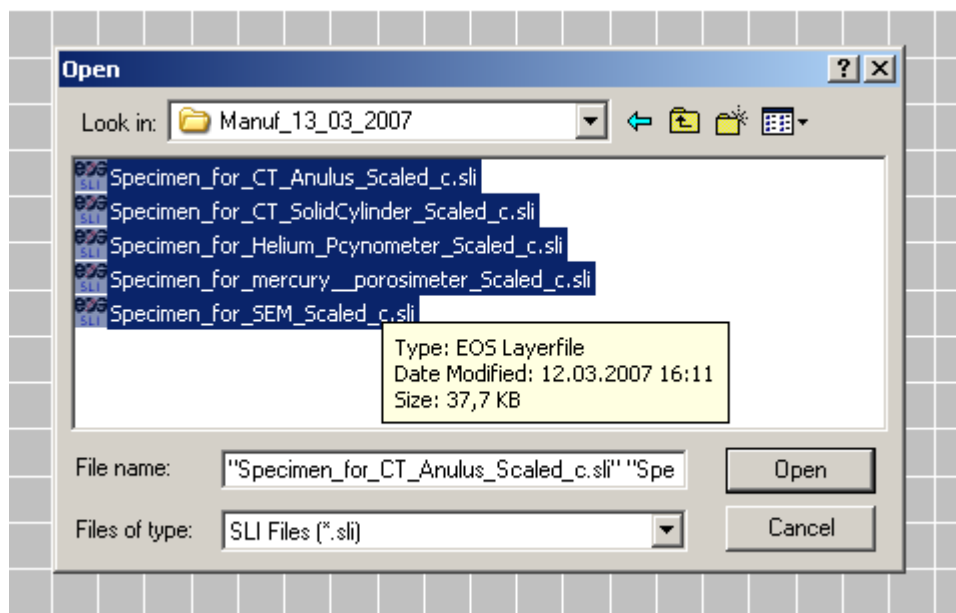
Figure C12: Choosing Parts and then load them
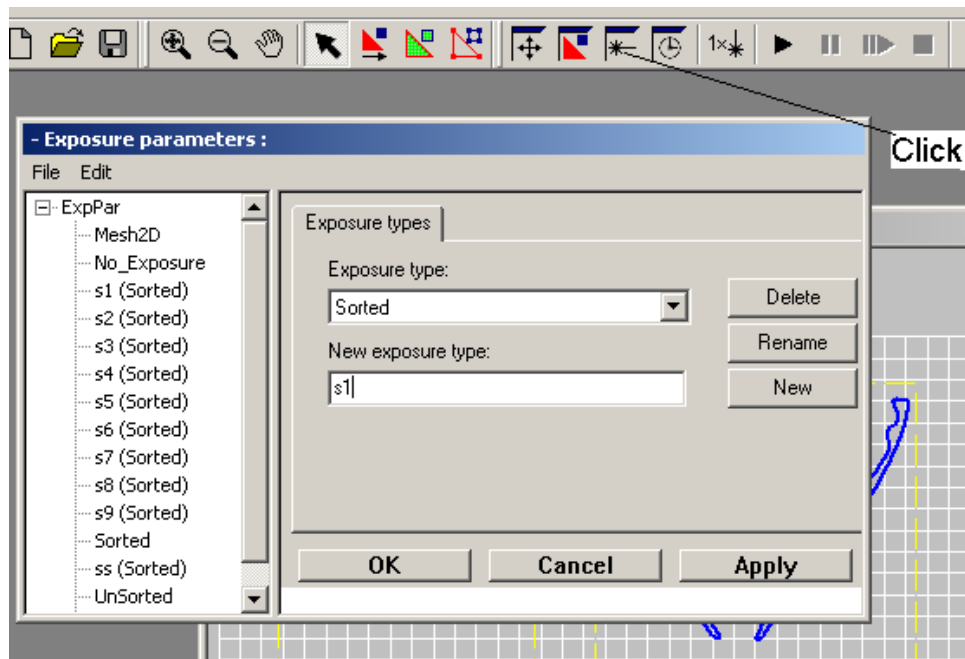
Figure C13: Naming exposure type
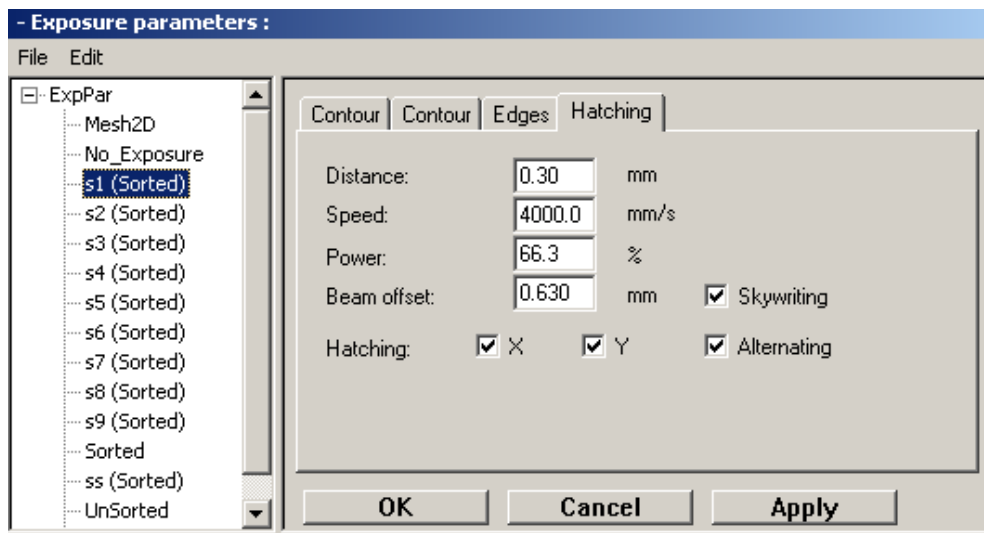
Figure C14: Entering the desired values of the exposure parameters

144
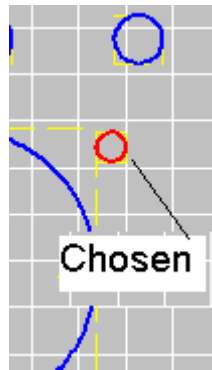
Figure C15: Chosen part
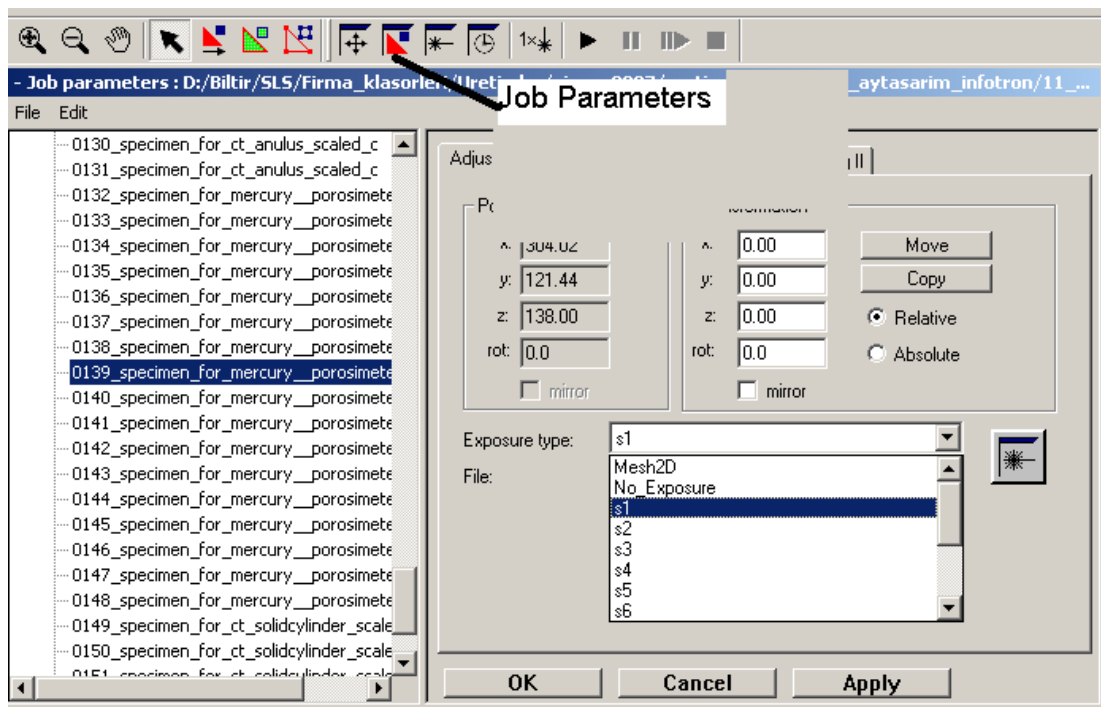
Figure C16: Example of assigning the desired exposure parameter setting onto the solid model to be sintered
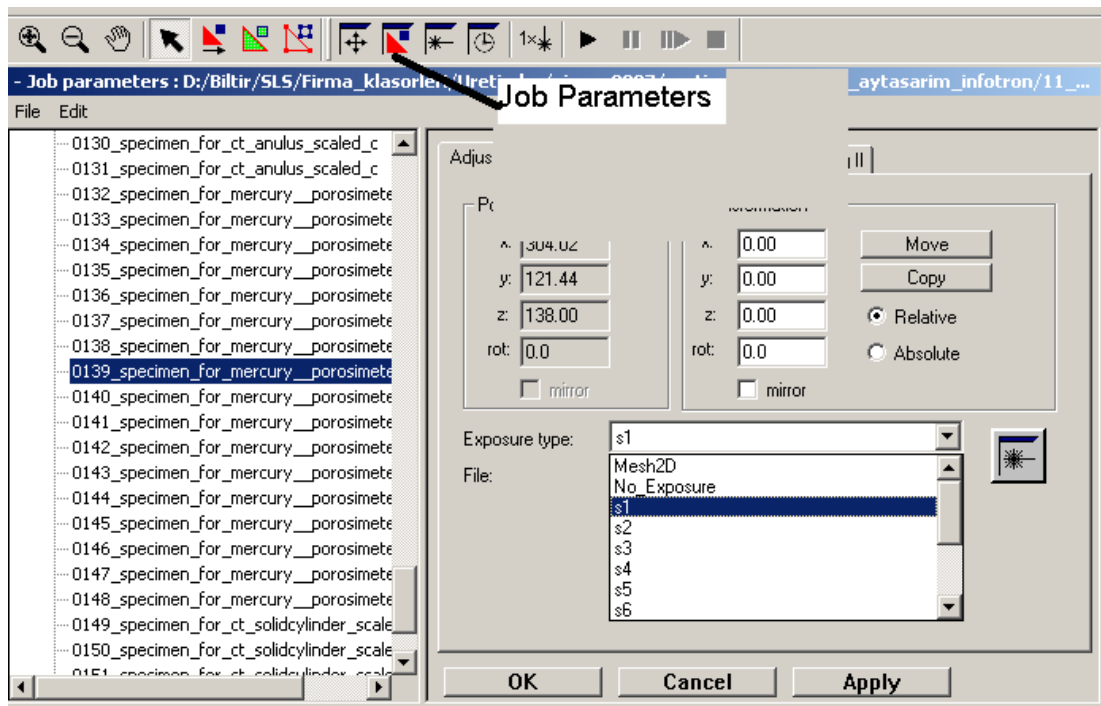
Figure C17: Assigning Job Parameters onto the specimen

Theoretical Process-Basics

a) Standard exposure types *sorted* and *unsorted*

Basically, there are two different standard exposure types: The Hatch types **"Sorted"** and **"Unsorted".** The "Sorted" strategy searches the shortest exposure way across the part, whereas the "Unsorted" strategy moves across the part in the easiest way (Figure C18).
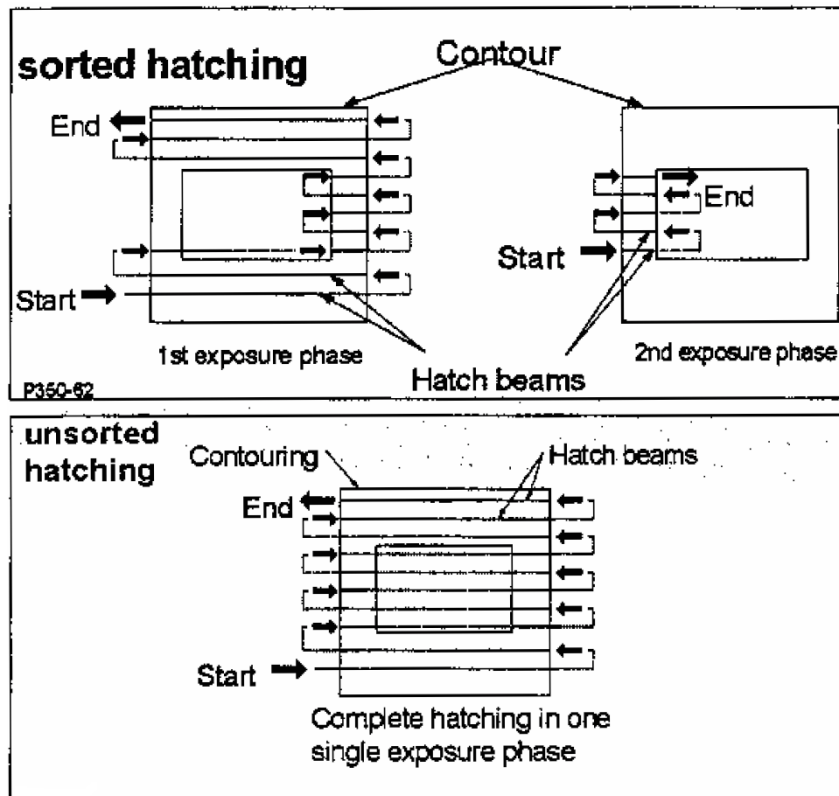
Figure C18: Exposure types sorted and unsorted

The sorted exposure type **sorted** is usually substantially faster than the **unsorted** type. For parts, on which the hatch on the surface is visible, it can lead to gaps or slight recesses, which can eventually get in the way (sorting **edges**). In the case that a high quality part surface is needed, the type **unsorted** should be used, which can however increase the building time substantially. In the window **Exposure parameters,** the exposure types sorted and unsorted have the same tabs with the same functions, as these types differ only in the exposure path over the part.

Contour tab
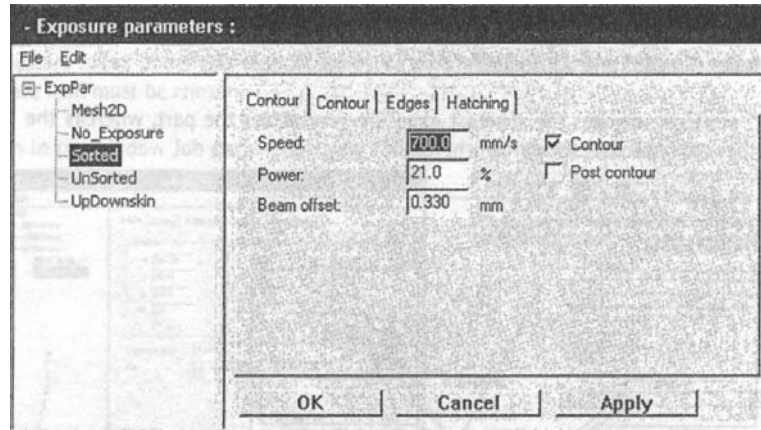
Figure C19: Contour Tab

<u>Speed</u>

Contour speed should not be chosen greater than 700mm/s for polyamide and 800mm/s for polystyrene. In the case of higher speeds, contouring errors arise through the inertia of the mirrors.

<u>Power</u>

The laser power is inputted as percentage of the maximum power of the laser. The inputted value depends on the material/layer thickness, with which the part is built. The standard values for the appropriate material is given in Watts.

Beam offset (displacement):

On exposure of the contour, offsets the path of the center of the laser beam

inwards by the value entered. (Fig.C20)
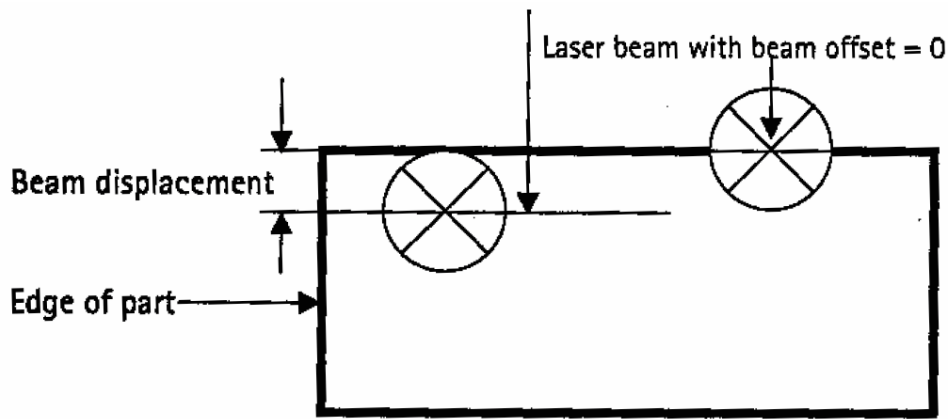
Figure C20: Beam displacement of contour

Contour selected:

The laser beam exposes the contour

Post Contour selected:

The contour is exposed after the exposure of the hatching.

Hatching tab
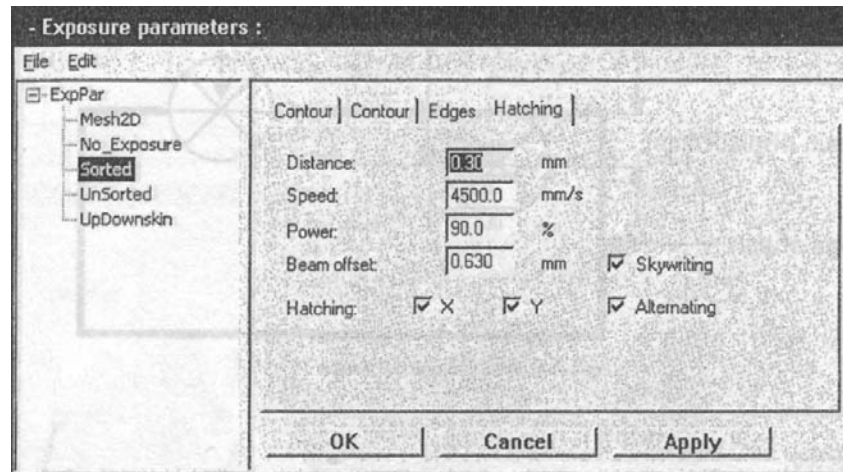
Figure C21: Hatching Tab

Distance:

Distance between the hatch lines in X and Y direction is inputted here. The distance between hatch lines is the measure by which the hatch beam is shifted after   each line 90° to the hatch direction. This spacing must be smaller than the beam diameter, otherwise a connection between the lines is not guaranteed.

Speed:

The hatching speed is dependent on the material.

Power:

Here the laser power is inputted as a percent of the maximum power of laser. The inputted value depends on the material/layer thickness, with which the part is built.

Beam offset:

During the exposure of the hatching, offsets the path of the center of the laser beam from   the   nominal contour of the part by the value entered towards the inside. The value of the beam offset for the hatching should always be larger than the value of the beam offset for the contour, otherwise the hatching moves outside the contour. This can lead to a bad surface quality of the part. Furthermore, the distance should be chosen in such a way that the laser beam forms an intersection between the contour and the hatching (C22).
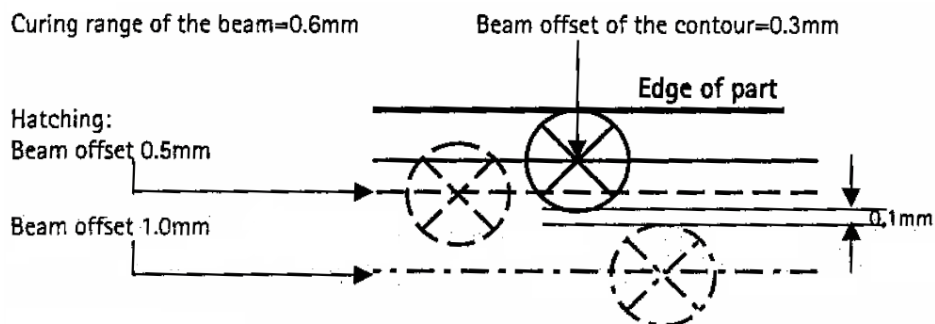
Figure C22: Example hatching beam offset.

Hatching:

1. only x-direction selected: Implies that each layer is hatched in X-direction
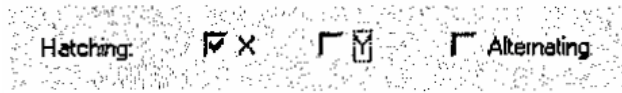
Figure 27: Hatching in X direction selected
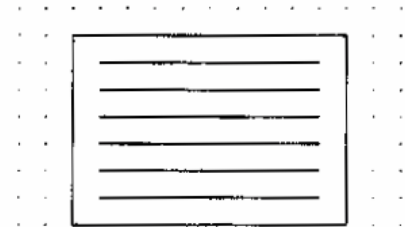
Hatching lines X direction

2. only y-direction selected: Implies that each layer is hatched in Y direction

Fig. 28 Hatching Y
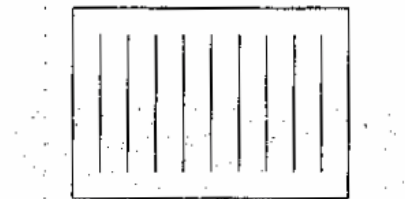
Hatching lines Y direction

3. x and y direction selected:

Each layer is hatched in X and in Y direction.
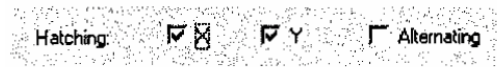
Fig. 29 Hatching X and Y
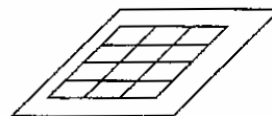
Hatching lines X and Y Direction

4. Alternating is selected(Standard):

Fig.30 Hatching Alternating

Alternating

-changes the direction of the hatch lines from layer to layer.

Skywriting:

Because of the mass inertia of the scanner mirrors, a certain time is needed in order to accelerate the mirrors to the desired speed. During this time the laser beam covers the distance $s=0.5*a*t^2$. Within this distance, the exposure speed is not constant. More energy is applied at the edges of the part than in the inside of the part. This may have an adverse effect on the quality of the part (Fig.C23). In order to guarantee a stable amount of energy, Skywriting is selected.
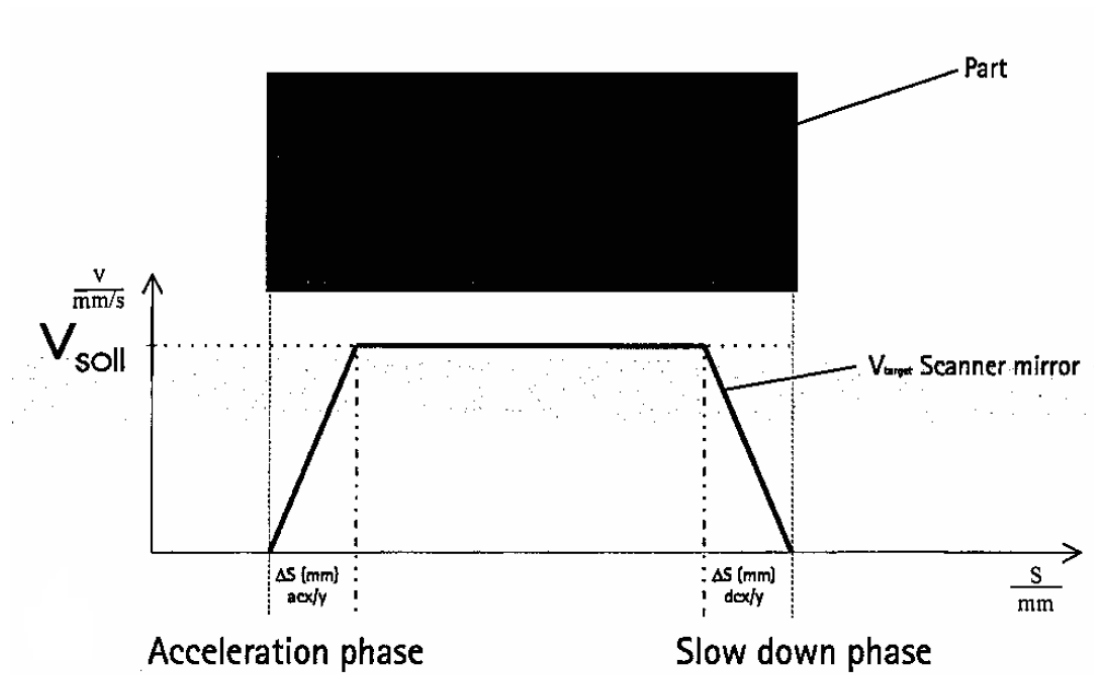
Fig.31: Speed progression (without Skywriting) of the scanner mirror in function to distance covered

Figure C23: Speed progression without skywritting

Figure C24: Skywriting is chosen

Edges tab

This function is needed for parts, which have points and/or very thin wall thickness. **Edges** first selected, when the peaks/walls are **<2xBeam offset (BO) of the contour** (this corresponds usually to the curing range of the laser beam) (C25 and C26).
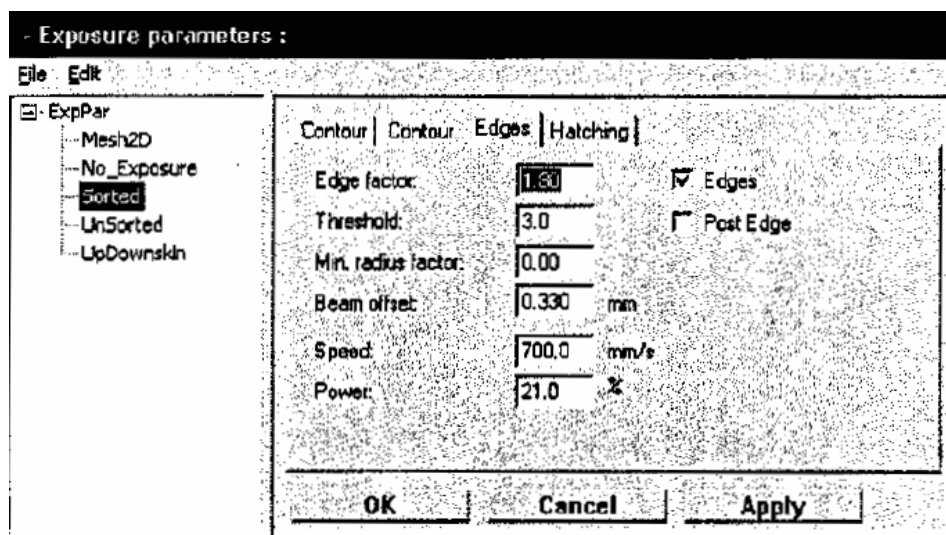
Figure C25: Edges
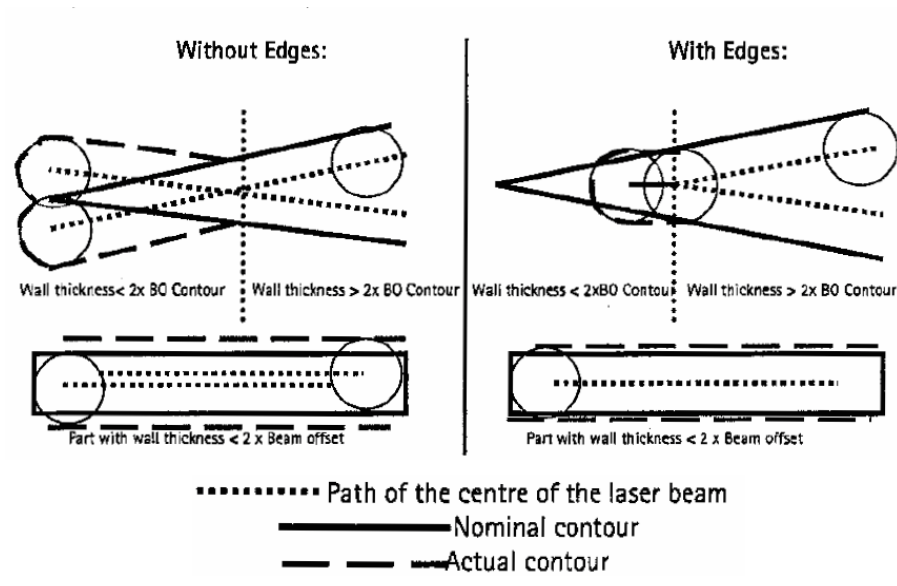
Figure C26: Edges as a function of wall thickness of part

Edge factor

This defines the level of exposure for points starting from the outermost points on the nominal contour. Exposure for points=edge factor x beam offset (Figure C27).

1 Path of the centre of the laser beam
2 Nominal contour
3 Actual contour
4 Exposure of points
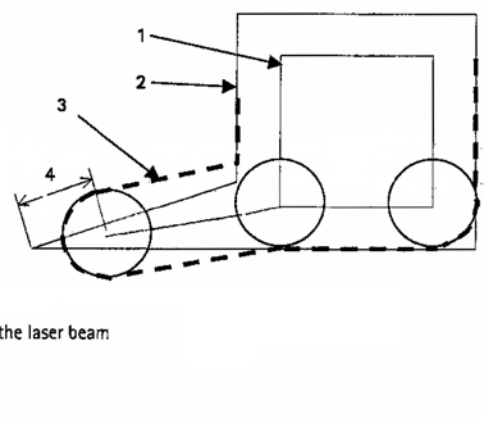
Figure C27: Level of exposure

Threshold:

If the distance from the actual contour **(3)** to the nominal contour **(2)** at a point exceeds the value **threshold x beam offset**, then this point is exposed with an **edge factor of 1.45.**

Min.radius factor:

This defines the level of exposure of the points as a function of the radius of the laser beam. This means that thin walls up to a wall thickness of 2 x radius factor are exposed, thinner walls are not exposed. Points are driven out up to a wall thickness of 2 x radius factor. The level of exposure of the points/thin-walled parts is defined either by the exposure for the points (edge factor x beam offset) or by the minimum radius factor. This is why the value "0" is entered as the standard value for the min. radius factor. Thus, this ensures that very thin-walled parts are also exposed and the boundary is regulated by the exposure of points.

Beam offset:

Beam offset defines the start point for the exposure of the points from the inside of the part. This value is additionally needed for the calculation of the exposure of the points. This value is the same as the value for the beam offset of the outermost contour.

Speed:

Speed for the exposure of the points. The speed that is used for the contour exposure is used as standard here.

Power

Laser power for the exposure of the points. The power that is used for the contour exposure is used likewise as standard here.

b) Basic exposure type UpDownskin

This exposure type is a mixture between sorted and unsorted. The building time moves therefore between the building times of sorted (fast) and unsorted (slower) (Figure C28). With this exposure type, the software checks in every layer, whether an exposed area is above or below the exposed area of the layer, i.e., whether it covers these. The .the result is Upskin, Downskin or Inskin. The tabs Contour, Edges and Hatching have the same functions as already described under exposure types sorted/unsorted.
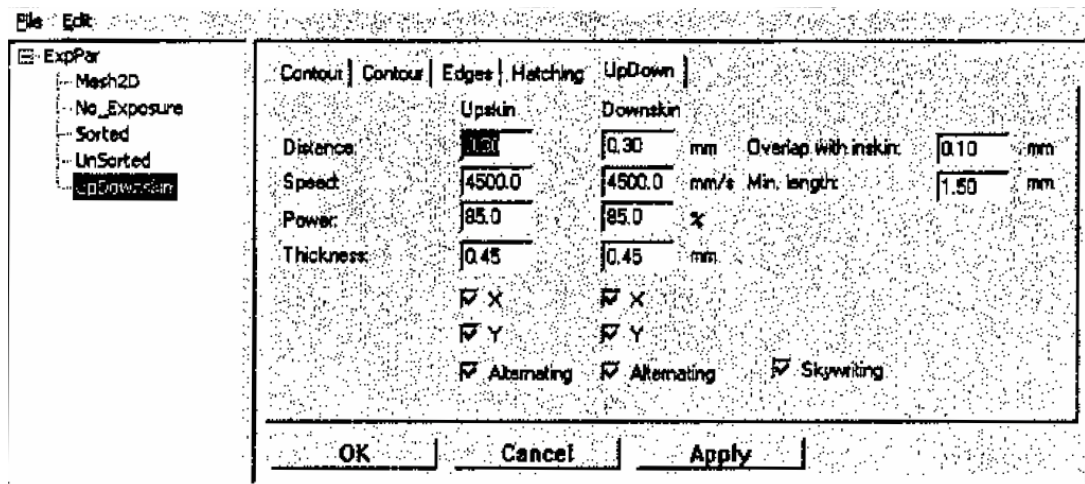
Figure C28: UpDownskin Tab

UpDown tab

1   Hatch   0   Upskin

2   Thickness Downskin   X   Downskin

    Overlapping   Inskin
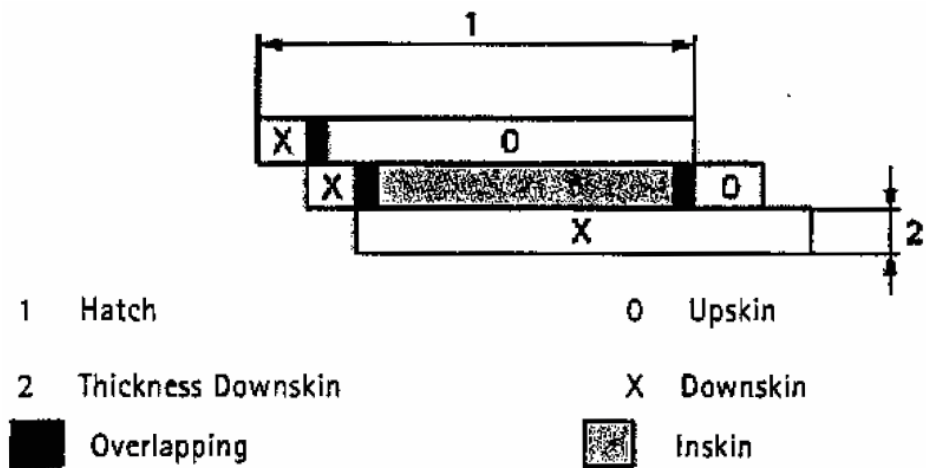
Figure C29: UpDown Tab

- **Upskin:**

  Exposes areas above which there is no exposed area. This area is exposed using "unsorted".

- **Downskin:**

  Exposes areas below which there is no exposed area. This area is exposed using "unsorted".

- **Inskin:**

  Exposes areas above and below which there are exposed areas. The parameters for this are found in register **Hatching.** This area is exposed using "sorted".

- **Overlapping:**

  Area for improved joint between inskin and upskin- or downkin

Distance Upskin and Downskin:

This is the distance between hatch lines in the **Upskin/Downskin.** As standard value, it is recommended the same value, as is inputted in the **Hatching tab** under **Distance.**

<u>Speed Upskin and Downskin:</u>

Speed for the exposure in the **Upskin/Downskin.** As standard value, it is recommended the same value, as is inputted in the **Hatching tab** under **Speed.**

<u>Power Upskin and Downskin:</u>

Laser power for the exposure in the **Upskin/Downskin.** As standard value, it is recommended the same value, as is inputted in the **Hatching tab** under **Power.**

<u>Thickness Upskin and Downskin:</u>

Defines how thick the **Upskin /Downskin** areas are for which the values entered apply. For layers of 0.15mm is a value of 0.45mm sufficient (equals 3 layers).

<u>Hatching X, Y and Alternating for Upskin and Downskin:</u>

Same function as under **Hatching** tab apply.

<u>Overlapping with inskin:</u>

Overlapping of **Upskin/Downskin** to **Inskin.** An overlap of 0.1mm is usually sufficient.

Min.length:

Minimum length of **Upskin/Downskin** hatch lines. If the **Upskin/Downskin** hatch lines are shorter than the minimum length, the values for the Upskin/Downskin hatch lines are added to the **inskin.** For this value of 1.5mm can be used as reference value.

c) Basic exposure type Mesh2D

The core is exposed by certain applications (i.e., Skin/Core) with this type of exposure (Figure C30). In place of continuous hatches, a mesh comprising of stripes is generated within the part. The tabs Contour and Edges have the same functions as described already under the exposure types sorted/unsorted. The function **Edges** is however not used here.
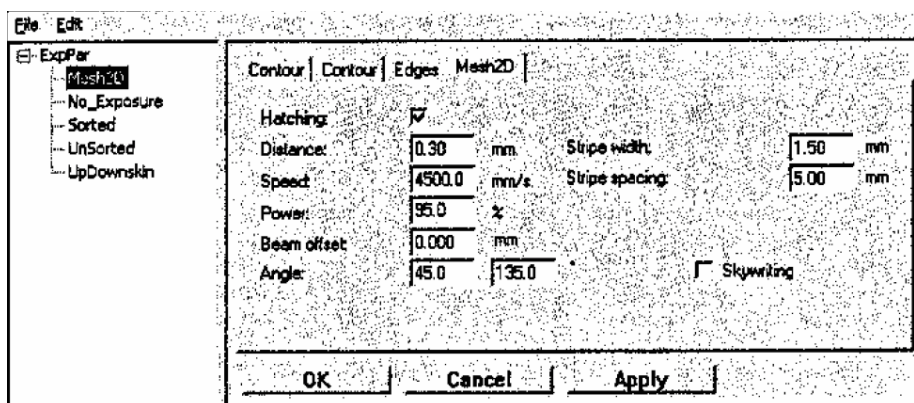
Figure C30: Mesh2D tab

Hatching: Hatches the stripes

Distance: Distance between the hatch lines within the stripes

Speed: Exposure speed for the hatching stripes

Power: Laser power for the hatching the stripes

Beam offset: During the exposure of the stripes, offsets the path of the center of the laser beam from the nominal contour of the part by the value entered towards the inside.

Angle: Angle of the stripes to the X axis

➢ left field: Angle α to the X axis(counter clockwise-see Fig.34)

➢ right field: Angle β to the X axis(counter clockwise-see Fig.34)

Stripe width: Width of the stripes

Stripe spacing: Distance between the stripes

Skywriting: Same function as described before. However, it is not used here.
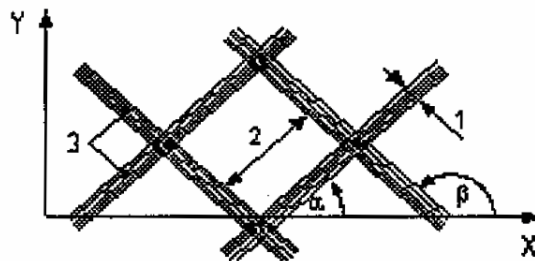
Fig.39. Mesh 2D

| | Stripe width | 3 | Hatch lines |
| 2 | Distance between stripes | α, β | Angle of the stripes to the X axis |

Figure C31: Parameters for the Mesh2D

d) Basic Exposure type No-Exposure

If this exposure type is assigned to a part, no exposure of the part takes place.

5. Loading the *filename.job* into the computer which is connected to the RP-Machine.

From step 4 the CAD is ready for manufacturing. Therefore, transfer the created folder example Manuf_13_03_2007-05-22 into the computer which is connected to the RP-Machine. Follow all necessary steps until the building process starts.

The procedures explained above have to be followed in producing other parts like graded materials and also refer to Chapter 3 in this thesis on how graded parts have to be produced via selective laser sintering process. Figure C32, C33, and C34 shows the assignment of process parameter into different grades of Type I-3 Grades graded porous parts. The highlighted ones indicate the name of the grade, and the process settings used to produce the respective grades are shown on the right.
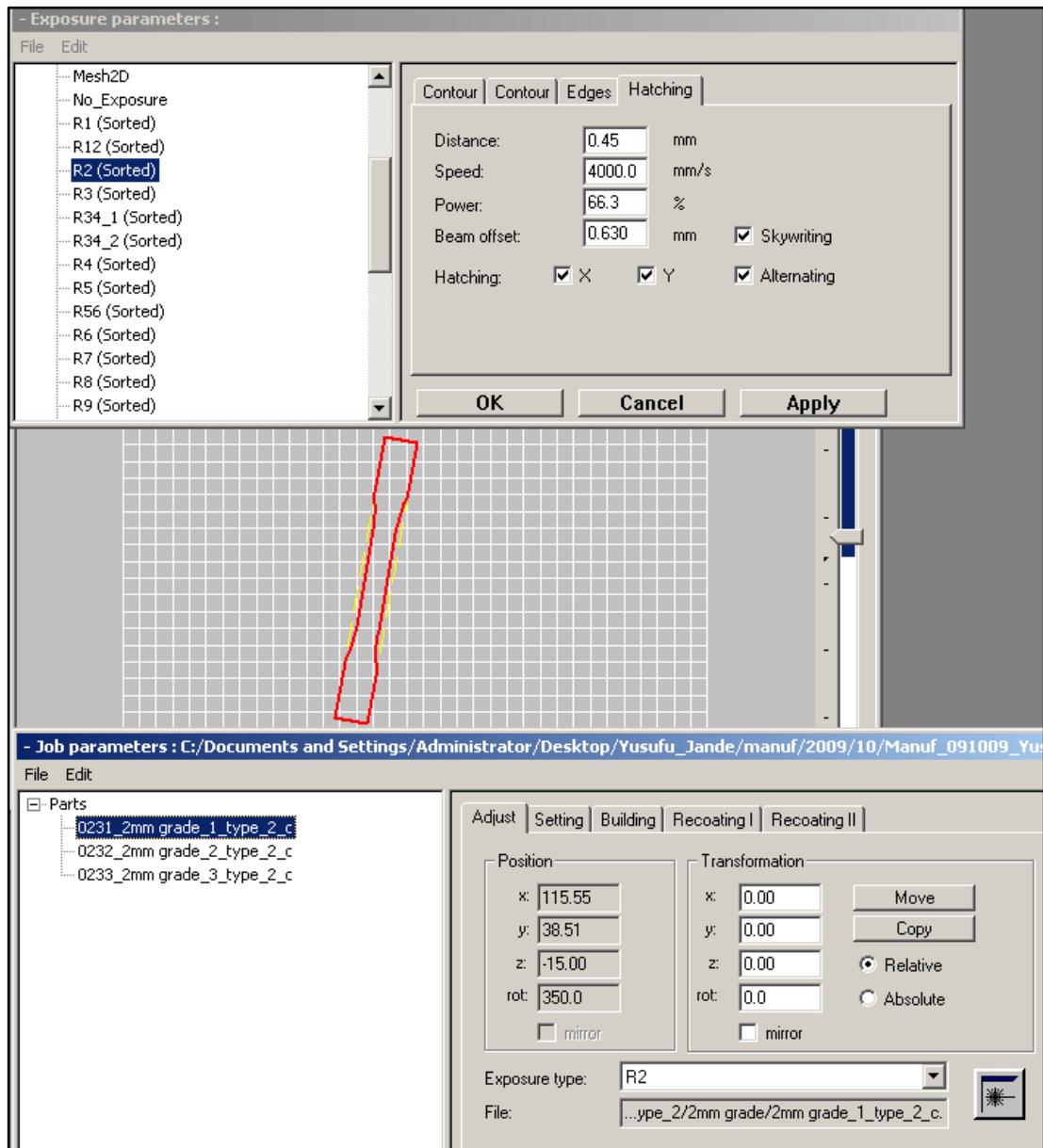
Figure C32: Assigning process parameter setting for Type II grade 1
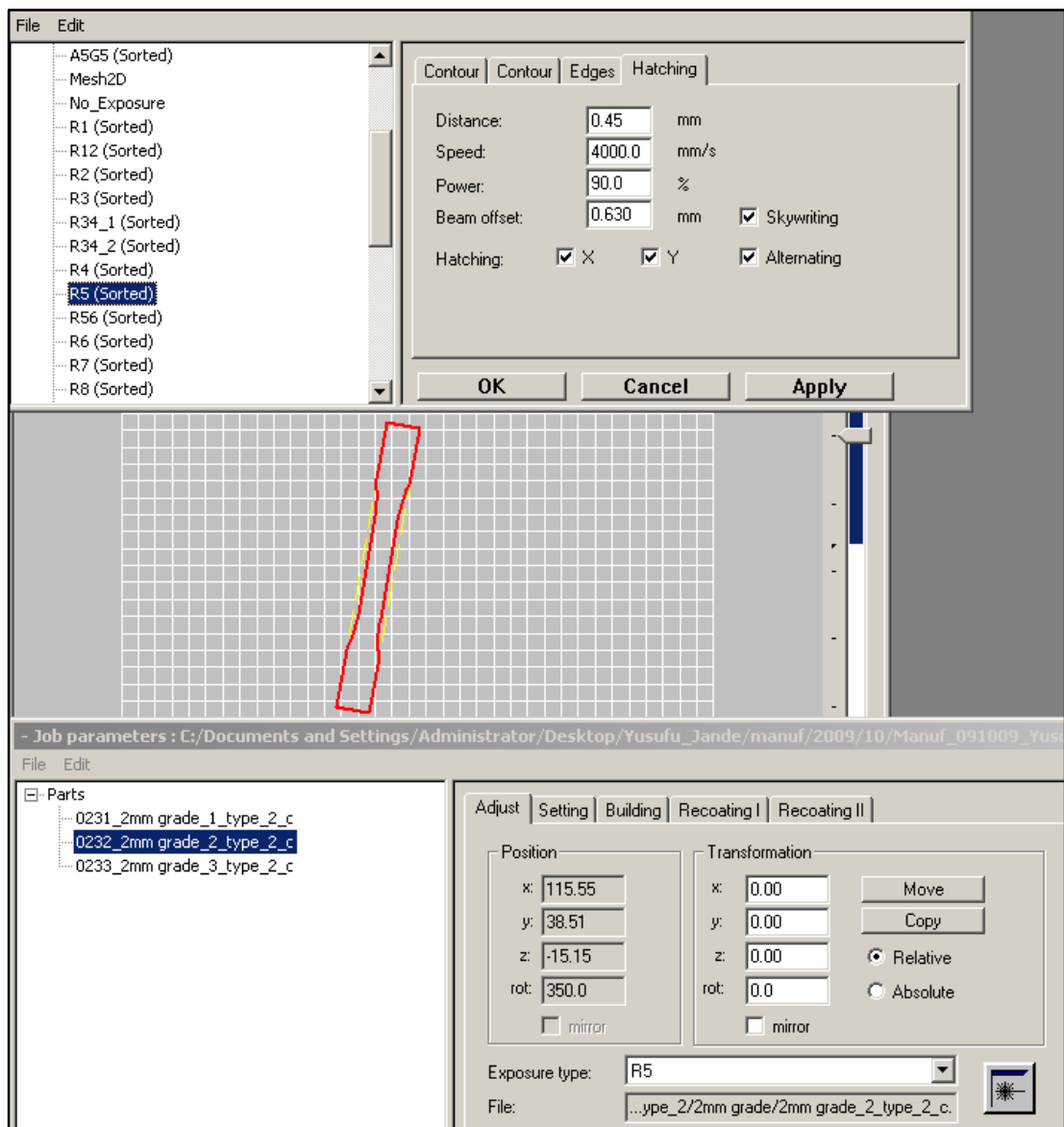
Figure C33: Assigning process parameter setting for Type II grade 2
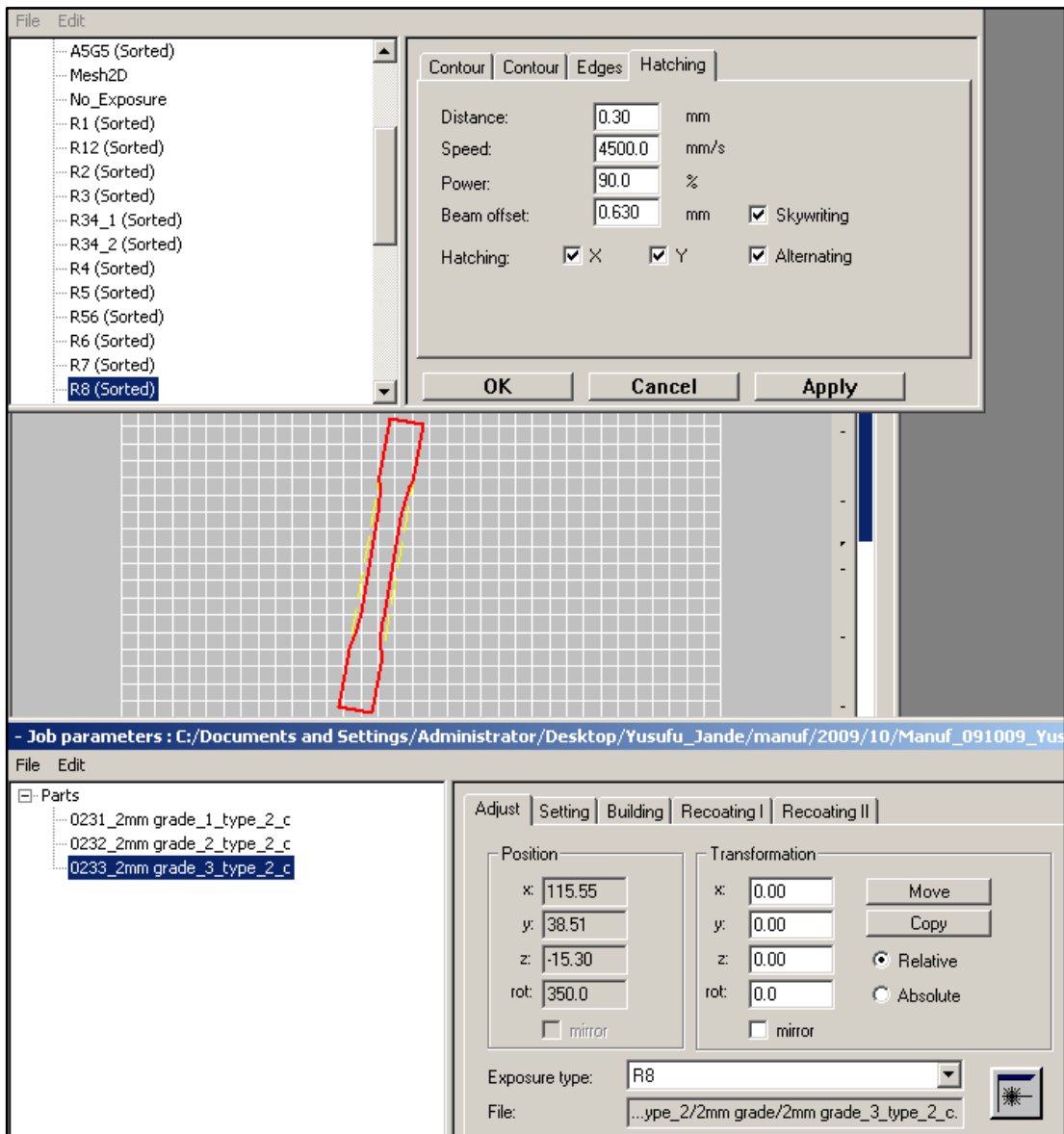
Figure 34: Assigning process parameter setting for Type II grade 3

APPENDIX D

CASING FOR SPECIMENS USED IN COMPUTED TOMOGRAPHY (CT) TEST
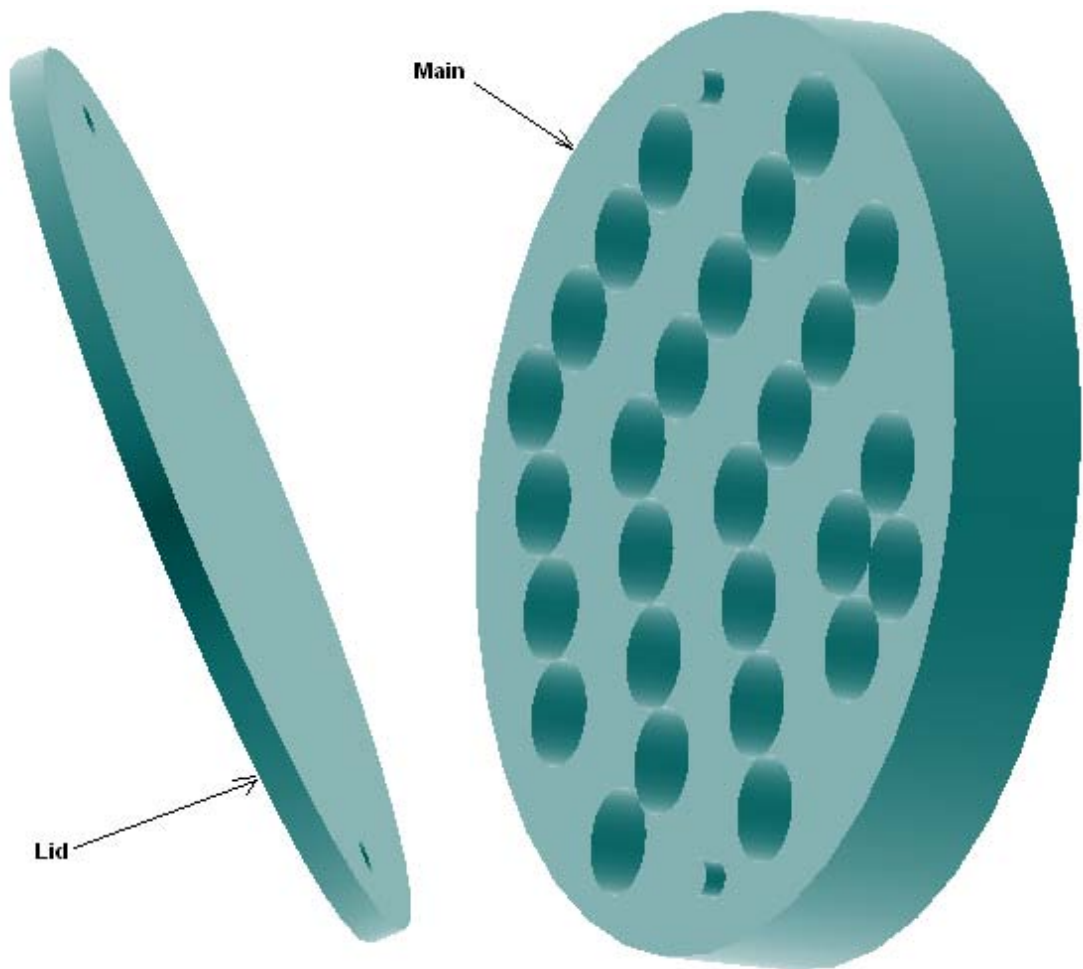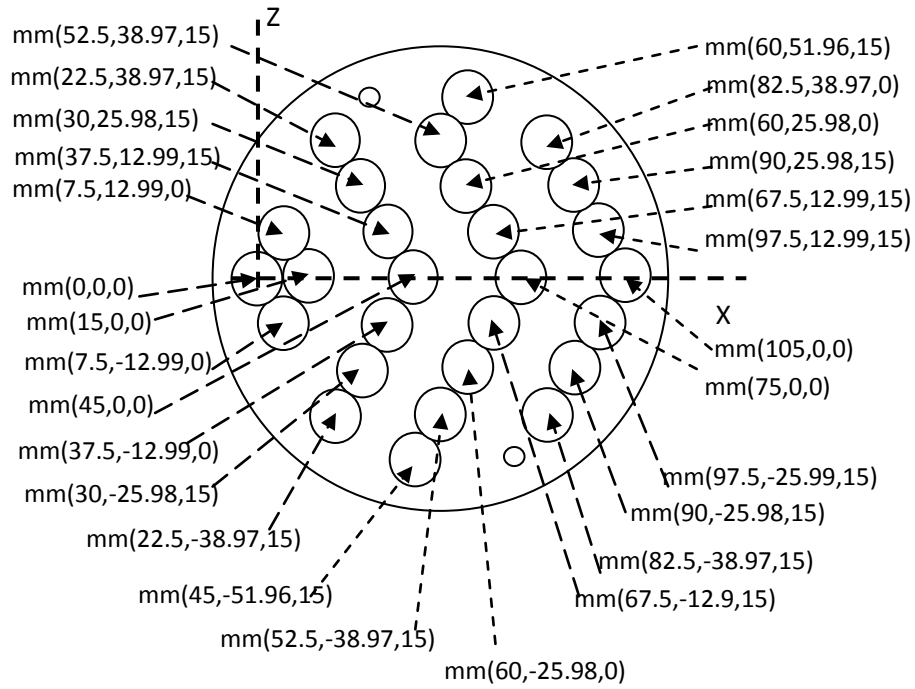
Figure D1: Position of sitting uniformly porous CT specimens in the casing

(centers with respect to xz plane)
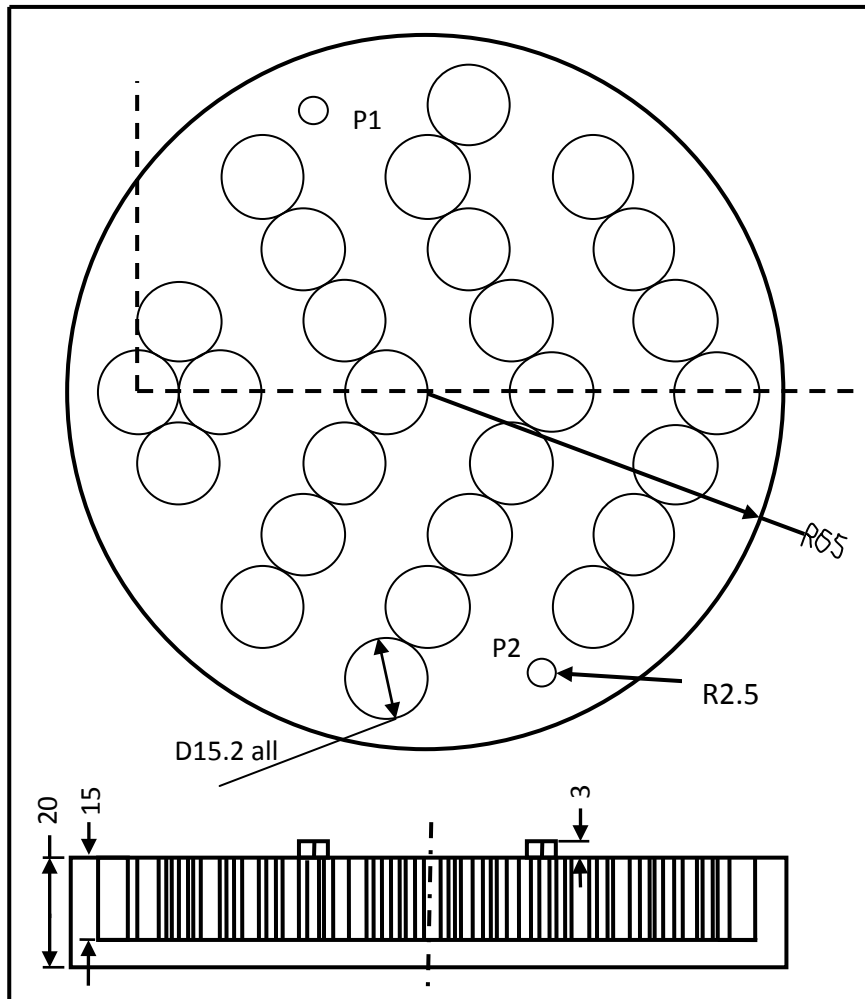
Figure D2: Dimensions of the casing body (dimensions in mm), P1 and P2
are guide pins
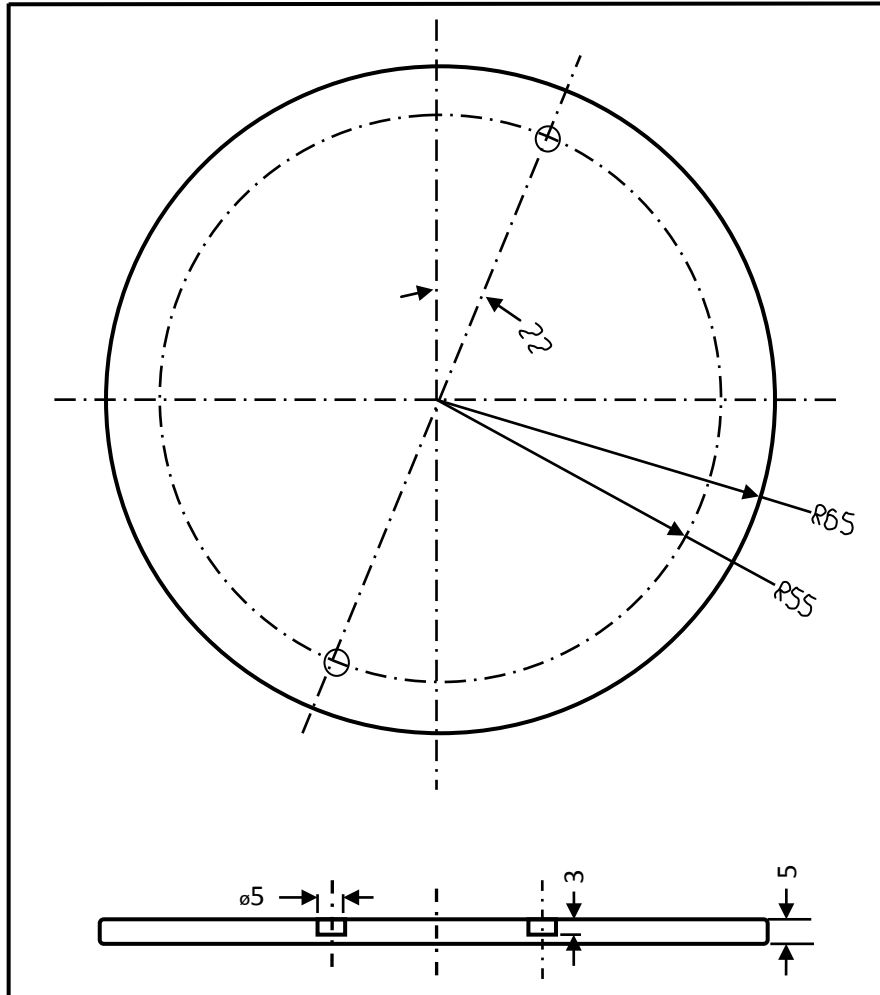
Figure D3: Lid Dimensions (in mm)

APPENDIX E

ADDITIONAL POROUS PART CHARACTERIZATION DATA

E1. Additional Porosimeter Results for Pore Size Distribution
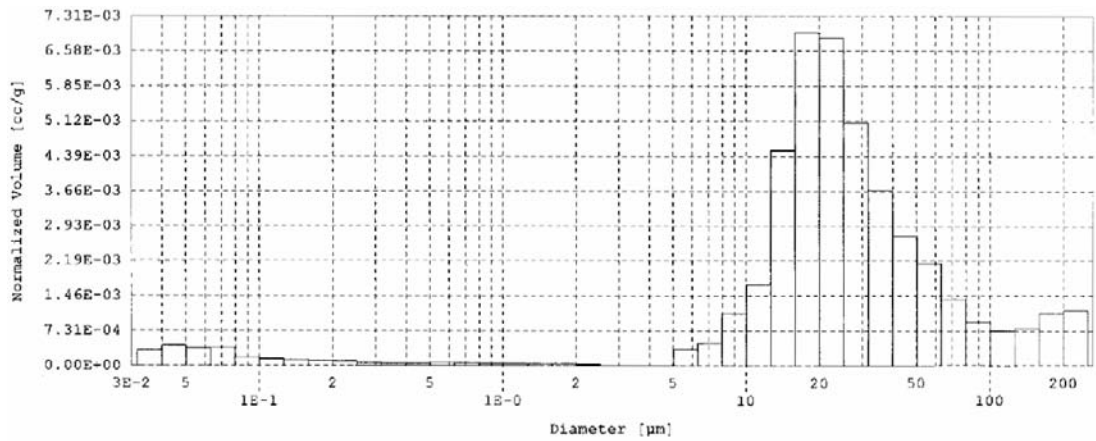
Figure E1: Pore Size Distribution for ED=0.019J/mm^2
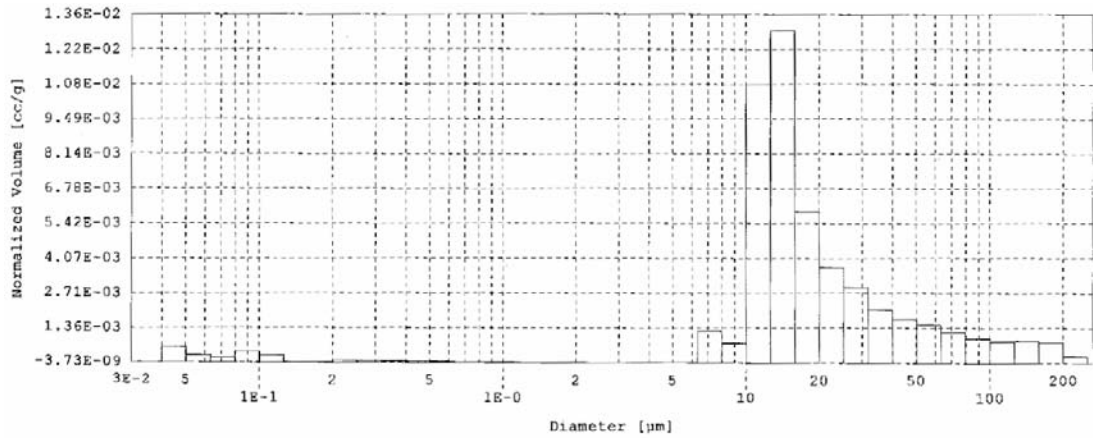
Figure E2: Pore Size Distribution for ED=0.020J/mm^2
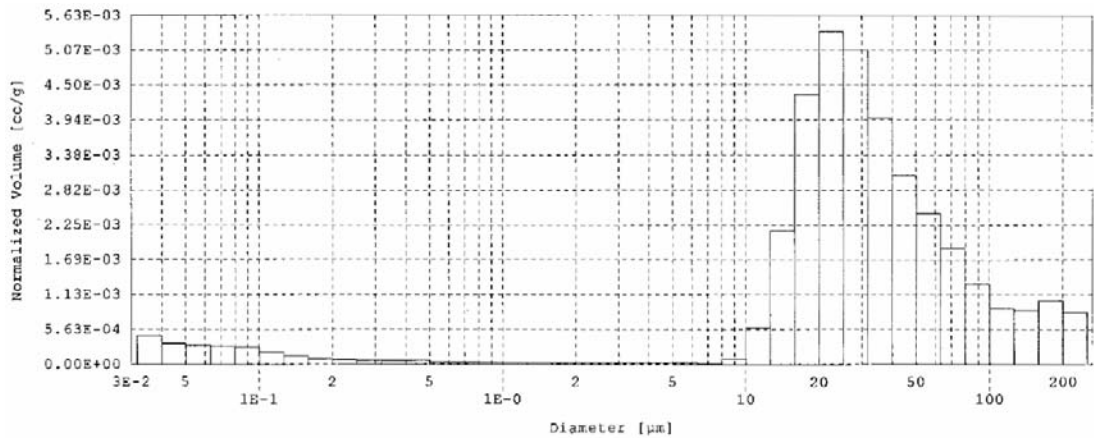
Figure E3: Pore Size Distribution for ED=0.023J/mm²
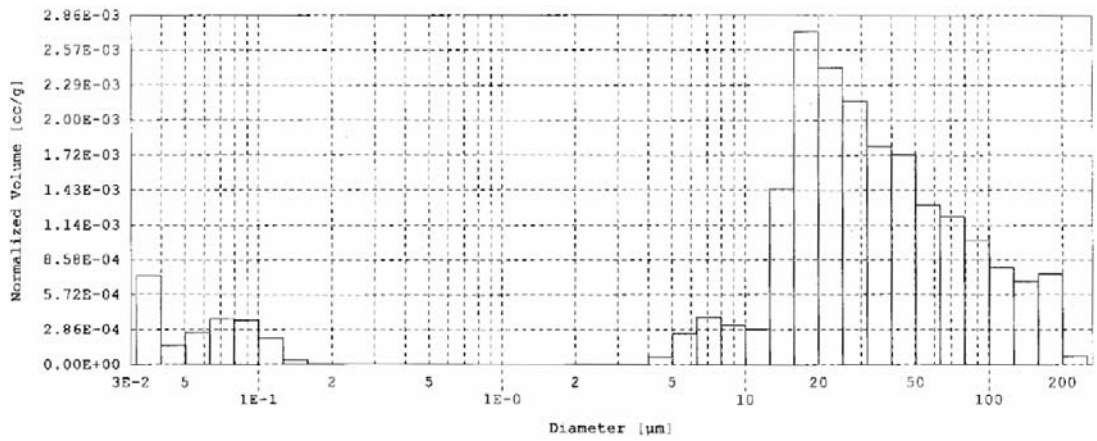
Figure E4: Pore Size Distribution for ED=0.029J/mm²
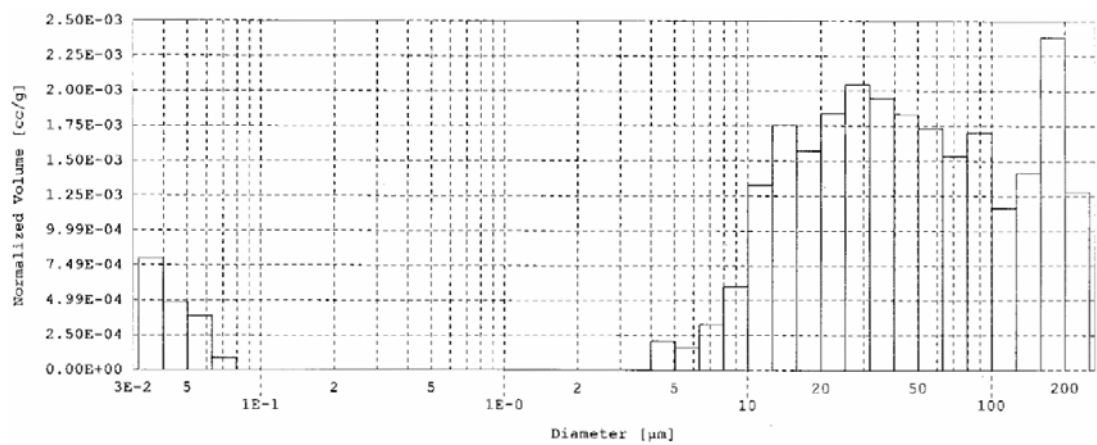
Figure E5: Pore Size Distribution for ED=0.030J/mm²

173
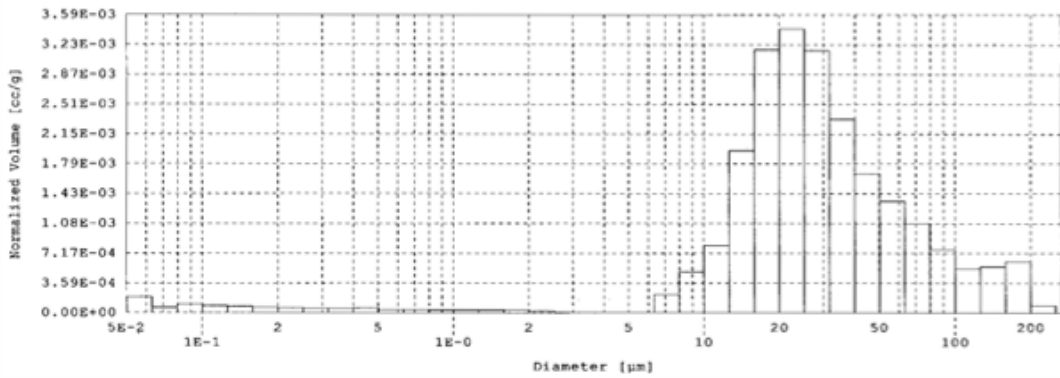
Figure E6: Pore Size Distribution for ED=0.033J/mm²

Numerical Data for Pore Size Distribution

Table E1: ED=0.029J/mm²

Report date: 08/10/2007   Merged File

QUANTACHROME INSTRUMENTS

QUANTACHROME POREMASTER FOR WINDOWS® DATA REPORT

VERSION 4.03

SAMPLE ID   CS1030407-8   FILE NAME   S780603H_Merged.PRM

SAMPLE WEIGHT   1.0000 grams   BULK SAMPLE VOLUME 1.0000 cc

SAMPLE DESCRIPTION M. TEKIN

COMMENTS   LP STATION 1

HG SURFACE TENSION 480.00 erg/cm²   HG CONTACT ANGLE   (I)140.00°,(E)140.00°

MINIMUM DELTA VOL. 0.000 % FS   MOVING POINT AVG. 11 (Scan Mode)

OPERATOR   K. BEHLULGIL   Mercury volume normalized by sample weight.

Pore Size Distribution By Volume - Intrusion

Printing every data point.

Pressure	Pore Diameter	Volume Intruded	Delta Volume	% Volume Intruded	Dv(d)	-dV/d(log d)
[PSI]	[µm]	[cc/g]	[cc/g]	%	[cc/(µm-g)]	[cc/g]
0.962	2.217E+02	0.0000	0.0000	0.00	5.355E-06	3.523E-03
0.990	2.156E+02	0.0000	0.0000	0.00	5.855E-06	3.994E-03
1.042	2.047E+02	0.0000	0.0000	0.00	6.648E-06	4.476E-03
1.135	1.879E+02	0.0002	0.0002	1.12	7.902E-06	4.955E-03
1.331	1.603E+02	0.0008	0.0005	3.65	1.045E-05	5.478E-03
1.571	1.358E+02	0.0013	0.0005	5.92	1.482E-05	6.008E-03
1.768	1.207E+02	0.0016	0.0003	7.54	2.186E-05	7.179E-03
1.991	1.071E+02	0.0020	0.0004	9.43	3.003E-05	8.237E-03
2.239	9.529E+01	0.0025	0.0004	11.51	4.081E-05	9.333E-03
2.508	8.504E+01	0.0030	0.0005	13.85	4.878E-05	9.972E-03
2.803	7.610E+01	0.0035	0.0005	16.38	5.734E-05	1.062E-02
3.122	6.834E+01	0.0041	0.0006	19.18	7.021E-05	1.165E-02
3.439	6.203E+01	0.0046	0.0005	21.45	8.488E-05	1.259E-02
3.756	5.680E+01	0.0051	0.0005	23.60	9.979E-05	1.344E-02
4.072	5.238E+01	0.0056	0.0005	25.81	1.154E-04	1.432E-02
4.390	4.859E+01	0.0060	0.0005	28.08	1.297E-04	1.492E-02
4.739	4.502E+01	0.0066	0.0006	30.88	1.455E-04	1.564E-02
5.117	4.169E+01	0.0072	0.0006	33.54	1.624E-04	1.628E-02
5.527	3.860E+01	0.0078	0.0006	36.21	1.863E-04	1.729E-02
5.968	3.574E+01	0.0084	0.0006	39.07	2.141E-04	1.835E-02

6.442	3.311E+01	0.0090	0.0006	41.67	2.444E-04	1.936E-02
6.948	3.070E+01	0.0096	0.0006	44.60	2.768E-04	2.028E-02
7.486	2.850E+01	0.0102	0.0006	47.59	3.051E-04	2.075E-02
8.055	2.648E+01	0.0110	0.0007	50.97	3.418E-04	2.159E-02
8.657	2.464E+01	0.0117	0.0007	54.41	3.843E-04	2.253E-02
9.291	2.296E+01	0.0125	0.0008	57.92	4.292E-04	2.336E-02
9.957	2.142E+01	0.0132	0.0008	61.43	4.860E-04	2.446E-02
10.625	2.008E+01	0.0139	0.0007	64.49	5.363E-04	2.500E-02
11.264	1.894E+01	0.0145	0.0007	67.61	5.825E-04	2.529E-02
11.875	1.796E+01	0.0152	0.0006	70.53	6.069E-04	2.475E-02
12.456	1.713E+01	0.0157	0.0006	73.20	6.193E-04	2.389E-02
13.038	1.636E+01	0.0163	0.0006	75.87	6.175E-04	2.261E-02
13.620	1.566E+01	0.0168	0.0005	78.08	6.040E-04	2.098E-02
14.201	1.502E+01	0.0172	0.0004	80.03	5.888E-04	1.938E-02
14.782	1.443E+01	0.0175	0.0003	81.39	5.555E-04	1.740E-02
15.361	1.389E+01	0.0177	0.0002	82.50	5.098E-04	1.524E-02
15.939	1.338E+01	0.0179	0.0002	83.28	4.534E-04	1.298E-02
16.514	1.292E+01	0.0180	0.0001	83.80	3.841E-04	1.062E-02
17.086	1.249E+01	0.0181	0.0001	84.19	3.187E-04	8.519E-03
17.685	1.206E+01	0.0182	0.0001	84.51	2.512E-04	6.512E-03
18.310	1.165E+01	0.0182	0.0001	84.77	2.025E-04	5.078E-03
18.962	1.125E+01	0.0183	0.0000	84.97	1.596E-04	3.885E-03
19.607	1.088E+01	0.0183	0.0000	85.16	1.285E-04	3.041E-03
20.247	1.054E+01	0.0184	0.0000	85.29	1.082E-04	2.492E-03
20.880	1.022E+01	0.0184	0.0000	85.36	9.305E-05	2.092E-03
21.506	9.919E+00	0.0184	0.0000	85.42	8.103E-05	1.788E-03

22.126	9.641E+00	0.0184	0.0000	85.49	9.219E-05	2.078E-03
22.737	9.382E+00	0.0184	0.0000	85.55	1.046E-04	2.346E-03
23.341	9.140E+00	0.0184	0.0000	85.62	1.191E-04	2.647E-03
23.936	8.912E+00	0.0184	0.0000	85.68	1.412E-04	3.075E-03
24.524	8.699E+00	0.0184	0.0000	85.75	1.708E-04	3.610E-03
25.103	8.498E+00	0.0185	0.0001	86.07	2.044E-04	4.194E-03
25.674	8.309E+00	0.0186	0.0001	86.33	2.410E-04	4.797E-03
26.213	8.138E+00	0.0186	0.0001	86.59	2.802E-04	5.418E-03
26.721	7.983E+00	0.0187	0.0001	86.85	3.237E-04	6.095E-03
27.221	7.837E+00	0.0187	0.0001	87.11	3.723E-04	6.835E-03
27.691	7.704E+00	0.0188	0.0001	87.37	4.240E-04	7.599E-03
28.154	7.577E+00	0.0189	0.0001	87.63	3.984E-04	6.972E-03
28.611	7.456E+00	0.0189	0.0001	87.89	3.780E-04	6.451E-03
29.038	7.346E+00	0.0190	0.0001	88.15	3.531E-04	5.888E-03
29.437	7.247E+00	0.0190	0.0001	88.41	3.232E-04	5.278E-03
29.830	7.151E+00	0.0191	0.0001	88.67	2.902E-04	4.647E-03
30.217	7.060E+00	0.0191	0.0000	88.67	2.522E-04	3.964E-03
30.598	6.972E+00	0.0191	0.0000	88.67	2.111E-04	3.258E-03
30.997	6.882E+00	0.0191	0.0000	88.67	1.671E-04	2.530E-03
31.414	6.791E+00	0.0191	0.0000	88.67	1.172E-04	1.741E-03
31.824	6.703E+00	0.0191	0.0000	88.67	6.073E-05	8.842E-04
32.250	6.615E+00	0.0191	0.0000	88.67	0.000E+00	0.000E+00
32.670	6.530E+00	0.0191	0.0000	88.67	0.000E+00	0.000E+00
33.084	6.448E+00	0.0191	0.0000	88.67	0.000E+00	0.000E+00
33.513	6.365E+00	0.0191	0.0000	88.67	0.000E+00	0.000E+00
33.958	6.282E+00	0.0191	0.0000	88.67	0.000E+00	0.000E+00

34.396	6.202E+00	0.0191	0.0000	88.67	0.000E+00	0.000E+00
34.845	6.122E+00	0.0191	0.0000	88.67	0.000E+00	0.000E+00
35.270	6.048E+00	0.0191	0.0000	88.67	0.000E+00	0.000E+00
35.687	5.978E+00	0.0191	0.0000	88.67	0.000E+00	0.000E+00
36.098	5.910E+00	0.0191	0.0000	88.67	0.000E+00	0.000E+00
36.503	5.844E+00	0.0191	0.0000	88.67	0.000E+00	0.000E+00
36.902	5.781E+00	0.0191	0.0000	88.67	0.000E+00	0.000E+00
37.294	5.720E+00	0.0191	0.0000	88.67	0.000E+00	0.000E+00
37.681	5.661E+00	0.0191	0.0000	88.67	0.000E+00	0.000E+00
38.062	5.605E+00	0.0191	0.0000	88.67	4.848E-05	6.590E-04
38.437	5.550E+00	0.0191	0.0000	88.67	9.971E-05	1.334E-03
38.806	5.497E+00	0.0191	0.0000	88.67	1.538E-04	2.027E-03
39.152	5.449E+00	0.0191	0.0000	88.67	2.105E-04	2.736E-03
39.510	5.399E+00	0.0191	0.0000	88.67	2.700E-04	3.462E-03
39.863	5.351E+00	0.0191	0.0000	88.80	3.324E-04	4.205E-03
40.210	5.305E+00	0.0191	0.0000	88.93	3.979E-04	4.966E-03
40.552	5.260E+00	0.0192	0.0000	89.06	4.662E-04	5.744E-03
40.889	5.217E+00	0.0192	0.0000	89.19	5.376E-04	6.541E-03
41.220	5.175E+00	0.0192	0.0000	89.32	6.120E-04	7.355E-03
41.546	5.135E+00	0.0192	0.0000	89.45	6.895E-04	8.189E-03
41.868	5.095E+00	0.0193	0.0000	89.58	6.416E-04	7.530E-03
42.184	5.057E+00	0.0193	0.0000	89.71	5.908E-04	6.855E-03
42.496	5.020E+00	0.0193	0.0000	89.84	5.370E-04	6.162E-03
42.803	4.984E+00	0.0194	0.0000	89.97	4.804E-04	5.453E-03
43.104	4.949E+00	0.0194	0.0000	90.10	4.209E-04	4.727E-03
43.402	4.915E+00	0.0194	0.0000	90.10	3.584E-04	3.984E-03

43.695	4.882E+00	0.0194	0.0000	90.10	2.929E-04	3.223E-03
43.983	4.850E+00	0.0194	0.0000	90.10	2.243E-04	2.445E-03
44.267	4.819E+00	0.0194	0.0000	90.10	1.527E-04	1.648E-03
44.547	4.789E+00	0.0194	0.0000	90.10	7.795E-05	8.340E-04
44.822	4.759E+00	0.0194	0.0000	90.10	0.000E+00	0.000E+00
45.094	4.731E+00	0.0194	0.0000	90.10	0.000E+00	0.000E+00
45.372	4.702E+00	0.0194	0.0000	90.10	0.000E+00	0.000E+00
45.657	4.672E+00	0.0194	0.0000	90.10	0.000E+00	0.000E+00
45.950	4.642E+00	0.0194	0.0000	90.10	0.000E+00	0.000E+00
46.251	4.612E+00	0.0194	0.0000	90.10	0.000E+00	0.000E+00
46.560	4.582E+00	0.0194	0.0000	90.10	0.000E+00	0.000E+00
46.856	4.553E+00	0.0194	0.0000	90.10	0.000E+00	0.000E+00
47.445	4.496E+00	0.0194	0.0000	90.10	0.000E+00	0.000E+00
48.377	4.410E+00	0.0194	0.0000	90.10	0.000E+00	0.000E+00
49.708	4.292E+00	0.0194	0.0000	90.10	0.000E+00	0.000E+00
51.535	4.139E+00	0.0194	0.0000	90.10	0.000E+00	0.000E+00
53.946	3.954E+00	0.0194	0.0000	90.10	0.000E+00	0.000E+00
57.077	3.737E+00	0.0194	0.0000	90.10	0.000E+00	0.000E+00
61.092	3.492E+00	0.0194	0.0000	90.10	0.000E+00	0.000E+00
66.196	3.223E+00	0.0194	0.0000	90.10	0.000E+00	0.000E+00
72.659	2.936E+00	0.0194	0.0000	90.10	0.000E+00	0.000E+00
80.812	2.640E+00	0.0194	0.0000	90.10	0.000E+00	0.000E+00
91.104	2.342E+00	0.0194	0.0000	90.10	0.000E+00	0.000E+00
103.647	2.058E+00	0.0194	0.0000	90.10	0.000E+00	0.000E+00
118.883	1.794E+00	0.0194	0.0000	90.10	0.000E+00	0.000E+00
137.184	1.555E+00	0.0194	0.0000	90.10	0.000E+00	0.000E+00

158.893	1.343E+00	0.0194	0.0000	90.10	0.000E+00	0.000E+00
184.351	1.157E+00	0.0194	0.0000	90.10	0.000E+00	0.000E+00
213.729	9.981E-01	0.0194	0.0000	90.10	0.000E+00	0.000E+00
247.178	8.630E-01	0.0194	0.0000	90.10	0.000E+00	0.000E+00
284.765	7.491E-01	0.0194	0.0000	90.10	0.000E+00	0.000E+00
326.431	6.535E-01	0.0194	0.0000	90.10	0.000E+00	0.000E+00
372.079	5.733E-01	0.0194	0.0000	90.10	0.000E+00	0.000E+00
421.467	5.061E-01	0.0194	0.0000	90.10	0.000E+00	0.000E+00
474.319	4.497E-01	0.0194	0.0000	90.10	0.000E+00	0.000E+00
530.368	4.022E-01	0.0194	0.0000	90.10	0.000E+00	0.000E+00
589.271	3.620E-01	0.0194	0.0000	90.10	0.000E+00	0.000E+00
650.720	3.278E-01	0.0194	0.0000	90.10	0.000E+00	0.000E+00
714.386	2.986E-01	0.0194	0.0000	90.10	0.000E+00	0.000E+00
779.990	2.735E-01	0.0194	0.0000	90.10	0.000E+00	0.000E+00
848.046	2.515E-01	0.0194	0.0000	90.10	0.000E+00	0.000E+00
918.370	2.323E-01	0.0194	0.0000	90.10	0.000E+00	0.000E+00
990.663	2.153E-01	0.0194	0.0000	90.10	0.000E+00	0.000E+00
1064.780	2.003E-01	0.0194	0.0000	90.10	0.000E+00	0.000E+00
1141.534	1.869E-01	0.0194	0.0000	90.10	6.705E-05	4.091E-05
1219.968	1.749E-01	0.0194	0.0000	90.10	1.520E-04	8.329E-05
1299.945	1.641E-01	0.0194	0.0000	90.10	3.406E-04	1.709E-04
1382.383	1.543E-01	0.0194	0.0000	90.10	7.577E-04	3.521E-04
1467.962	1.453E-01	0.0194	0.0000	90.10	1.268E-03	5.396E-04
1555.859	1.371E-01	0.0194	0.0000	90.16	1.995E-03	7.804E-04
1645.672	1.296E-01	0.0194	0.0000	90.21	2.867E-03	1.031E-03
1737.481	1.228E-01	0.0194	0.0000	90.32	3.897E-03	1.290E-03

1831.377	1.165E-01	0.0195	0.0000	90.53	5.251E-03	1.611E-03
1926.905	1.107E-01	0.0195	0.0000	90.74	6.829E-03	1.944E-03
2024.611	1.054E-01	0.0196	0.0001	91.00	8.662E-03	2.290E-03
2123.043	1.005E-01	0.0196	0.0001	91.27	1.054E-02	2.612E-03
2222.926	9.596E-02	0.0197	0.0001	91.53	1.266E-02	2.944E-03
2324.261	9.178E-02	0.0198	0.0001	91.85	1.478E-02	3.244E-03
2426.321	8.792E-02	0.0198	0.0001	92.17	1.629E-02	3.396E-03
2528.382	8.437E-02	0.0199	0.0001	92.48	1.790E-02	3.552E-03
2630.170	8.111E-02	0.0200	0.0001	92.80	1.901E-02	3.598E-03
2732.594	7.807E-02	0.0200	0.0001	93.12	2.012E-02	3.639E-03
2835.470	7.523E-02	0.0201	0.0001	93.44	2.160E-02	3.757E-03
2938.710	7.259E-02	0.0202	0.0001	93.70	2.238E-02	3.746E-03
3042.404	7.012E-02	0.0202	0.0001	93.97	2.311E-02	3.730E-03
3145.281	6.782E-02	0.0203	0.0000	94.18	2.377E-02	3.711E-03
3249.427	6.565E-02	0.0203	0.0000	94.39	2.385E-02	3.597E-03
3353.756	6.361E-02	0.0204	0.0001	94.65	2.380E-02	3.476E-03
3458.901	6.167E-02	0.0204	0.0000	94.87	2.309E-02	3.263E-03
3564.409	5.985E-02	0.0205	0.0000	95.08	2.220E-02	3.019E-03
3669.826	5.813E-02	0.0205	0.0000	95.29	2.167E-02	2.860E-03
3776.695	5.648E-02	0.0205	0.0000	95.45	2.159E-02	2.760E-03
3884.290	5.492E-02	0.0206	0.0000	95.61	2.144E-02	2.661E-03
3991.612	5.344E-02	0.0206	0.0000	95.71	1.975E-02	2.383E-03
4099.750	5.203E-02	0.0206	0.0000	95.77	1.856E-02	2.176E-03
4207.436	5.070E-02	0.0206	0.0000	95.87	1.716E-02	1.961E-03
4316.209	4.942E-02	0.0206	0.0000	95.98	1.553E-02	1.740E-03
4423.985	4.822E-02	0.0207	0.0000	96.08	1.458E-02	1.598E-03

4532.668	4.706E-02	0.0207	0.0000	96.14	1.349E-02	1.453E-03
4641.080	4.596E-02	0.0207	0.0000	96.19	1.317E-02	1.388E-03
4750.488	4.491E-02	0.0207	0.0000	96.24	1.473E-02	1.524E-03
4859.988	4.389E-02	0.0207	0.0000	96.30	1.633E-02	1.680E-03
4970.123	4.292E-02	0.0207	0.0000	96.35	1.801E-02	1.836E-03
5080.983	4.198E-02	0.0207	0.0000	96.40	2.297E-02	2.341E-03
5192.840	4.108E-02	0.0208	0.0000	96.46	2.604E-02	2.584E-03
5304.518	4.022E-02	0.0208	0.0000	96.56	3.121E-02	3.028E-03
5416.920	3.938E-02	0.0208	0.0000	96.72	4.110E-02	3.922E-03
5530.593	3.857E-02	0.0208	0.0000	96.88	6.105E-02	5.753E-03
5644.992	3.779E-02	0.0209	0.0001	97.20	9.088E-02	8.424E-03
5759.501	3.704E-02	0.0209	0.0000	97.35	1.025E-01	9.146E-03
5874.722	3.631E-02	0.0210	0.0001	97.59	1.168E-01	1.003E-02
5990.509	3.561E-02	0.0211	0.0001	98.02	1.324E-01	1.097E-02
6105.004	3.494E-02	0.0213	0.0002	98.83	1.498E-01	1.201E-02
6221.430	3.429E-02	0.0215	0.0003	100.00	1.726E-01	1.338E-02

Table E2: ED=0.037J/mm²

Report date: 08/10/2007   Merged File

QUANTACHROME INSTRUMENTS

QUANTACHROME POREMASTER FOR WINDOWS® DATA REPORT

VERSION 4.03

SAMPLE ID   CS2030407_10   FILE NAME   S780604H_Merged.PRM

SAMPLE WEIGHT   1.0000 grams   BULK SAMPLE VOLUME 1.0000 cc

SAMPLE DESCRIPTION M. TEKIN

COMMENTS   LP STATION 1

HG SURFACE TENSION 480.00 erg/cm²   HG CONTACT ANGLE (I)140.00°,(E)140.00°

MINIMUM DELTA VOL. 0.000 % FS   MOVING POINT AVG. 11 (Scan Mode)

OPERATOR   K. BEHLULGIL   Mercury volume normalized by sample weight.

Pore Size Distribution By Volume - Intrusion

Printing every data point.

Pressure	Pore Diameter	Volume Intruded	Delta Volume	% Volume Intruded	Dv(d)	-dV/d(log d)
[PSI]	[μm]	[cc/g]	[cc/g]	%	[cc/(μm-g)]	[cc/g]
0.901	2.369E+02	0.0000	0.0000	0.00	6.596E-06	5.688E-03
1.071	1.991E+02	0.0004	0.0004	2.07	7.958E-06	6.398E-03
1.203	1.773E+02	0.0006	0.0003	3.73	1.063E-05	7.138E-03
1.510	1.413E+02	0.0014	0.0008	8.24	1.529E-05	8.002E-03
1.918	1.112E+02	0.0022	0.0008	12.62	2.462E-05	8.915E-03
2.363	9.028E+01	0.0030	0.0008	17.03	3.828E-05	9.690E-03
2.748	7.762E+01	0.0037	0.0007	21.06	5.879E-05	1.125E-02
3.165	6.741E+01	0.0044	0.0008	25.42	7.637E-05	1.250E-02
3.618	5.896E+01	0.0053	0.0009	30.42	9.653E-05	1.371E-02
4.119	5.179E+01	0.0062	0.0010	35.99	1.178E-04	1.478E-02
4.645	4.593E+01	0.0071	0.0009	41.24	1.459E-04	1.593E-02
5.178	4.119E+01	0.0080	0.0008	45.92	1.765E-04	1.685E-02
5.718	3.731E+01	0.0088	0.0008	50.52	2.058E-04	1.746E-02

6.256	3.410E+01	0.0095	0.0007	54.79	2.321E-04	1.768E-02
6.799	3.138E+01	0.0102	0.0007	58.91	2.514E-04	1.742E-02
7.347	2.904E+01	0.0109	0.0007	62.78	2.623E-04	1.666E-02
7.903	2.699E+01	0.0115	0.0006	66.17	2.731E-04	1.606E-02
8.466	2.520E+01	0.0120	0.0005	69.16	2.825E-04	1.541E-02
9.036	2.361E+01	0.0124	0.0004	71.58	2.855E-04	1.453E-02
9.609	2.220E+01	0.0127	0.0003	73.44	2.832E-04	1.349E-02
10.190	2.093E+01	0.0130	0.0002	74.73	2.747E-04	1.234E-02
10.749	1.985E+01	0.0132	0.0003	76.18	2.588E-04	1.104E-02
11.281	1.891E+01	0.0134	0.0002	77.39	2.402E-04	9.816E-03
11.790	1.809E+01	0.0136	0.0002	78.36	2.220E-04	8.798E-03
12.300	1.734E+01	0.0137	0.0001	79.17	2.080E-04	8.022E-03
12.815	1.665E+01	0.0138	0.0001	79.89	1.974E-04	7.353E-03
13.335	1.600E+01	0.0139	0.0001	80.46	1.958E-04	7.000E-03
13.854	1.540E+01	0.0140	0.0001	80.94	1.783E-04	6.100E-03
14.375	1.484E+01	0.0141	0.0001	81.51	1.607E-04	5.275E-03
14.897	1.432E+01	0.0142	0.0001	82.07	1.448E-04	4.563E-03
15.418	1.384E+01	0.0143	0.0001	82.47	1.307E-04	3.959E-03
15.935	1.339E+01	0.0144	0.0001	82.88	1.166E-04	3.406E-03
16.480	1.294E+01	0.0144	0.0000	82.96	1.062E-04	2.984E-03
17.053	1.251E+01	0.0144	0.0000	83.04	9.706E-05	2.620E-03
17.655	1.208E+01	0.0144	0.0000	83.12	7.988E-05	2.065E-03
18.258	1.168E+01	0.0144	0.0000	83.20	6.304E-05	1.595E-03
18.860	1.131E+01	0.0144	0.0000	83.28	5.462E-05	1.384E-03
19.459	1.096E+01	0.0144	0.0000	83.36	4.455E-05	1.162E-03
20.057	1.064E+01	0.0145	0.0000	83.44	5.115E-05	1.304E-03

20.650	1.033E+01	0.0145	0.0000	83.44	5.860E-05	1.457E-03
21.241	1.004E+01	0.0145	0.0000	83.52	6.695E-05	1.619E-03
21.830	9.772E+00	0.0145	0.0000	83.68	7.604E-05	1.786E-03
22.414	9.517E+00	0.0145	0.0000	83.84	8.591E-05	1.959E-03
22.994	9.277E+00	0.0146	0.0000	84.01	9.655E-05	2.138E-03
23.568	9.051E+00	0.0146	0.0000	84.17	1.080E-04	2.322E-03
24.137	8.838E+00	0.0146	0.0000	84.33	1.259E-04	2.611E-03
24.700	8.637E+00	0.0146	0.0000	84.49	1.327E-04	2.657E-03
25.257	8.446E+00	0.0147	0.0000	84.65	1.262E-04	2.442E-03
25.808	8.266E+00	0.0147	0.0000	84.81	1.185E-04	2.220E-03
26.354	8.095E+00	0.0147	0.0000	84.97	1.097E-04	1.991E-03
26.893	7.932E+00	0.0148	0.0000	85.14	9.957E-05	1.754E-03
27.425	7.778E+00	0.0148	0.0000	85.22	8.813E-05	1.508E-03
27.950	7.632E+00	0.0148	0.0000	85.22	7.534E-05	1.254E-03
28.469	7.493E+00	0.0148	0.0000	85.22	6.117E-05	9.907E-04
28.980	7.361E+00	0.0148	0.0000	85.22	4.556E-05	7.192E-04
29.463	7.240E+00	0.0148	0.0000	85.22	2.847E-05	4.389E-04
29.917	7.130E+00	0.0148	0.0000	85.22	9.899E-06	1.498E-04
30.345	7.030E+00	0.0148	0.0000	85.22	1.360E-05	2.368E-04
30.767	6.934E+00	0.0148	0.0000	85.22	2.818E-05	4.803E-04
31.182	6.841E+00	0.0148	0.0000	85.22	4.379E-05	7.307E-04
31.591	6.753E+00	0.0148	0.0000	85.22	6.041E-05	9.876E-04
31.995	6.667E+00	0.0148	0.0000	85.22	7.720E-05	1.237E-03
32.393	6.585E+00	0.0148	0.0000	85.30	9.419E-05	1.480E-03
32.785	6.507E+00	0.0148	0.0000	85.38	1.108E-04	1.709E-03
33.171	6.431E+00	0.0148	0.0000	85.46	1.283E-04	1.943E-03

33.552	6.358E+00	0.0148	0.0000	85.54	1.467E-04	2.185E-03
33.948	6.284E+00	0.0148	0.0000	85.62	1.662E-04	2.432E-03
34.360	6.209E+00	0.0149	0.0000	85.70	1.868E-04	2.687E-03
34.803	6.129E+00	0.0149	0.0000	85.78	1.736E-04	2.450E-03
35.241	6.053E+00	0.0149	0.0000	85.86	1.594E-04	2.207E-03
35.671	5.980E+00	0.0149	0.0000	85.94	1.439E-04	1.956E-03
36.096	5.910E+00	0.0149	0.0000	86.03	1.273E-04	1.699E-03
36.514	5.842E+00	0.0149	0.0000	86.11	1.104E-04	1.450E-03
36.925	5.777E+00	0.0149	0.0000	86.11	9.341E-05	1.207E-03
37.330	5.715E+00	0.0149	0.0000	86.11	7.696E-05	9.784E-04
37.729	5.654E+00	0.0149	0.0000	86.11	5.942E-05	7.436E-04
38.122	5.596E+00	0.0149	0.0000	86.11	4.075E-05	5.023E-04
38.510	5.539E+00	0.0149	0.0000	86.11	2.097E-05	2.547E-04
38.891	5.485E+00	0.0149	0.0000	86.11	0.000E+00	0.000E+00
39.249	5.435E+00	0.0149	0.0000	86.11	0.000E+00	0.000E+00
39.602	5.387E+00	0.0149	0.0000	86.11	0.000E+00	0.000E+00
39.950	5.340E+00	0.0149	0.0000	86.11	0.000E+00	0.000E+00
40.292	5.294E+00	0.0149	0.0000	86.11	0.000E+00	0.000E+00
40.629	5.250E+00	0.0149	0.0000	86.11	0.000E+00	0.000E+00
40.961	5.208E+00	0.0149	0.0000	86.11	0.000E+00	0.000E+00
41.289	5.167E+00	0.0149	0.0000	86.11	0.000E+00	0.000E+00
41.611	5.127E+00	0.0149	0.0000	86.11	0.000E+00	0.000E+00
41.928	5.088E+00	0.0149	0.0000	86.11	0.000E+00	0.000E+00
42.241	5.050E+00	0.0149	0.0000	86.11	0.000E+00	0.000E+00
42.549	5.014E+00	0.0149	0.0000	86.11	0.000E+00	0.000E+00
42.852	4.978E+00	0.0149	0.0000	86.11	0.000E+00	0.000E+00

43.152	4.944E+00	0.0149	0.0000	86.11	0.000E+00	0.000E+00
43.446	4.910E+00	0.0149	0.0000	86.11	0.000E+00	0.000E+00
43.736	4.878E+00	0.0149	0.0000	86.11	0.000E+00	0.000E+00
44.022	4.846E+00	0.0149	0.0000	86.11	0.000E+00	0.000E+00
44.303	4.815E+00	0.0149	0.0000	86.11	0.000E+00	0.000E+00
44.581	4.785E+00	0.0149	0.0000	86.11	0.000E+00	0.000E+00
44.854	4.756E+00	0.0149	0.0000	86.11	0.000E+00	0.000E+00
45.123	4.728E+00	0.0149	0.0000	86.11	4.100E-05	4.618E-04
45.399	4.699E+00	0.0149	0.0000	86.11	8.186E-05	9.137E-04
45.682	4.670E+00	0.0149	0.0000	86.11	1.243E-04	1.375E-03
45.972	4.640E+00	0.0149	0.0000	86.11	1.469E-04	1.609E-03
46.259	4.612E+00	0.0149	0.0000	86.11	1.620E-04	1.756E-03
46.553	4.582E+00	0.0149	0.0000	86.19	1.730E-04	1.857E-03
46.856	4.553E+00	0.0150	0.0000	86.27	1.817E-04	1.931E-03
47.154	4.524E+00	0.0150	0.0000	86.35	1.889E-04	1.989E-03
47.751	4.467E+00	0.0150	0.0000	86.43	1.962E-04	2.035E-03
48.710	4.379E+00	0.0150	0.0000	86.51	2.057E-04	2.073E-03
50.149	4.254E+00	0.0150	0.0000	86.59	2.184E-04	2.105E-03
52.163	4.090E+00	0.0150	0.0000	86.67	1.809E-04	1.643E-03
54.878	3.887E+00	0.0150	0.0000	86.75	1.416E-04	1.191E-03
58.480	3.648E+00	0.0150	0.0000	86.83	9.455E-05	7.291E-04
63.189	3.376E+00	0.0151	0.0000	86.91	7.191E-05	4.960E-04
69.282	3.079E+00	0.0151	0.0000	86.99	5.794E-05	3.486E-04
77.150	2.765E+00	0.0151	0.0000	86.99	4.858E-05	2.480E-04
87.228	2.446E+00	0.0151	0.0000	86.99	4.121E-05	1.735E-04
100.011	2.133E+00	0.0151	0.0000	86.99	3.420E-05	1.158E-04

115.676	1.844E+00	0.0151	0.0000	86.99	2.612E-05	6.968E-05
134.525	1.586E+00	0.0151	0.0000	86.99	1.532E-05	3.183E-05
156.922	1.359E+00	0.0151	0.0000	86.99	0.000E+00	0.000E+00
183.206	1.164E+00	0.0151	0.0000	86.99	0.000E+00	0.000E+00
213.552	9.989E-01	0.0151	0.0000	86.99	0.000E+00	0.000E+00
248.076	8.599E-01	0.0151	0.0000	86.99	0.000E+00	0.000E+00
286.741	7.440E-01	0.0151	0.0000	86.99	0.000E+00	0.000E+00
329.511	6.474E-01	0.0151	0.0000	86.99	0.000E+00	0.000E+00
376.159	5.671E-01	0.0151	0.0000	86.99	0.000E+00	0.000E+00
426.437	5.002E-01	0.0151	0.0000	86.99	0.000E+00	0.000E+00
480.075	4.444E-01	0.0151	0.0000	86.99	3.030E-05	5.464E-05
536.705	3.975E-01	0.0151	0.0000	86.99	7.517E-05	1.125E-04
596.125	3.578E-01	0.0151	0.0000	86.99	1.819E-04	2.333E-04
657.930	3.242E-01	0.0151	0.0000	86.99	3.280E-04	3.595E-04
721.770	2.956E-01	0.0151	0.0000	86.99	5.217E-04	4.926E-04
787.710	2.708E-01	0.0151	0.0000	87.13	9.899E-04	8.424E-04
855.537	2.493E-01	0.0151	0.0000	87.26	1.606E-03	1.216E-03
925.796	2.304E-01	0.0152	0.0000	87.52	2.394E-03	1.612E-03
998.436	2.137E-01	0.0152	0.0000	87.78	3.398E-03	2.040E-03
1072.557	1.989E-01	0.0153	0.0000	88.05	4.645E-03	2.499E-03
1148.154	1.858E-01	0.0154	0.0001	88.70	6.165E-03	2.985E-03
1223.835	1.743E-01	0.0155	0.0001	89.36	7.584E-03	3.342E-03
1299.671	1.641E-01	0.0156	0.0001	90.02	9.209E-03	3.713E-03
1374.046	1.553E-01	0.0157	0.0001	90.67	1.057E-02	3.932E-03
1447.336	1.474E-01	0.0158	0.0001	91.33	1.204E-02	4.157E-03
1519.915	1.404E-01	0.0159	0.0001	91.99	1.361E-02	4.382E-03

1591.947	1.340E-01	0.0160	0.0001	92.51	1.342E-02	4.032E-03
1664.251	1.282E-01	0.0161	0.0001	93.04	1.300E-02	3.659E-03
1735.739	1.229E-01	0.0162	0.0001	93.43	1.232E-02	3.263E-03
1807.861	1.180E-01	0.0163	0.0001	93.82	1.133E-02	2.835E-03
1881.436	1.134E-01	0.0163	0.0001	94.22	1.003E-02	2.376E-03
1956.643	1.090E-01	0.0163	0.0000	94.22	8.399E-03	1.889E-03
2035.388	1.048E-01	0.0163	0.0000	94.22	6.941E-03	1.478E-03
2116.674	1.008E-01	0.0163	0.0000	94.22	5.197E-03	1.049E-03
2202.223	9.687E-02	0.0163	0.0000	94.22	3.725E-03	7.093E-04
2292.127	9.307E-02	0.0163	0.0000	94.22	1.997E-03	3.583E-04
2385.388	8.943E-02	0.0163	0.0000	94.22	0.000E+00	0.000E+00
2481.370	8.597E-02	0.0163	0.0000	94.22	0.000E+00	0.000E+00
2579.348	8.270E-02	0.0163	0.0000	94.22	0.000E+00	0.000E+00
2680.320	7.959E-02	0.0163	0.0000	94.22	0.000E+00	0.000E+00
2781.745	7.669E-02	0.0163	0.0000	94.22	0.000E+00	0.000E+00
2883.715	7.397E-02	0.0163	0.0000	94.22	3.757E-04	7.705E-05
2987.318	7.141E-02	0.0163	0.0000	94.22	8.074E-04	1.566E-04
3089.923	6.904E-02	0.0163	0.0000	94.22	1.293E-03	2.376E-04
3193.798	6.679E-02	0.0163	0.0000	94.22	1.841E-03	3.213E-04
3298.217	6.468E-02	0.0163	0.0000	94.22	2.453E-03	4.070E-04
3402.455	6.270E-02	0.0163	0.0000	94.28	3.126E-03	4.939E-04
3506.602	6.083E-02	0.0164	0.0000	94.35	3.862E-03	5.821E-04
3611.928	5.906E-02	0.0164	0.0000	94.42	4.676E-03	6.736E-04
3716.891	5.739E-02	0.0164	0.0000	94.48	5.560E-03	7.663E-04
3822.309	5.581E-02	0.0164	0.0000	94.55	7.790E-03	1.050E-03
3929.269	5.429E-02	0.0164	0.0000	94.61	1.027E-02	1.344E-03

4037.498	5.284E-02	0.0164	0.0000	94.68	1.508E-02	1.964E-03
4144.730	5.147E-02	0.0164	0.0000	94.75	2.037E-02	2.598E-03
4253.322	5.015E-02	0.0164	0.0000	94.81	2.622E-02	3.253E-03
4361.915	4.891E-02	0.0165	0.0000	95.01	3.255E-02	3.916E-03
4469.600	4.773E-02	0.0165	0.0000	95.21	3.945E-02	4.597E-03
4577.738	4.660E-02	0.0166	0.0001	95.67	4.688E-02	5.290E-03
4685.967	4.552E-02	0.0167	0.0001	96.13	5.493E-02	6.000E-03
4793.199	4.451E-02	0.0167	0.0001	96.59	6.350E-02	6.719E-03
4901.428	4.352E-02	0.0168	0.0001	97.05	7.267E-02	7.448E-03
5009.204	4.259E-02	0.0169	0.0001	97.51	7.810E-02	7.764E-03
5117.434	4.169E-02	0.0170	0.0001	97.96	8.365E-02	8.069E-03
5225.391	4.082E-02	0.0171	0.0001	98.42	7.886E-02	7.372E-03
5334.074	3.999E-02	0.0171	0.0001	98.88	7.346E-02	6.659E-03
5443.301	3.919E-02	0.0172	0.0001	99.34	6.733E-02	5.922E-03
5552.529	3.842E-02	0.0173	0.0001	99.67	6.061E-02	5.175E-03
5664.115	3.766E-02	0.0173	0.0001	100.00	5.317E-02	4.409E-03
5773.938	3.695E-02	0.0173	0.0000	100.00	4.953E-02	3.992E-03
5887.495	3.623E-02	0.0173	0.0000	100.00	4.414E-02	3.459E-03
6002.484	3.554E-02	0.0173	0.0000	100.00	3.645E-02	2.778E-03
6118.110	3.487E-02	0.0173	0.0000	100.00	2.536E-02	1.883E-03
6237.196	3.420E-02	0.0173	0.0000	100.00	1.521E-02	1.098E-03

Table E3: ED=0.023J/mm²

QUANTACHROME POREMASTER FOR WINDOWS® DATA REPORT

VERSION 4.03

SAMPLE ID   CS3030407_12   FILE NAME   S780605H_Merged.PRM

SAMPLE WEIGHT   1.0000 grams   BULK SAMPLE VOLUME 1.0000 cc

SAMPLE DESCRIPTION M. TEKIN

COMMENTS   LP STATION 1

HG SURFACE TENSION 480.00 erg/cm²   HG CONTACT ANGLE   (I)140.00°,(E)140.00°

MINIMUM DELTA VOL. 0.000 % FS   MOVING POINT AVG. 11 (Scan Mode)

OPERATOR   K. BEHLULGIL   Mercury volume normalized by sample weight.

Pore Size Distribution By Volume - Intrusion

Printing every data point.

Pressure	Pore Diameter	Volume Intruded	Delta Volume	% Volume Intruded	Dv(d)	-dV/d(log d)
[PSI]	[µm]	[cc/g]	[cc/g]	%	[cc/(µm-g)]	[cc/g]
0.931	2.290E+02	0.0000	0.0000	0.00	1.138E-05	1.028E-02
1.051	2.029E+02	0.0008	0.0008	2.12	1.295E-05	1.206E-02
1.462	1.459E+02	0.0022	0.0014	6.01	2.081E-05	1.378E-02
1.995	1.069E+02	0.0033	0.0011	8.95	3.934E-05	1.552E-02
2.570	8.300E+01	0.0046	0.0013	12.60	6.826E-05	1.718E-02
3.166	6.738E+01	0.0061	0.0016	16.89	1.079E-04	1.910E-02
3.699	5.766E+01	0.0077	0.0015	21.12	1.697E-04	2.318E-02

4.276	4.989E+01	0.0093	0.0016	25.59	2.059E-04	2.632E-02
4.908	4.347E+01	0.0111	0.0018	30.43	2.683E-04	3.018E-02
5.540	3.850E+01	0.0128	0.0017	35.09	3.551E-04	3.418E-02
6.175	3.454E+01	0.0146	0.0018	40.05	4.504E-04	3.795E-02
6.813	3.131E+01	0.0165	0.0019	45.32	5.527E-04	4.157E-02
7.453	2.862E+01	0.0184	0.0019	50.59	6.520E-04	4.423E-02
8.094	2.636E+01	0.0203	0.0019	55.75	7.546E-04	4.651E-02
8.736	2.442E+01	0.0220	0.0017	60.48	8.571E-04	4.832E-02
9.350	2.281E+01	0.0236	0.0016	64.83	9.545E-04	4.955E-02
9.938	2.147E+01	0.0251	0.0015	68.99	1.028E-03	4.970E-02
10.527	2.026E+01	0.0264	0.0013	72.56	1.074E-03	4.870E-02
11.088	1.924E+01	0.0275	0.0011	75.72	1.100E-03	4.712E-02
11.651	1.831E+01	0.0286	0.0011	78.64	1.105E-03	4.497E-02
12.215	1.746E+01	0.0295	0.0009	81.22	1.096E-03	4.234E-02
12.749	1.673E+01	0.0303	0.0007	83.26	1.070E-03	3.944E-02
13.254	1.609E+01	0.0308	0.0006	84.84	1.015E-03	3.603E-02
13.761	1.550E+01	0.0314	0.0005	86.26	9.549E-04	3.265E-02
14.267	1.495E+01	0.0318	0.0004	87.49	8.845E-04	2.919E-02
14.774	1.444E+01	0.0322	0.0003	88.45	7.994E-04	2.548E-02
15.311	1.393E+01	0.0325	0.0003	89.38	7.115E-04	2.187E-02
15.874	1.344E+01	0.0328	0.0003	90.22	6.375E-04	1.887E-02
16.437	1.298E+01	0.0330	0.0002	90.84	5.729E-04	1.631E-02
17.026	1.253E+01	0.0332	0.0002	91.38	5.058E-04	1.388E-02
17.612	1.211E+01	0.0333	0.0001	91.73	4.375E-04	1.158E-02
18.195	1.172E+01	0.0334	0.0001	91.96	3.827E-04	9.783E-03
18.802	1.135E+01	0.0335	0.0001	92.23	3.207E-04	7.916E-03

19.435	1.098E+01	0.0336	0.0001	92.46	2.613E-04	6.246E-03
20.062	1.063E+01	0.0337	0.0001	92.65	2.168E-04	5.022E-03
20.684	1.031E+01	0.0337	0.0000	92.76	1.768E-04	3.991E-03
21.299	1.002E+01	0.0338	0.0000	92.88	1.525E-04	3.349E-03
21.907	9.737E+00	0.0338	0.0000	92.92	1.384E-04	2.951E-03
22.483	9.488E+00	0.0338	0.0000	92.96	1.123E-04	2.327E-03
23.027	9.264E+00	0.0338	0.0000	92.99	8.877E-05	1.797E-03
23.539	9.063E+00	0.0338	0.0000	93.03	6.718E-05	1.336E-03
24.044	8.872E+00	0.0338	0.0000	93.07	5.387E-05	1.048E-03
24.542	8.692E+00	0.0338	0.0000	93.11	3.904E-05	7.489E-04
25.034	8.521E+00	0.0338	0.0000	93.11	3.466E-05	6.455E-04
25.519	8.359E+00	0.0338	0.0000	93.11	2.946E-05	5.334E-04
25.998	8.205E+00	0.0338	0.0000	93.11	2.336E-05	4.115E-04
26.469	8.059E+00	0.0338	0.0000	93.11	1.626E-05	2.790E-04
26.933	7.920E+00	0.0338	0.0000	93.11	8.482E-06	1.420E-04
27.391	7.788E+00	0.0338	0.0000	93.11	0.000E+00	0.000E+00
27.867	7.655E+00	0.0338	0.0000	93.11	0.000E+00	0.000E+00
28.362	7.521E+00	0.0338	0.0000	93.11	0.000E+00	0.000E+00
28.875	7.388E+00	0.0338	0.0000	93.11	0.000E+00	0.000E+00
29.380	7.261E+00	0.0338	0.0000	93.11	0.000E+00	0.000E+00
29.877	7.140E+00	0.0338	0.0000	93.11	8.629E-07	1.861E-05
30.367	7.025E+00	0.0338	0.0000	93.11	1.382E-06	3.246E-05
30.849	6.915E+00	0.0338	0.0000	93.11	1.773E-06	4.591E-05
31.319	6.811E+00	0.0338	0.0000	93.11	2.101E-06	6.035E-05
33.818	6.308E+00	0.0338	0.0000	93.11	2.545E-06	7.617E-05
43.710	4.880E+00	0.0339	0.0000	93.17	3.887E-06	9.372E-05

61.721	3.456E+00	0.0339	0.0000	93.23	7.637E-06	1.133E-04
88.035	2.423E+00	0.0339	0.0000	93.30	1.620E-05	1.348E-04
122.560	1.741E+00	0.0339	0.0000	93.36	3.340E-05	1.581E-04
165.752	1.287E+00	0.0340	0.0000	93.42	6.717E-05	2.087E-04
217.609	9.803E-01	0.0340	0.0000	93.49	1.263E-04	2.649E-04
277.862	7.677E-01	0.0340	0.0000	93.55	1.598E-04	2.947E-04
346.965	6.148E-01	0.0340	0.0000	93.61	2.158E-04	3.355E-04
425.915	5.009E-01	0.0341	0.0000	93.67	2.966E-04	3.826E-04
514.175	4.149E-01	0.0341	0.0000	93.80	4.079E-04	4.349E-04
609.250	3.501E-01	0.0341	0.0000	93.92	5.563E-04	4.927E-04
706.048	3.021E-01	0.0342	0.0000	94.02	7.424E-04	5.555E-04
804.480	2.652E-01	0.0342	0.0000	94.11	9.661E-04	6.220E-04
904.998	2.357E-01	0.0342	0.0000	94.21	1.235E-03	6.930E-04
1007.149	2.118E-01	0.0343	0.0000	94.30	1.642E-03	8.360E-04
1109.664	1.922E-01	0.0343	0.0000	94.39	1.919E-03	8.912E-04
1212.722	1.759E-01	0.0343	0.0000	94.49	2.216E-03	9.465E-04
1317.595	1.619E-01	0.0344	0.0000	94.58	2.675E-03	1.056E-03
1423.284	1.499E-01	0.0344	0.0000	94.67	3.196E-03	1.168E-03
1528.974	1.395E-01	0.0345	0.0001	94.83	3.782E-03	1.284E-03
1635.933	1.304E-01	0.0345	0.0000	94.93	4.549E-03	1.450E-03
1744.344	1.223E-01	0.0345	0.0000	95.02	5.413E-03	1.618E-03
1853.118	1.151E-01	0.0346	0.0000	95.14	6.378E-03	1.788E-03
1962.164	1.087E-01	0.0346	0.0000	95.27	7.458E-03	1.964E-03
2070.938	1.030E-01	0.0347	0.0000	95.40	8.645E-03	2.141E-03
2179.893	9.786E-02	0.0347	0.0001	95.55	9.145E-03	2.143E-03
2290.300	9.314E-02	0.0348	0.0001	95.71	1.050E-02	2.330E-03

2401.977	8.881E-02	0.0348	0.0001	95.87	1.199E-02	2.521E-03
2514.107	8.485E-02	0.0349	0.0001	96.02	1.284E-02	2.551E-03
2627.598	8.119E-02	0.0350	0.0001	96.18	1.370E-02	2.578E-03
2741.543	7.781E-02	0.0350	0.0000	96.27	1.515E-02	2.733E-03
2855.397	7.471E-02	0.0351	0.0001	96.43	1.600E-02	2.772E-03
2970.068	7.182E-02	0.0351	0.0001	96.59	1.685E-02	2.811E-03
3085.736	6.913E-02	0.0351	0.0000	96.68	1.771E-02	2.851E-03
3202.040	6.662E-02	0.0352	0.0000	96.77	1.853E-02	2.881E-03
3319.069	6.427E-02	0.0352	0.0001	96.93	1.934E-02	2.912E-03
3437.187	6.206E-02	0.0353	0.0000	97.06	2.110E-02	3.051E-03
3555.759	5.999E-02	0.0353	0.0000	97.18	2.143E-02	2.995E-03
3674.330	5.806E-02	0.0354	0.0000	97.31	2.168E-02	2.936E-03
3796.168	5.619E-02	0.0354	0.0000	97.43	2.302E-02	2.998E-03
3918.187	5.444E-02	0.0355	0.0000	97.56	2.440E-02	3.059E-03
4041.113	5.279E-02	0.0355	0.0000	97.68	2.449E-02	2.983E-03
4165.218	5.122E-02	0.0355	0.0000	97.78	2.512E-02	2.966E-03
4289.505	4.973E-02	0.0356	0.0000	97.87	2.570E-02	2.947E-03
4414.428	4.832E-02	0.0356	0.0000	97.96	2.620E-02	2.924E-03
4540.347	4.698E-02	0.0356	0.0000	98.06	2.676E-02	2.912E-03
4669.080	4.569E-02	0.0357	0.0000	98.15	2.961E-02	3.181E-03
4801.532	4.443E-02	0.0357	0.0000	98.25	3.262E-02	3.445E-03
4934.981	4.323E-02	0.0357	0.0000	98.34	3.548E-02	3.642E-03
5068.703	4.209E-02	0.0358	0.0000	98.43	4.054E-02	4.070E-03
5200.430	4.102E-02	0.0358	0.0000	98.53	4.324E-02	4.209E-03
5332.609	4.000E-02	0.0359	0.0001	98.72	5.128E-02	4.902E-03
5467.783	3.901E-02	0.0360	0.0001	98.90	6.119E-02	5.729E-03

5602.644	3.808E-02	0.0360	0.0001	99.04	6.701E-02	6.021E-03
5743.288	3.714E-02	0.0361	0.0001	99.26	7.391E-02	6.371E-03
5877.694	3.629E-02	0.0361	0.0000	99.38	8.218E-02	6.799E-03
6009.354	3.550E-02	0.0362	0.0001	99.66	9.213E-02	7.332E-03
6156.714	3.465E-02	0.0364	0.0001	100.00	9.763E-02	7.509E-03

Table E4: ED=0.030J/mm²

Report date: 08/10/2007   Merged File

QUANTACHROME INSTRUMENTS

QUANTACHROME POREMASTER FOR WINDOWS® DATA REPORT

VERSION 4.03

SAMPLE ID   CS4030407_14   FILE NAME   S781001H_Merged.PRM

SAMPLE WEIGHT   1.0000 grams   BULK SAMPLE VOLUME 1.0000 cc

SAMPLE DESCRIPTION M. TEKIN

COMMENTS   LP STATION 1

HG SURFACE TENSION 480.00 erg/cm²   HG CONTACT ANGLE   (I)140.00°,(E)140.00°

MINIMUM DELTA VOL. 0.000 % FS   MOVING POINT AVG. 11 (Scan Mode)

OPERATOR   Leyla MOLU   Mercury volume normalized by sample weight.

Pore Size Distribution By Volume - Intrusion

Printing every data point.

| Pressure | Pore | Volume | Delta | % Volume | Dv(d) | -dV/d(log d) |

	Diameter	Intruded	Volume	Intruded		
[PSI]	[μm]	[cc/g]	[cc/g]	%	[cc/(μm-g)]	[cc/g]
0.952	2.240E+02	0.0000	0.0000	0.00	2.347E-05	1.599E-02
1.133	1.883E+02	0.0019	0.0019	7.15	2.647E-05	1.611E-02
1.236	1.726E+02	0.0030	0.0011	11.14	3.224E-05	1.623E-02
1.411	1.512E+02	0.0040	0.0011	15.25	3.768E-05	1.602E-02
1.706	1.250E+02	0.0051	0.0011	19.27	4.943E-05	1.606E-02
2.087	1.022E+02	0.0061	0.0010	22.89	6.961E-05	1.621E-02
2.418	8.821E+01	0.0071	0.0011	26.95	1.020E-04	1.783E-02
2.786	7.658E+01	0.0082	0.0010	30.90	1.106E-04	1.723E-02
3.181	6.706E+01	0.0090	0.0008	34.01	1.121E-04	1.638E-02
3.622	5.890E+01	0.0099	0.0009	37.49	1.219E-04	1.639E-02
4.105	5.196E+01	0.0109	0.0010	41.13	1.431E-04	1.711E-02
4.617	4.621E+01	0.0118	0.0009	44.56	1.721E-04	1.798E-02
5.157	4.137E+01	0.0127	0.0009	47.94	1.947E-04	1.829E-02
5.704	3.740E+01	0.0135	0.0008	50.99	2.182E-04	1.861E-02
6.257	3.409E+01	0.0143	0.0008	53.89	2.479E-04	1.911E-02
6.814	3.131E+01	0.0151	0.0008	56.79	2.733E-04	1.928E-02
7.370	2.895E+01	0.0158	0.0007	59.43	2.960E-04	1.932E-02
7.930	2.690E+01	0.0164	0.0006	61.86	3.169E-04	1.918E-02
8.495	2.511E+01	0.0170	0.0006	64.18	3.341E-04	1.882E-02
9.063	2.354E+01	0.0176	0.0006	66.29	3.528E-04	1.860E-02
9.640	2.213E+01	0.0181	0.0005	68.13	3.691E-04	1.828E-02
10.222	2.087E+01	0.0185	0.0005	69.87	3.790E-04	1.772E-02
10.803	1.975E+01	0.0189	0.0004	71.35	3.936E-04	1.752E-02

11.387	1.873E+01	0.0193	0.0003	72.61	4.097E-04	1.743E-02
11.972	1.782E+01	0.0196	0.0003	73.93	4.192E-04	1.703E-02
12.529	1.703E+01	0.0199	0.0003	75.09	4.276E-04	1.665E-02
13.063	1.633E+01	0.0202	0.0003	76.09	4.394E-04	1.647E-02
13.601	1.568E+01	0.0205	0.0003	77.31	4.534E-04	1.642E-02
14.114	1.511E+01	0.0208	0.0003	78.47	4.769E-04	1.670E-02
14.627	1.458E+01	0.0211	0.0003	79.42	5.048E-04	1.707E-02
15.144	1.409E+01	0.0213	0.0002	80.31	5.250E-04	1.713E-02
15.633	1.365E+01	0.0215	0.0002	81.16	5.454E-04	1.719E-02
16.095	1.325E+01	0.0217	0.0002	82.00	5.638E-04	1.719E-02
16.556	1.288E+01	0.0220	0.0002	82.90	5.596E-04	1.657E-02
17.021	1.253E+01	0.0222	0.0002	83.74	5.503E-04	1.586E-02
17.485	1.220E+01	0.0224	0.0002	84.48	5.513E-04	1.544E-02
17.977	1.187E+01	0.0226	0.0002	85.22	5.551E-04	1.511E-02
18.498	1.153E+01	0.0228	0.0002	85.90	5.536E-04	1.460E-02
19.020	1.122E+01	0.0229	0.0001	86.43	5.378E-04	1.373E-02
19.569	1.090E+01	0.0231	0.0001	86.96	5.021E-04	1.241E-02
20.117	1.060E+01	0.0232	0.0001	87.49	4.661E-04	1.117E-02
20.661	1.032E+01	0.0233	0.0001	88.01	4.345E-04	1.011E-02
21.232	1.005E+01	0.0235	0.0001	88.49	4.067E-04	9.239E-03
21.827	9.773E+00	0.0236	0.0001	88.86	3.896E-04	8.656E-03
22.419	9.515E+00	0.0236	0.0001	89.07	3.812E-04	8.248E-03
23.006	9.272E+00	0.0237	0.0001	89.28	3.623E-04	7.623E-03
23.589	9.043E+00	0.0237	0.0001	89.49	3.398E-04	6.978E-03
24.169	8.826E+00	0.0238	0.0001	89.75	3.131E-04	6.310E-03
24.742	8.622E+00	0.0239	0.0001	90.07	2.920E-04	5.786E-03

25.309	8.429E+00	0.0240	0.0001	90.33	2.829E-04	5.502E-03
25.868	8.247E+00	0.0240	0.0000	90.49	2.916E-04	5.537E-03
26.422	8.074E+00	0.0240	0.0000	90.65	3.002E-04	5.571E-03
26.970	7.910E+00	0.0241	0.0000	90.81	3.087E-04	5.606E-03
27.510	7.754E+00	0.0241	0.0000	90.97	2.920E-04	5.176E-03
28.044	7.607E+00	0.0242	0.0000	91.12	2.555E-04	4.426E-03
28.571	7.466E+00	0.0242	0.0000	91.28	2.233E-04	3.781E-03
29.092	7.333E+00	0.0243	0.0000	91.44	2.162E-04	3.585E-03
29.605	7.206E+00	0.0243	0.0000	91.60	2.085E-04	3.394E-03
30.111	7.084E+00	0.0243	0.0000	91.65	1.996E-04	3.194E-03
30.610	6.969E+00	0.0243	0.0000	91.65	1.895E-04	2.987E-03
31.081	6.864E+00	0.0243	0.0000	91.65	1.779E-04	2.772E-03
31.524	6.767E+00	0.0243	0.0000	91.70	1.648E-04	2.548E-03
31.941	6.679E+00	0.0243	0.0000	91.76	1.502E-04	2.316E-03
32.352	6.594E+00	0.0243	0.0000	91.81	1.343E-04	2.076E-03
32.757	6.512E+00	0.0244	0.0000	91.86	1.421E-04	2.172E-03
33.156	6.434E+00	0.0244	0.0000	91.92	1.631E-04	2.448E-03
33.549	6.358E+00	0.0244	0.0000	91.97	1.842E-04	2.716E-03
33.937	6.286E+00	0.0244	0.0000	92.02	1.733E-04	2.509E-03
34.318	6.216E+00	0.0244	0.0000	92.07	1.605E-04	2.285E-03
34.694	6.149E+00	0.0244	0.0000	92.13	1.469E-04	2.056E-03
35.064	6.084E+00	0.0244	0.0000	92.18	1.321E-04	1.821E-03
35.450	6.018E+00	0.0245	0.0000	92.23	1.164E-04	1.579E-03
35.851	5.950E+00	0.0245	0.0000	92.23	9.977E-05	1.330E-03
36.267	5.882E+00	0.0245	0.0000	92.23	8.203E-05	1.075E-03
36.675	5.817E+00	0.0245	0.0000	92.23	6.311E-05	8.128E-04

37.078	5.753E+00	0.0245	0.0000	92.23	4.294E-05	5.438E-04
37.474	5.692E+00	0.0245	0.0000	92.23	2.148E-05	2.677E-04
37.865	5.634E+00	0.0245	0.0000	92.23	0.000E+00	0.000E+00
38.250	5.577E+00	0.0245	0.0000	92.23	0.000E+00	0.000E+00
38.629	5.522E+00	0.0245	0.0000	92.23	2.493E-05	3.336E-04
39.003	5.469E+00	0.0245	0.0000	92.23	5.122E-05	6.752E-04
39.371	5.418E+00	0.0245	0.0000	92.23	7.885E-05	1.024E-03
39.733	5.369E+00	0.0245	0.0000	92.23	1.080E-04	1.383E-03
40.090	5.321E+00	0.0245	0.0000	92.23	1.384E-04	1.749E-03
40.441	5.275E+00	0.0245	0.0000	92.29	1.704E-04	2.124E-03
40.787	5.230E+00	0.0245	0.0000	92.34	2.038E-04	2.507E-03
41.129	5.187E+00	0.0245	0.0000	92.39	2.704E-04	3.294E-03
41.464	5.145E+00	0.0245	0.0000	92.44	3.399E-04	4.098E-03
41.795	5.104E+00	0.0245	0.0000	92.50	4.125E-04	4.920E-03
42.121	5.064E+00	0.0245	0.0000	92.55	4.881E-04	5.759E-03
42.442	5.026E+00	0.0246	0.0000	92.60	5.013E-04	5.856E-03
42.759	4.989E+00	0.0246	0.0000	92.71	5.147E-04	5.955E-03
43.071	4.953E+00	0.0246	0.0000	92.81	5.283E-04	6.055E-03
43.378	4.918E+00	0.0246	0.0000	92.92	5.420E-04	6.156E-03
43.681	4.884E+00	0.0247	0.0000	93.02	5.560E-04	6.260E-03
43.979	4.851E+00	0.0247	0.0000	93.07	5.702E-04	6.364E-03
44.273	4.818E+00	0.0247	0.0000	93.13	5.845E-04	6.469E-03
44.562	4.787E+00	0.0247	0.0000	93.18	5.181E-04	5.682E-03
44.848	4.757E+00	0.0247	0.0000	93.23	4.486E-04	4.878E-03
45.128	4.727E+00	0.0247	0.0000	93.28	3.759E-04	4.056E-03
45.405	4.698E+00	0.0248	0.0000	93.34	3.001E-04	3.217E-03

45.678	4.670E+00	0.0248	0.0000	93.39	2.623E-04	2.786E-03
45.958	4.642E+00	0.0248	0.0000	93.39	2.229E-04	2.346E-03
46.245	4.613E+00	0.0248	0.0000	93.39	1.818E-04	1.896E-03
46.538	4.584E+00	0.0248	0.0000	93.39	1.391E-04	1.438E-03
46.840	4.554E+00	0.0248	0.0000	93.39	9.456E-05	9.674E-04
47.150	4.524E+00	0.0248	0.0000	93.39	4.819E-05	4.881E-04
47.468	4.494E+00	0.0248	0.0000	93.39	0.000E+00	0.000E+00
47.795	4.463E+00	0.0248	0.0000	93.39	0.000E+00	0.000E+00
48.102	4.435E+00	0.0248	0.0000	93.39	0.000E+00	0.000E+00
48.465	4.402E+00	0.0248	0.0000	93.39	0.000E+00	0.000E+00
48.878	4.364E+00	0.0248	0.0000	93.39	0.000E+00	0.000E+00
49.355	4.322E+00	0.0248	0.0000	93.39	0.000E+00	0.000E+00
49.886	4.276E+00	0.0248	0.0000	93.39	0.000E+00	0.000E+00
50.474	4.226E+00	0.0248	0.0000	93.39	0.000E+00	0.000E+00
51.119	4.173E+00	0.0248	0.0000	93.39	0.000E+00	0.000E+00
51.835	4.115E+00	0.0248	0.0000	93.39	0.000E+00	0.000E+00
52.607	4.055E+00	0.0248	0.0000	93.39	0.000E+00	0.000E+00
53.455	3.991E+00	0.0248	0.0000	93.39	0.000E+00	0.000E+00
54.360	3.924E+00	0.0248	0.0000	93.39	0.000E+00	0.000E+00
55.356	3.854E+00	0.0248	0.0000	93.39	0.000E+00	0.000E+00
56.372	3.784E+00	0.0248	0.0000	93.39	0.000E+00	0.000E+00
57.409	3.716E+00	0.0248	0.0000	93.39	0.000E+00	0.000E+00
58.447	3.650E+00	0.0248	0.0000	93.39	0.000E+00	0.000E+00
59.506	3.585E+00	0.0248	0.0000	93.39	0.000E+00	0.000E+00
60.577	3.522E+00	0.0248	0.0000	93.39	0.000E+00	0.000E+00
61.672	3.459E+00	0.0248	0.0000	93.39	0.000E+00	0.000E+00

62.777	3.398E+00	0.0248	0.0000	93.39	0.000E+00	0.000E+00
63.906	3.338E+00	0.0248	0.0000	93.39	0.000E+00	0.000E+00
65.034	3.280E+00	0.0248	0.0000	93.39	0.000E+00	0.000E+00
66.197	3.223E+00	0.0248	0.0000	93.39	0.000E+00	0.000E+00
67.379	3.166E+00	0.0248	0.0000	93.39	0.000E+00	0.000E+00
68.592	3.110E+00	0.0248	0.0000	93.39	0.000E+00	0.000E+00
69.849	3.054E+00	0.0248	0.0000	93.39	0.000E+00	0.000E+00
71.148	2.998E+00	0.0248	0.0000	93.39	0.000E+00	0.000E+00
72.484	2.943E+00	0.0248	0.0000	93.39	0.000E+00	0.000E+00
73.870	2.888E+00	0.0248	0.0000	93.39	0.000E+00	0.000E+00
75.294	2.833E+00	0.0248	0.0000	93.39	0.000E+00	0.000E+00
76.766	2.779E+00	0.0248	0.0000	93.39	0.000E+00	0.000E+00
78.333	2.723E+00	0.0248	0.0000	93.39	0.000E+00	0.000E+00
80.027	2.666E+00	0.0248	0.0000	93.39	0.000E+00	0.000E+00
81.792	2.608E+00	0.0248	0.0000	93.39	0.000E+00	0.000E+00
83.643	2.550E+00	0.0248	0.0000	93.39	0.000E+00	0.000E+00
85.627	2.491E+00	0.0248	0.0000	93.39	0.000E+00	0.000E+00
87.757	2.431E+00	0.0248	0.0000	93.39	0.000E+00	0.000E+00
89.998	2.370E+00	0.0248	0.0000	93.39	0.000E+00	0.000E+00
92.420	2.308E+00	0.0248	0.0000	93.39	0.000E+00	0.000E+00
94.969	2.246E+00	0.0248	0.0000	93.39	0.000E+00	0.000E+00
97.654	2.184E+00	0.0248	0.0000	93.39	0.000E+00	0.000E+00
100.496	2.123E+00	0.0248	0.0000	93.39	0.000E+00	0.000E+00
103.467	2.062E+00	0.0248	0.0000	93.39	0.000E+00	0.000E+00
106.556	2.002E+00	0.0248	0.0000	93.39	0.000E+00	0.000E+00
109.834	1.942E+00	0.0248	0.0000	93.39	0.000E+00	0.000E+00

113.311	1.883E+00	0.0248	0.0000	93.39	0.000E+00	0.000E+00
116.962	1.824E+00	0.0248	0.0000	93.39	0.000E+00	0.000E+00
120.804	1.766E+00	0.0248	0.0000	93.39	0.000E+00	0.000E+00
124.902	1.708E+00	0.0248	0.0000	93.39	0.000E+00	0.000E+00
129.221	1.651E+00	0.0248	0.0000	93.39	0.000E+00	0.000E+00
133.850	1.594E+00	0.0248	0.0000	93.39	0.000E+00	0.000E+00
138.821	1.537E+00	0.0248	0.0000	93.39	0.000E+00	0.000E+00
144.174	1.480E+00	0.0248	0.0000	93.39	0.000E+00	0.000E+00
149.937	1.423E+00	0.0248	0.0000	93.39	0.000E+00	0.000E+00
156.149	1.366E+00	0.0248	0.0000	93.39	0.000E+00	0.000E+00
162.898	1.310E+00	0.0248	0.0000	93.39	0.000E+00	0.000E+00
170.242	1.253E+00	0.0248	0.0000	93.39	0.000E+00	0.000E+00
178.216	1.197E+00	0.0248	0.0000	93.39	0.000E+00	0.000E+00
186.912	1.141E+00	0.0248	0.0000	93.39	0.000E+00	0.000E+00
196.419	1.086E+00	0.0248	0.0000	93.39	0.000E+00	0.000E+00
206.818	1.031E+00	0.0248	0.0000	93.39	0.000E+00	0.000E+00
218.231	9.775E-01	0.0248	0.0000	93.39	0.000E+00	0.000E+00
230.805	9.243E-01	0.0248	0.0000	93.39	0.000E+00	0.000E+00
244.626	8.720E-01	0.0248	0.0000	93.39	0.000E+00	0.000E+00
259.897	8.208E-01	0.0248	0.0000	93.39	0.000E+00	0.000E+00
276.777	7.707E-01	0.0248	0.0000	93.39	0.000E+00	0.000E+00
295.386	7.222E-01	0.0248	0.0000	93.39	0.000E+00	0.000E+00
315.957	6.752E-01	0.0248	0.0000	93.39	0.000E+00	0.000E+00
338.665	6.299E-01	0.0248	0.0000	93.39	0.000E+00	0.000E+00
363.694	5.865E-01	0.0248	0.0000	93.39	0.000E+00	0.000E+00
391.217	5.453E-01	0.0248	0.0000	93.39	0.000E+00	0.000E+00

421.431	5.062E-01	0.0248	0.0000	93.39	0.000E+00	0.000E+00
454.478	4.694E-01	0.0248	0.0000	93.39	0.000E+00	0.000E+00
490.528	4.349E-01	0.0248	0.0000	93.39	0.000E+00	0.000E+00
529.674	4.027E-01	0.0248	0.0000	93.39	0.000E+00	0.000E+00
571.984	3.730E-01	0.0248	0.0000	93.39	0.000E+00	0.000E+00
617.519	3.455E-01	0.0248	0.0000	93.39	0.000E+00	0.000E+00
666.342	3.201E-01	0.0248	0.0000	93.39	0.000E+00	0.000E+00
718.416	2.969E-01	0.0248	0.0000	93.39	0.000E+00	0.000E+00
773.744	2.757E-01	0.0248	0.0000	93.39	0.000E+00	0.000E+00
831.367	2.566E-01	0.0248	0.0000	93.39	0.000E+00	0.000E+00
892.987	2.389E-01	0.0248	0.0000	93.39	0.000E+00	0.000E+00
958.009	2.227E-01	0.0248	0.0000	93.39	0.000E+00	0.000E+00
1026.849	2.077E-01	0.0248	0.0000	93.39	0.000E+00	0.000E+00
1099.331	1.940E-01	0.0248	0.0000	93.39	0.000E+00	0.000E+00
1175.842	1.814E-01	0.0248	0.0000	93.39	0.000E+00	0.000E+00
1255.066	1.700E-01	0.0248	0.0000	93.39	0.000E+00	0.000E+00
1337.998	1.594E-01	0.0248	0.0000	93.39	0.000E+00	0.000E+00
1424.879	1.497E-01	0.0248	0.0000	93.39	0.000E+00	0.000E+00
1515.443	1.408E-01	0.0248	0.0000	93.39	0.000E+00	0.000E+00
1610.341	1.325E-01	0.0248	0.0000	93.39	0.000E+00	0.000E+00
1710.042	1.247E-01	0.0248	0.0000	93.39	0.000E+00	0.000E+00
1812.557	1.177E-01	0.0248	0.0000	93.39	0.000E+00	0.000E+00
1917.339	1.113E-01	0.0248	0.0000	93.39	0.000E+00	0.000E+00
2024.116	1.054E-01	0.0248	0.0000	93.39	0.000E+00	0.000E+00
2133.253	1.000E-01	0.0248	0.0000	93.39	0.000E+00	0.000E+00
2243.841	9.507E-02	0.0248	0.0000	93.39	0.000E+00	0.000E+00

2358.240	9.046E-02	0.0248	0.0000	93.39	0.000E+00	0.000E+00
2474.543	8.621E-02	0.0248	0.0000	93.39	0.000E+00	0.000E+00
2591.754	8.231E-02	0.0248	0.0000	93.39	0.000E+00	0.000E+00
2709.963	7.872E-02	0.0248	0.0000	93.39	1.387E-03	3.152E-04
2828.172	7.543E-02	0.0248	0.0000	93.39	3.020E-03	6.406E-04
2947.197	7.238E-02	0.0248	0.0000	93.39	4.908E-03	9.750E-04
3067.311	6.955E-02	0.0248	0.0000	93.39	7.037E-03	1.312E-03
3188.785	6.690E-02	0.0248	0.0000	93.39	9.463E-03	1.661E-03
3311.621	6.442E-02	0.0248	0.0001	93.60	1.220E-02	2.018E-03
3435.091	6.210E-02	0.0249	0.0001	93.82	1.525E-02	2.383E-03
3559.650	5.993E-02	0.0249	0.0001	94.03	1.864E-02	2.758E-03
3687.566	5.785E-02	0.0250	0.0001	94.25	2.241E-02	3.141E-03
3815.935	5.590E-02	0.0251	0.0001	94.46	2.658E-02	3.534E-03
3945.394	5.407E-02	0.0251	0.0001	94.68	3.116E-02	3.938E-03
4076.031	5.234E-02	0.0252	0.0001	94.89	3.300E-02	4.036E-03
4207.757	5.070E-02	0.0252	0.0001	95.11	3.489E-02	4.132E-03
4340.663	4.915E-02	0.0253	0.0001	95.32	3.684E-02	4.229E-03
4474.113	4.768E-02	0.0253	0.0001	95.54	3.901E-02	4.344E-03
4608.289	4.629E-02	0.0254	0.0001	95.75	4.123E-02	4.457E-03
4743.008	4.498E-02	0.0255	0.0001	95.97	4.655E-02	4.934E-03
4878.816	4.372E-02	0.0255	0.0001	96.18	5.226E-02	5.417E-03
5015.532	4.253E-02	0.0256	0.0001	96.39	5.906E-02	5.980E-03
5149.254	4.143E-02	0.0256	0.0001	96.61	7.128E-02	7.095E-03
5284.064	4.037E-02	0.0257	0.0001	96.82	7.487E-02	7.204E-03
5421.688	3.935E-02	0.0258	0.0001	97.21	8.485E-02	7.961E-03
5560.489	3.836E-02	0.0259	0.0001	97.60	9.807E-02	8.982E-03

5697.125	3.744E-02	0.0260	0.0001	98.01	1.071E-01	9.417E-03
5834.854	3.656E-02	0.0262	0.0002	98.65	1.177E-01	9.936E-03
5975.590	3.570E-02	0.0262	0.0001	98.87	1.302E-01	1.056E-02
6121.354	3.485E-02	0.0264	0.0001	99.37	1.457E-01	1.134E-02
6272.373	3.401E-02	0.0265	0.0002	100.00	1.561E-01	1.170E-02

Table E5: ED=0.019J/mm²

Report date: 08/10/2007   Merged File

QUANTACHROME INSTRUMENTS

QUANTACHROME POREMASTER FOR WINDOWS® DATA REPORT

VERSION 4.03

SAMPLE ID   CS5030407_16   FILE NAME   S781002H_Merged.PRM

SAMPLE WEIGHT   1.0000 grams   BULK SAMPLE VOLUME 1.0000 cc

SAMPLE DESCRIPTION M. TEKIN

COMMENTS   LP STATION 1

HG SURFACE TENSION 480.00 erg/cm²   HG CONTACT ANGLE   (I)140.00°,(E)140.00°

MINIMUM DELTA VOL. 0.000 % FS   MOVING POINT AVG. 11 (Scan Mode)

OPERATOR   Leyla MOLU   Mercury volume normalized by sample weight.

Pore Size Distribution By Volume - Intrusion

Printing every data point.

Pressure	Pore Diameter	Volume Intruded	Delta Volume	% Volume Intruded	Dv(d)	-dV/d(log d)
[PSI]	[μm]	[cc/g]	[cc/g]	%	[cc/(μm-g)]	[cc/g]
0.926	2.303E+02	0.0000	0.0000	0.00	1.067E-05	9.430E-03
1.132	1.885E+02	0.0016	0.0016	3.61	1.297E-05	1.092E-02
1.518	1.405E+02	0.0026	0.0011	6.01	2.131E-05	1.247E-02
2.073	1.029E+02	0.0036	0.0010	8.23	3.900E-05	1.418E-02
2.685	7.946E+01	0.0047	0.0010	10.60	6.818E-05	1.591E-02
3.323	6.420E+01	0.0059	0.0012	13.43	1.093E-04	1.801E-02
3.896	5.476E+01	0.0073	0.0014	16.54	1.736E-04	2.211E-02
4.515	4.725E+01	0.0088	0.0015	19.94	1.992E-04	2.507E-02
5.175	4.122E+01	0.0104	0.0017	23.69	2.673E-04	2.953E-02
5.863	3.639E+01	0.0121	0.0017	27.56	3.654E-04	3.488E-02
6.549	3.257E+01	0.0140	0.0019	31.82	4.871E-04	4.056E-02
7.238	2.947E+01	0.0160	0.0020	36.26	6.217E-04	4.579E-02
7.929	2.690E+01	0.0180	0.0020	40.84	7.656E-04	5.076E-02
8.621	2.474E+01	0.0201	0.0021	45.57	9.180E-04	5.507E-02
9.315	2.290E+01	0.0223	0.0022	50.62	1.074E-03	5.866E-02
10.009	2.131E+01	0.0245	0.0022	55.70	1.238E-03	6.191E-02
10.703	1.993E+01	0.0266	0.0021	60.40	1.387E-03	6.392E-02
11.366	1.877E+01	0.0285	0.0019	64.81	1.517E-03	6.493E-02
11.998	1.778E+01	0.0302	0.0017	68.59	1.621E-03	6.511E-02
12.629	1.689E+01	0.0317	0.0015	71.99	1.693E-03	6.418E-02
13.229	1.612E+01	0.0331	0.0014	75.07	1.706E-03	6.131E-02
13.829	1.543E+01	0.0342	0.0012	77.74	1.670E-03	5.714E-02

14.427	1.479E+01	0.0353	0.0010	80.09	1.629E-03	5.322E-02
14.992	1.423E+01	0.0362	0.0009	82.09	1.547E-03	4.848E-02
15.525	1.374E+01	0.0369	0.0007	83.71	1.451E-03	4.387E-02
16.054	1.329E+01	0.0374	0.0005	84.85	1.343E-03	3.927E-02
16.582	1.286E+01	0.0377	0.0004	85.67	1.216E-03	3.446E-02
17.105	1.247E+01	0.0381	0.0004	86.53	1.098E-03	3.028E-02
17.656	1.208E+01	0.0384	0.0003	87.23	9.805E-04	2.628E-02
18.233	1.170E+01	0.0387	0.0003	87.87	8.691E-04	2.269E-02
18.806	1.134E+01	0.0389	0.0002	88.37	7.722E-04	1.971E-02
19.403	1.099E+01	0.0391	0.0002	88.82	7.125E-04	1.772E-02
19.994	1.067E+01	0.0393	0.0002	89.26	6.813E-04	1.645E-02
20.577	1.037E+01	0.0395	0.0002	89.61	6.242E-04	1.470E-02
21.184	1.007E+01	0.0396	0.0002	89.99	5.882E-04	1.349E-02
21.813	9.779E+00	0.0398	0.0002	90.41	5.623E-04	1.256E-02
22.435	9.509E+00	0.0400	0.0002	90.75	5.525E-04	1.201E-02
23.047	9.256E+00	0.0401	0.0001	91.07	5.548E-04	1.176E-02
23.653	9.019E+00	0.0402	0.0001	91.29	5.410E-04	1.117E-02
24.249	8.797E+00	0.0403	0.0001	91.52	5.402E-04	1.085E-02
24.812	8.598E+00	0.0404	0.0001	91.74	5.258E-04	1.031E-02
25.342	8.418E+00	0.0405	0.0001	91.96	5.041E-04	9.698E-03
25.840	8.256E+00	0.0406	0.0001	92.18	4.813E-04	9.084E-03
26.330	8.102E+00	0.0407	0.0001	92.34	4.606E-04	8.548E-03
26.813	7.956E+00	0.0407	0.0001	92.50	4.576E-04	8.325E-03
27.289	7.817E+00	0.0408	0.0001	92.63	4.329E-04	7.697E-03
27.758	7.685E+00	0.0409	0.0001	92.75	4.117E-04	7.185E-03
28.219	7.559E+00	0.0409	0.0000	92.85	3.838E-04	6.589E-03

28.674	7.440E+00	0.0409	0.0000	92.95	3.482E-04	5.901E-03
29.122	7.325E+00	0.0410	0.0000	93.04	3.292E-04	5.500E-03
29.562	7.216E+00	0.0410	0.0000	93.07	3.077E-04	5.083E-03
30.021	7.106E+00	0.0410	0.0000	93.14	2.952E-04	4.818E-03
30.496	6.995E+00	0.0410	0.0000	93.20	2.698E-04	4.337E-03
30.990	6.884E+00	0.0411	0.0000	93.26	2.542E-04	4.016E-03
31.475	6.778E+00	0.0411	0.0000	93.33	2.369E-04	3.685E-03
31.954	6.676E+00	0.0411	0.0000	93.39	2.177E-04	3.343E-03
32.425	6.579E+00	0.0412	0.0000	93.45	2.243E-04	3.380E-03
32.888	6.486E+00	0.0412	0.0000	93.49	2.180E-04	3.237E-03
33.345	6.397E+00	0.0412	0.0000	93.52	2.121E-04	3.109E-03
33.795	6.312E+00	0.0412	0.0000	93.55	2.069E-04	2.996E-03
34.237	6.231E+00	0.0412	0.0000	93.58	2.008E-04	2.877E-03
34.674	6.152E+00	0.0412	0.0000	93.61	1.940E-04	2.754E-03
35.102	6.077E+00	0.0412	0.0000	93.64	1.864E-04	2.626E-03
35.525	6.005E+00	0.0413	0.0000	93.68	1.939E-04	2.700E-03
35.940	5.935E+00	0.0413	0.0000	93.71	2.215E-04	3.062E-03
36.350	5.868E+00	0.0413	0.0000	93.74	2.504E-04	3.433E-03
36.753	5.804E+00	0.0413	0.0000	93.77	2.808E-04	3.812E-03
37.150	5.742E+00	0.0413	0.0000	93.80	3.125E-04	4.198E-03
37.541	5.682E+00	0.0413	0.0000	93.84	3.227E-04	4.277E-03
37.926	5.625E+00	0.0414	0.0000	93.90	3.331E-04	4.357E-03
38.305	5.569E+00	0.0414	0.0000	93.96	3.437E-04	4.437E-03
38.679	5.515E+00	0.0414	0.0000	94.03	3.545E-04	4.520E-03
39.047	5.463E+00	0.0414	0.0000	94.09	3.654E-04	4.604E-03
39.410	5.413E+00	0.0415	0.0000	94.12	3.766E-04	4.689E-03

39.767	5.364E+00	0.0415	0.0000	94.15	3.878E-04	4.775E-03
40.119	5.317E+00	0.0415	0.0000	94.19	3.454E-04	4.200E-03
40.465	5.272E+00	0.0415	0.0000	94.22	3.003E-04	3.611E-03
40.806	5.228E+00	0.0415	0.0000	94.25	2.527E-04	3.007E-03
41.142	5.185E+00	0.0415	0.0000	94.28	2.026E-04	2.388E-03
41.472	5.144E+00	0.0415	0.0000	94.31	1.778E-04	2.071E-03
41.798	5.104E+00	0.0415	0.0000	94.31	1.517E-04	1.747E-03
42.119	5.065E+00	0.0415	0.0000	94.31	1.242E-04	1.414E-03
42.435	5.027E+00	0.0415	0.0000	94.31	9.527E-05	1.073E-03
42.746	4.991E+00	0.0415	0.0000	94.31	6.492E-05	7.233E-04
43.052	4.955E+00	0.0415	0.0000	94.31	3.320E-05	3.660E-04
43.353	4.921E+00	0.0415	0.0000	94.31	0.000E+00	0.000E+00
43.651	4.887E+00	0.0415	0.0000	94.31	0.000E+00	0.000E+00
43.944	4.854E+00	0.0415	0.0000	94.31	0.000E+00	0.000E+00
44.233	4.823E+00	0.0415	0.0000	94.31	0.000E+00	0.000E+00
44.517	4.792E+00	0.0415	0.0000	94.31	0.000E+00	0.000E+00
44.798	4.762E+00	0.0415	0.0000	94.31	0.000E+00	0.000E+00
45.074	4.733E+00	0.0415	0.0000	94.31	0.000E+00	0.000E+00
45.346	4.704E+00	0.0415	0.0000	94.31	0.000E+00	0.000E+00
45.614	4.677E+00	0.0415	0.0000	94.31	0.000E+00	0.000E+00
45.889	4.649E+00	0.0415	0.0000	94.31	0.000E+00	0.000E+00
46.172	4.620E+00	0.0415	0.0000	94.31	0.000E+00	0.000E+00
46.462	4.591E+00	0.0415	0.0000	94.31	0.000E+00	0.000E+00
46.728	4.565E+00	0.0415	0.0000	94.31	0.000E+00	0.000E+00
47.284	4.512E+00	0.0415	0.0000	94.31	0.000E+00	0.000E+00
48.183	4.427E+00	0.0415	0.0000	94.31	0.000E+00	0.000E+00

49.499	4.310E+00	0.0415	0.0000	94.31	0.000E+00	0.000E+00
51.309	4.158E+00	0.0415	0.0000	94.31	0.000E+00	0.000E+00
53.728	3.970E+00	0.0415	0.0000	94.31	0.000E+00	0.000E+00
56.894	3.749E+00	0.0415	0.0000	94.31	0.000E+00	0.000E+00
60.990	3.498E+00	0.0415	0.0000	94.31	2.535E-06	3.533E-05
66.220	3.221E+00	0.0415	0.0000	94.31	5.362E-06	6.848E-05
72.880	2.927E+00	0.0415	0.0000	94.31	8.795E-06	1.002E-04
81.334	2.623E+00	0.0415	0.0000	94.31	1.325E-05	1.311E-04
92.091	2.316E+00	0.0415	0.0000	94.31	1.938E-05	1.616E-04
105.363	2.025E+00	0.0416	0.0000	94.36	2.804E-05	1.922E-04
121.623	1.754E+00	0.0416	0.0000	94.42	4.041E-05	2.234E-04
141.275	1.510E+00	0.0416	0.0000	94.47	5.821E-05	2.555E-04
164.837	1.294E+00	0.0416	0.0000	94.52	8.624E-05	3.057E-04
192.680	1.107E+00	0.0417	0.0000	94.57	1.267E-04	3.581E-04
225.046	9.479E-01	0.0417	0.0000	94.62	1.844E-04	4.134E-04
262.135	8.138E-01	0.0417	0.0000	94.67	2.124E-04	3.977E-04
303.994	7.017E-01	0.0417	0.0000	94.73	2.453E-04	3.853E-04
350.606	6.084E-01	0.0418	0.0000	94.80	2.909E-04	3.975E-04
401.833	5.309E-01	0.0418	0.0000	94.88	3.459E-04	4.135E-04
457.356	4.664E-01	0.0418	0.0000	94.96	4.118E-04	4.329E-04
516.937	4.127E-01	0.0418	0.0000	94.98	4.895E-04	4.551E-04
580.181	3.677E-01	0.0418	0.0000	95.01	5.798E-04	4.793E-04
646.776	3.298E-01	0.0419	0.0000	95.06	7.289E-04	5.635E-04
716.218	2.978E-01	0.0419	0.0000	95.11	8.357E-04	6.046E-04
788.189	2.706E-01	0.0419	0.0000	95.17	9.549E-04	6.493E-04
862.666	2.473E-01	0.0419	0.0000	95.22	1.084E-03	6.942E-04

940.359	2.269E-01	0.0420	0.0000	95.27	1.356E-03	7.779E-04
1020.735	2.090E-01	0.0420	0.0000	95.37	1.678E-03	8.642E-04
1103.692	1.933E-01	0.0420	0.0000	95.45	1.976E-03	9.329E-04
1187.828	1.796E-01	0.0421	0.0000	95.53	2.309E-03	1.002E-03
1275.525	1.672E-01	0.0421	0.0000	95.60	2.680E-03	1.072E-03
1366.768	1.561E-01	0.0421	0.0000	95.68	3.101E-03	1.144E-03
1460.972	1.460E-01	0.0422	0.0000	95.76	3.670E-03	1.262E-03
1556.791	1.370E-01	0.0422	0.0000	95.84	3.836E-03	1.236E-03
1655.676	1.288E-01	0.0422	0.0000	95.91	4.242E-03	1.285E-03
1757.464	1.214E-01	0.0423	0.0000	95.99	4.665E-03	1.331E-03
1860.976	1.146E-01	0.0423	0.0000	96.07	5.127E-03	1.381E-03
1966.303	1.085E-01	0.0424	0.0000	96.17	5.629E-03	1.435E-03
2073.988	1.029E-01	0.0424	0.0000	96.23	6.172E-03	1.492E-03
2182.217	9.775E-02	0.0424	0.0000	96.30	7.123E-03	1.659E-03
2293.985	9.299E-02	0.0424	0.0000	96.38	8.423E-03	1.895E-03
2405.752	8.867E-02	0.0425	0.0000	96.46	9.907E-03	2.142E-03
2517.974	8.472E-02	0.0425	0.0000	96.54	1.152E-02	2.384E-03
2630.286	8.110E-02	0.0426	0.0000	96.61	1.270E-02	2.522E-03
2744.503	7.773E-02	0.0426	0.0001	96.74	1.465E-02	2.757E-03
2858.176	7.464E-02	0.0427	0.0001	96.90	1.609E-02	2.877E-03
2971.939	7.178E-02	0.0427	0.0001	97.05	1.764E-02	3.003E-03
3089.785	6.904E-02	0.0428	0.0001	97.21	1.966E-02	3.200E-03
3210.261	6.645E-02	0.0429	0.0001	97.34	2.187E-02	3.402E-03
3330.375	6.405E-02	0.0429	0.0001	97.47	2.507E-02	3.753E-03
3454.571	6.175E-02	0.0430	0.0000	97.57	2.631E-02	3.777E-03
3578.949	5.960E-02	0.0430	0.0000	97.67	2.648E-02	3.651E-03

3703.962	5.759E-02	0.0431	0.0001	97.80	2.647E-02	3.518E-03
3828.884	5.571E-02	0.0431	0.0001	97.93	2.641E-02	3.394E-03
3954.985	5.394E-02	0.0432	0.0001	98.11	2.803E-02	3.506E-03
4080.906	5.227E-02	0.0433	0.0000	98.22	2.966E-02	3.614E-03
4211.725	5.065E-02	0.0433	0.0000	98.29	3.221E-02	3.806E-03
4343.360	4.911E-02	0.0433	0.0000	98.37	3.494E-02	4.000E-03
4472.908	4.769E-02	0.0434	0.0000	98.45	3.628E-02	4.030E-03
4600.461	4.637E-02	0.0434	0.0001	98.58	3.755E-02	4.055E-03
4728.921	4.511E-02	0.0435	0.0001	98.71	3.714E-02	3.935E-03
4855.023	4.394E-02	0.0435	0.0001	98.84	3.910E-02	4.031E-03
4981.396	4.282E-02	0.0436	0.0001	98.97	4.221E-02	4.224E-03
5109.131	4.175E-02	0.0436	0.0000	99.07	4.681E-02	4.564E-03
5237.409	4.073E-02	0.0437	0.0000	99.17	4.837E-02	4.550E-03
5365.416	3.976E-02	0.0437	0.0000	99.28	4.948E-02	4.545E-03
5494.692	3.882E-02	0.0438	0.0000	99.38	5.642E-02	5.130E-03
5621.066	3.795E-02	0.0438	0.0000	99.48	5.317E-02	4.678E-03
5747.218	3.712E-02	0.0439	0.0001	99.62	5.436E-02	4.636E-03
5873.606	3.632E-02	0.0439	0.0000	99.67	5.684E-02	4.691E-03
6001.511	3.554E-02	0.0439	0.0000	99.77	5.944E-02	4.748E-03
6126.651	3.482E-02	0.0440	0.0001	100.00	6.209E-02	4.806E-03
6256.381	3.410E-02	0.0440	0.0000	100.00	6.497E-02	4.873E-03

Table E6: ED=0.025J/mm²

SAMPLE ID   CS6030407_18   FILE NAME   S781003H_Merged.PRM

SAMPLE WEIGHT   1.0000 grams   BULK SAMPLE VOLUME 1.0000 cc

SAMPLE DESCRIPTION M. TEKIN

COMMENTS   LP STATION 1

HG SURFACE TENSION 480.00 erg/cm²   HG CONTACT ANGLE   (I)140.00°,(E)140.00°

MINIMUM DELTA VOL. 0.000 % FS   MOVING POINT AVG. 11 (Scan Mode)

OPERATOR   Leyla MOLU   Mercury volume normalized by sample weight.

Pore Size Distribution By Volume - Intrusion

Printing every data point.

Pressure	Pore Diameter	Volume Intruded	Delta Volume	% Volume Intruded	Dv(d)	-dV/d(log d)
[PSI]	[µm]	[cc/g]	[cc/g]	%	[cc/(µm-g)]	[cc/g]
1.080	1.975E+02	0.0000	0.0000	0.00	1.277E-05	8.852E-03
1.397	1.527E+02	0.0018	0.0018	6.31	1.667E-05	9.636E-03
1.709	1.248E+02	0.0028	0.0009	9.46	2.538E-05	1.001E-02
2.020	1.056E+02	0.0033	0.0006	11.41	3.524E-05	1.023E-02

2.335	9.136E+01	0.0039	0.0005	13.26	4.678E-05	1.060E-02
2.658	8.027E+01	0.0044	0.0005	15.10	6.045E-05	1.113E-02
2.980	7.158E+01	0.0051	0.0007	17.53	8.259E-05	1.266E-02
3.309	6.447E+01	0.0057	0.0006	19.49	8.546E-05	1.290E-02
3.645	5.853E+01	0.0062	0.0005	21.21	9.797E-05	1.379E-02
3.989	5.348E+01	0.0068	0.0005	23.08	1.161E-04	1.484E-02
4.332	4.924E+01	0.0073	0.0006	25.08	1.373E-04	1.606E-02
4.676	4.562E+01	0.0079	0.0006	26.99	1.610E-04	1.738E-02
5.025	4.245E+01	0.0085	0.0006	29.05	1.819E-04	1.847E-02
5.372	3.971E+01	0.0091	0.0006	31.05	2.095E-04	1.992E-02
5.720	3.730E+01	0.0096	0.0005	32.87	2.422E-04	2.156E-02
6.067	3.516E+01	0.0102	0.0006	34.78	2.735E-04	2.282E-02
6.415	3.325E+01	0.0108	0.0006	36.79	3.069E-04	2.421E-02
6.763	3.154E+01	0.0114	0.0006	38.84	3.455E-04	2.584E-02
7.106	3.002E+01	0.0120	0.0006	40.94	3.834E-04	2.729E-02
7.449	2.864E+01	0.0126	0.0006	43.05	4.245E-04	2.885E-02
7.803	2.734E+01	0.0132	0.0006	44.96	4.774E-04	3.099E-02
8.159	2.614E+01	0.0138	0.0006	47.06	5.369E-04	3.339E-02
8.523	2.503E+01	0.0144	0.0007	49.30	6.007E-04	3.583E-02
8.881	2.402E+01	0.0151	0.0006	51.45	6.621E-04	3.786E-02
9.256	2.305E+01	0.0157	0.0007	53.75	7.216E-04	3.958E-02
9.637	2.214E+01	0.0165	0.0008	56.33	7.795E-04	4.093E-02
10.031	2.127E+01	0.0173	0.0008	59.19	8.495E-04	4.263E-02
10.431	2.045E+01	0.0182	0.0009	62.16	9.030E-04	4.325E-02
10.839	1.968E+01	0.0190	0.0008	64.93	9.517E-04	4.359E-02
11.260	1.895E+01	0.0198	0.0008	67.60	9.979E-04	4.368E-02

11.687	1.825E+01	0.0205	0.0007	70.09	1.039E-03	4.354E-02
12.107	1.762E+01	0.0212	0.0007	72.52	1.053E-03	4.230E-02
12.540	1.701E+01	0.0218	0.0006	74.53	1.031E-03	3.975E-02
12.978	1.644E+01	0.0224	0.0006	76.49	9.832E-04	3.642E-02
13.436	1.588E+01	0.0229	0.0005	78.35	9.316E-04	3.313E-02
13.889	1.536E+01	0.0235	0.0005	80.12	8.718E-04	2.979E-02
14.352	1.486E+01	0.0239	0.0004	81.55	8.109E-04	2.669E-02
14.818	1.440E+01	0.0242	0.0003	82.51	7.397E-04	2.358E-02
15.289	1.395E+01	0.0243	0.0002	83.18	6.872E-04	2.123E-02
15.770	1.353E+01	0.0245	0.0002	83.75	6.256E-04	1.879E-02
16.254	1.312E+01	0.0247	0.0001	84.23	5.627E-04	1.648E-02
16.741	1.274E+01	0.0248	0.0001	84.71	4.844E-04	1.388E-02
17.232	1.238E+01	0.0250	0.0002	85.23	4.223E-04	1.187E-02
17.724	1.204E+01	0.0251	0.0002	85.76	3.906E-04	1.073E-02
18.220	1.171E+01	0.0252	0.0001	86.24	3.748E-04	1.001E-02
18.718	1.140E+01	0.0254	0.0001	86.67	3.653E-04	9.492E-03
19.220	1.110E+01	0.0255	0.0001	86.95	3.623E-04	9.149E-03
19.727	1.081E+01	0.0255	0.0001	87.24	3.533E-04	8.665E-03
20.231	1.054E+01	0.0256	0.0001	87.53	3.279E-04	7.811E-03
20.738	1.029E+01	0.0257	0.0001	87.76	3.037E-04	7.068E-03
21.242	1.004E+01	0.0258	0.0001	88.00	2.763E-04	6.280E-03
21.744	9.810E+00	0.0258	0.0001	88.24	2.564E-04	5.723E-03
22.251	9.587E+00	0.0259	0.0001	88.43	2.514E-04	5.488E-03
22.758	9.373E+00	0.0259	0.0000	88.53	2.457E-04	5.258E-03
23.264	9.170E+00	0.0260	0.0000	88.67	2.385E-04	5.015E-03
23.769	8.975E+00	0.0260	0.0000	88.77	2.366E-04	4.886E-03

24.271	8.789E+00	0.0260	0.0000	88.91	2.338E-04	4.753E-03
24.773	8.611E+00	0.0261	0.0000	89.06	2.302E-04	4.615E-03
25.268	8.442E+00	0.0261	0.0000	89.20	2.411E-04	4.774E-03
25.764	8.280E+00	0.0262	0.0000	89.34	2.678E-04	5.196E-03
26.258	8.124E+00	0.0262	0.0000	89.49	2.796E-04	5.318E-03
26.747	7.976E+00	0.0262	0.0000	89.63	3.001E-04	5.579E-03
27.233	7.833E+00	0.0263	0.0000	89.77	3.037E-04	5.523E-03
27.716	7.697E+00	0.0263	0.0001	89.96	3.079E-04	5.484E-03
28.195	7.566E+00	0.0264	0.0001	90.15	3.114E-04	5.437E-03
28.673	7.440E+00	0.0264	0.0000	90.30	3.039E-04	5.189E-03
29.147	7.319E+00	0.0265	0.0000	90.44	3.068E-04	5.146E-03
29.619	7.202E+00	0.0265	0.0000	90.54	3.092E-04	5.099E-03
30.066	7.095E+00	0.0265	0.0000	90.63	3.110E-04	5.050E-03
30.510	6.992E+00	0.0266	0.0000	90.73	2.880E-04	4.609E-03
30.948	6.893E+00	0.0266	0.0000	90.77	2.631E-04	4.158E-03
31.382	6.798E+00	0.0266	0.0000	90.87	2.484E-04	3.873E-03
31.812	6.706E+00	0.0266	0.0000	90.96	2.325E-04	3.583E-03
32.238	6.617E+00	0.0267	0.0000	91.06	2.282E-04	3.468E-03
32.659	6.532E+00	0.0267	0.0000	91.11	2.214E-04	3.322E-03
33.075	6.450E+00	0.0267	0.0000	91.16	2.140E-04	3.173E-03
33.487	6.370E+00	0.0267	0.0000	91.20	2.207E-04	3.225E-03
33.892	6.294E+00	0.0267	0.0000	91.25	1.951E-04	2.805E-03
34.292	6.221E+00	0.0267	0.0000	91.30	1.676E-04	2.376E-03
34.707	6.146E+00	0.0267	0.0000	91.35	1.385E-04	1.937E-03
35.117	6.075E+00	0.0268	0.0000	91.40	1.245E-04	1.711E-03
35.521	6.005E+00	0.0268	0.0000	91.44	1.096E-04	1.480E-03

35.921	5.939E+00	0.0268	0.0000	91.44	9.354E-05	1.242E-03
36.315	5.874E+00	0.0268	0.0000	91.44	7.728E-05	1.012E-03
36.702	5.812E+00	0.0268	0.0000	91.44	5.953E-05	7.708E-04
37.086	5.752E+00	0.0268	0.0000	91.44	4.152E-05	5.346E-04
37.463	5.694E+00	0.0268	0.0000	91.44	2.235E-05	2.922E-04
37.805	5.643E+00	0.0268	0.0000	91.44	2.241E-06	5.246E-05
45.277	4.711E+00	0.0268	0.0000	91.48	3.249E-06	7.884E-05
60.244	3.541E+00	0.0268	0.0000	91.52	5.942E-06	1.075E-04
83.884	2.543E+00	0.0268	0.0000	91.56	1.261E-05	1.498E-04
115.564	1.846E+00	0.0268	0.0000	91.60	2.671E-05	1.961E-04
155.647	1.371E+00	0.0268	0.0000	91.68	5.359E-05	2.460E-04
204.132	1.045E+00	0.0269	0.0000	91.79	1.027E-04	3.138E-04
262.019	8.141E-01	0.0269	0.0000	91.91	1.478E-04	3.625E-04
328.311	6.498E-01	0.0270	0.0000	92.07	2.257E-04	4.241E-04
403.370	5.289E-01	0.0270	0.0000	92.22	3.518E-04	5.162E-04
488.285	4.369E-01	0.0270	0.0000	92.38	5.398E-04	6.185E-04
582.181	3.664E-01	0.0271	0.0001	92.57	7.633E-04	6.992E-04
678.980	3.142E-01	0.0271	0.0000	92.73	1.014E-03	7.766E-04
778.137	2.741E-01	0.0272	0.0000	92.88	1.344E-03	8.889E-04
877.204	2.432E-01	0.0272	0.0001	93.08	1.659E-03	9.668E-04
977.722	2.182E-01	0.0273	0.0001	93.27	2.017E-03	1.049E-03
1079.057	1.977E-01	0.0274	0.0000	93.43	2.430E-03	1.138E-03
1182.841	1.803E-01	0.0274	0.0000	93.58	2.779E-03	1.180E-03
1287.169	1.657E-01	0.0275	0.0001	93.78	3.213E-03	1.234E-03
1393.403	1.531E-01	0.0275	0.0000	93.93	3.673E-03	1.288E-03
1500.544	1.422E-01	0.0275	0.0000	94.09	4.045E-03	1.317E-03

1607.322	1.327E-01	0.0276	0.0000	94.24	4.606E-03	1.431E-03
1715.733	1.243E-01	0.0276	0.0000	94.36	5.331E-03	1.568E-03
1823.872	1.170E-01	0.0277	0.0000	94.48	6.006E-03	1.662E-03
1932.464	1.104E-01	0.0277	0.0000	94.59	6.400E-03	1.676E-03
2043.052	1.044E-01	0.0277	0.0000	94.71	6.955E-03	1.716E-03
2154.911	9.899E-02	0.0278	0.0001	94.91	7.706E-03	1.810E-03
2267.495	9.408E-02	0.0278	0.0001	95.10	8.690E-03	1.958E-03
2379.444	8.965E-02	0.0279	0.0000	95.26	1.022E-02	2.204E-03
2492.118	8.560E-02	0.0279	0.0000	95.37	1.192E-02	2.457E-03
2605.428	8.188E-02	0.0280	0.0000	95.49	1.379E-02	2.713E-03
2719.645	7.844E-02	0.0280	0.0000	95.64	1.586E-02	2.978E-03
2835.223	7.524E-02	0.0281	0.0001	95.84	1.682E-02	3.018E-03
2951.617	7.227E-02	0.0281	0.0001	96.07	1.810E-02	3.122E-03
3068.103	6.953E-02	0.0282	0.0001	96.31	1.980E-02	3.272E-03
3186.039	6.696E-02	0.0283	0.0001	96.54	2.202E-02	3.477E-03
3303.976	6.457E-02	0.0283	0.0001	96.77	2.442E-02	3.687E-03
3425.541	6.227E-02	0.0284	0.0000	96.93	2.653E-02	3.844E-03
3548.558	6.012E-02	0.0284	0.0001	97.12	2.777E-02	3.862E-03
3672.119	5.809E-02	0.0285	0.0001	97.32	2.847E-02	3.820E-03
3795.680	5.620E-02	0.0285	0.0001	97.51	2.904E-02	3.770E-03
3919.696	5.442E-02	0.0286	0.0001	97.71	2.954E-02	3.718E-03
4044.799	5.274E-02	0.0287	0.0001	97.90	2.932E-02	3.578E-03
4173.440	5.111E-02	0.0287	0.0000	98.06	3.044E-02	3.580E-03
4302.263	4.958E-02	0.0288	0.0000	98.21	3.020E-02	3.423E-03
4432.719	4.812E-02	0.0288	0.0000	98.37	3.046E-02	3.350E-03
4563.357	4.675E-02	0.0288	0.0000	98.52	3.132E-02	3.363E-03

4694.447	4.544E-02	0.0289	0.0000	98.64	3.213E-02	3.375E-03
4822.726	4.423E-02	0.0289	0.0000	98.76	3.205E-02	3.287E-03
4951.640	4.308E-02	0.0289	0.0000	98.83	3.288E-02	3.287E-03
5082.187	4.197E-02	0.0290	0.0000	98.95	3.274E-02	3.182E-03
5213.550	4.092E-02	0.0290	0.0000	99.11	3.363E-02	3.197E-03
5345.457	3.991E-02	0.0291	0.0000	99.26	3.701E-02	3.472E-03
5477.456	3.895E-02	0.0291	0.0000	99.38	3.801E-02	3.462E-03
5607.367	3.804E-02	0.0291	0.0000	99.50	3.639E-02	3.197E-03
5736.684	3.719E-02	0.0291	0.0000	99.57	3.925E-02	3.318E-03
5866.763	3.636E-02	0.0292	0.0000	99.69	4.104E-02	3.350E-03
5998.917	3.556E-02	0.0292	0.0001	99.91	4.113E-02	3.255E-03
6129.645	3.480E-02	0.0293	0.0000	100.00	4.060E-02	3.121E-03
6263.367	3.406E-02	0.0293	0.0000	100.00	4.171E-02	3.105E-03

Table E7: ED=0.016J/mm²

Report date: 08/10/2007   Merged File

QUANTACHROME INSTRUMENTS

QUANTACHROME POREMASTER FOR WINDOWS® DATA REPORT

VERSION 4.03

SAMPLE ID   CS7030407_20   FILE NAME   S781004H_Merged.PRM

SAMPLE WEIGHT   1.0000 grams   BULK SAMPLE VOLUME 1.0000 cc

SAMPLE DESCRIPTION M. TEKIN

COMMENTS   LP STATION 1

HG SURFACE TENSION 480.00 erg/cm²   HG CONTACT ANGLE   (I)140.00°,(E)140.00°

MINIMUM DELTA VOL. 0.000 % FS   MOVING POINT AVG. 11 (Scan Mode)

OPERATOR   Leyla MOLU   Mercury volume normalized by sample weight.

Pore Size Distribution By Volume - Intrusion

Printing every data point.

Pressure	Pore Diameter	Volume Intruded	Delta Volume	% Volume Intruded	Dv(d)	-dV/d(log d)
[PSI]	[μm]	[cc/g]	[cc/g]	%	[cc/(μm-g)]	[cc/g]
1.019	2.094E+02	0.0000	0.0000	0.00	7.364E-06	5.854E-03
1.180	1.808E+02	0.0003	0.0003	0.51	9.097E-06	7.319E-03
1.402	1.522E+02	0.0009	0.0006	1.42	1.356E-05	9.286E-03
1.842	1.158E+02	0.0016	0.0007	2.60	2.303E-05	1.153E-02
2.390	8.924E+01	0.0024	0.0008	3.91	4.192E-05	1.402E-02
2.989	7.136E+01	0.0033	0.0010	5.47	7.225E-05	1.686E-02
3.508	6.081E+01	0.0044	0.0011	7.31	1.248E-04	2.262E-02
4.074	5.237E+01	0.0059	0.0015	9.77	1.886E-04	2.952E-02
4.689	4.549E+01	0.0077	0.0018	12.74	2.744E-04	3.736E-02
5.350	3.988E+01	0.0098	0.0021	16.17	4.006E-04	4.639E-02
6.037	3.533E+01	0.0122	0.0024	20.08	5.718E-04	5.634E-02
6.728	3.171E+01	0.0152	0.0030	24.98	7.880E-04	6.697E-02
7.419	2.875E+01	0.0186	0.0034	30.61	1.034E-03	7.708E-02
8.112	2.630E+01	0.0223	0.0036	36.59	1.301E-03	8.627E-02
8.807	2.422E+01	0.0260	0.0038	42.78	1.588E-03	9.453E-02

221

9.503	2.245E+01	0.0299	0.0038	49.10	1.888E-03	1.016E-01
10.199	2.092E+01	0.0337	0.0039	55.50	2.186E-03	1.072E-01
10.895	1.958E+01	0.0374	0.0037	61.50	2.423E-03	1.090E-01
11.591	1.840E+01	0.0407	0.0033	67.00	2.588E-03	1.074E-01
12.288	1.736E+01	0.0438	0.0030	72.01	2.695E-03	1.039E-01
12.984	1.643E+01	0.0465	0.0027	76.49	2.742E-03	9.883E-02
13.678	1.560E+01	0.0489	0.0024	80.47	2.714E-03	9.195E-02
14.371	1.484E+01	0.0507	0.0018	83.39	2.600E-03	8.316E-02
15.030	1.419E+01	0.0520	0.0012	85.44	2.429E-03	7.382E-02
15.657	1.362E+01	0.0529	0.0010	87.05	2.211E-03	6.430E-02
16.250	1.313E+01	0.0537	0.0008	88.36	1.958E-03	5.491E-02
16.839	1.267E+01	0.0544	0.0006	89.40	1.692E-03	4.606E-02
17.425	1.224E+01	0.0548	0.0004	90.13	1.419E-03	3.771E-02
18.006	1.185E+01	0.0552	0.0003	90.71	1.208E-03	3.128E-02
18.582	1.148E+01	0.0554	0.0003	91.14	1.061E-03	2.676E-02
19.152	1.114E+01	0.0557	0.0002	91.51	9.309E-04	2.292E-02
19.715	1.082E+01	0.0559	0.0002	91.86	8.041E-04	1.938E-02
20.272	1.052E+01	0.0560	0.0002	92.16	7.082E-04	1.678E-02
20.822	1.025E+01	0.0562	0.0001	92.39	6.482E-04	1.507E-02
21.395	9.971E+00	0.0563	0.0002	92.66	6.058E-04	1.380E-02
21.991	9.700E+00	0.0565	0.0002	92.92	5.809E-04	1.290E-02
22.609	9.435E+00	0.0566	0.0001	93.12	5.668E-04	1.225E-02
23.218	9.188E+00	0.0568	0.0001	93.35	5.483E-04	1.154E-02
23.818	8.956E+00	0.0569	0.0001	93.56	5.361E-04	1.100E-02
24.410	8.739E+00	0.0570	0.0001	93.74	5.385E-04	1.077E-02
24.994	8.535E+00	0.0571	0.0001	93.90	5.226E-04	1.022E-02

25.568	8.343E+00	0.0572	0.0001	94.07	5.127E-04	9.821E-03
26.134	8.163E+00	0.0573	0.0001	94.20	5.084E-04	9.507E-03
26.692	7.992E+00	0.0574	0.0001	94.34	4.793E-04	8.749E-03
27.242	7.831E+00	0.0575	0.0001	94.48	4.532E-04	8.088E-03
27.783	7.678E+00	0.0575	0.0001	94.59	4.303E-04	7.515E-03
28.315	7.534E+00	0.0576	0.0001	94.71	4.236E-04	7.268E-03
28.840	7.397E+00	0.0577	0.0001	94.80	4.147E-04	7.004E-03
29.335	7.272E+00	0.0577	0.0000	94.85	4.124E-04	6.860E-03
29.801	7.158E+00	0.0577	0.0000	94.89	3.966E-04	6.502E-03
30.260	7.050E+00	0.0577	0.0000	94.94	3.798E-04	6.153E-03
30.691	6.951E+00	0.0578	0.0000	95.01	3.554E-04	5.674E-03
31.116	6.856E+00	0.0578	0.0000	95.08	3.281E-04	5.174E-03
31.534	6.765E+00	0.0579	0.0000	95.15	3.261E-04	5.094E-03
31.925	6.682E+00	0.0579	0.0000	95.19	3.433E-04	5.289E-03
32.289	6.607E+00	0.0579	0.0000	95.24	3.736E-04	5.701E-03
32.649	6.534E+00	0.0579	0.0000	95.26	4.052E-04	6.124E-03
33.004	6.464E+00	0.0579	0.0000	95.28	4.025E-04	6.024E-03
33.353	6.396E+00	0.0580	0.0000	95.33	3.990E-04	5.920E-03
33.718	6.327E+00	0.0580	0.0000	95.38	3.961E-04	5.827E-03
34.098	6.256E+00	0.0580	0.0000	95.44	3.734E-04	5.411E-03
34.473	6.188E+00	0.0581	0.0000	95.51	3.479E-04	4.989E-03
34.863	6.119E+00	0.0581	0.0000	95.56	3.390E-04	4.810E-03
35.248	6.052E+00	0.0581	0.0000	95.61	3.285E-04	4.627E-03
35.615	5.990E+00	0.0582	0.0000	95.65	2.945E-04	4.154E-03
42.857	4.978E+00	0.0582	0.0001	95.74	3.128E-04	3.709E-03
56.157	3.799E+00	0.0583	0.0001	95.93	3.853E-04	3.014E-03

75.132	2.839E+00	0.0585	0.0001	96.13	4.753E-04	2.307E-03
99.601	2.142E+00	0.0586	0.0001	96.32	6.143E-04	1.888E-03
129.293	1.650E+00	0.0587	0.0001	96.50	6.568E-04	1.462E-03
163.484	1.305E+00	0.0588	0.0001	96.67	3.914E-04	1.011E-03
202.899	1.051E+00	0.0589	0.0001	96.82	5.276E-04	1.051E-03
247.085	8.634E-01	0.0590	0.0001	96.97	6.028E-04	9.592E-04
297.858	7.162E-01	0.0591	0.0001	97.12	6.857E-04	8.736E-04
354.854	6.012E-01	0.0591	0.0001	97.27	7.629E-04	7.853E-04
419.447	5.086E-01	0.0592	0.0001	97.42	8.478E-04	7.010E-04
485.400	4.395E-01	0.0593	0.0001	97.53	8.898E-04	6.074E-04
552.806	3.859E-01	0.0593	0.0000	97.53	9.063E-04	5.192E-04
624.475	3.416E-01	0.0593	0.0000	97.53	8.613E-04	4.225E-04
699.954	3.048E-01	0.0593	0.0000	97.53	7.551E-04	3.206E-04
780.060	2.735E-01	0.0593	0.0000	97.53	5.703E-04	2.118E-04
865.247	2.465E-01	0.0593	0.0000	97.53	2.985E-04	9.786E-05
954.516	2.235E-01	0.0593	0.0000	97.53	0.000E+00	0.000E+00
1048.684	2.034E-01	0.0593	0.0000	97.53	0.000E+00	0.000E+00
1145.483	1.862E-01	0.0593	0.0000	97.53	0.000E+00	0.000E+00
1246.908	1.711E-01	0.0593	0.0000	97.53	0.000E+00	0.000E+00
1351.599	1.578E-01	0.0593	0.0000	97.53	0.000E+00	0.000E+00
1458.650	1.462E-01	0.0593	0.0000	97.53	0.000E+00	0.000E+00
1567.695	1.361E-01	0.0593	0.0000	97.53	0.000E+00	0.000E+00
1677.286	1.272E-01	0.0593	0.0000	97.53	0.000E+00	0.000E+00
1787.420	1.193E-01	0.0593	0.0000	97.53	0.000E+00	0.000E+00
1898.462	1.124E-01	0.0593	0.0000	97.53	0.000E+00	0.000E+00
2009.867	1.061E-01	0.0593	0.0000	97.53	6.443E-04	2.091E-04

2122.269	1.005E-01	0.0593	0.0000	97.53	2.697E-03	8.091E-04
2236.123	9.540E-02	0.0593	0.0000	97.53	5.456E-03	1.508E-03
2351.157	9.073E-02	0.0593	0.0000	97.53	8.819E-03	2.250E-03
2466.100	8.650E-02	0.0593	0.0000	97.53	1.283E-02	3.031E-03
2581.133	8.265E-02	0.0594	0.0000	97.60	1.759E-02	3.864E-03
2696.439	7.911E-02	0.0595	0.0001	97.81	2.316E-02	4.748E-03
2809.023	7.594E-02	0.0596	0.0001	98.03	2.955E-02	5.675E-03
2919.430	7.307E-02	0.0598	0.0001	98.26	3.697E-02	6.683E-03
3028.294	7.044E-02	0.0599	0.0001	98.48	4.541E-02	7.758E-03
3134.074	6.807E-02	0.0600	0.0001	98.71	5.495E-02	8.903E-03
3237.224	6.590E-02	0.0602	0.0001	98.93	6.158E-02	9.501E-03
3338.649	6.389E-02	0.0603	0.0001	99.16	6.121E-02	9.006E-03
3434.722	6.211E-02	0.0604	0.0001	99.38	5.901E-02	8.306E-03
3527.348	6.048E-02	0.0606	0.0001	99.61	5.595E-02	7.565E-03
3616.526	5.899E-02	0.0607	0.0001	99.83	5.209E-02	6.783E-03
3703.073	5.761E-02	0.0608	0.0001	99.98	4.731E-02	5.950E-03
3787.806	5.632E-02	0.0608	0.0000	100.00	4.163E-02	5.067E-03
3876.349	5.503E-02	0.0608	0.0000	100.00	3.515E-02	4.140E-03
3967.523	5.377E-02	0.0608	0.0000	100.00	2.749E-02	3.132E-03
4059.241	5.255E-02	0.0608	0.0000	100.00	1.866E-02	2.057E-03
4152.593	5.137E-02	0.0608	0.0000	100.00	8.525E-03	9.114E-04
4248.212	5.021E-02	0.0608	0.0000	100.00	1.009E-03	1.052E-04
4348.277	4.906E-02	0.0608	0.0000	100.00	0.000E+00	0.000E+00
4454.238	4.789E-02	0.0608	0.0000	100.00	0.000E+00	0.000E+00
4565.371	4.673E-02	0.0608	0.0000	100.00	0.000E+00	0.000E+00
4682.491	4.556E-02	0.0608	0.0000	100.00	0.000E+00	0.000E+00

4805.054	4.440E-02	0.0608	0.0000	100.00	0.000E+00	0.000E+00
4930.430	4.327E-02	0.0608	0.0000	100.00	2.704E-07	3.098E-08
5057.166	4.218E-02	0.0608	0.0000	100.00	5.630E-07	6.207E-08
5187.804	4.112E-02	0.0608	0.0000	100.00	8.894E-07	9.438E-08
5321.617	4.009E-02	0.0608	0.0000	100.00	1.237E-06	1.263E-07
5458.604	3.908E-02	0.0608	0.0000	100.00	1.302E-06	1.263E-07
5597.729	3.811E-02	0.0608	0.0000	100.00	1.506E-06	1.389E-07
5739.941	3.716E-02	0.0608	0.0000	100.00	1.760E-06	1.543E-07
5880.164	3.628E-02	0.0608	0.0000	100.00	2.080E-06	1.736E-07
6025.728	3.540E-02	0.0608	0.0000	100.00	2.495E-06	1.984E-07
6161.778	3.462E-02	0.0608	0.0000	100.00	3.050E-06	2.315E-07

Table E8: ED=0.020J/mm²

Report date: 08/10/2007   Merged File

QUANTACHROME INSTRUMENTS

QUANTACHROME POREMASTER FOR WINDOWS® DATA REPORT

VERSION 4.03

SAMPLE ID   CS8030407_22   FILE NAME   S781005H_Merged.PRM

SAMPLE WEIGHT   1.0000 grams   BULK SAMPLE VOLUME 1.0000 cc

SAMPLE DESCRIPTION M. TEKIN

COMMENTS   LP STATION 1

HG SURFACE TENSION 480.00 erg/cm²   HG CONTACT ANGLE   (I)140.00°,(E)140.00°

MINIMUM DELTA VOL. 0.000 % FS   MOVING POINT AVG. 11 (Scan Mode)

OPERATOR   Leyla MOLU   Mercury volume normalized by sample weight.

Pore Size Distribution By Volume - Intrusion

Printing every data point.

Pressure	Pore Diameter	Volume Intruded	Delta Volume	% Volume Intruded	Dv(d)	-dV/d(log d)
[PSI]	[µm]	[cc/g]	[cc/g]	%	[cc/(µm-g)]	[cc/g]
0.973	2.192E+02	0.0000	0.0000	0.00	8.113E-06	6.872E-03
1.166	1.830E+02	0.0005	0.0005	0.92	9.748E-06	7.655E-03
1.443	1.478E+02	0.0013	0.0008	2.57	1.439E-05	8.438E-03
1.867	1.143E+02	0.0022	0.0009	4.37	2.301E-05	9.283E-03
2.294	9.301E+01	0.0029	0.0007	5.84	3.572E-05	9.949E-03
2.817	7.572E+01	0.0038	0.0009	7.62	5.329E-05	1.075E-02
3.294	6.475E+01	0.0047	0.0008	9.28	8.207E-05	1.259E-02
3.820	5.584E+01	0.0056	0.0009	11.06	1.064E-04	1.413E-02
4.388	4.862E+01	0.0065	0.0010	12.98	1.322E-04	1.587E-02
4.993	4.272E+01	0.0074	0.0009	14.76	1.690E-04	1.806E-02
5.629	3.790E+01	0.0084	0.0010	16.71	2.163E-04	2.040E-02
6.265	3.405E+01	0.0093	0.0009	18.57	2.706E-04	2.277E-02
6.933	3.077E+01	0.0103	0.0010	20.57	3.318E-04	2.520E-02
7.635	2.794E+01	0.0115	0.0012	22.91	4.061E-04	2.796E-02
8.338	2.558E+01	0.0128	0.0012	25.35	4.904E-04	3.078E-02
9.043	2.359E+01	0.0140	0.0012	27.74	5.980E-04	3.442E-02
9.749	2.188E+01	0.0151	0.0012	30.08	7.257E-04	3.869E-02
10.455	2.040E+01	0.0163	0.0012	32.44	9.036E-04	4.510E-02

227

11.129	1.917E+01	0.0175	0.0012	34.83	1.137E-03	5.361E-02
11.773	1.812E+01	0.0187	0.0011	37.11	1.398E-03	6.252E-02
12.383	1.723E+01	0.0199	0.0012	39.56	1.677E-03	7.137E-02
12.993	1.642E+01	0.0213	0.0014	42.28	1.996E-03	8.083E-02
13.601	1.568E+01	0.0231	0.0018	45.87	2.351E-03	9.044E-02
14.209	1.501E+01	0.0253	0.0022	50.26	2.748E-03	1.004E-01
14.813	1.440E+01	0.0276	0.0023	54.79	3.145E-03	1.091E-01
15.414	1.384E+01	0.0298	0.0022	59.24	3.554E-03	1.172E-01
16.011	1.332E+01	0.0321	0.0023	63.77	3.939E-03	1.237E-01
16.604	1.285E+01	0.0343	0.0022	68.22	4.274E-03	1.280E-01
17.192	1.241E+01	0.0366	0.0023	72.69	4.445E-03	1.272E-01
17.807	1.198E+01	0.0387	0.0021	76.95	4.420E-03	1.209E-01
18.448	1.156E+01	0.0408	0.0021	81.09	4.295E-03	1.120E-01
19.114	1.116E+01	0.0428	0.0020	84.98	4.114E-03	1.021E-01
19.774	1.079E+01	0.0444	0.0017	88.29	3.827E-03	9.055E-02
20.425	1.044E+01	0.0456	0.0012	90.60	3.472E-03	7.856E-02
21.068	1.013E+01	0.0462	0.0006	91.85	2.997E-03	6.503E-02
21.704	9.829E+00	0.0466	0.0004	92.57	2.506E-03	5.228E-02
22.331	9.553E+00	0.0468	0.0003	93.10	1.984E-03	3.994E-02
22.951	9.295E+00	0.0470	0.0001	93.35	1.457E-03	2.839E-02
23.561	9.054E+00	0.0471	0.0001	93.57	9.548E-04	1.811E-02
24.162	8.829E+00	0.0471	0.0000	93.57	5.728E-04	1.062E-02
24.754	8.618E+00	0.0471	0.0000	93.57	3.524E-04	6.369E-03
25.337	8.419E+00	0.0471	0.0000	93.57	2.166E-04	3.808E-03
25.912	8.233E+00	0.0471	0.0000	93.57	1.082E-04	1.856E-03
26.455	8.064E+00	0.0471	0.0000	93.57	1.251E-04	2.359E-03

26.965	7.911E+00	0.0471	0.0000	93.57	1.539E-04	3.058E-03
27.467	7.766E+00	0.0471	0.0000	93.57	2.481E-04	4.784E-03
27.939	7.635E+00	0.0471	0.0000	93.57	3.501E-04	6.565E-03
28.403	7.511E+00	0.0471	0.0000	93.57	4.598E-04	8.397E-03
28.860	7.392E+00	0.0472	0.0001	93.79	5.776E-04	1.028E-02
29.288	7.283E+00	0.0473	0.0001	94.01	6.967E-04	1.211E-02
29.689	7.185E+00	0.0474	0.0001	94.24	8.162E-04	1.388E-02
30.082	7.091E+00	0.0475	0.0001	94.46	9.423E-04	1.570E-02
30.469	7.001E+00	0.0476	0.0001	94.68	1.070E-03	1.747E-02
30.850	6.915E+00	0.0477	0.0001	94.90	1.203E-03	1.929E-02
31.249	6.827E+00	0.0479	0.0001	95.13	1.134E-03	1.783E-02
31.665	6.737E+00	0.0480	0.0001	95.35	1.053E-03	1.624E-02
32.075	6.651E+00	0.0481	0.0001	95.57	9.603E-04	1.451E-02
32.501	6.563E+00	0.0482	0.0001	95.79	8.592E-04	1.273E-02
32.922	6.480E+00	0.0483	0.0001	96.02	7.500E-04	1.090E-02
33.336	6.399E+00	0.0483	0.0000	96.02	6.319E-04	9.011E-03
33.765	6.318E+00	0.0483	0.0000	96.02	5.135E-04	7.188E-03
34.208	6.236E+00	0.0483	0.0000	96.02	3.946E-04	5.418E-03
34.646	6.157E+00	0.0483	0.0000	96.02	2.670E-04	3.597E-03
35.077	6.082E+00	0.0483	0.0000	96.02	1.379E-04	1.823E-03
35.500	6.009E+00	0.0483	0.0000	96.02	0.000E+00	0.000E+00
35.917	5.939E+00	0.0483	0.0000	96.02	0.000E+00	0.000E+00
36.328	5.872E+00	0.0483	0.0000	96.02	0.000E+00	0.000E+00
36.733	5.807E+00	0.0483	0.0000	96.02	0.000E+00	0.000E+00
37.130	5.745E+00	0.0483	0.0000	96.02	0.000E+00	0.000E+00
37.522	5.685E+00	0.0483	0.0000	96.02	0.000E+00	0.000E+00

37.908	5.627E+00	0.0483	0.0000	96.02	0.000E+00	0.000E+00
38.289	5.571E+00	0.0483	0.0000	96.02	0.000E+00	0.000E+00
38.663	5.517E+00	0.0483	0.0000	96.02	0.000E+00	0.000E+00
39.032	5.465E+00	0.0483	0.0000	96.02	0.000E+00	0.000E+00
39.395	5.415E+00	0.0483	0.0000	96.02	0.000E+00	0.000E+00
39.753	5.366E+00	0.0483	0.0000	96.02	0.000E+00	0.000E+00
40.105	5.319E+00	0.0483	0.0000	96.02	0.000E+00	0.000E+00
40.451	5.274E+00	0.0483	0.0000	96.02	0.000E+00	0.000E+00
40.792	5.230E+00	0.0483	0.0000	96.02	0.000E+00	0.000E+00
41.129	5.187E+00	0.0483	0.0000	96.02	0.000E+00	0.000E+00
41.459	5.145E+00	0.0483	0.0000	96.02	0.000E+00	0.000E+00
41.785	5.105E+00	0.0483	0.0000	96.02	0.000E+00	0.000E+00
42.106	5.066E+00	0.0483	0.0000	96.02	0.000E+00	0.000E+00
42.422	5.029E+00	0.0483	0.0000	96.02	0.000E+00	0.000E+00
42.734	4.992E+00	0.0483	0.0000	96.02	0.000E+00	0.000E+00
43.040	4.956E+00	0.0483	0.0000	96.02	0.000E+00	0.000E+00
43.341	4.922E+00	0.0483	0.0000	96.02	0.000E+00	0.000E+00
43.639	4.888E+00	0.0483	0.0000	96.02	0.000E+00	0.000E+00
43.933	4.856E+00	0.0483	0.0000	96.02	0.000E+00	0.000E+00
44.221	4.824E+00	0.0483	0.0000	96.02	0.000E+00	0.000E+00
44.505	4.793E+00	0.0483	0.0000	96.02	0.000E+00	0.000E+00
44.785	4.763E+00	0.0483	0.0000	96.02	0.000E+00	0.000E+00
45.060	4.734E+00	0.0483	0.0000	96.02	0.000E+00	0.000E+00
45.332	4.706E+00	0.0483	0.0000	96.02	0.000E+00	0.000E+00
45.600	4.678E+00	0.0483	0.0000	96.02	0.000E+00	0.000E+00
45.874	4.650E+00	0.0483	0.0000	96.02	0.000E+00	0.000E+00

46.156	4.622E+00	0.0483	0.0000	96.02	0.000E+00	0.000E+00
46.446	4.593E+00	0.0483	0.0000	96.02	0.000E+00	0.000E+00
47.069	4.532E+00	0.0483	0.0000	96.02	0.000E+00	0.000E+00
48.100	4.435E+00	0.0483	0.0000	96.02	0.000E+00	0.000E+00
49.613	4.300E+00	0.0483	0.0000	96.02	0.000E+00	0.000E+00
51.733	4.124E+00	0.0483	0.0000	96.02	0.000E+00	0.000E+00
54.593	3.908E+00	0.0483	0.0000	96.02	0.000E+00	0.000E+00
58.403	3.653E+00	0.0483	0.0000	96.02	0.000E+00	0.000E+00
63.413	3.364E+00	0.0483	0.0000	96.02	0.000E+00	0.000E+00
69.922	3.051E+00	0.0483	0.0000	96.02	0.000E+00	0.000E+00
78.350	2.723E+00	0.0483	0.0000	96.02	0.000E+00	0.000E+00
89.217	2.391E+00	0.0483	0.0000	96.02	0.000E+00	0.000E+00
103.068	2.070E+00	0.0483	0.0000	96.02	0.000E+00	0.000E+00
120.144	1.776E+00	0.0483	0.0000	96.02	0.000E+00	0.000E+00
140.871	1.514E+00	0.0483	0.0000	96.02	0.000E+00	0.000E+00
165.815	1.287E+00	0.0483	0.0000	96.02	0.000E+00	0.000E+00
195.258	1.093E+00	0.0483	0.0000	96.02	5.991E-06	3.495E-05
229.453	9.297E-01	0.0483	0.0000	96.02	1.607E-05	7.239E-05
268.524	7.944E-01	0.0483	0.0000	96.02	3.220E-05	1.124E-04
312.462	6.827E-01	0.0483	0.0000	96.02	5.689E-05	1.550E-04
361.256	5.905E-01	0.0483	0.0000	96.02	9.323E-05	2.003E-04
414.158	5.151E-01	0.0483	0.0000	96.06	1.448E-04	2.486E-04
470.511	4.534E-01	0.0484	0.0000	96.11	2.152E-04	2.997E-04
530.155	4.024E-01	0.0484	0.0000	96.15	3.082E-04	3.536E-04
592.995	3.597E-01	0.0484	0.0000	96.20	4.284E-04	4.105E-04
658.955	3.237E-01	0.0484	0.0000	96.24	5.804E-04	4.701E-04

727.463	2.932E-01	0.0484	0.0000	96.29	7.692E-04	5.328E-04
798.821	2.670E-01	0.0485	0.0000	96.33	8.252E-04	4.979E-04
872.829	2.444E-01	0.0485	0.0000	96.38	8.693E-04	4.604E-04
949.243	2.247E-01	0.0485	0.0000	96.43	8.975E-04	4.204E-04
1028.458	2.074E-01	0.0485	0.0000	96.47	9.060E-04	3.778E-04
1109.822	1.922E-01	0.0486	0.0000	96.52	8.906E-04	3.325E-04
1193.836	1.787E-01	0.0486	0.0000	96.52	8.454E-04	2.842E-04
1281.180	1.665E-01	0.0486	0.0000	96.52	7.672E-04	2.332E-04
1372.739	1.554E-01	0.0486	0.0000	96.52	1.226E-03	4.706E-04
1466.955	1.454E-01	0.0486	0.0000	96.52	1.803E-03	7.207E-04
1563.672	1.364E-01	0.0486	0.0000	96.52	2.530E-03	9.890E-04
1663.009	1.283E-01	0.0486	0.0000	96.52	3.402E-03	1.265E-03
1764.252	1.209E-01	0.0486	0.0000	96.52	4.783E-03	1.618E-03
1868.127	1.142E-01	0.0486	0.0001	96.67	6.426E-03	1.985E-03
1972.365	1.082E-01	0.0487	0.0001	96.83	8.360E-03	2.368E-03
2075.242	1.028E-01	0.0488	0.0001	96.99	1.058E-02	2.764E-03
2179.752	9.787E-02	0.0489	0.0001	97.15	1.310E-02	3.171E-03
2285.169	9.335E-02	0.0490	0.0001	97.31	1.598E-02	3.594E-03
2391.493	8.920E-02	0.0490	0.0001	97.47	1.923E-02	4.035E-03
2497.818	8.540E-02	0.0491	0.0001	97.62	1.907E-02	3.743E-03
2605.412	8.188E-02	0.0492	0.0001	97.78	1.865E-02	3.436E-03
2714.186	7.860E-02	0.0493	0.0001	97.94	1.794E-02	3.108E-03
2823.232	7.556E-02	0.0494	0.0001	98.10	1.694E-02	2.769E-03
2932.187	7.275E-02	0.0494	0.0001	98.26	1.564E-02	2.416E-03
3041.233	7.014E-02	0.0494	0.0000	98.26	1.400E-02	2.050E-03
3151.821	6.768E-02	0.0494	0.0000	98.26	1.199E-02	1.666E-03

3265.584	6.532E-02	0.0494	0.0000	98.26	1.048E-02	1.425E-03
3380.074	6.311E-02	0.0494	0.0000	98.26	1.092E-02	1.561E-03
3496.015	6.102E-02	0.0494	0.0000	98.26	1.137E-02	1.700E-03
3612.318	5.905E-02	0.0494	0.0000	98.26	1.174E-02	1.828E-03
3729.166	5.720E-02	0.0494	0.0000	98.26	1.632E-02	2.418E-03
3846.468	5.546E-02	0.0495	0.0000	98.30	2.140E-02	3.024E-03
3966.400	5.378E-02	0.0495	0.0001	98.46	2.702E-02	3.641E-03
4086.060	5.221E-02	0.0496	0.0001	98.62	3.323E-02	4.277E-03
4207.716	5.070E-02	0.0497	0.0001	98.78	4.011E-02	4.936E-03
4328.375	4.928E-02	0.0498	0.0001	98.94	4.764E-02	5.613E-03
4449.396	4.794E-02	0.0499	0.0001	99.09	5.568E-02	6.288E-03
4571.324	4.667E-02	0.0499	0.0001	99.25	6.110E-02	6.627E-03
4692.890	4.546E-02	0.0500	0.0001	99.41	5.837E-02	6.083E-03
4813.275	4.432E-02	0.0501	0.0001	99.57	5.504E-02	5.522E-03
4933.389	4.324E-02	0.0502	0.0001	99.73	5.123E-02	4.953E-03
5056.769	4.219E-02	0.0503	0.0001	99.89	4.679E-02	4.363E-03
5180.512	4.118E-02	0.0503	0.0001	100.00	4.178E-02	3.758E-03
5302.803	4.023E-02	0.0503	0.0000	100.00	3.616E-02	3.140E-03
5426.727	3.931E-02	0.0503	0.0000	100.00	2.983E-02	2.504E-03
5552.919	3.842E-02	0.0503	0.0000	100.00	2.273E-02	1.845E-03
5676.884	3.758E-02	0.0503	0.0000	100.00	1.635E-02	1.285E-03
5802.116	3.677E-02	0.0503	0.0000	100.00	7.892E-03	6.023E-04
5938.318	3.592E-02	0.0503	0.0000	100.00	5.523E-07	4.621E-08
6071.174	3.514E-02	0.0503	0.0000	100.00	6.604E-07	5.281E-08
6216.539	3.432E-02	0.0503	0.0000	100.00	8.066E-07	6.161E-08

Table E9-True Density of Polyamide

Mass(g)	True Volume(cc)	True Density(g/cc)	Energy Density(J/mm^2)
0.9425	0.8975	1.0501	0.016
1.0260	1.0043	1.0216	0.019
1.0255	1.0058	1.0196	0.020
1.0702	1.0808	0.9902	0.024
1.0798	1.0911	0.9896	0.025
1.0690	1.0693	0.9997	0.029
1.1139	1.1277	0.9878	0.030
1.1195	1.1145	1.0045	0.033
1.1202	1.1529	0.9716	0.037

E2. Additional physical/mechanical characterization data

Table E 10: Apparent density of uniformly parts

ED (J/mm^2)	Density(g/cc)					
	Replicate 1	Replicate 2	Replicate 3	Replicate 4	Average	Stdev
0.016	0.7194	0.6911	0.7243	0.7051	0.7100	0.0150
0.019	0.7886	0.8145	0.7742	0.8132	0.7976	0.0196
0.020	0.8010	0.8387	0.7939	0.8266	0.8151	0.0211
0.024	0.9039	0.9038	0.9037	0.9063	0.9044	0.0013
0.025	0.9241	0.9082	0.9037	0.9121	0.9120	0.0088
0.029	0.9503	0.9359	0.9363	0.9392	0.9404	0.0067
0.030	0.9280	0.9365	0.9366	0.9370	0.9345	0.0044
0.033	0.9460	0.9419	0.9514	0.9471	0.9466	0.0039
0.037	0.9533	0.9651	0.9407	0.9430	0.9505	0.0112

Table E 11: Macroscopic porosities of the uniformly porous parts

ED (J/mm^2)	Porosity (%)					
	Replicate 1	Replicate 2	Replicate 3	Replicate 4	Average	Stdev
0.016	27.57	29.49	28.06	30.89	29.00	1.50
0.019	22.58	18.68	21.14	18.55	20.24	1.96
0.020	20.61	17.34	19.9	16.13	18.50	2.11
0.024	9.63	9.37	9.61	9.62	9.56	0.13
0.025	9.63	8.79	7.59	9.18	8.80	0.88
0.029	6.37	6.08	4.97	6.41	5.96	0.67
0.030	6.34	6.3	7.2	6.35	6.55	0.44
0.033	5.4	5.81	4.86	5.29	5.34	0.39
0.037	5.93	5.7	4.67	3.49	4.95	1.12

Table E12: UTS of uniformly porous parts

ED J/mm^2	UTS(MPa)						
	Replicate 1	Replicate 2	Replicate 3	Replicate 4	Replicate 5	Average	Stdev
0.016	19.93	18.87	20.31	21.3	19.49	19.98	0.91
0.019	30.64	31.36	30.96	32.41	32.73	31.62	0.91
0.020	31.72	33.25	31.82	32.78	34.54	32.82	1.16
0.024	39.99	39.67	40.48	41.1	40.87	40.42	0.60
0.025	42.08	42.27	42.27	41.31	42.7	42.13	0.51
0.029	43.7	42.92	43.95	43.48	43.42	43.49	0.38
0.030	42.73	43.09	43.16	43.36	44.17	43.30	0.54
0.033	42.53	42.95	43.07	43.80	43.52	43.15	1.30
0.037	43.88	43.68	43.66	43.81	43.65	43.74	0.10

Table E 13: Normalized weight gains for the epoxy-PA

ED	ρ	Sample 1				Sample 2				Sample 3				Average	stdev
		M1	v1	m1	WG1	M2	v2	m2	WG2	M3	v3	m3	WG3	WG	
(J/mm^2)	(g/cc)	(g)	(cc)	(g)	(g/cc)	(g)	(cc)	(g)	(g/cc)	(g)	(cc)	(g)	(g/cc)	(g/cc)	(g/cc)
0.016	0.7100	4.04	4.22	3.00	0.25	4.05	4.05	2.88	0.29	3.99	3.95	2.81	0.30	0.28	0.028
0.019	0.7976	3.87	3.92	3.12	0.19	3.95	4.15	3.31	0.15	3.87	4.18	3.34	0.13	0.16	0.031
0.020	0.8151	3.94	4.08	3.33	0.15	3.96	4.05	3.30	0.16	4.11	4.30	3.50	0.14	0.15	0.010
0.024	0.9044	3.6	3.76	3.40	0.05	3.67	3.81	3.45	0.06	3.77	3.86	3.49	0.07	0.06	0.010
0.025	0.9120	3.69	3.89	3.55	0.04	3.56	3.67	3.35	0.06	3.55	3.67	3.35	0.05	0.05	0.012
0.029	0.9404	3.88	4.01	3.77	0.03	3.71	3.86	3.63	0.02	3.74	3.93	3.70	0.01	0.02	0.009
0.030	0.9345	3.7	3.87	3.62	0.02	3.66	3.79	3.54	0.03	3.69	3.83	3.58	0.03	0.03	0.005
0.033	0.9466	3.69	3.98	3.77	-0.02	3.71	3.91	3.70	0.00	3.65	3.83	3.63	0.01	0.00	0.014
0.037	0.9505	3.9	4.12	3.92	0.00	3.8	4.00	3.80	0.00	3.75	4.03	3.83	-0.02	-0.01	0.010

where ED:energy density, ρ:apparent density of the porous parts, M:after infiltration, v:volume, m:mass before infiltration (mass of porous parts), WG:normalized weight gain (M-m divide by v).

Table E 14: Porosity left after epoxy infiltration into uniform porous medium

po(%)	Sample 1			Sample 2			Sample3			average	stdev
	Vr1(cc)	Vpore1(cc)	po-l1 (%)	Vr2(cc)	Vpore2 (cc)	po-l2 (%)	Vr3 (cc)	Vpore3 (cc)	po-l3 (%)	po-l(%)	(%)
29.0	0.9	1.2	6.6	1.0	1.2	5.4	1.1	1.1	1.8	4.6	2.5
20.2	0.7	0.8	2.9	0.8	0.8	2.1	0.5	0.8	8.6	4.6	3.5
18.5	0.6	0.8	4.9	0.6	0.7	4.3	0.6	0.8	5.7	5.0	0.7
9.6	0.2	0.4	4.8	0.2	0.4	3.2	0.3	0.4	2.9	3.6	1.0
8.8	0.1	0.3	5.5	0.0	0.3	8.5	0.2	0.3	3.9	5.9	2.3
6.0	0.1	0.2	3.4	-0.1	0.2	7.3	0.0	0.2	5.0	5.2	2.0
6.5	0.1	0.3	4.6	0.0	0.2	5.5	0.1	0.3	4.0	4.7	0.8
5.3	-0.1	0.2	7.2	-0.1	0.2	6.8	0.0	0.2	4.9	6.3	1.3
4.9	0.0	0.2	5.3	-0.1	0.2	7.6	-0.1	0.2	6.7	6.5	1.1

where po: porosity of uniformly porous structures, Vr: amount of resin infiltrated (=density of epoxy(1.1 g/cc)*v, Vpore: volume of pores (=po*v/100), po-l: porosity left (=(Vpore-Vr)/v*100).

Table E 15: Normalized weight gains for the epoxy-PA graded porous structures (epoxy infiltrated graded porous Type I PA parts)

	uW (g)			iW(g)			V(cc)			normalized weight gains (g/cc)				
	w1	w2	w3	Iw1	Iw2	Iw3	V1	V2	V3	Wg1	Wg2	Wg3	average	stdev
Type I-3 Grades	2.98	3.03	2.94	3.35	3.56	3.28	3.71	3.70	3.40	0.10	0.14	0.10	0.11	0.02
Type I-5 Grades	2.67	2.84	2.69	3.3	3.31	3.27	3.40	3.37	3.42	0.19	0.14	0.17	0.16	0.02
Type I-7 Grades	2.71	2.57	2.65	3.54	3.52	3.45	3.72	3.61	3.57	0.22	0.26	0.22	0.24	0.02

where uW: weight of uninfiltrated sample, iW: weight of infiltrated sample, V: volume of infiltrated sample, Wgi (i=1,2,3) weight gains of ith sample.

ARALDITE 564 AND HARDENER XB 3486 DATASHEET

APPLICATIONS   Industrial composites

PROPERTIES

Laminating system with low viscosity and high flexibility. The reactivity may easily be adjusted to demands through the combination of both hardeners. The long pot life of XB 3486 facilitates the production of very large industrial parts. The systems are qualified by Germanischer Lloyd.

Table F1: Key Data

Araldite® LY 564		
Aspect (visual)	clear liquid	
Colour (Gardner, ISO 4630)	1-2	
Viscosity at 25 °C (ISO 12058-1B)	1200 - 1400	[mPa s]
Density at 25 °C (ISO 1675)	1.1 - 1.2	[g/cm^3]
Flash point (ISO 2719)	185	[°C]
Storage temperature (see expiry date on original container)	2 - 40	[°C]
Hardener XB 3486		
Aspect (visual)	clear colourless to slightly yellow liquid	
Viscosity at 25 °C (ISO 12058-1B)	10 - 20	[mPa s]
Density at 25 °C (ISO 1675)	0.94 - 0,95	[g/cm^3]
Flash point (ISO 2719)	123	[°C]
Storage temperature	2 - 40	[°C]

(see expiry date on original container)

STORAGE

Provided that Araldite® LY 564 and Hardener XB 3486 are stored in a dry place in their original, properly closed containers at the above mentioned storage temperatures they will have the shelf lives indicated on the labels.Partly emptied containers should be closed immediately after use.

PROCESSING DATA

Table F2: Mix Ratio

Components	Parts by Weight	Parts by Volume
Araldite® LY 564	100	100
Hardener XB 3486	34	41

We recommend that the components are weighed with an accurate balance to prevent mixing inaccuracies which can affect the properties of the matrix system. The components should be mixed thoroughly to ensure homogeneity. It is important that the side and the bottom of the vessel are incorporated into the mixing process. When processing large quantities of mixture the pot life will decrease due to exothermic reaction. It is advisable to divide large mixes into several smaller containers.

Initial Mix Viscosity: 200 – 300 MPas at 25°C.

Table F3: Pot Life

		[g]	[min]
(TECAM, 23°C, 65 % RH)	LY 564 /XB 3486	100	560 - 620
		1000	180 - 230

Table F4: Gel Time (Hot Plate)

		[°C]	[min]
LY 564 /XB 3486		at 60	110 - 130
		at 80	33 - 43
		at 100	13 - 17
		at 120	5 - 9

The values shown are for small amounts of pure resin/hardener mix. In composite structures the gel time can differ significantly from the given values depending on the fiber content and the laminate thickness.

Table F5: Properties of the Cured, Neat Formulation

Glass transition		Cure	T_G (°C)
Temperature	(IEC	2 days 23 °C	33-37
1006,		8 days 23 °C	49 - 53
DSC, 10 K/MIN)		20 h 40 °C	52-56
		15 h 50 °C	66 - 70
		24 h 50 °C	66-70
		10 h 60 °C	67 - 71
		16 h 60 °C	68-72
		4 h 80 °C	77 - 81

	8 h 80 °C	80 - 84
	2 h 100 °C	78 - 82
	5 h 100 °C	80 - 84

Tensile Test (ISO 527)		Cure: 15h 50 °C	Cure: 8h 80 °C
	Tensile strength[MPa]	74 - 78	70 - 74
	Elongation at tensile strength[%]	4.0 - 4.2	4.6 - 5.0
	Ultimate strength[MPa]	62 - 68	60 - 64
	Ultimate elongation[%]	5.8 – 6.2	8.0 - 8.5
	Tensile modulus[MPa]	3100 - 3250	2860 - 3000

Flexural Test (ISO 178)

	Cure: 7 days 23 °C	Cure: 15 h 50 °C	Cure: 8 h 80 °C
Flexural strength[MPa]	80 - 90	120 - 135	118 - 130
Elongation at flexural strength[%]	2.1 - 2.5	5.2 - 5.6	5.5 - 6.5
Ultimate strength[MPa]	80 - 90	78 - 85	88 - 100
Ultimate elongation[%]	2.1 - 2.5	9.0 - 11.5	10.5 - 12.5
Flexural modulus[MPa]	3500 - 3700	3100 - 3300	2900 - 3050

Fracture Properties Bend notch test (PM 258-0/90)

	Cure: 5 h 100 °C
Fracture toughness K_{1C} [MPa√m]	0.95 - 1.05
Fracture energy $G_{1C[J/m^2]}$	260 - 310

APPENDIX G

FACTORIAL DESIGN

The 2^3 Factorial Designs

In this report two experiments are considered, density and ultimate tensile strength for the parts build via selective laser sintering (sls) method. There are many factors contributing to these responses, however only hatching distance, laser power, and laser scanning speed will be considered.

Let A=Hatching distance (mm), B=Laser power (%), and C=Laser scanning speed (mm/s), then Table G-1 gives their levels.

Table G-1: Factor levels for the density and ultimate tensile strength experiment

Factor	Factor Levels	
	Low(-)	High(+)
A(mm)	0.30	0.45
B (%)	66.3	90
C(mm/s)	4000	5000

G.1. Density Experiment

In this experiment four replicates are used. Table G-2 gives the details of the response for each run and for each replicate and Figure G-1 shows the geometric view of treatment combination

Table G-2: The Density Experiment

Run	Coded Factors			Labels	Density(g/cc)			
	A	B	C		Replicate 1	Replicate 2	Replicate 3	Replicate 4
1	1	-1	1	ac	0.7194	0.6911	0.7243	0.7051
2	1	-1	-1	a	0.7886	0.8145	0.7742	0.8132
3	1	1	1	abc	0.8010	0.8387	0.7939	0.8266
4	-1	-1	1	c	0.9039	0.9038	0.9037	0.9063
5	1	1	-1	ab	0.9241	0.9082	0.9037	0.9121
6	-1	-1	-1	(l)	0.9503	0.9359	0.9363	0.9392
7	-1	1	1	bc	0.9280	0.9365	0.9366	0.9370
8	-1	1	-1	b	0.9533	0.9651	0.9407	0.9430
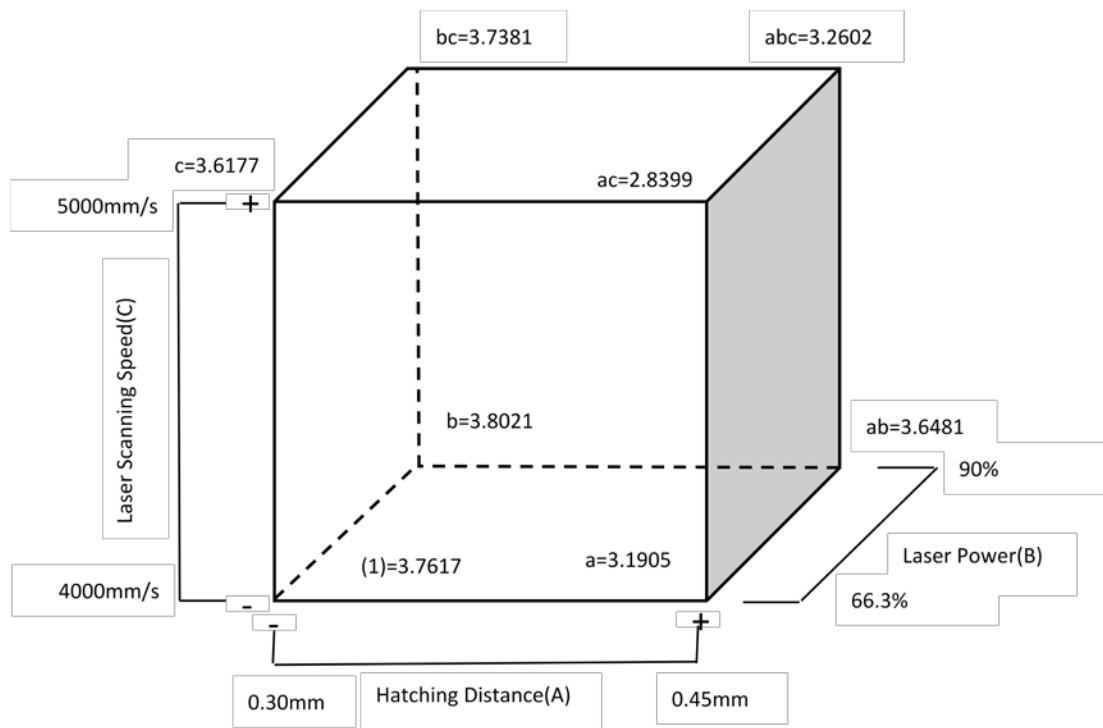
Figure G-1: Treatment Combinations for the density experiment

The values in Figure G-1 are obtained by summing up all densities in a given run as shown in Table G-1.

For example, for Run 1:

$$ac=0.7194+0.6911+0.7243+0.7051=2.8399$$

$$a=0.7886+0.8145+0.7742+0.8132=3.1905$$

In the same way the values of the other Runs are obtained. The effects of A, B, C, AB, AC, BC, and ABC on the density are found as follows with n=4(number of replicates):

$$A = \frac{[a-(1)+ab-b+ac-c+abc-bc]}{4n} \quad \text{i.e.,} \quad A=-0.124$$

$$B = \frac{[b+ab+bc+abc-(1)-a-c-ac]}{4n} \quad B= 0.065$$

$$C = \frac{[c+ac+bc+abc-(1)-a-b-ab]}{4n} \quad C=-0.059$$

$$AB = \frac{[ab-a-b+(1)+abc-bc-ac+c]}{4n} \quad AB=0.045$$

$$AC = \frac{[(1)-a+b-ab-c+ac-bc+abc]}{4n} \quad AC=-0.033$$

$$BC = \frac{[(1)+a-b-ab-c-ac+bc+abc]}{4n} \quad BC=2.66 \times 10^{-3} \text{ and}$$

$$ABC = \frac{[abc-bc-ac+c-ab+b+a-(1)]}{4n} \quad ABC=-7.331 \times 10^{-3}$$

The A main effect seems to have largest effects than all, about -0.124, followed by B(0.065), C(-0.059), AB(0.045), AC(-0.033), ABC(-7.331x10^{-3}), and BC(2.669x10^{-3}). BC interaction has smallest effects. The summary of the treatment effects are shown in Table G-3 and their standardized effects are shown in Table G-4.

Table G-3: Effect Estimate summary for the density experiment

Factor	Effect Estimate	Sum of Squares	Percent Contribution
A	-0.124	0.123	57.47663551
B	0.065	0.034	15.88785047
C	-0.059	0.028	13.08411215
AB	0.045	0.016	7.476635514
AC	-0.033	8.795E-03	4.11
BC	0.002669	5.70E-05	0.026626
ABC	-0.007331	4.30E-04	0.2009
Pure Error		0.00371802	1.737392523
Total		0.214	

Sum of Squares in Table G-3 and Table G-4 are achieved as follows for every factor.

$$SS_A = \frac{[a-(1)+ab-b+ac-c+abc-bc]^2}{8n} \qquad i.e., \quad SS_A = 0.123$$

$$SS_B = \frac{[b+ab+bc+abc-(1)-a-c-ac]^2}{8n} \qquad SS_B = 0.034$$

$$SS_C = \frac{[c+ac+bc+abc-(1)-a-b-ab]^2}{8n} \qquad SS_C = 0.028$$

$$SS_{AB} = \frac{[ab-a-b+(1)+abc-bc-ac+c]^2}{8n} \qquad SS_{AB} = 0.016$$

$$SS_{AC} = \frac{[(1)-a+b-ab-c+ac-bc+abc]^2}{8n} \qquad SS_{AC} = 8.795 \times 10^{-3}$$

$$SS_{BC} = \frac{[(1)+a-b-ab-c-ac+bc+abc]^2}{8n} \qquad SS_{BC} = 5.698 \times 10^{-5}$$

$$SS_{ABC} = \frac{[abc-bc-ac+c-ab+b+a-(1)]^2}{8n} \qquad SS_{ABC} = 4.3 \times 10^{-4}$$

Since there are 4 replicates i.e., n=4, the total sum of squares can be found as follows:

$$SS_T = \sum_{i=1}^{2}\sum_{j=1}^{2}\sum_{k=1}^{2}\sum_{m=1}^{n} y_{ijkm}^2 - \frac{y_t^2}{8n}$$

where $y_t = (1) + a + b + c + ab + ac + bc + abc$

Defining

$$\sum_{i=1}^{2}\sum_{j=1}^{2}\sum_{k=1}^{2}\sum_{m=1}^{n} y_{ijkm}^{2} = \sum_{i=0}^{r-1}\sum_{j=0}^{p-1} \rho_{i,j}^{2}$$

where r=8 (number of rows of the density matrix), p=4(number of columns of the density matrix), and the density matrix is defined as:

$$\rho = \begin{pmatrix} 0.7194 & 0.6911 & 0.7243 & 0.7051 \\ 0.7886 & 0.8145 & 0.7742 & 0.8132 \\ 0.8010 & 0.8387 & 0.7939 & 0.8266 \\ 0.9039 & 0.9038 & 0.9037 & 0.9063 \\ 0.9241 & 0.9082 & 0.9037 & 0.9121 \\ 0.9503 & 0.9359 & 0.9363 & 0.9392 \\ 0.9280 & 0.9365 & 0.9366 & 0.9370 \\ 0.9533 & 0.9651 & 0.9407 & 0.9430 \end{pmatrix}$$

$$SS_T = \sum_{i=0}^{7}\sum_{j=0}^{3} \rho_{i,j}^{2} - \frac{y_t^2}{8n} \qquad i.e., SS_T = 0.214$$

Table G-4: The standardized effects for density (DoF: degree of freedom, Coef.: coefficient, SE Coef.: Standard Errors for coefficients, SE: Standardized effects, and Z: score)

Term	Effect	Coef.	Sum of Squares	DoF	Mean Square	SE Coef.	SE	Z
A	-0.124	-0.062	0.123	1	0.123	0.0022	-28.18	-1.69
B	0.065	0.0325	0.034	1	0.034	0.0022	14.77	1.26
C	-0.059	-0.0295	0.028	1	0.028	0.0022	-13.41	-0.68
AB	0.045	0.0225	0.016	1	0.016	0.0022	10.23	0.95
AC	-0.033	-0.0165	8.795E-03	1	8.795E-03	0.0022	-7.50	-0.27
BC	2.669E-3	1.3345E-3	5.70E-05	1	5.70E-05	0.0022	0.61	0.29
ABC	-7.331E-3	-3.6655E-3	4.30E-04	1	4.30E-04	0.0022	-1.67	0.13
Error			0.003718	24	1.54917E-4			
Total			0.214	31				

In Table G-4 coefficients are found by taking one-half of the corresponding effect. For example, the coefficient in the row of factor A is (-0.124)/2=-0.062.

The same procedure is followed for the rest. Mean square in Table G-4 is obtained by dividing the sum of squares by the corresponding degree of freedom. For example, the mean square in the row of factor A is (0.123)/1=0.123. The same procedure is followed for the rest. The procedure on how to find sum of squares have been shown in page 4.

The Standard Errors for coefficients is achieved by using the following formula

$$SE\ coef = \sqrt{\frac{MSE}{N}}$$

where MSE= 1.54917×10^{-4}, mean square error (in Table G-4) and N=32, total number of observation.

The Standard error coefficient is the same for all effects, since MSE and N are the same for all. And lastly, the standardized effects are achieved by just dividing coefficient by the standard errors coefficient. For example, the standardized effect in the row of term A is (-0.062/0.0022)= -28.18 as found in Table G-4. The same procedure can be followed for the rest of the data.

The score labeled Z in Table G-4 is found by first finding the average (μ) and the standard deviation (σ) of the standardized effects (SE). Then, by using the formula

$$Z = \frac{SE - \mu}{\sigma}$$

the desired Z-score can be found.

Density Regression Model

The model has been generated using the Minitab software. The regression model for the density is given as:

$$\rho=2.39221-3.70746H-0.0216498P-1.52721 \times 10^{-4}S+00623347HP+$$

$$2.02572 \times 10^{-4}HS+3.31857 \times 10^{-6}PS-8.24895 \times 10^{-6}HPS$$

where H: hatching distance (mm), P: laser power (%), and S: laser scan speed (mm/s), for example if power is 30% input 30.

G.2. Ultimate Tensile Strength Experiment

Similar procedure is followed as in Density Experiment. Table G-7 and Figure G-2 give the treatment combination.

Table G-7: The Ultimate Tensile Strength Experiment

Run	Coded Factors			Labels	UTS(MPa)				
	A	B	C		Replicate 1	Replicate 2	Replicate 3	Replicate 4	Replicate 5
1	1	-1	1	ac	19.93	18.87	20.31	21.3	19.49
2	1	-1	-1	a	30.64	31.36	30.96	32.41	32.73
3	1	1	1	abc	31.72	33.25	31.82	32.78	34.54
4	-1	-1	1	c	39.99	39.67	40.48	41.1	40.87
5	1	1	-1	ab	42.08	42.27	42.27	41.31	42.7
6	-1	-1	-1	(l)	43.7	42.92	43.95	43.48	43.42
7	-1	1	1	bc	42.73	43.09	43.16	43.36	44.17
8	-1	1	-1	b	43.88	43.68	43.66	43.81	43.65

Figure G-2: The Ultimate Tensile Strength Experiment

The effects of the predetermined factors are found as follows, see next page:

Note that the number of replicates in this problem is n=5 and not 4(see Table G-7).

$$A = \frac{[a-(1)+ab-b+ac-c+abc-bc]}{4n}$$ i.e., A=-11.102

$$B = \frac{[b+ab+bc+abc-(1)-a-c-ac]}{4n}$$ B= 6.617

$$C = \frac{[c+ac+bc+abc-(1)-a-b-ab]}{4n}$$ C=-6.113

$$AB = \frac{[ab-a-b+(1)+abc-bc-ac+c]}{4n}$$ AB=5.057

$$AC = \frac{[(1)-a+b-ab-c+ac-bc+abc]}{4n}$$ AC=-4.359

$$BC = \frac{[(1)+a-b-ab-c-ac+bc+abc]}{4n}$$ BC=1.244 and

$$ABC = \frac{[abc-bc-ac+c-ab+b+a-(1)]}{4n}$$ ABC=-0.075

The A factor seems to have largest effects than all, about -11.102, followed by B(6.617), C(-6.113), AB(5.057), AC(-4.359), BC(1.244), and lastly ABC(-0.075). ABC interaction has the smallest effect. The summary of the treatment effects are shown in Table G-8 and their standardized effects are shown in Table G-9.

Table G-8: Effect Estimate summary for the UTS experiment

Factor	Effect Estimate	Sum of Squares	Percent Contribution
A	-11.102	1232	48.86949623
B	6.617	437.913	17.3706069
C	-6.113	373.627	14.82058707
AB	5.057	255.682	10.14208647
AC	-4.359	190.052	7.54
BC	1.244	15.463	0.613368
ABC	-0.075	0.057	0.0023
Pure Error		16.206	0.642840143
Total		2521	

Sum of Squares in Table G-8 and Table G-9 are achieved as follows for every factor.

$$SS_A = \frac{[a-(1)+ab-b+ac-c+abc-bc]^2}{8n} \qquad \text{i.e.,} \quad SS_A = 1.23 \times 10^3$$

$$SS_B = \frac{[b+ab+bc+abc-(1)-a-c-ac]^2}{8n} \qquad SS_B = 437.913$$

$$SS_C = \frac{[c+ac+bc+abc-(1)-a-b-ab]^2}{8n} \qquad SS_C = 373.627$$

$$SS_{AB} = \frac{[ab-a-b+(1)+abc-bc-ac+c]^2}{8n} \qquad SS_{AB} = 255.682$$

$$SS_{AC} = \frac{[(1)-a+b-ab-c+ac-bc+abc]^2}{8n} \qquad SS_{AC} = 190.052$$

$$SS_{BC} = \frac{[(1)+a-b-ab-c-ac+bc+abc]^2}{8n} \qquad SS_{BC} = 15.463$$

$$SS_{ABC} = \frac{[abc-bc-ac+c-ab+b+a-(1)]^2}{8n} \qquad SS_{ABC} = 0.057$$

Since there are 5 replicates i.e., n=5 the total sum of squares can be found as follows:

$$SS_T = \sum_{i=1}^{2}\sum_{j=1}^{2}\sum_{k=1}^{2}\sum_{m=1}^{n} uy_{ijkm}^{2} - \frac{u_t^{2}}{8n}$$

where $u_t = (1) + a + b + c + ab + ac + bc + abc$

Define UTS matrix as:

$$u = \begin{pmatrix} 19.93 & 18.87 & 20.31 & 21.3 & 19.49 \\ 30.64 & 31.36 & 30.96 & 32.41 & 32.73 \\ 31.72 & 33.25 & 31.82 & 32.78 & 34.54 \\ 39.99 & 39.67 & 40.48 & 41.1 & 40.87 \\ 42.08 & 42.27 & 42.27 & 41.31 & 42.7 \\ 43.7 & 42.92 & 43.95 & 43.48 & 43.42 \\ 42.73 & 43.09 & 43.16 & 43.36 & 44.17 \\ 43.88 & 43.68 & 43.66 & 43.81 & 43.65 \end{pmatrix}$$

and

$$\sum_{i=1}^{2}\sum_{j=1}^{2}\sum_{k=1}^{2}\sum_{m=1}^{n} u_{ijkm}^{2} = \sum_{i=0}^{r-1}\sum_{j=0}^{p-1} u_{i,j}^{2}$$

where r=8 (number of rows of the UTS matrix), p=4(number of columns of the UTS matrix)

Therefore,

$$SS_T = \sum_{i=0}^{7}\sum_{j=0}^{3} u_{i,j}^{2} - \frac{u_t^{2}}{8n} \qquad i.e., SS_T = 2.521x10^{3}$$

Table G-9: The standardized effects for UTS (DoF: degree of freedom, Coef.: coefficient, SE Coef.: Standard Errors for coefficients, SE: Standardized effects, and Z: score)

Term	Effect	Coef.	Sum of Squares	DoF	Mean Square	SE Coef.	SE	Z
A	-11.102	-5.551	1232	1	1232	0.112521	-49.33	-1.56
B	6.617	3.3085	437.913	1	437.913	0.112521	29.40	1.24
C	-6.113	-3.0565	373.627	1	373.627	0.112521	-27.16	-0.77
AB	5.057	2.5285	255.682	1	255.682	0.112521	22.47	1.00
AC	-4.359	-2.1795	190.052	1	190.052	0.112521	-19.37	-0.49
BC	1.244	0.622	15.463	1	15.463	0.112521	5.53	0.39
ABC	-0.075	-0.0375	0.057	1	0.057	0.112521	-0.33	0.19
Error			16.206	32	0.5064375			
Total			2521	39	66.6410256			

In Table G-9 coefficients are found by taking one-half of the corresponding effect. For example, the coefficient in the row of factor A is (-11.102)/2=-11.102. The same procedure is followed for the rest. Mean square in Table G-9 is obtained by dividing the sum of squares by the corresponding degree of freedom. For example, the mean square in the row of factor A is (1232)/1=1232. The same procedure is followed for the rest. The procedure on how to find sum of squares have been shown in page 9.

The Standard Errors for coefficients is achieved by using the following formula

$$SE\ coef = \sqrt{\frac{MSE}{N}}$$

where MSE= 0.5064375, mean square error (in Table G-9) and N=40, total number of observation.

The Standard error coefficient is the same for all effects, since MSE and N are the same for all. And lastly, the standardized effects are achieved by just dividing coefficient by the standard errors coefficient. For example, the standardized effect in the row of term A is (--5.551/0.112521)= -49.33 as found in the Table G-9. The same procedure can be followed for the rest of the data. The score labeled Z in Table G-9 is found by first finding the average (μ) and the standard deviation (σ) of the standardized effects (SE).

Then, by using the formula

$$Z = \frac{SE - \mu}{\sigma}$$

the desired Z-score can be found.

UTS Regression Model

The model has been generated using the Minitab software. The regression model for the ultimate tensile strength is given as:

$$U=104.013-64.6304H-1.40312P+4.99461 \times 10^{-3}S+3.227HP-$$

$$5.14878 \times 10^{-2}HS+1.36793 \times 10^{-4}PS-8.495081 \times 10^{-5}HPS$$

where H: hatching distance (mm), P: laser power (%), and S: laser scan speed (mm/s), for example if power is 30%, input 30.